Molecular and biochemical characterisation of mycobacterial cell wall drug targets - Lipoarabinomannan

A thesis submitted to the

University of Birmingham

for the degree of Doctor of Philosophy

January 2014

Shipra Grover, M. Sc.

Abstract

A recent surge in emergence of drug resistant strains of *Mycobacterium tuberculosis*, the etiological agent of tuberculosis has highlighted the importance of developing new therapeutics and devising novel strategies for effective management of this disease. The cell wall of *M. tuberculosis* is a major determinant of high level drug resistance demonstrated by this pathogen. Therefore pathways for the synthesis of its components and their regulation have remained an attractive drug target. In this study, the pathway for decaprenyl phosphate recycling emerges as a new target and illustrates a possible mechanism of resistance to the recently discovered anti-tubercular compounds, Benzothiazinones. Additionally, the newly identified Lac-I type transcriptional regulator IpsA, sheds light on an intricate regulatory network for the synthesis of cell wall components, such as the phosphatidyl inositol based lipoglycans. Since the pathway is critical for growth in members of *Corynebacterineae*, it provides for an untapped resource for designing novel inhibitors against the pathogenic species *M. tuberculosis* and *Corynebacterium diphtheriae*. This work also explores new approaches for the design of anti-tubercular compounds against cell wall glycosyltransferases, such as 'co-targeting' of interacting transferases as revealed by protein-protein interaction studies and utilising the concept of 'polar hydrophobicity' in the design of 'suicide inhibitors' of transferase activity.

Declaration

I do hereby declare that the work described in this thesis has been carried out under the supervision of Prof. Gurdyal S. Besra in the School of Biosciences, University of Birmingham, Birmingham, U.K. B15 2TT. The work in this thesis is original except where acknowledged by reference. The thesis Chapters 1, 2 and 3 resulted in four publications; two with Monika Jankute as the co-author, one as a first author and one as the third author that may bear similarities to the thesis chapters. These similar sections included in the thesis are my original work with no significant contribution to the text by either Monika Jankute or Prof. Gurdyal S. Besra. This work or part thereof has not been submitted elsewhere for any other diploma or degree at any other university.

Monika Jankute

Prof. Gurdyal S. Besra

Acknowledgements

I deeply attribute completion of this work to my supervisor Prof. Gurdyal S. Besra, whose guidance and supervision has made it possible for me to make any worthwhile progress. His motivating attitude, critical analysis and timely suggestions let me work more and produce valued results. I will forever be indebted to him for shaping my career as a reseacher.

I express my gratefulness to Dr. Apoorva Bhatt for providing his expertise throughout the doctoral period. A special thanks to Dr. Luke Alderwick for being a source of constant encouragement and for his timely suggestions that helped me throughout.

I would like to thank Dr. Lothar Eggeling and his lab from Institute of Bio- and Geosciences, Jülich, for performing some of the molecular biology experiments in this work and Dr. Julia Frunzke and her lab from the Institute of Bio- and Geosciences, Jülich, for providing me with an opportunity to work with them. Also, I am thankful to Dr. Bruno Linclau, University of Southampton for generating some of the compounds used in this thesis.

My special thanks to all the present and past members of this lab who have made this experience memorable. I appreciate the assistance provided by Dr.Arun K. Mishra and Dr. Sudagar Gurucha. I appreciate the affection and assistance provided by Monika, Amrita, Natacha and Veemal in my difficult times and for making life in England an experience to be cherished. I also thank Usha, Cristian, Albel, Vijay and Mimi for making my time in the lab more enjoyable. I am forever indebted to my parents and my brother for their unconditional love and support at all times.

This thesis is dedicated to my family

Table of Contents

List of Figures

List of Tables

List of Abbreviations

A	adenine
Aa	amino acid
ACP	Acyl carrier protein
ADP	adenosine diphosphate
Ag85A	Antigen 85 complex
AMP	adenosine monophosphate
AftA	Arabinofuranosyltransferase A
AftB	Arabinofuranosyltransferase B
AftC	Arabinofuranosyltransferase C
AftD	Arabinofuranosyltransferase D
AftE	Arabinofuranosyltransferase E
AG	arabinogalactan
AIDS	Acquired immuno-deficiency syndrome
Ara	arabinose
Ara*f*	arabino*furanose*
AraLAM	un-capped LAM
ATP	Adenosine triphosphate
BCA	bicinchoninic protein assay
BCG	bacillus Calmette-Guérin
BHI	brain heart infusion
BHIS	brain heart infusion sorbitol
BSA	bovine serum albumin
BTZ	benzothiazinone
C	cytosine

°C	degrees centigrade
CAP	catabolite activator protein
CDP-DAG	cytidine diphosphate-diacylglycerol
Ci	Curie
CoA	Coenzyme A
CPM	counts per minute
DAG	diacylglycerol
DAP	diaminopimelic acid
DAT	diacyl trehalose
DMSO	dimethylsulphoxide
DNA	deoxyribonucleic acid
DPA	decaprenyl-phosphate-D-arabinose
DPG	diphosphatidyl glycerol
DPM	decaprenyl-phospho-mannose
DPPR	decaprenylphosphoryl-5- phosphoribose
DPR	decaprenyl-phosphate-D-ribose
DXD	Aspartic acid residue motif in glycosyltransferases
EDTA	ethylenediaminetetraacetic acid
EMB	ethambutol
f	furanose
FAD	Flavin adenine dinucleotide
FAME	Fatty acid methyl esters
FAS	fatty acid synthase
FQ	Fluoroqinolones
g	grams

G	guanine
Gal	galactose
Gal*f*	galactofuranose
GAT	Gatifloxacin
GC/MS	gas chromatography-mass spectrometry
GDP-Man*p*	guanosine diphospho-mannose *pyranose*
GlcNAc	N-acetylglucosamine
GMCM	glucose monocorynomycolate
Gro	glycerol
HCl	hydrochloric acid
His-tag	6 histidine residue tag
HIV	human immuno-deficiency virus
Hz	hertz
IPTG	isopropylthio-β-D-galactoside
INH	Isoniazid
kDa	kilo Dalton
kPa	kilo Pascal
L	litre
LAM	lipoarabinomannan
LB	Luria-Bertani
LM	lipomannan
LOSs	lipooligosaccharides
LPS	lipopolysaccharide
LU	linkage unit
M	molar

MAC	*Mycobacterium avium* complex
mAGP	mycolyl-arabinogalactan-peptidoglycan complex
MALDI-TOF	matrix assisted laser desorption ionisation-time of flight
ManLAM	mannosyl capped LAM
Man*p*	mannopyranose
MDR	multi-drug resistant
mg	milligram
MgtA	α-mannosyl-glucopyranosyluronic acid-transferase A
mL	millilitre
mM	millimolar
MOPS	4-morpholine propane sulfonic acid
MPA	molybdophosphoric acid
MPI	mannosyl-phosphatidyl-myo-inositol
MptA	α(1→6) mannospyranosyltransferase A
MptB	α(1→6) mannospyranosyltransferase B
MptC	α(1→2) mannospyranosyltransferase C
MptD	α(1→2) mannospyranosyltransferase D
MS	mass spectrometry
MSH	mycothiol
Mur	muramic acid
nm	nanometres
NAD	Nicotinamide adenine dincleotide
NADH	Reduced nicotinamide adenine dincleotide
NADP	Nicotinamide adenine dincleotide phosphate

NADPH	Reduced nicotinamide adenine dincleotide phosphate
NMR	nuclear magnetic resonance
OD	optical density
ORF	open reading frame
P	phosphate
p.p.m.	parts per million
PAGE	polyacrylamide gel electrophoresis
PCR	polymerase chain reaction
PE	phosphatidyl ethanolamine
PG	peptidoglycan
PGls	phenolic glycolipids
PI	phosphatidyl-myo-inositol
PILAM	LAM with phosphoinositide caps
PIM	phosphatidyl-myo-inositol mannoside
PPM	polyprenyl monophosphate
pRpp	5-phosphoribofuranose pyrophosphate
Rha	rhamnose
sec	second
SDS	sodium dodecyl sulfate
SL	sulfolipid
t	terminal
T	thymine
TAE	Tris-acetate EDTA
TB	tuberculosis
TBAH	tetra butylammonium hydroxide

TDM	trehalose dimycolate
TFA	trifluoroacetic acid
TLC	thin-layer chromatography
TMCM	trehalose monocorynomycolate
TMM	trehalose monomycolate
U	uracil
UDP-Gal	uridine diphospho-galactose
UDP-GlcA	UDP-D-glucuronic acid
v/v	volume/volume
w/v	weight per volume
μg	microgram
μl	microlitre
μM	micromolar

Published work associated with this thesis

- S. Grover*, M. Jankute*, A. K. Rana, G. S. Besra, Arabinogalactan and lipoarabinomannan biosynthesis: structure, biogenesis and their potential as drug targets. *Future Microbiol* 7, 129 (Jan, 2012)

- Meike Baumgart, Kerstin Luder, Shipra Grover, Cornelia Gätgens , Gurdyal S. Besra, Julia Frunzke, IpsA, a novel LacI-type regulator, is required for inositol-1 derived lipid formation in Corynebacteria and Mycobacteria *BMC Biology* 2013, 11:122

- S. Grover*, M. Jankute*, H. Birch, G.S. Besra, Genetics of Arabinogalactan and Lipoarabinomannan biosynthesis. *Molecular Genetics of Mycobacteria* Second Ed. ASM Press. (Accepted, In press)

- S. Grover,L. J. Alderwick, A. K. Mishra, A. Bhatt, G.S. Besra, Benzothiazinones mediate killing of *Corynebacterianeae* by blocking decaprenyl phosphate recycling involved in cell wall biosynthesis. J. Biol. Chem, 2014. (In press

)

Chapter 1

1 Introduction

1.1 Mycobacteria and related species

In 1882, Robert Koch isolated *Mycobacterium tuberculosis* (MTB), the etiologic agent of tuberculosis (TB) from the lungs of infected animals using methylene blue based dye and described it as a rod shaped Gram positive bacteria classified under the genus *Mycobacterium*. The members of the genus *Mycobacterium* are aerobic Actinomycetales that are rod shaped, acid-alcohol fast, non-capsular, non-endosporous, and non-motile with the exception of *Mycobacterium marnium* that exhibits motility in macrophages (Stamm *et al.*, 2003). *Mycobacterium* forms a part of the *Corynebacterium-Mycobacterium-Nocardia* (CMN) branch in the sub-order *Corynebacterineae* of the actinomycete group. The genus *Rhodococcus* is designated as the fourth member of this sub-order. The organisms under this branch have a characteristic type IV cell wall with distinctive structures such as *meso*-diaminopimelic acid, N-acetyl glucosamine and N-glycolated muramic acid. In addition, the cell wall contains a unique polysaccharide, arabinoglactan (AG), substituted with long chain fatty acids, termed mycolic acids (Dobson, 1985; Minnikin, 1982; Minnikin, 1980). The classification of organisms in the *Corynebacterineae* sub-order is based on the composition of their cell envelope. The mycolates in *Corynebacterium* are the smallest in size with 22-38 carbons, whilst those in *Nocardia* and *Rhodococcus* are intermediate in size with 40-60 carbon atoms. The largest and the most complex mycolates are synthesised in *Mycobacterium* and contain 60-90 carbon atoms (Brennan and Nikaido, 1995; Iain C. Sutcliffe, 2010).

The species in the *Mycobacterium* group have been divided into two sub-groups based on their growth rate. The first group of slow-growing species of mycobacteria with a

generation time of 15-20 hours include; MTB, *Mycobacterium bovis* BCG, *Mycobacterium avium, Mycobacterium canetti, Mycobacterium kansasii,* and the non-culturable *Mycobacterium leprae.* The second group comprises of fast-growing species of mycobacteria with a generation time of 3-4 hours with *Mycobacterim smegmatis* and *Mycobacterium chelonae* being the most significant. The fast growers are also characterised by the presence of α'-mycolates in their cell walls (Brennan and Nikaido, 1995).

MTB is a part of the *M. tuberculosis* complex (MTBC) that includes four other TB-causing mycobacteria; *M. africanum*, *M. bovis*, *M. microti* and *M. canetti.* While *M. africanum* and *M. canetti* are causative agents of TB in parts of Africa, infection with *M. microti* is considered to be opportunistic and prevalent in immuno-compromised individuals, *M. bovis* is common in cattle and can cause TB in humans if unpasteurised milk is routinely consumed. Other virulent strains of mycobacteria include *M. leprae* and the opportunistic pathogens, *M. marinum, M. avium* and *M. kansasii*. The virulent strains of *M. tuberculosis* also occur in chains and forms unique serpentine cords. These characteristic structures are attributed to presence of 'cord factor' i.e. trehalose dimycolate (TDM) in the cell wall of virulent strains of *M. tuberculosis* and related species.

1.2 Tuberculosis

1.2.1 Origins of Tuberculosis

TB is considered to be an ancient scourge. Evidence for its occurrence have been reported in prehistoric literary works, including Deuteronomy and Leviticus, using the ancient Hebrew word 'schachepheth' (Daniel and Daniel, 1999). In 400 BC Hippocrates described TB as the condition associated with fever, cough and loss of appetite and termed it as "phthisis". It has also been referred to as "Consumption", "King's Evil", "Pott's disease", "Scofula" and "The White Plague" in various literary records.

The evolution and phylogeny of the MTB complex remains poorly understood. The most popular hypothesis on TB evolution was suggested by Aidan Cockburn in 1963 who proposed *M. bovis* as the ancestor of MTB. Cockburn argued that the pathogen had transmitted from cattle to humans as a consequence of domestication and evolved into its present respiratory form due to urbanisation of human settlements (A. R. Zink, 2007). This classical theory of TB evolution has been challenged by (Brosch *et al.*, 2002)) who recently proposed MTB to be the common ancestor for the entire MTB complex. The genus *Mycobacterium* is hypothesised to have originated 150 million years ago and the modern strains of MTB appear to have diversified 20,000- 15,000 years ago from a common ancestor as a result of a genetic evolutionary bottleneck (Hayman, 1984). *M. bovis* is therefore a derivative of the parent MTB strain that branched off later during development of other pathogenic mycobacteria. Brosch's hypothesis is based on modern techniques for genotyping and are supported by ancient DNA studies. Genetic and molecular evidence from the skeletal remains of Egyptian

mummies have established the presence of pathogen in Egypt over 5000 years ago (Crubezy *et al.*, 1998; Helen D. Donoghue, 2010; Nerlich *et al.*, 1997) and designated East Africa as the birth place of TB. The disease was well established in this region by the 19th century and later spread to other parts of the world with inter-continental movement (Wirth *et al.*, 2008).

1.2.2 Clinical manifestations

TB is a dreadful communicative infectious disease that spreads through small airborne droplets generated by sneezing, coughing or talking with an infected individual. Although the bacteria mainly colonises the lung tissue and causes pulmonary TB, it is also capable of infecting other parts of the body, such as lymph nodes, bones/joints or meninges and results in extra-pulmonary TB. The etiologic agent of TB in cattle is *M. bovis* that also causes extra-pulmonary TB in humans. Not all individuals exposed to TB develop an active form of the disease, as the immune system successfully wards off the infection in healthy individuals. However, persons a with weak immune system, such as HIV patients, are more susceptible to TB and can develop latent or active TB upon exposure to the bacteria.

An encounter with MTB sets off an immune response in the lungs and marcophages are recruited for phagocytosis. Although the macrophages are able to engulf the bacteria, its digestion is prevented due to the waxy cell wall. The bacteria continues to divide inside the macrophage. Once the macrophage bursts open, the bacteria gets engulfed by other macrophages and forms a scar tissue. This stage of TB infection is called primary TB and is usually asymptomatic and the individual is non-infectious. The scar tissue and lymph nodes may eventually harden as Ca^{2+} is recruited from the

blood stream to the infected area. This process of calcification of scar tissue results in formation of a quarantined area within the lung and is called a tubercle or a granuloma. These calcified scars can easily be detected using radiology. MTB can remain in this state of latent or dormant infection for many years in a healthy individual.

If the immune system is weakened or suppressed, the bacteria can rupture the scar tissue and cause active TB referred to as secondary TB or reactivation of TB. A rare form of TB is called disseminated TB, that occurs when infected macrophages moving through the circulatory system transport the bacteria to other sites in the body. The symptoms of disseminated TB depend on the location infected.

1.2.3 Epidemiology

TB is one of the most fatal diseases to have affected mankind since the ancient times. Nearly one third of the world's population is estimated to be suffering from one or the other form of the disease (Murray and Salomon, 1998). According to WHO Global TB report of 2012, 8.7 million people had contracted TB in 2011 of which 1.1 million reported cases were of individuals with HIV co-infection. Of the total number of infected individuals reported, 12% of the infected population, including 430,000 cases of those co-infected with HIV had died from the disease. Geographically, the highest numbers of TB incidences are reported from Asia and Africa, with India and China alone accounting for 40% of the total TB cases (Fig 1.1). Africa accounts for 24% of the cases and suffers from highest number of deaths *per* capita. The remaining numbers of cases are reported from South-East Asia and Western Pacific regions. Although the mortality rate from TB infection has reduced to 41% since 1990, TB still continues to be a treat owing to the evolution of drug resistant strains.

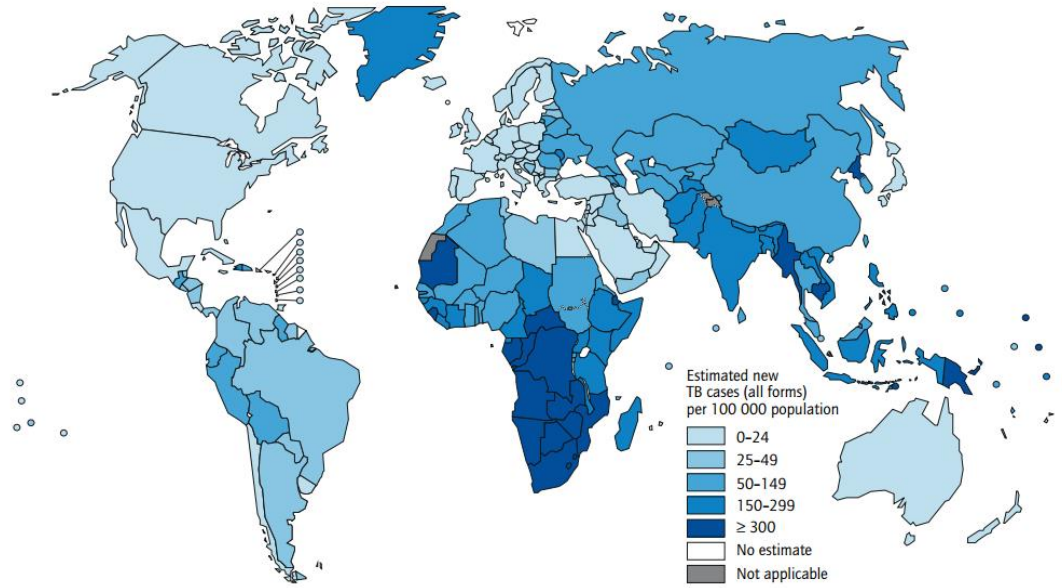

Figure 1.1: Estimated number of TB cases worldwide accoding to Global Tuberculosis Report 2012.-WHO, 2012.

These drug resistant strains are classified as multidrug resistant (MDR), which includes organisms that are resistant to the most effective anti-TB drugs – isoniazid and rifampicin, and extensively drug resistant (XDR), which refers to MDR strains resistant to second line drugs, such as amikacin, kanamycin, capreomycin and fluoroquinolone. Recently, a new class of drug resistant TB, termed totally drug resistant TB (TDR-TB) has been reported in Iran, Italy, India and South Africa (Klopper *et al.*, 2013; Loewenberg, 2012). These strains are reported to be resistant to all first and second line drugs currently used for the treatment of TB.

It is now estimated that 3.7% of new TB patients in the world i.e. 310,000 have MDR-TB, with Brazil, India, China, Russia and South Africa accounting for 60% of the total cases. Approximately 9% of the MDR cases are also reported to be XDR with at least one case of XDR in 84 countries. In case of HIV positive individuals, TB is the most

common and deadliest of all opportunistic infections and puts them at the highest risk. The severity of infection increases several folds in such individuals due to their weak immune system and renders them difficult to treat (Aids Control and Prevention (Aidscap) Project of Family Health Internal, 1996). According to WHO nearly one third of the HIV infected patients in the world suffer from latent TB of which 80% of infected individuals reside in Africa. The increase in number of patients being affected by drug resistant strains of TB, has prompted the need for new drugs and better vaccines. Clinical trials are underway for many new potential drug and vaccine candidates for effective treatment in future.

1.2.4 Treatment

In the late eighteenth century, TB that was commonly referred to as "consumption" resulted in the death of one in every four individuals in England. The major factors that attributed to this high mortality rate was the lack of hygiene and sanitation, poor nutrition and absence of adequate medical care (Davis, 2000). However, during the nineteenth century, with improvements in the socio-economic conditions and a grave realisation that TB is an infectious disease; a downward trend in the death rate was observed. The treatment of TB during this time was based on a regimen of nutritious diet, bed-rest and fresh air provided in a "sanatorium". Since antibiotics had not been discovered yet, sanatorium was the sole way for helping patients cope with the disease. Robert Koch's discovery of the TB bacteria in 1882 not only won him the Nobel Prize in Medicine but also paved the way for the identification of antibiotics targeted to pulmonary lesions and cavitation, a characteristic of TB infection that revolutionised the treatment of TB. After isolating MTB, Koch made several attempts to find a cure for the disease. One such attempt was the use of "tuberculin", a glycerine extract from

MTB which Koch reported could inhibit the growth of the pathogen (Koch, 1891). Tuberculin was immediately adopted as a cure for TB but the treatment suffered a major setback when its administration resulted in several critical reactions in TB patients (Gradmann, 2006). Subsequently, Tuberculin was determined to be non-therapeutic but had significant diagnostic value as it could be utilised for detecting "latent TB". It is still used today and is known as "Mantoux Test" (Daniel, 2006).

The first breakthrough in the treatment of TB was achieved in 1908 when the avirulent form of *M. bovis*, known as *M. bovis* BCG (Bacillus Calmette Guerin) was isolated by Albert Calmette and Camille Guerin. This BCG strain lost its virulence after its 39th passage and paved the way for the first vaccine against TB. At present, BCG is widely used as a vaccine to prevent extra-pulmonary infection in children under the age of 5 with maximum efficiency (Bloom and Murray, 1992).

The idea of treatment of TB with chemotherapeutics originated in 1946 and streptomycin (SM) was the first antibiotic to be tested. The results of early clinical trials showed that SM could effectively reduce mortality rates. However, *M. tuberculosis* developed resistance by modifying the ribosome protein S12 and 16S rRNA within five years of drug trials (Musser, 1992). In 1948, *p*-aminosalicylic acid (PAS), a folic acid inhibitor was introduced for the treatment of TB. However, owing to its low efficacy, PAS was used in combination with SM and resulted in a decrease in incidences of resistance. The effective three drug combination regimen was adopted in 1952 with the addition of isoniazid (INH) to the existing therapy consisting of SM and PAS. Later in 1966, rifampicin (RIF) and pyrazinamide (PZA) were added to the six-month regimen of standard TB treatment which was introduced in the 1970s (Saltini, 2006). The current therapy for TB treatment known as Directly Observed Therapy-

Short course (DOTS) comprises of five elements. These include a (i) political commitment from the governments for designing and implementation of adequate disease management strategies and financial help, (ii) case detection through sputum smear test and drug susceptibility testing (DST), (iii) standardised treatment under supervision with adequate patient support, (iv) a system for ensuring regular supply of quality anti-TB drugs, (v) a system for regular monitoring and assessment of the treatment received on a case by case basis. The element of chemotherapy in DOTS follows a tiered approach, where attempts are made to cure infection with the first line drugs: INH, RIF, Ethambutol (EMB), SM and PZA. Referred to as the initial phase, it makes use of three or more drugs for two months to kill actively dividing bacteria. Post-treatment with the first-line drugs in the initiation phase, the patient now enters into the second-phase, the 'continuation phase' that makes use of fewer drugs, mostly RIF and INH for four to seven months in order to kill the remaining or dormant bacteria and prevent relapse. The patient is considered cured at six months. INH alone is administered for six-nine months to a patient suffering from latent TB. If resistance is found for any one of the above drugs or side effects are observed in the patient, less effective second line drugs that include quinolones, cycloserine, amikacin, SM, kanamycin, ethinonamide and PAS are then administered. The third line of therapeutics, include amoxicillin-clavulanate, clofazamine, clarithromycin, imipenem, thioacetazone, and high-doses of INH that are prescribed in the case of MDR and XDR TB (Caminero *et al.*, 2010).

1.3 Drugs for treatment of TB

The emergence of MDR and XDR strains that are tough to control with present chemotherapeutics, calls for the hastening of efforts for generating new delivery systems, different regimes and novel drugs with effective anti-mycobacterial activity, for improved treatment. Drug resistance is not just limited to MDR and XDR-TB. Recently reported in four countries across the world, TDR-TB has attracted the attention of many researchers and health organisations to its potential threat. However, despite the rise in number of incidences of TDR-TB being reported each year, WHO doesn't acknowledge it as a new class and instead includes them under the category of XDR-TB, as currently there are no defined and internationally accepted methods available to test the drug susceptibility in such cases. Moreover, the new drugs being developed are yet to be tested on these TDR-TB strains. Therefore, on grounds of insufficient data to support the status, WHO recommends not using the term TDR-TB in practice, even though the concept is clearly understandable in theory.

The present TB treatment comprises of INH, RIF, PZA and EMB as the major drugs, with each having a unique mode of action. The course of therapy consists of a mix of four drugs to help in combating the problem of increase of drug resistance. No new drug has been included in this standard regimen, since its introduction in 1970. Recently two new drugs, bedaquiline and delamanid were proposed to be included in this short course regimen to treat MDR-TB. However, by early 2013, only bedaquiline was approved by the American and European Regulatory Authorities and was incorporated as a novel second-line drug, the first in 40 years since the treatment came into effect (Osborne, 2013). Delamanid was initially declined by the Committee for Medicinal Products for Human Use (CHMP), the European Medical Agency on

grounds of insufficient evidence to prove effectiveness and accurate dosage of the drug in the treatment of MDR-TB. In addition, clinical trials conducted to test the potency of delamanid only tested the drug for a short duration of two months and could not demonstrate its efficacy over the course of 6 months, a requirement of the standard DOTS regimen. However, in a revised statement issued by European Regulatory Authorities later in 2013, Otsuka Pharmaceutical Co., Ltd. (Otsuka) was granted a marketing authorization for Deltyba(TM) (delamanid) for treatment of MDR-TB in adults. Although, the initial failure of delamanid was a huge set back for a new chemotherapeutic, hopes are being pinned on the REMoxTB therapy that is currently in Phase III clinical trials. REMoxTB therapy is a global venture between Bayer Healthcare AG, the Medical Research Council and University College London to evaluate the response of a moxifloxacin containing TB regime in TB patients in 9 countries across the world. The therapy tests moxifloxacin as a replacement of INH and EMB, and is to be used in conjunction with other current first line drugs for TB treatment. The preliminary results are promising and suggest that the inclusion of moxifloxacin in the present regimen can reduce the course of therapy from 6 to 4 months. The new drug pipeline (Fig 1.2) comprises of several new candidates and regimens being evaluated for their potential as future TB drugs and therapies. The new therapeutic agents developed for TB treatment have to fulfill a well defined criterion that includes, validated safety reporting, greater potency than existing drugs, a novel target and mechanism of action, no harmful drug-drug interactions with existing TB drugs, and high compatibility with anti-retroviral therapies to treat HIV co-infection cases (Zumla *et al.*, 2013).

Several new options are currently being explored for the treatment of TB. These include re-purposing of drugs such as rifamycin, fluoroquinolones, riminophenazines, oxazolidinones that are currently used to treat other infections. In addition, the use of adjunct immunotherapies, such as either cytokines or their inhibitors and other immunomodulatory compounds that increase the immune response to the pathogen. Finally, novel anti-mycobacterial agents such as bedaquiline, benzothiazinones nitroimidazoles, dipiperidine, SQ109, capuramycin, and the caparazene nucleoside (Figure 1.2) are being developed. The mechanism of action of main TB drugs that are in clinical use has been studied in detail while that of several novel candidates in pre-clinical development phase are yet to be elucidated.

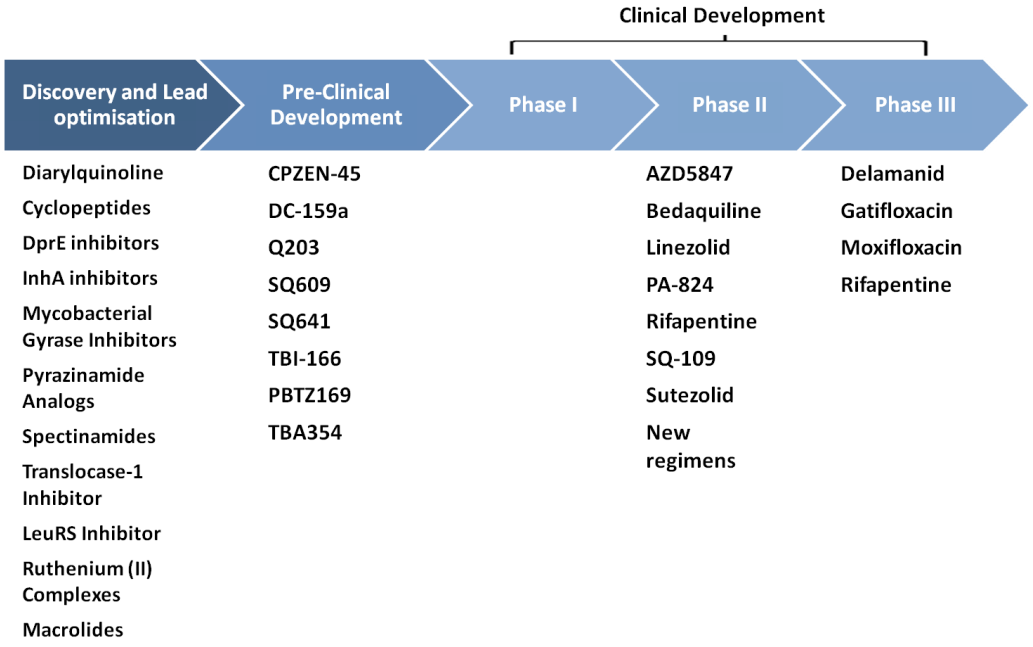

Figure 1.2: Global TB Drug Pipeline -Adapted from Working Group, Stop TB partnership on www.newtbdrugs.com

1.3.1 Drugs in DOTS

1.3.1.1 Isoniazid

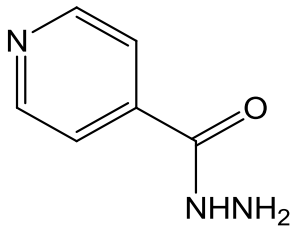

Figure 1.3: Structure of Isoniazid

Isoniazid (INH: isonicotinic acid hydrazide, Figure 1.3) is one of the most powerful drugs against TB and forms the core of anti-TB therapy. Administered as a pro-drug, it gets activated by a catalase-peroxidase *katG* (Zhang *et al.*, 1992). INH inhibits the biosynthesis of the cell wall by targeting mycolic acids (Banerjee *et al.*, 1994; Mdluli *et al.*, 1998), and shows bactericidal activity. However, it exhibits bacteriostatic activity against resting bacilli. INH was first used in anti-TB treatment in 1952 (Saltini, 2006), and it possesses very low minimum inhibitory concentration (MIC) values of ≤ 0.02 µg/mL (Zhang *et al.*, 1992) against *M. tuberculosis* H37Rv. Use of INH as an anti-TB drug initiated a global search for its target in MTB. The first contribution was made by Middlebrook in 1954 who observed that INH resistant MTB strains had a decreased catalase activity (Middlebrook and Dressler, 1954). Several years later, analysis of clinical isolates of MTB strains sensitive to INH revealed peroxidase KatG as the activator of INH (Zhang *et al.*, 1992). In the same study, 3′-deletion mutants of MTB *katG* in shuttle vectors when expressed in *E. coli* could confer susceptibility to inherently INH resistant *E. coli* that varied with the level of enzyme expressed. There are three possible targets of INH reported using independent studies. Firstly, mycolic acid biosynthesis, secondly, NAD^+ (nicotinamide dinucleotide) metabolism through

interference of NADH dehydrogenase II (Ndh II), and thirdly, pyridoxal phosphate metabolism (Lee *et al.*, 2001). Mycolic acid biosynthesis is widely accepted as the primary target (Banerjee *et al.*, 1994; Kremer *et al.*, 2003; Winder and Collins, 1970). Resistance to INH is observed in *M. smegmatis* when the enoyl-ACP reductase, InhA is over-expressed (Marrakchi *et al.*, 2000). Similar effects are observed in clinical isolates of *M. tuberculosis* with a Ser94Ala mutation in InhA (Morlock *et al.*, 2003). In normal metabolism, mycolic acids are reduced by InhA using NADH as a co-factor. However in the presence of INH, NAD complexes with INH, to form an isonicotinic acyl radical and generates an INH-NAD adduct that interacts with InhA and impedes the reduction of mycolic acids (Broussy *et al.*, 2003; Rozwarski *et al.*, 1998). This inhibitory effect is hindered in the protein with a Ser94Ala mutation, and results in resistance to INH (Pantano *et al.*, 2002). Another set of mutations that contribute to INH resistance have been isolated in the β-ketoacyl-ACP synthase KasA, that elongates the meromycolate chain (Kremer *et al.*, 2000). Mutations that confer resistance to INH due to over-expression of KasA have been isolated (Mdluli *et al.*, 1996), however, *in vitro* studies on the other hand have demonstrated that activated INH does not inhibit KasA and its over-expression has no effect on the MIC of INH (Choi *et al.*, 2000; Kremer *et al.*, 2000; Larsen *et al.*, 2002).

1.3.1.2 Rifampicin

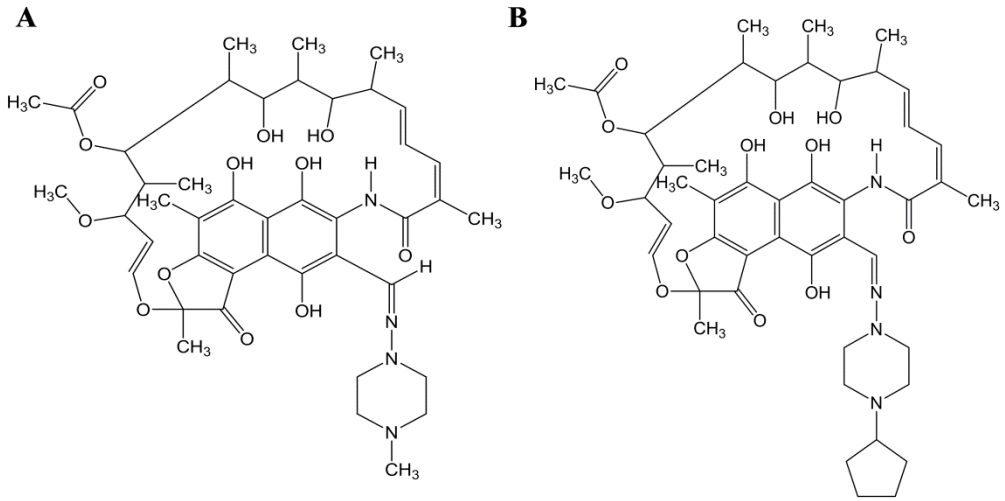

Figure 1.4: Structure of A. Rifampicin and B. Rifapentine

Rifampicin or rifampin (RIF, Fig 1.4 A) targets the β-subunit of RNA polymerase (RpoB) thereby inhibiting transcription. This antibiotic has effective bactericidal activity against actively dividing and non-dividing bacilli. Mutations occurring in the 81 bp region of the target gene *rpoB* results in resistance to RIF (Taniguchi *et al.*, 1996). The most suitable dose of RIF has never been determined and currently 600 mg *per* day is prescribed for TB treatment (Steingart *et al.*, 2011; Van Ingen *et al.*, 2011). A HIGHRIF trial is an initiative to establish the optimum concentration of RIF, both in terms of efficacy against the bacilli and tolerance by the host. An improvement over RIF is rifapentine (Fig 1.4 B) that has a similar mechanism of inhibition as RIF but a longer half-life. This characteristic gives a significant advantage to rifapentine, as its inclusion in TB therapy as a replacement for RIF could aid in shortening therapy (Udwadia, 2012).

1.3.1.3 Pyrazinamide

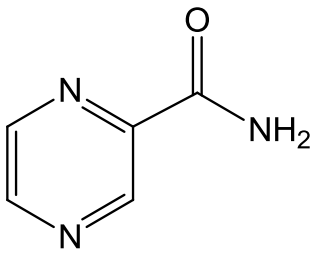

Figure 1.5: Structure of Pyrazinamide

Pyrazinamide (PZA: pyrazinoic acid amide, Fig 1.5) is highly specific to mycobacteria and displays activity against both latent and persistent bacilli. Introduction of PZA to the DOTS regimen was a turning point in TB chemotherapy as the duration of therapy was then reduced from nine to six months. The mechanism of action of PZA is still unclear. Earlier hypothesis suggested by Scorpio and Zhang *et. al.* illustrate PZA as a prodrug that is activated by mycobacterial pyrazinamidase PncA (Scorpio and Zhang, 1996). PZA is easily diffusible through the cell wall and gets converted into its non-diffusible active form pyrazinoic acid (POA) in the cytosol. The weakly acidic non diffusible POA accumulates in cytosol and supplements enough protons to create an imbalance in the proton gradient across the membrane (Zhang and Mitchison, 2003; Zhang *et al.*, 2003b). This imbalance disrupts the membrane energetics which proves lethal for mycobacteria. However, an alternative mechanism was recently proposed by (Shi *et al.*, 2011)) that purported PZA to inhibit *trans*-translation by bindng to RpsA. RpsA-PZA complex prevents the binding of RpsA to tmRNA and impedes the core mechanism responsible for tagging damaged proteins for proteolysis and rescuing stalled ribosomes. Inhibition of this process by PZA renders the ribosomes unavailable for cellular function and is particularly detrimental for latent TB bacilli where

ribosomes are already in short supply (Shi *et al.*, 2011). These findings have questioned PZA's status as a prodrug and have revealed RpsA and the *trans*-translation machinery as an appealing target for developing novel therapeutics against TB.

1.3.1.4 Ethambutol

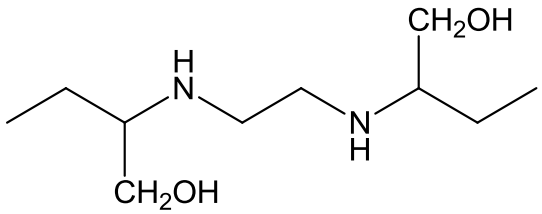

Figure 1.6: Structure of Ethambutol

Ethambutol (EMB: (2,2(ethylenediimino)di-1-butanol, Figure 1.6) is a bacteriostatic agent that targets the synthesis of the arabinan component of arabinogalactan (AG) in the mycobacterial cell wall. The anti-mycobacterial activity of EMB was first reported in 1961 (Thomas *et al.*, 1961) which led to its inclusion in the DOTS regimen. Since the drug forms the most vulnerable component of DOTS, several of its analogues and replacements are currently being tested (Protopopova *et al.*, 2005). The mode of action and mechanisms of resistance to EMB are only partially understood. EMB targets AG biosynthesis by inhibiting the glycosyltransferases encoded by *embCAB* operon (Belanger *et al.*, 1996; Telenti *et al.*, 1997), in particular EmbB (Alcaide *et al.*, 1997; Mikusova *et al.*, 1995; Sreevatsan *et al.*, 1997).

Genome sequence analysis of EMB resistant clinical isolates illustrated an EMB resistance determining region (ERDR) in the gene *embB* (Alcaide *et al.*, 1997; Telenti *et al.*, 1997) to harbor missense mutations in codon 306 that resulted in Met306Leu,

Met306Val or Met306Ile substitutions in 68-70% of the EMB resistant clinical isolates (Ramaswamy *et al.*, 2000; Sreevatsan *et al.*, 1997). These findings branded codon 306 as a molecular marker for EMB resistance. However, it is also implicated that mutations in codon 306 could alter the drug-enzyme interaction and mediate resistance against the drug (Sreevatsan *et al.*, 1997).

Treatment of mycobacteria with EMB causes accumulation of decaprenyl-phospho-arabinose (DPA), the sole arabinose donor employed for production of the arabinan component of AG and lipoarabinomannan (LAM). The drug causes bacteria to synthesise modified LAMs with decreased arabinose content and AG is completely devoid of the arabinan component (Mikusova *et al.*, 1995). Consequently, accumulation of mycolates, such as trehalose mono- and dimycolates is observed as these mycolic acid esters that are otherwise attached to terminal arabinose (Ara) residues of AG are unable to be deposited into the defective AG polymer that is synthesised in presence of EMB (Wolucka *et al.*, 1994). Lack of mycolates in the cell wall reduces its impermeability and makes the bacteria more susceptible to drugs. Therefore, EMB when administered along with other drugs of the DOTS therapy increases the effectiveness of these drugs.

1.3.1.5 Streptomycin

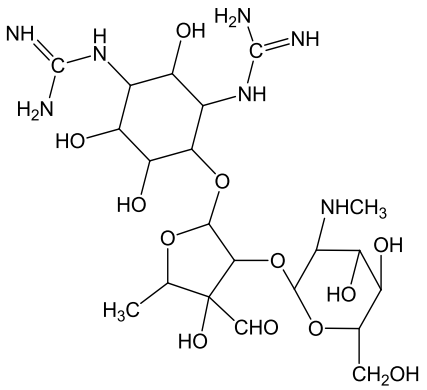

Figure 1.7: Structure of Streptomycin

Streptomycin (SM, Figure 1.7) an aminoglycoside obtained from *Streptomyces griseus*, inhibits translation by binding to 16S rRNA of the 30S subunit of the bacterial ribosome, therefore preventing the binding of formyl-methionine tRNA to the 30S subunit. The drug has bactericidal activity when consumed in large doses and shows bacteriostatic effects when a low dosage is given. SM was the first antibiotic proven to have anti-mycobacterial activity and was introduced for TB treatment over 70 years ago. The effectiveness of SM lasts for up to the first three months of therapy and reduces thereafter as the bacteria starts to develop resistance to the antibiotic (Marshall, 1949). The development of resistance to the antibiotic in a short duration led to a realisation that the problem of TB can only be tackled with use of a cocktail of drugs. SM is included as a second line anti-TB drug and administered only in cases of failure of infection and response to first-line drugs.

1.3.1.6 Ethionamide

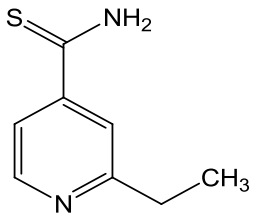

Figure 1.8: Structure of Ethionamide

Ethionamide (ETH, 2-ethylthioisonicotinamide, Figure 1.8) is a bacteriostatic anti-mycobacterial agent that was discovered in 1956 and employed in the treatment of TB in 1961. ETH is a structural analogue of INH and inhibits mycolic acid biosynthesis (Winder *et al.*, 1971) with a different mode of action to INH. Mutations that confer resistance to ETH have been associated with gene loci *ethA* and *inhA* (Banerjee *et al.*, 1994; Morlock *et al.*, 2003). Lack of cross-resistance between INH and ETH in clinical isolates of mycobacteria, especially ones with mutations in *katG* led to the idea of ETH being a *pro*-drug requiring an alternative enzyme to KatG for its activation (Baulard *et al.*, 2000; Debarber *et al.*, 2000). The mode of action of ETH became clearer when isolates of MTB with mutations in EthA, a flavin monooxygenase encoded by *Rv3854c* (*ethA* or *etaA*) were found to be resistant to ETH (Debarber *et al.*, 2000; Morlock *et al.*, 2003). Based on over-expression studies, EthA was designated as the activator of the *pro*-drug ETH (Banerjee *et al.*, 1994; Debarber *et al.*, 2000). The enzyme EthR (EtaR, *etaR* or *ethR*) encoded by *Rv3855* downstream of *ethA*, was hypothesised to be responsible for the negative regulation of EthA synthesis as its over-expression led to an increase in resistance to ETH (Baulard *et al.*, 2000; Debarber *et al.*, 2000). Genetic knockout experiments in *M. bovis* BCG confirmed EthR as the transcriptional repressor of EthA (Baulard *et al.*, 2000), as its inactivation resulted in hypersensitivity to the

drug. Sequence analysis of EthR highlighted its high similarity to members of the TetR family of transcriptional repressors (Baulard *et al.*, 2000; Debarber *et al.*, 2000). ETH is oxidised at the sulphide group by EthA to generate the corresponding S-oxide. This S-oxide is further oxidised by EthA to yield 2-ethyl-4-aminopyridine. The intermediary S-oxide is highly toxic to mycobacteria, but the final product 2-ethyl-4-aminopyridine is devoid of any anti-mycobacterial properties (Vannelli *et al.*, 2002). Studies conducted in various species of mycobacteria have also reported that ETH targets InhA similar to INH and inhibits biosynthesis of mycolic acids in mycobacteria (Banerjee *et al.*, 1994; Baulard *et al.*, 2000)

1.3.1.7 *Para*-aminosalicylic acid

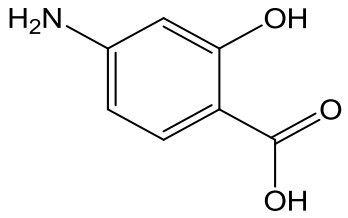

Figure 1.9: *p*-aminosalicylic acid

Para-aminosalicylic acid (PAS, Figure 1.9) is a bacteriostatic agent that was introduced for the treatment of TB alongside SM and INH as a first-line drug in the earliest of all regimens practiced. However, due to harmful side-effects and the inclusion of more potent drugs, such as RIF, PAS was removed as a first-line agent and incorporated into second-line drug regimens. PAS is now used for treatment of MDR-TB and XDR-TB (Rengarajan *et al.*, 2004). The mechanism of action of PAS has not been elucidated yet and the target is still unknown. However, recently analysed isolates of MTB and transposon mutagenesis of genes in *M. bovis* BCG

revealed mutations in the thymidylate synthase (*thyA*) an enzyme responsible for regulating intracellular folate levels, that either result in reduced levels of ThyA or a decrease in activity of the enzyme play a crucial role in imparting resistance to the drug (Rengarajan *et al.*, 2004). Interestingly, mutations in ThyA also account for resistance to other drugs that inhibit folate synthesis. PAS is hypothesised to work as an inhibitor of enzyme dihydropteroate synthase due to its close structural similarity to the actual substrate, *para*-amino benzoic acid (Iwainsky, 1988). However, *in vitro* studies that evaluated the inhibitory effect of PAS, were unable to deduce notable PAS activity implying that PAS may function as a pro-drug and gets activated inside the cell (Chakraborty *et al.*, 2013). The use of PAS is limited to MDR-TB and XDR-TB, due to its harmful side effects mainly in the gastro-intestinal tract.

1.3.1.8 Fluoroquinolones

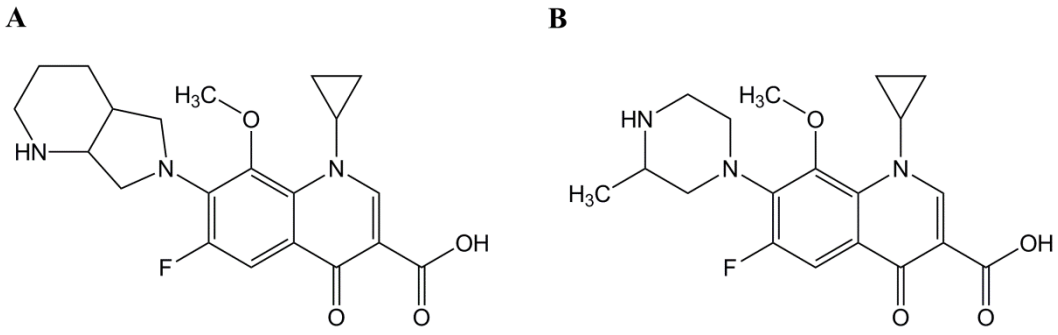

Figure 1.10: Structure of fluoroquinolones A. Moxifloxacin **B.** Gatifloxacin

Antimicrobials, such as ciprofloxacin, gatifloxacin, levofloxacin, moxifloxacin and ofloxacin belong to a single group of broad-spectrum antibiotics referred to as fluoroquinolones (FQs). FQs are routinely prescribed in case of infections and are administered as second-line drugs for MDR-TB treatment. This group of anti-microbials target DNA gyrase, a type II topoisomerase consisting of two subunits that

are encoded by *gyrA* and *gyrB* (Takiff *et al.*, 1994). Mutations occur frequently in the quniolone resistance determining region (QRDR) of *gyrA*, mainly in codons 90, 91 and 94, and less frequently in the *gyrB* (Alangaden *et al.*, 1995; Ginsburg *et al.*, 2005; Takiff *et al.*, 1994). Recently, studies in mouse models employing FQs as part of a first-line regimen have demonstrated that these anti-microbials can effectively reduce the duration of chemotherapy by two months (Nuermberger *et al.*, 2004), thus highlighting their potential usefulness as first-line agents. Efforts are currently underway to test new regimens with moxifloxacin (Fig 1.10 A) as a replacement of EMB or INH, and gatifloxacin (Fig 1.10 B) as a substitute for EMB (Skovierova *et al.*, 2010). In addition, new inhibitors that target either the DNA gyrase and/or are based on FQs are currently being developed.

1.3.1.9 Aminoglycosides

Alongside SM, other aminoglycosides, such as capreomycin, kanamycin and amikacin are second-line drugs prescribed for the treatment of drug-resistant TB. These antibiotics are verified inhibitors of protein translation and are not used as first-line agents due to a problem of cross-resistance (Alangaden *et al.*, 1998; Maus *et al.*, 2005a). The resistance to all aminoglycosides can occur due to mutations in 16S rRNA (*rrs*), however mutations in *tlyA*, a rRNA methyltransferase are also accountable for capreomycin resistance (Alangaden *et al.*, 1998; Johansen *et al.*, 2006; Maus *et al.*, 2005b; Via *et al.*, 2010). Methylation by TlyA enhances the effect of capreomycin, whereas mutations in TlyA that prevent methylation of rRNA render capreomycin ineffective. Methylation of rRNA is a mechanism used by aminoglycoside producing bacteria to become resistant to their own metabolites.

However, in case of capreomycin the effect is reversed as methylation assists in its action.

1.3.2 New TB Drugs

The problem of emerging drug resistance in MTB has highlighted the need of new drugs, vaccines and treatment regimens. Recently, a multitude of compounds with anti-tubercular activity have been generated with combined efforts of industry and academia, and several of these compounds have emerged as promising drug candidates. These efforts have led to the formulation of a drug pipeline (Fig 1.2), depicting the state of development for each of compound with potential to be an anti-TB drug in the near future.

The drug pipeline holds immense promise in terms of new compounds with a prospect of future anti-TB drugs. However, there is an extensive lag between the pre-clinical and clinical stages, as most of the new compounds are either being evaluated for safe use or are rejected owing to toxic effects. This is a grave problem that requires immediate attention and considerable efforts to bridge the existing gap and increasing the likelihood of the candidates for successful progression to the clinical stage.

1.3.2.1 Clofazimine

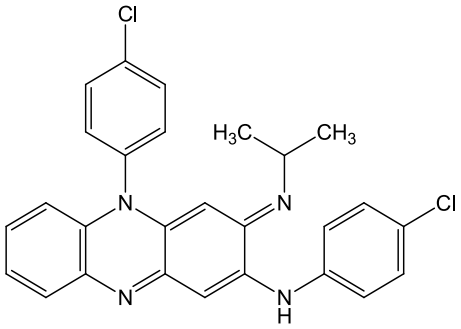

Figure 1.11: Structure of Clofazimine

Clofazimine (Figure 1.11) is a hydrophobic riminophenazine antibiotic discovered in 1957 (Barry *et al.*, 1957) and employed for the treatment of leprosy in 1962. The hydrophobic and anti-inflammatory properties of clofazimine makes it ideal for the treatment of leprosy as it accumulates in the nerves and skin, which are the main sites of *M. leprae* infection, and also prevents adverse immune reactions, thereby evading the complications that may arise in chemotherapy (Anderson, 1983; Dutta, 1980; Imkamp, 1981). Clofazimine is currently a part of a three-drug regimen along with RIF and dapsone for the treatment of leprosy as advised by WHO. Although clofazimine is inactive against pulmonary TB, its lipophilicity and anti-inflammatory properties have found their use in formulation of new riminophenazine based compounds with a novel mechanism of action. Clofazimine and drugs based on clofazimine may prove useful in the treatment of HIV individuals with suppressed immune system, especially in tackling immune reconstitution inflammatory syndrome (IRIS) (Cholo *et al.*, 2012).

1.3.2.2 Oxazolindinones

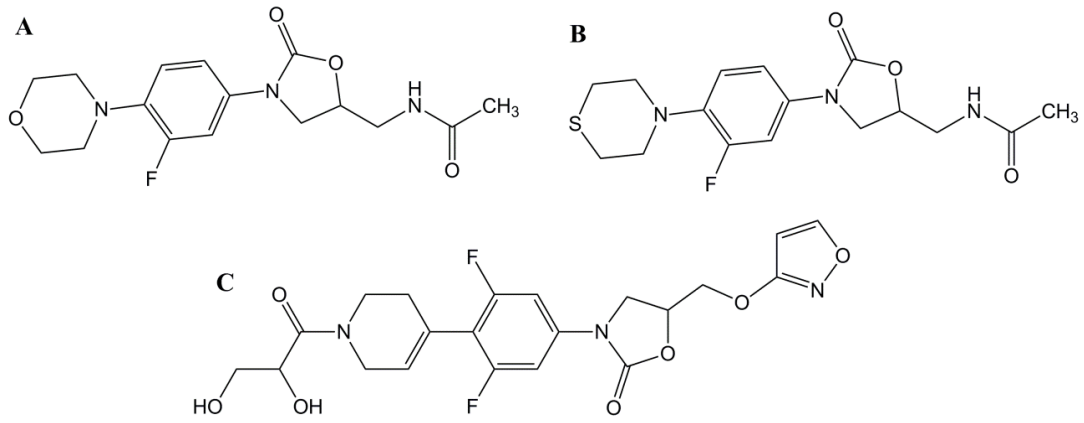

Figure 1.12: Structure of oxazolindinones A. Linezolid **B**. Sutezolid **C.** AZD5847

Oxazolindinones are a class of drugs that inhibit protein synthesis by binding to the 23S subunit of the ribosome. Linezolid (Figure 1.12 A) is a drug from this class with bacteriostatic activity against TB bacilli and also shows activity against MDR-TB (Fortun *et al.*, 2005; Lee *et al.*, 2012b). Resistance to linezolid could develop if mutations arise either in *rplC* or in 23S rRNA (Lee *et al.*, 2012b), that disturb the *van der waal* forces of interaction responsible for arrangement of a functional ribosome. The drawback of linezolid is its ability to damage nerves and cause bone marrow suppression when administered to patients (Sotgiu *et al.*, 2012). Linezolid is recommended for patients suffering from MDR-TB and should be prescribed with caution. The toxic effects of linezolid have led to development of structural analogues that are currently being examined for their anti-mycobacterial activity. Sutezolid (PNU-100480, Figure 1.12 B) is a more potent analogue of linezolid that is currently in Phase II clinical trials and has been tested for its effectiveness in conjuction with TMC207/SQ109 and PA824 (Wallis *et al.*, 2012; Wallis *et al.*, 2010). Trials with sutezolid and SQ109/TMC207 combination produced additive effects, whereas

deleterious or not significantly beneficial effects were observed with PA824 rendering it unsuitable for use with PA824 (Wallis *et al.*, 2010). AZD5847 (Figure 1.12 C) is not an analogue of linezolid, but has similar mode of action to linezolid. The drug-drug interaction studies with AZD5847 have yielded no interference and the compound has progressed to Phase II clinical trials (Zumla *et al.*, 2013).

1.3.2.3 Nitroimidazoles

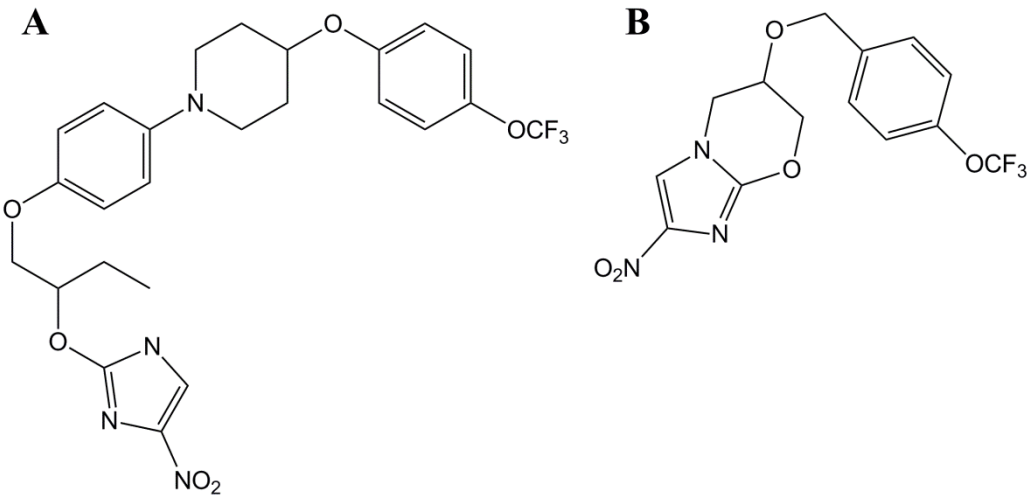

Figure 1.13: Structure of nitroimidazoles A. Delamanid **B.** PA-824

Nitroimidazoles are a class of antibiotics used for the treatment of anaerobic infections. This property of nitroimidazoles has implicated their use in treatment of latent TB infections (Migliori *et al.*, 2013). Delamanid (OPC67683, Fig 1.13 A) and PA824 (Fig 1.13 B) are leading nitroimidazoles, with Delamanid being the most recently licensed drug to be used for treatment of MDR-TB. Both, delamanid and PA824 are *pro*-drugs that require intracellular activation (Manjunatha *et al.*, 2006a). Delamanid (nitrodihydroimidazooxazole) is an inhibitor of mycolic acid biosynthesis in mycobacteria (Matsumoto *et al.*, 2006). Delamanid is activated by the enzyme Ddn, a nitroreductase that utilises deazaflavin as a coenzyme. This enzyme is specific for

MTB and is absent in *M. leprae (Manjunatha et al., 2006b).* Mutations in *ddn* or in genes for deazaflavin synthesis can lead to the development of resistance in bacteria against delamanid (Arora *et al.*, 2011; Manjunatha *et al.*, 2006a; Manjunatha *et al.*, 2006b). In addition to inhibition of mycolic acid biosynthesis, delamanid is proposed to kill mycobacteria by overproduction of DNA damaging free radicals (Hurdle *et al.*, 2008; Singh *et al.*, 2008). The chemical nature of these free radicals has not been determined but their production is attributed to des-nitro-imidazooxazole that is generated as a result of the reduction process. PA824 is similar to delamanid as it also requires activation by Ddn. The active form of PA824 is a reactive nitrogen species, including nitric oxide. These harmful radicals lead to cellular toxicity that ultimately kills the bacteria. Resistance to PA824 can develop if synthesis of the Coenzyme is inhibited as it inactivates Ddn (Lin *et al.*, 2012). PA824 also inhibits mycolic acid biosynthesis in mycobacteria but in aerobic conditions. In the absence of oxygen, cellular toxicity is mediated by inhibition of Cytochrome C oxidase by nitric oxide (Manjunatha *et al.*, 2006a).

1.3.2.4 Diarylquinolones

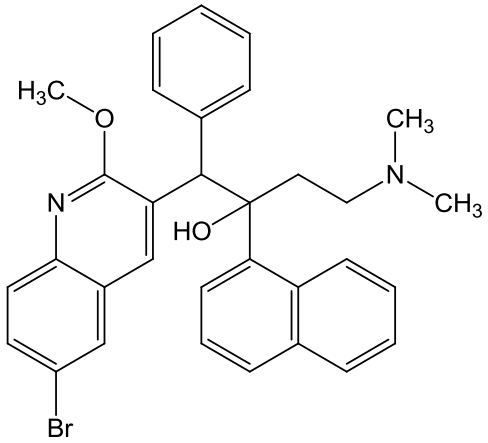

Figure 1.14: Structure of Bedaquiline

Bedaquiline or sirturo (TMC207, Figure 1.14) a diarylquinolone, is a new inclusion in DOTS therapy, the first in 40 years. Whole genome sequencing of bedaquiline resistant mutants revealed that missense mutations in *atpE* resulted in Asp32Val and Ala63Pro substitutions in the ε-subunit of the ATP synthase (Andries *et al.*, 2005; Huitric *et al.*, 2010). Bedaquiline inhibits the synthesis of ATP as it binds the ε-subunit, thus disturbing the association between the ε-subunit and the C-ring of the ATP synthase (Koul *et al.*, 2007). This leads to energy deficiency in cells and disturbs the proton gradient across the membrane. The target ATP synthase is common to both mycobacteria and humans but differ in terms of sensitivity to bedaquiline, as the human ATP synthase is 20,000-fold less sensitive to the drug (Haagsma *et al.*, 2009). Bedaquiline has several advantages including action against both active and latent forms of TB infection, a very long half-life and significantly low levels of MIC in comparison to INH and RIF when used for the treatment of MDR-TB strains (Huitric *et al.*, 2010; Veziris *et al.*, 2009).

1.3.2.5 SQ109 and EMB analogues

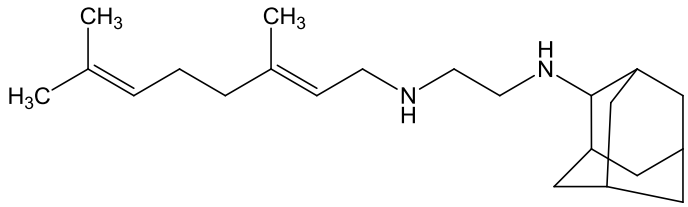

Figure 1.15 Structure of SQ109

One of the major candidates that could be introduced for therapy against TB in the near future includes EMB analogues. EMB, is among the foremost chemotherapeutic that targets proteins in AG biosynthesis (Takayama and Kilburn, 1989). Using combinatorial chemistry, EMB derivatives have been synthesised, of which NIH241 and SQ109 are the most promising. SQ109,[N-(2-adamantyl)-N-[(2E)-3,7-dimethylocta-2,6-dienyl]ethane-1,2-diamine] (Figure 1.15), has low cytotoxicity and better *in vivo* efficacy against MTB than EMB (Protopopova *et al.*, 2005). The EMB-like diaminated compound SQ109, possess very efficient anti-mycobacterial activity and is effective against MDR-TB strains. SQ109 accumulates in the lungs, at the site of TB infection. The mechanism of action of SQ109 is considered to be different to EMB, as neither the EMB resistant nor MDR strains of MTB show any cross-resistance to SQ109 (Sacksteder *et al.*, 2012). Recently, it has been reported that SQ109 acts by preventing the incorporation of mycolic acids into the cell wall by inhibiting a trehalose monomycolate (TMM) transporter MmpL3, without altering the total cellular mycolic acid levels (Tahlan *et al.*, 2012). The total mycolate levels are maintained in the cell since the reduction in trehalose dimycolate (TDM) levels leads to a corresponding increase in TMM levels, once TMM transport is stalled in presence of the drug. However, since the study did not use any direct spontaneous mutants

against the drug, it is likely that the compound has secondary targets or inhibits the protein by binding to essential residues critical for function and survival.

The safety profile of SQ109 has been established and it is a well-tolerated drug with a long plasma half-life. SQ109 has progressed to Phase II clinical trials (Ginsberg). Strong synergistic activity with bedaquiline, INH and RIF renders SQ109 a promising new drug to reduce the duration of TB treatment (Nikonenko *et al.*, 2007). The highly synergistic effects of SQ109 and bedaquiline can be attributed to the function of SQ109 to weaken the cell wall by inhibiting the deposition of mycolates thereby allowing easy access to the ATP synthase for bedaquiline. This combination therapy is currently being investigated in Phase II clinical trials. SQ109 has a narrow spectrum, being active against *M. tuberculosis, M. bovis, M. smegmatis* and *M. avium.*

1.3.2.6 Benzothiazinones and dinitrobenzamides

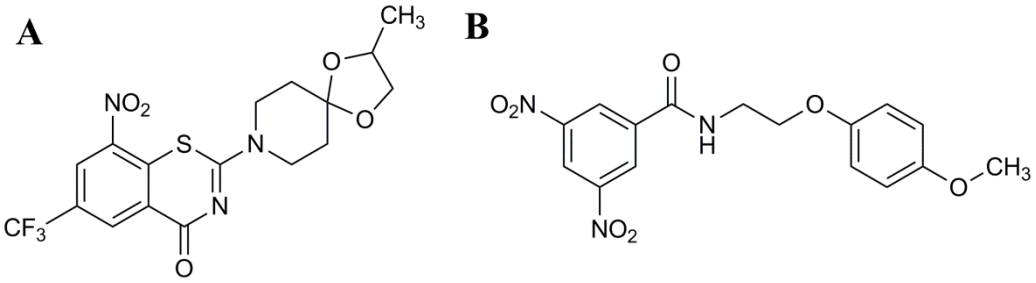

Figure 1.16: Structure of A. Benzothiazinone lead compound BTZ043 and B. Dinitrobenzamide lead compound DNB1

Discovered under the "New Medicines for TB", European consortium project, the sulphur-containing heterocycles benzothiazinones (BTZ or 1,4 dioxa-8-azaspiro[4.5]dec-8-yl-8-nitro-6-(trifluoromethyl)-4H-1,3-benzothiazin-4-one) is a novel and highly potent anti-mycobacterial agent. The lead compound of the series is

BTZ043 (Fig 1.16 A) (Makarov *et al.*, 2006). BTZ targets the enzyme decaprenyl-phosphoryl-β-D-ribose epimerase, encoded by *dprE1* (*Rv3790*) and *dprE2* (*Rv3791*), responsible for epimerisation of DPR to DPA (Christophe *et al.*, 2009; Makarov *et al.*, 2009; Mikusova *et al.*, 2005). The lipid based sugar donor, DPA is a precursor molecule supplying arabinofuranose residues to AG and LAM (Mikusova *et al.*, 2005; Wolucka, 2008). *Rv3790* is highly conserved in orthologous genes from various actinomycetales, including *NCgl0187* in *C. glutamicum* (Meniche *et al.*, 2008)

BTZs are bactericidal and reduce bacterial activity by more than 1000-fold in less than 72 hours (Makarov *et al.*, 2009). The compound targets active cellular metabolism and causes the bacteria to swell before lysis. The compounds display very low MICs for the MTB complex (1-30 ng/mL) and for fast-growing *Mycobacterium* species (0.1-80 ng/mL) (Makarov *et al.*, 2009). They are relatively non-toxic (Makarov *et al.*, 2009) and have high potency for MDR-TB and XDR-TB strains (Pasca *et al.*, 2010).

The target of BTZ was determined through analysis of spontaneous resistant mutants of *M. smegmatis* and *M. tuberculosis* to BTZ. The resistant strains were found to harbor a mis-sense mutation in *MSMEG_6382* and *Rv3790*. These mutants showed a Cys387 conversion to either Ser/Gly and the MICs increased by 250-10,000 fold, respectively (Makarov *et al.*, 2009). Interestingly, *M. avium* and *M. aurum* are naturally resistant to BTZs, as Cys387 residue is naturally substituted by Ser/Ala. These findings suggest that BTZs target DprE1 at the Cys387 residue, which abolishes the oxidase activity of the enzyme (Makarov *et al.*, 2009). The nitro-group of BTZ is proposed to be reduced to a nitroso-group by the action of DprE1. The nitroso-group forms a semi-mercaptal linkage to the conserved cystine residue (Cys387) in the active site of the enzyme, thus rendering it non-functional (Trefzer *et al.*, 2010; Trefzer *et al.*, 2012). Therefore, BTZs

are also classified as suicide substrates for the FAD dependant DprE1 enzyme (Trefzer *et al.*, 2012).

Dinitrobenzamides (DNBs, Figure 1.16 B) are nitro-compounds that target decaprenylphosphoryl-β-D-ribose 2' epimerase similar to BTZs (Christophe *et al.*, 2009; Makarov *et al.*, 2009). They were identified as potent anti-TB compounds from a library of compounds screened using fluorescence microscopy (Christophe *et al.*, 2009). DNBs exhibit a similar mechanism of action to BTZ as it undergoes reduction by DprE1 (Trefzer *et al.*, 2010; Trefzer *et al.*, 2012). Recent studies have demonstrated that mis-sense mutations in Cys387 can confer resistance to both drugs (Christophe *et al.*, 2009; Makarov *et al.*, 2009). BTZs and DNBs can also be inactivated by the nitroreductase NfnB in *M. smegmatis* (Manina *et al.*, 2010). While orthologues of *nfnB* are absent in MTB, its presence in eukaryotes questions the efficacy of BTZ and DNB as anti-TB drugs (Manina *et al.*, 2010). The lead compound BTZ043 is in late stages of pre-clinical trials and has successfully demonstrated high bactericidal activity against MDR-TB strains, thus paving way for the clinical trials (Pasca *et al.*, 2010). The vulnerability of DprE1 to antimycobacterial agents, such as DNBs and BTZs and its essentiality in various mycobacterial species, highlights its potential as a suitable target for development of new therapeutics.

1.4 The mycobacterial cell wall

The cell envelope of mycobacteria is critical as it imparts high resistance and tolerance to several anti-mycobacterial agents and also contributes towards the patho-physiological properties of the bacteria. Electron microscopic studies revealed that the cell envelope of mycobacteria consists of four components: an innermost layer of plasma membrane, consecutively three distinct layers of peptidoglycan (PG), a third layer of low electron density comprising AG and an outermost asymmetric layer of mycolic acids, phospholipids and glycolipids. Of these four components, PG, AG, mycolic acids and other lipids form the core of the mycobacterial cell wall. The classic chemotype IV cell wall of MTB comprises of PG; an insoluble matrix of alternating N-glycolated muramic acid and N-acetyl glucosamine acid residues that are cross-linked by *meso*-diamonopimelic acid (Severn *et al.*, 1998). This thickly cross-linked PG layer is in turn attached to a unique polysaccharide; AG decorated with long chain fatty acids, termed mycolic acids at its distal ends (Vilkas and Lederer, 1956). Many unusual free soluble lipids, which are non-covalently linked to the cell envelope, also exist, of which, trehalose-based lipooligosaccharides (LOS) and lipoarabinomannan (LAM) (Khoo *et al.*, 1995b), are the most significant ones. Together, these components form an asymmetric bilayer of exceptional thickness. The cell wall also consists of protein channels called porins to allow the passage of the hydrophilic solutes including inhibitors and nutrients.

The structural features and distribution of cell wall components and its effects on fluidity have been described in a model proposed by (Minnikin *et al.*, 2002)) as illustrated in Figure 1.17. This model suggests that the cell wall consist of two layers; an outer layer of extractable lipids which includes the LOSs, glycopeptidolipids and

phenolic glycolipids and an inner layer consisting of mycolic acids which are perpendicularly arranged to the plane of the cell surface. Together, these two layers impart an asymmetric appearance and variable fluidity to the cell wall. The entire packaging of the cell wall is responsible for providing a highly effective permeability barrier that can only be distorted by adding surfactants. Due to the permeability barrier MTB is resistant to common antibiotics, therapeutics, alkali and disinfectants, while sensitive to aminoglycosides, RIF, FQ, ETH, PZA, PAS and EMB like antimicrobials (Birch *et al.*, 2010; Chatterjee *et al.*, 1991).

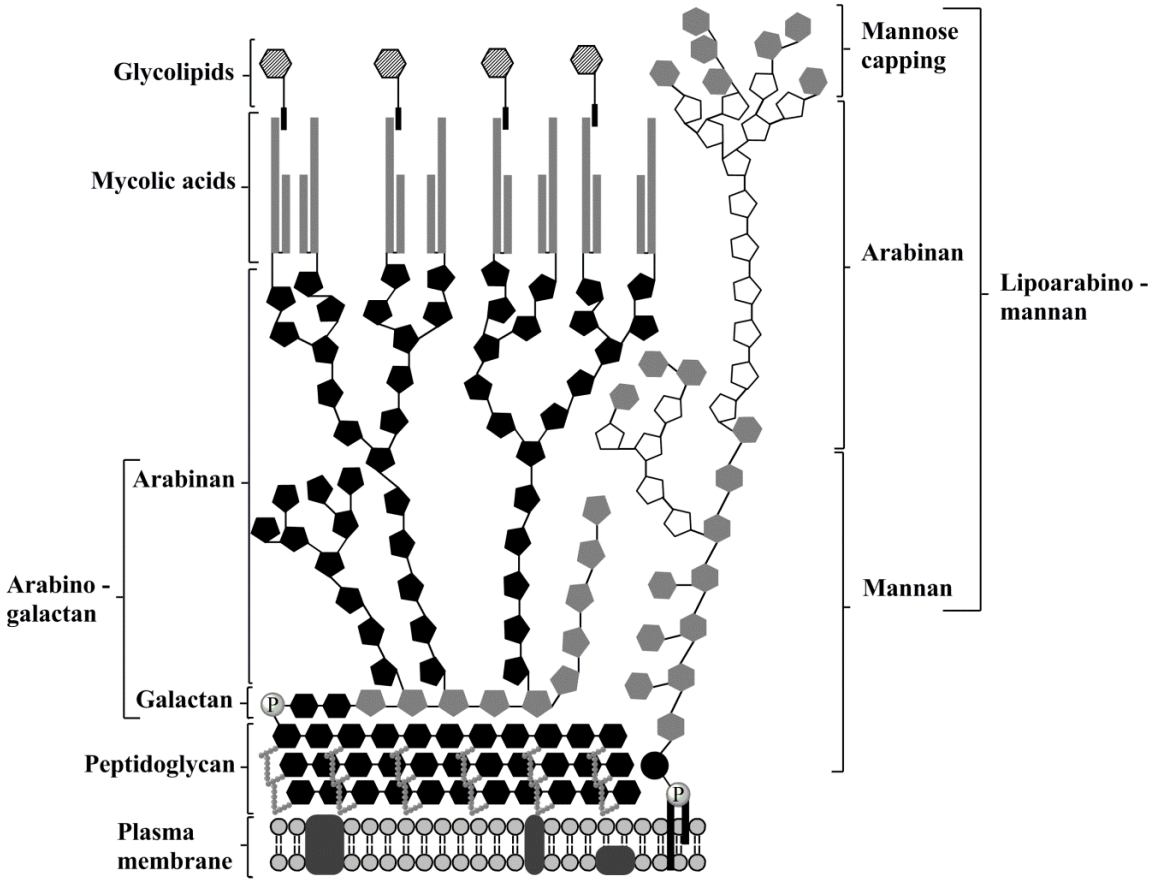

Figure 1.17: Structural features of mycobacterial cell wall. The cell wall of *M. tuberculosis* consists of an inner-most layer of plasma membrane, a middle layer of cell wall core consisting of the components; peptidoglycan (PG), arabinogalactan (AG) comprising of arabinan and galactan and mycolates which extend to the outer layer of the cell envelope.The plasma membrane is also linked to lipoarabinomannan (LAM) formed of mannan and arabinan, capped with mannose residues which extends into the interior of cell wall. – Adapted from Grover S. & Jankute M. *et al.*, 2012.

Sixteen mycolate residues are attached at the non-reducing end of the branched arabinan motif of AG (Besra *et al.*, 1995). The galactan core of AG is linked to PG *via* a rhamnose-N-acetylglucosamine-phosphate linker unit. Together the mycolates, AG and PG are referred to as the mycolyl-arabinogalactan-peptidoglycan (mAGP) complex. The lipoglycans, LAM and LM are presumably anchored to the outer leaflet of the cell wall. The arrangement of these components in the cell wall creates a hydrophobic interior that stops hydrophilic polysaccharides and solutes from entering the cell. The various components in the cell wall are extracted for analysis based on their polarity using different solvent systems. The free lipids, proteins, LAM and PIMs get solubilised, while the mAGP complex remains in the insoluble fraction. The soluble components behave as signalling effector molecules in the disease process while the insoluble core is essential for the viability of the mycobacteria.

1.4.1 Plasma membrane

The plasma membrane of mycobacteria is asymmetrical with characteristic regions of extra thickness harbouring the carbohydrate rich phosphatidyl-inositol mannosides (PIMs), lipomannan (LM) and LAM. These soluble conjugates are one of the major structural components of the mycobacterial plasma membrane and are involved in interactions with the host-immune system. Aside the PIMs, phospholipids, such as phosphatidyl ethanolamine (PE), phosphatidyl inositol (PI), phosphatidyl glycerol and cardiolipid (CL), pol yterpene based products, glycosyl phosphopolyprenols, such as β-mannopyranosyl phosphodecaprenol (PPM), DPA and β-D-ribofuranosyl phosphodecaprenol (DPR), which are involved in cell wall biosynthesis are also hypothesised to be associated with the plasma membrane. The mycobacterial membrane is rich in PE and PI, but contains modest levels of phosphatidyl glycerol.

The genes involved in PI biosynthesis are essential in *M. smegmatis* indicating its vital role in the growth and viability of mycobacteria (Jackson *et al.*, 2000). PIs undergo extensive glycosylations to generate PIMs, LM and LAM that are unique components with a specific structural and biological role in mycobacteria including modulation of the host immune response in favour of the pathogen.

1.4.2 Peptidoglycan

The PG layer is an important component of the bacterial cell envelope. Largely consisting of alternating N-acetyl glucosamine (GlcNAc) – N-glycolated muramic acid (MurNGly) units (1984; Wietzerbin *et al.*, 1974), linked to each other *via* β-1,4 linkages, with L-alanine-D-glutamate-D-isoglutaminsyl-*meso*-diaminopimelyl (DAP)-D-alanine-D-alanine penta-peptide side chains also referred to as the stem peptide on the 4^{th} position of the muramic acid units (Goffin and Ghuysen, 2002). The cross-linking of the disaccharide unit includes a portion between two DAP residues and between DAP and D-alanine (Wietzerbin *et al.*, 1974). The biosynthesis of PG in MTB has not been investigated in detail. However, much detail has been elucidated from the PG biosynthesis pathway in *E. coli* (Van Heijenoort, 2001a; b). The first step in the synthesis of PG requires synthesis of UDP-N-acetyl muramic acid (UDP-MurNAc) from UDP-GlcNAc *via* a two step reaction catalysed by enzymes MurA (*Rv1315*) and MurB (*Rv0482*) (Belanger *et al.*, 2000; De Smet *et al.*, 1999). UDP-MurNAc thus generated is converted to UDP-MurNGly *via* a UDP-N-acetylmuramic acid hydroxylase encoded by *namH* (*Rv3818*) (Raymond *et al.*, 2005). The enzymes MurC (*Rv2152c*), MurD (*Rv2155c*), MurE (*Rv2158c*), and MurF (*Rv2157c*) are required for synthesis of the penta-peptide stem (Belanger *et al.*, 2000; Crick *et al.*, 2001; Mahapatra *et al.*, 2000). The penta-peptide synthesised on UDP-MurNGly is

transferred onto a molecule of undecaprenyl phosphate, Lipid I, *via* a translocase, MurX (*Rv2156c*). Addition of a unit of GlcNAc to Lipid I by a transferase MurG (*Rv2153c*) affords Lipid II carrying glycopeptides, which is then translocated to the periplasm for PG assembly.

1.4.3 Linker Unit

The AG component of the mAGP complex is attached to some MurNGly units of PG *via* a linker unit (LU) comprising of α-L-rhamnopyranose-(1→3)-α-D-GlcNAc-(1→P) bridge (Daffe *et al.*, 1990). Synthesis of the linker unit requires transfer of GlcNAc-1-P from UDP-GlcNAc to the lipid carrier decaprenyl monophosphate (C_{50}-P) catalysed by a UDP-GlcNAc transferase WecA (Rfe, *Rv1302*) (Mikusova *et al.*, 1996). The Rha*p* component of the LU is synthesised *via* a four-step reaction process that (Ma *et al.*, 2002) utilises the enzymes RmlA (*Rv0334*), an α-D-glucose-1-phosphate thymidylyltransferase, RmlB (*Rv3465*), a dTDP-D-glucose-4, 6-dehydratase, RmlC (*Rv3464*), a dTDP-4-keto-6-deoxy-glucose-3,5-epimerase and RmlD (*Rv3266c*), a dTDP-6-deoxy-L-lyxo-4-hexulose reductase which act sequentially to mediate the conversion of glucose-1-phosphate and thymidine-triphosphate to generate dTDP-Rha*p* (Giraud *et al.*, 2000). In the last step, the rhamnopyranosyl unit is transferred to C_{50}-P-P-GlcNAc *via* a rhamnosyltransferase, WbbL encoded by *Rv3265c* to yield C_{50}-P-P-GlcNAc-Rha (Mills *et al.*, 2004). Recent genetic and mutational studies in *M. smegmatis* have demonstrated *rmlB*, *rmlC* and *rmlD* to be essential for viability rendering the pathway for biogenesis of LU and the genes involved as attractive targets for drug devlopment (Li *et al.*, 2006; Ma *et al.*, 2002).

1.4.4 Arabinogalactan

1.4.4.1 Structure

Measuring up to 35% of the total cell wall of mycobacteria, AG is an important structural element that aids in anchoring mycolates to the PG. AG is a hetero-polysaccharide comprising of arabinose (Ara) and galactose (Gal) sugar units in furanose ring form (Mcneil *et al.*, 1987) arranged in a distinctive pattern to generate motifs (Fig 1.18) that are characteristic of the polysaccharide (Daffe *et al.*, 1990). AG rests at the centre of the mAGP complex where it is linked to mycolates at the non reducing end (Kaur *et al.*, 2009) and attached to the LU at the reducing end. The LU attaches mAG to the PG at the C-6 position of selected MurNGly residues (Mcneil *et al.*, 1990). The galactan core comprises of approximately 30 alternating β(1→5) and β(1→6) galactofuranose (Gal*f*) residues arranged linearly. The arabinan component is highly branched and built on the galactan. Each galactan core is linked to three arabinan chains of approximately 30 arabinofuranosyl (Ara*f*) residues, at the C-5 position of some β(1→6) Gal*f* residues (Bhamidi *et al.*, 2008; Daffe *et al.*, 1990). Mass spectrometric analysis of AG in *Corynebacterium glutamicum* revealed that the arabinan chains are attached at the 8^{th}, 10^{th} and 12^{th} Gal*f* residue in the galactan core (Alderwick *et al.*, 2006b). The Ara*f* residues in the backbone of arabinan core comprise of a linearly arranged α(1→5) linked α-D-Ara*f* residues with branching at the C-3 hydroxyl (Daffe *et al.*, 1990).

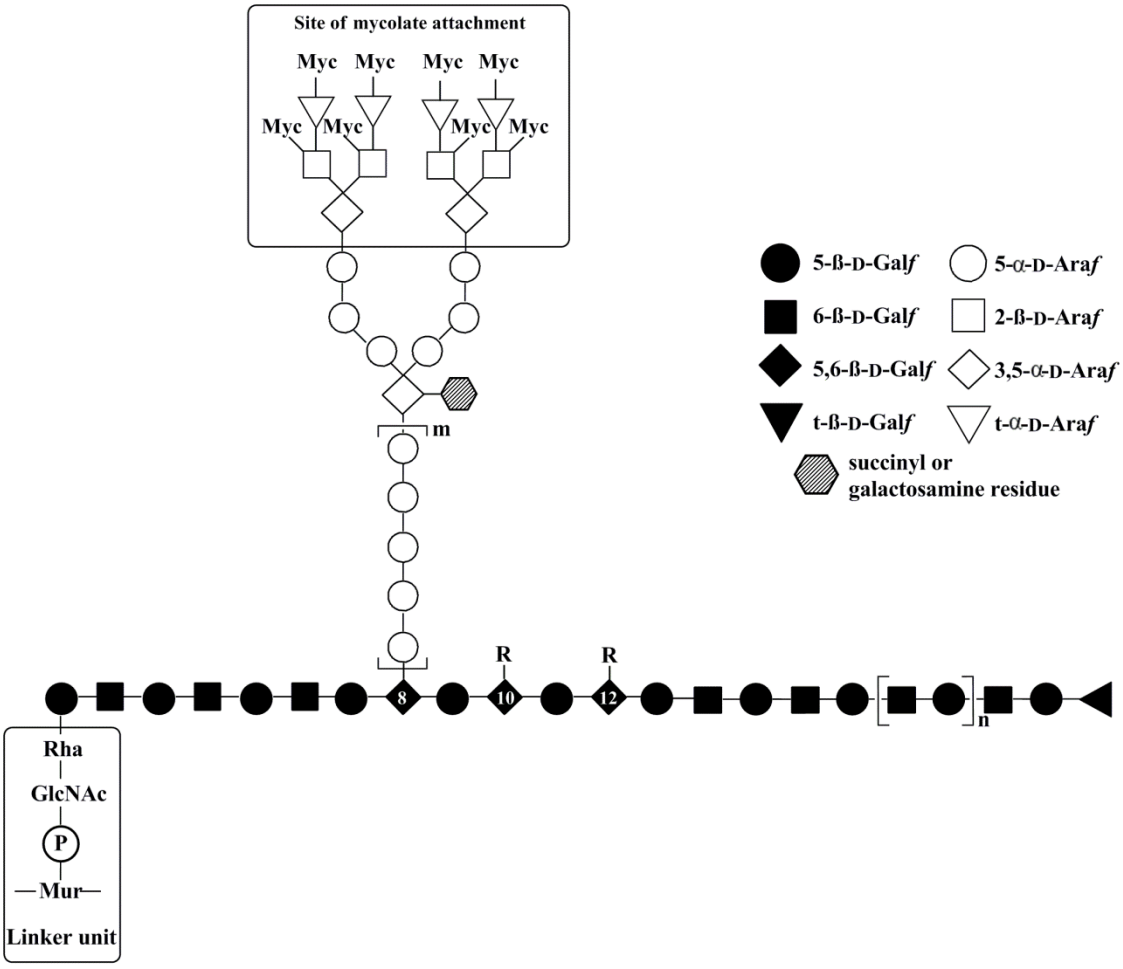

Figure 1.18: Structural features of AG. Arabinogalactan is a polysaccharide of linearly arranged galactose and highly branched arabinose residues decorated with mycolates at the distil end of arabinan domain. AG is attached to peptidoglyan *via* a rhamnopyranosyl-N-acetylglucosamine linker unit. – Adapted from Grover S. & Jankute M. *et al.,* 2012.

The non-reducing termini of arabinan structure consists of a characteristic hexa-arabinofuranosyl motif [β-D-Ara*f*-(1→2)-α-D-Ara*f*]$_2$-3,5-α-D-Ara*f*-(1→5)-α-D-Ara*f*], with mycolates attached to C-5 of both the terminal β-D-Ara*f* units and the penultimate 2-α-D-Ara*f* units (Mcneil *et al.,* 1991). Each hexa-arabinofuranosyl motif can potentially be attached to four mycolyl residues. However, only two-thirds of the total available sites get mycolated under physiological conditions (Mcneil *et al.,* 1991). The complete AG structure has a few modifications that vary from species to species. For

example slow-growing mycobacteria, such as MTB have a non-acylated galactosamine (D-GalN) residue attached to the C-2 position of some 3, 5-α-D-Ara*f* units in the core (Draper *et al.*, 1997; Lee *et al.*, 2006). In addition, the non-mycolated chains of arabinan are capped by succinyl residues (Bhamidi *et al.*, 2008), suggesting a possible negative control mechanism for mycolylation. Together, both the protonated D-GalN and the negatively charged succinates impart rigidity and stability to AG (Bhamidi *et al.*, 2008).

1.4.4.2 Biosynthesis of decaprenyl phosphoarabinose (DPA)

The furanose cyclic form of D-arabinose (Ara*f*) is a key component of both AG and LAM in mycobacteria. The sugar donor for Ara*f* is a lipid-linked decaprenyl-phospho-arabinose (DPA, C_{50}-P-Ara*f*) (Wolucka *et al.*, 1994). The majority of DPA in mycobacteria is generated by the pentose phosphate pathway (Marks, 1956). The first step of the DPA biosynthesis pathway is the formation of D-ribose-5-phosphate from sedoheptulose 7-phosphate, catalysed by *Rv1449* transketolase, and/or the isomerisation of D-ribulose 5-phosphate, catalysed by *Rv2465* D-ribose 5-phosphate isomerase (Roos *et al.*, 2004; Roos *et al.*, 2005). Subsequently, ribose 5-phosphate is converted into 5-phosphoribosyl-α-1-pyrophosphate (pRpp) (Alderwick *et al.*, 2011b), in a reaction catalysed by ribose-5-phosphate diphosphokinase (PrsA) encoded by *Rv1017c*.

The synthesis of DPA and DPR from pRpp occurs by a two-step epimerisation of DPR (Mikusova *et al.*, 2005; Scherman *et al.*, 1996). In the first step, pRpp is transferred to a decaprenyl-phosphate molecule to form decaprenylphosphoryl-β-D-5-phosphoribose (DPPR) *via* a 5-phospho-α-D-ribose-1-diphosphate: decaprenyl-phosphate-5-phospho-

ribosyltransferase, UbiA (*Rv3806c*) (Huang *et al.*, 2005). The dephosphorylation of DPPR to DPR is the first committed step of the pathway and is suggested to be catalysed by the putative phospholipid phosphatase, Rv3807. The gene *Rv3807c*, is present in the AG biosynthetic cluster (*Rv3779-Rv3809c*) and is known to encode an unknown poly-(A)-polymerase2 (PAP2)-superfamily phospholipid phosphatase. The dephosphorylated product, DPR is subsequently oxidised at 2-OH of ribose to yield decaprenylphosphoryl-2-keto-β-D-erythro-pentofuranose (DPX), which is then reduced to form DPA. DprE1 (*Rv3790*) and DprE2 (*Rv3791*) form a heteromer and catalyse the epimerisation of the ribosyl unit of DPR yielding the essential DPA donor (Mikusova *et al.*, 2005). Interestingly, recent studies have also confirmed *Rv3790* as the target of BTZs, a new class of antitubercular drugs. Besides being the Ara*f* donor for the biosynthesis of the arabinan domain in LAM, DPA also donates Ara*f* residues for the biosynthesis of AG, where the Ara*f* residues are transferred directly onto a previously generated intermediate, C_{50}-P-P-GlcNAc-Rha-Galf_{30}, utilising the only known mycobacterial Ara*f* donor DPA (Wolucka *et al.*, 1994).

1.4.4.3 Biosynthesis of arabinogalactan

The linker unit assembled on decaprenyl-phosphate functions as a primer for sequential addition of approximately 30 Gal*f* residues that are arranged in a linear fashion. The first two Gal*f* residues are added to Rha in the linker unit from UDP-Gal*f* by a galactofuranosyl transferase enzyme GlfT1 encoded by *Rv3782*. The remaining Gal*f* residues are added by a second transferase GlfT2 encoded by *Rv3808c* (Kremer *et al.*, 2001; Szczepina *et al.*, 2010). GlfT2 exhibits dual activity, as it acts both as a UDP-Gal*f*:β-D-(1→5) GalT and a UDP-Gal*f*:β-D-(1→6) GalT, and is responsible for sequentially polymerising the bulk of the galactan polysaccharide in alternating

β(1→5) and β(1→6) linkages (Kremer *et al.*, 2001). The activity of GlfT1 and GlfT2 together generates the galactan intermediate C_{50}-P-P-GlcNAc-Rha-Galf_{30} to which arabinose residues are added by arabinofuranoyltransferases (Ara*f*Ts) utilising the Ara*f* donor DPA (Wolucka *et al.*, 1994). The galactan intermediate is then primed for synthesis of the arabinan core by addition of arabinose residues from DPA onto the positions 8, 10 and 12 of the galactan chain (Figure 1.19). This reaction is catalysed by a novel α(1→5) Ara*f*T, AftA (*Rv3792*) (Alderwick *et al.*, 2006b). The arabinan chains on the primed galactan core are synthesised by several α(1→5) Ara*f*T namely, EmbA and EmbB (*Rv3794* and *Rv3795*), that are predicted to act as a heterodimer (Escuyer *et al.*, 2001) (Fig 1.19). Although, AG is a vital component of the mycobacterial cell wall, disruption of homologues of either *Rv3794* or *Rv3795* in *M. smegmatis* generates a viable mutant with an impaired AG structure (Escuyer *et al.*, 2001). Similarly, just one orthologue of the non-essential *emb* gene exists in *C. glutamicum* (Alderwick *et al.*, 2005) and its deletion results in synthesis of a truncated AG structure with only terminal Ara*f* residues (Alderwick *et al.*, 2005). A novel mycobacterial Ara*f*T, AftC (*Rv2673*), introduces α-1, 3 branches (Figure 1.19) by addition of α(1→3) linked Ara*f* units to the α(1→5) arabinose chain at the non-reducing end (Birch *et al.*, 2010; Birch *et al.*, 2008).

In addition AftC, another Ara*f*T with α-1,3-branching activity encoded by *aftD* (*Rv0236c*) has recently been described in *M. tuberculosis* (Skovierova *et al.*, 2009). The transfer of terminal β(1→2) Ara*f* units from DPA onto the arabinan domain is catalysed by AftB (*Rv3805c*) (Belisle *et al.*, 1997; Seidel *et al.*, 2007a). The complete AG structure is now ready for mycolation with four mycolic acid units *per* AG

molecule. Attachment of mycolates to the complete AG structure is predicted to be catalysed by the Antigen 85 Complex (Belisle *et al.*, 1997) composed of three closely related proteins FbpA, FbpB and FbpC (*Rv3804c*, *Rv1886c* and *Rv0129c* respectively) (Jackson *et al.*, 1999). However in *C. glutamicum*, mycolyltransferases encoded by *cmytA* and *cmytB* attach mycolic acid residues to AG (Kacem *et al.*, 2004).

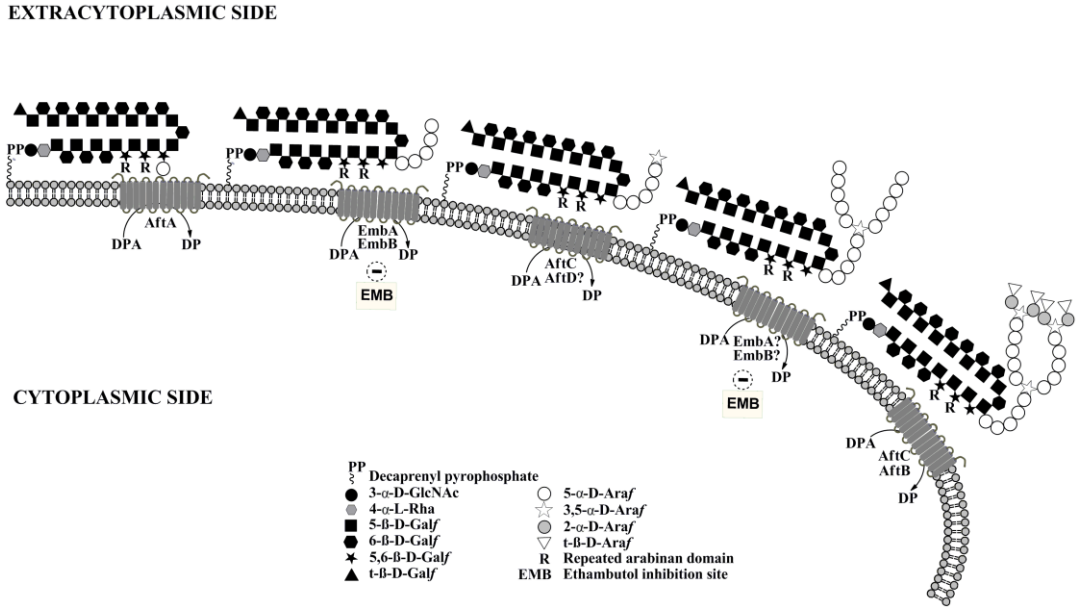

Figure 1.19: Biosynthesis of arabinan in AG and site of EMB action. The highly branched arabinan domain in AG is synthesised by several arabinofuranosyl transferases. Synthesis of a complete arabinan domain is stalled by EMB which inhibits the activity of EmbA and EmbB. – Adapted from Grover S. & Jankute M. *et al.*, 2012.

1.4.5 Phosphatidyl-*myo*-inositol based glycolipids

The plasma membrane of mycobacteria is rich in free lipids such as phospholipids; PE, PI, PIMs, LM, LAM and CL that forms the major structural components. The glycophospholipids such as PIMs, LM and LAM are built on a common phosphatidyl-*myo*-inositol (PI) backbone that undergoes a series of modifications. The spatial distribution of these PI based glycophospholipids in the cell envelope is still unclear. However, recent surface labelling experiments have indicated the likelihood of

occurrence of lipoglycans at the surface of mycobacteria predominantly in the outer leaflet of the outer membrane (Pitarque *et al.*, 2008). These surface exposed lipoglycans which include PIMs, LM and LAM exhibit immunomodulatory properties as they modulate immune response in macrophages, including cytokine production, inhibition of phagosome maturation, apoptosis in the host and are also instrumental in providing cross-protective immunity to mycobacteria (Mishra *et al.*, 2011b).

Based on experimental evidences the modifications of the PI anchor have been deduced to follow the order: PI → PIM → LM → LAM (Mishra *et al.*, 2011b). Sequential mannosylation of the PI anchor with up to six mannose residues generates PIMs that serve as the building blocks of higher lipoglycans, such as LM and LAM with highly branched mannose and arabinose units. Biogenesis of early PIM species utilises mannosyltransferases and acyltransferases encoded by genes present in an operon of six open reading frames that is conserved in the *Corynebacterineae* family (Cole *et al.*, 1998). These open reading frames (ORFs) include a probable threonyl-tRNA synthase (*Rv2614c*), a protein of unknown function with probable involvement in nucleotide biosynthesis (*Rv2613c*), PgsA (*Rv2612c*), a protein involved in PI synthesis and an acyltransferase (*Rv2611c*) (Kordulakova *et al.*, 2003). The fifth ORF PimA (*Rv2610c*), is an α-mannopyranosyltransferase of the GT-B superfamily that catalyses the production of PIM_1 (Guerin *et al.*, 2007). The last ORF of this gene cluster is a putative GDP-Man*p* hydrolase (*Rv2609c*) with a conserved MutT domain (Kordulakova *et al.*, 2002). The *embCAB* operon that encodes for Ara*f*Ts, such as EmbA, EmbB and EmbC in mycobacteria (Belanger *et al.*, 1996; Telenti *et al.*, 1997), is in another gene cluster comprising of enzymes employed in the biosynthesies of arabinan domains in LAM (Zhang *et al.*, 2003a) and AG (Escuyer *et al.*, 2001). These

complex lipoglycans are synonymous with the cell envelopes of all mycobacterial species (Besra and Brennan, 1997; Hunter and Brennan, 1990; Nigou *et al.*, 2003).

1.4.5.1 Structural features of PIMs

PIMs are all based on a common PI unit, a *sn*-glycero-3-phosphate-(1-D-*myo*-inositol) with glycerol phosphate attached to the L-1-position of *myo*-inositol (Ballou and Lee, 1964; Ballou *et al.*, 1963). The mannosyl-phosphate inositol anchor (MPI anchor) that binds these PIMs to the cell envelope is essentially a PI unit substituted with mannose residues on positions C-2 and C-6 of the inositol ring (Fig 1.20) (Nigou *et al.*, 2004; Severn *et al.*, 1998). The number, location and nature of the fatty acids attached to the MPI anchor are highly variable. Acylated PIM species are generated by acylation of the MPI anchor which harbours up to four potential acylation sites with two residing in the glycerol unit, one in the Man*p* unit linked to C-2 of *myo*-inositol and another at the C-3 position of the *myo*-inositol ring (Brennan and Ballou, 1968; Khoo *et al.*, 1996).

Sequential glycosylation of the MPI anchor generates PIMs with PIM_1, PIM_2, PIM_4 and PIM_6. The PI residue in the MPI anchor undergoes mannosylation with an α-D-mannopyranosyl (Man*p*) residue at position *O*-2 to yield PIM_1, whilst mannosylations with Man*p* at both *O*-2 and *O*-6 generates PIM_2 (Fig 1.20). A series of glycosylations of the MPI anchor generates the terminal PIM species PIM_6 with the structure Man*p*-α(1→2)-Man*p*-α(1→2)-Man*p*-α(1→6)-Man*p*-α(1→6)-Man*p*-α(1→.) attached to the MPI anchor (Nigou *et al.*, 1999) (Fig 1.21). Whilst mycobacteria accumulate acylated PIMs, such as Ac_1PIM_2 and Ac_1PIM_6, with acylation occurring at the Man*p* residue attached to C-2 of *myo*-inositol, the diacyl forms of PIMs, such as Ac_2PIM_2 and Ac_2PIM_6 also exist. The complex lipoglycans, such as LM and LAM and higher PIM

species, such as PIM_6 are built on Ac_1PIM_2 following a series of glycosylations mediated by mannosyltransferases and arabinosyltransferases (Chatterjee *et al.*, 1992).

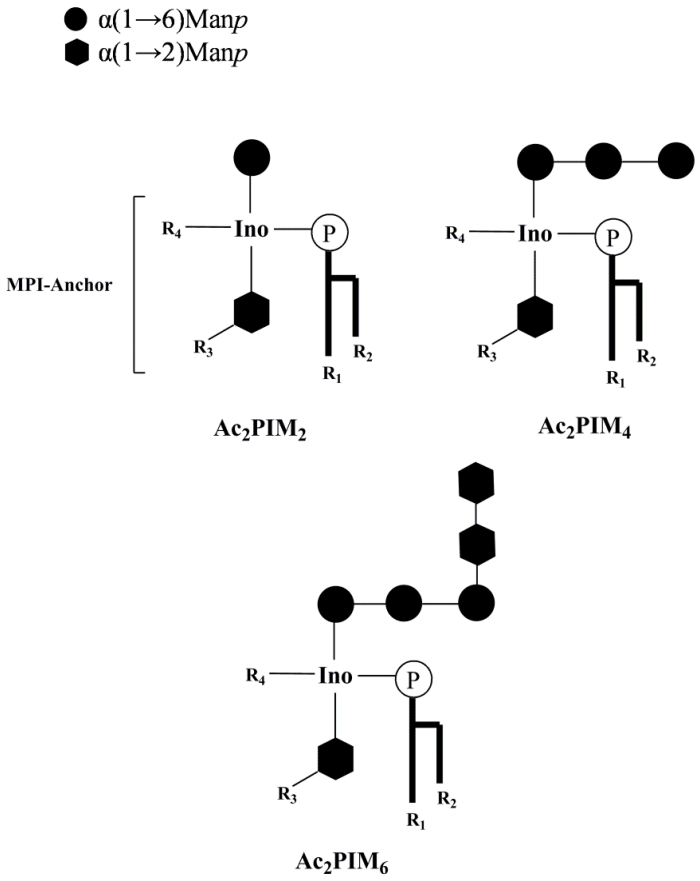

Figure 1.20: Structural features of PIMs. PIMs are based on a common PI anchor which attaches them to the membrane. The MPI anchor is glycosylated at 2-OH and 6-OH of inositol to generate PIM_2. Sequential addition of another two α(1→6) Man*p* residues generates PIM_4. The higher PIM species, PIM_6 is formed by addition of two α(1→2) Man*p* residues to PIM_4. The acylation sites in MPI anchor are represented by R_1, R_2, R_3 and R_4.

1.4.5.2 Structural features of LM and LAM

The extension of PIMs with 20-30 mannose residues generates the mannan core of LM and LAM. The C-6 position of the inositol ring is the initiation point to which the first Man*p* residue is attached (Chatterjee *et al.*, 1991; Khoo *et al.*, 1996) (Fig 1.21). The mannan backbone comprises of 21-34 linearly linked α(1→6) mannose residues with

branching introduced by 5-10 units of single α(1→2) Man*p* units at C-2 of some of the mannose residues in the backbone in all mycobacterial species (Mishra *et al.*, 2011a) except in *M. chelonae*, where branching occurs at the C-3 position (Chatterjee *et al.*, 1992; Guerardel *et al.*, 2002).

The arabinan domain in LAM consists of 55-70 Ara*f* units (Khoo *et al.*, 1996) with a linear backbone of α(1→5)-linked Ara*f* residues harbouring occasional branching at the 3rd position of some Ara*f* residues (Birch *et al.*, 2010; Kaur *et al.*, 2008) (Figure 1.21). The branched arabinan domain in LAM is similar to that of AG as it contains the hexa-arabinoside motif comprising of [β-D-Ara*f* (1→2)-α-D-Ara*f*]$_2$-3,5-α-D-Ara*f* (1→5)-α-D-Ara*f* as found in AG. In addition to the hexa-motif, a linear tetra-arabinoside comprising of β-D-Ara*f* (1→2)-α-D-Ara*f* (1→5)-α-D-Ara*f* (1→5)-α-D-Ara*f* is a second motif in the arabinan domain of LAM (Chatterjee *et al.*, 1991; Chatterjee *et al.*, 1993). The non-reducing end of both hexa-and the tetra-motifs are identified by a distinctive disaccharide unit, Ara*f*-β(1→2)-Ara*f*-α(1→.) (Chatterjee *et al.*, 1991; Chatterjee *et al.*, 1993; Mcneil *et al.*, 1994).

The β(1→2)-linked terminal Ara*f* units in LAM are capped with capping motifs that differ with respect to different mycobacterial species. Three different capping units have been identified in mycobateria: mannose capped LAM (Man-LAM) an attribute of slow-growing and mostly pathogenic mycobacteria, such as *M. tuberculosis, M. bovis, M. bovis BCG, M. leprae, M. avium, M. xenopi, M. marinum,* and *M. kansasii* (Chatterjee *et al.*, 1993), PI-capped LAM (PI-LAM) which is mainly found in fast-growing species of mycobacteria, such as *M. smegmatis* and *M. fortuitum* (Khoo *et al.*, 1995a), and non-capped LAM (Ara-LAM) that was recently identified in *M. chelonae*

(Guerardel *et al.*, 2002). The 'Man caps' in mycobacteria predominantly occur as dimannosides of α(1→2) Man*p*, whilst single and tri-mannosides also exist (Chatterjee *et al.*, 1992; Chatterjee *et al.*, 1993). In addition to the caps, Man-LAM isolated from *M. bovis* BCG (Glaxo, Pasteur, Japanese and Copenhagen strains) is modified with succinyl residues on the C-2 of the 3,5-di-α-D-Ara*f* units that can vary from one to four *per* LAM molecule (Delmas *et al.*, 1997).

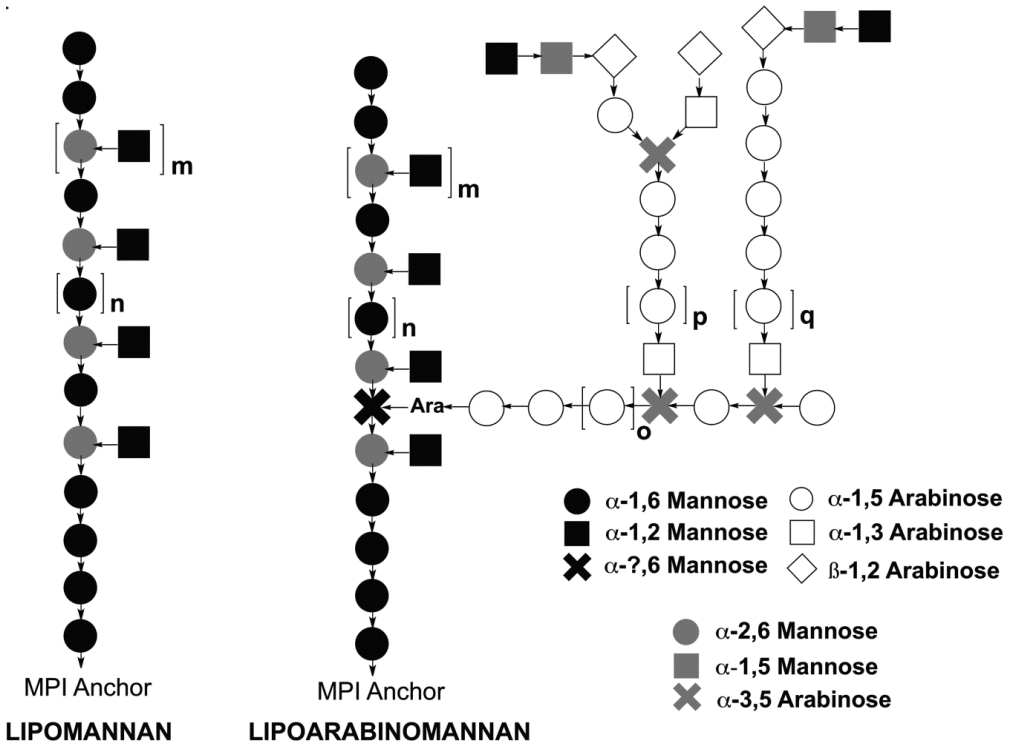

Figure 1.21: Structural features of LM and LAM. LM and LAM are formed by extensive glycosylation of PIM_4. The mannan in both LM and LAM comprises of 21-34 linearly linked α(1→6) man*p* residues occasionally branched by addition of α(1→2) man*p* residues. The arabinan domain consists of a branched hexa-motif; [β-D-Ara*f* (1→2)-α-D-Ara*f*]$_2$-3,5-α-D-Ara*f* (1→5)-α-D-Ara*f* which is similar to that of AG and a linear tetra motif: β-D-Ara*f* (1→2)-α-D-Ara*f* (1→5)-α-D-Ara*f* (1→5)-α-D-Ara*f*. A distinctive disaccharide unit, Ara*f*-β(1→2)-Ara*f*-α(1→.) decorates the non reducing ends. 'Man-LAM' in mycobacteria is capped by two or three α(1→2) man*p* residues.

1.4.5.3 Biosynthesis of PIMs, LM and LAM

1.4.5.3.1 GDP-Man*p* and polyprenol monophosphomannose biosynthesis

Mannose is an indispensable component of various glycolipids, lipoglycans, glycoproteins and polymethylated polysaccharides prevalent in mycobacteria (Jackson and Brennan, 2009). Mycobacteria is capable of sequestering mannose directly from the extracellular environment *via* the sugar transporters which is then phosphorylated by hexokinase (*Rv2702*) (Kowalska *et al.*, 1980) to generate mannose-1-phosphate. In an alternative mechanism, mycobacteria obtain mannose from the glycolytic pathway, by converting fructose-6-phosphate to mannose-6-phosphate *via* a phosphomannose isomerase (PMI), ManA (*Rv3255c)* (Patterson *et al.*, 2003) (Figure 1.22). The mannose-6-phosphate thus generated is converted to mannose-1-phosphate by a phosphotransferase, ManB (*Rv3257c)* (Mccarthy *et al.*, 2005). The mannose-1-phosphate thus synthesised is then transferred to guanosine diphosphate (GDP) by ManC to generate the intracellular nucleotide-derived mannose donor, GDP-Man*p* (Ma *et al.*, 2001; Ning and Elbein, 1999) that provides Man*p* residues to the GT-A/B superfamily glycosyltransferases for synthesis of several glycolipids in mycobacteria (Liu and Mushegian, 2003).

Polyprenyl-phosphate based mannose donors such as C_{50}-decaprenol-phospho-mannose (C_{50}-P-Man*p*, PPM) identified in *M. tuberculosis* (Takayama and Goldman, 1970) and *M. smegmatis* (Wolucka and De Hoffmann, 1998), are employed by the GT-C superfamily of glycosyltransferases for the synthesis of higher PIMs, LM and LAM. In addition to the C_{50}-polyprenol-based mannolipid, Takayama *et al*.(1973) also identified a C_{35}-octahydroheptaprenyl-phospho-mannose, C_{35}-P-Man*p*, in *M.*

smegmatis (Takayama *et al.*, 1973), thus establishing the existence of two prenyl-based phosphomannose donors in *M. smegmatis* that are utilised in the synthesis of cell wall components. Synthesis of these prenyl based phosphomannose donors is catalysed by a polyprenol monophosphomannose synthase (PPM synthase), Ppm1 (*Rv2051c*) that transfers Man*p* from GDP-Man to C_{35}/C_{50}-P to afford PPM (Gurcha *et al.*, 2002) (Figure 1.22). Recently, in a study conducted by Scherman *et. al.* (2009) the gene *Rv3779* was suggested to encode a second PPM synthase implicated in the synthesis of the $C_{35/50}$-P-Man*p* donor (Scherman *et al.*, 2009). However, in a second investigation by Skovierova *et al.* (2010), Rv3779 was identified as a glycosyltransferase that catalyses the transfer of a galactosamine residue from a polyprenyl-phospho-N-acetylgalactosamine to AG in mycobacteria (Skovierova *et al.*, 2010). The contradictory results thus obtained resulted in a re-examination of the role of Rv2051 and Rv3779, where a conditional mutant of *ppm1* in *M. smegmatis* was analysed for gain of function *in vivo* when complemented with a plasmid encoded copy of *Rv2051c* and *Rv3779.* The results obtained implicated *Rv2051c* as the true PPM synthase as it could successfully restore the wild type phenotype (Rana *et al.*, 2012).

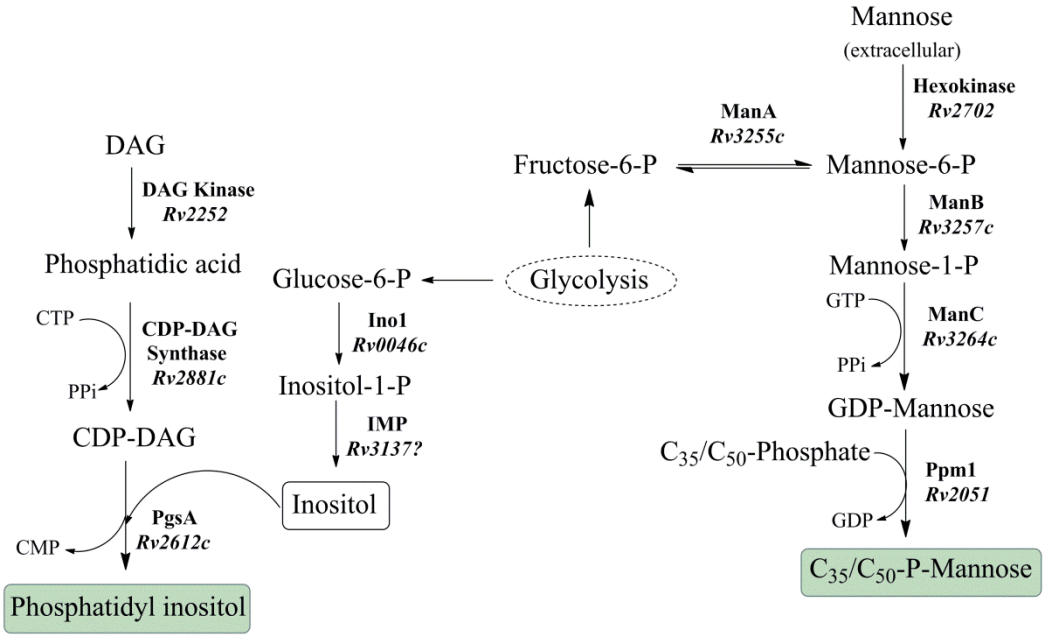

Figure 1.22: Biosynthesis of PI and PPM. PI is synthesised by a three step process which is initiated by conversion of glucose-6-P to inositol-1-P by Ino1. An IMP synthase converts inositol-1-P to *myo*-inositol which is loaded onto diacylglycerol by PgsA to afford the PI anchor. The pathway for PPM biosynthesis obtains mannose either exogenously or by converting the glycolysis intermediate fructose-6-P to mannose-6-P. PPM is generated by transfer of mannose residue from GDP-Man donor to the C_{35}/C_{50}-Phosphate carrier mediated by Ppm1. – Adapted from Grover S. and Jankute M. *et. al.*, Genetics of Arabinogalactan and Lipoarabinomannan, Molecular Genetics of Mycobacteria, 2nd Ed. (In Press).

1.4.5.3.2 Biosynthesis of PI

The PI moiety functions both as a building block for synthesis of PIMs, LM and LAM, and as an anchor for high molecular weight lipoglycans, LM and LAM. PI synthesis is a three-step process initiated by cyclisation of glucose-6-phosphate *via* inositol phosphate synthase InO1 (*Rv0046c)*, to afford *myo*-inositol-1-phosphate that is consequently dephosphorylated by inositol mono-phosphatase (IMP) to generate *myo*-inositol (Bachhawat and Mande, 1999a; Movahedzadeh *et al.*, 2004a) (Figure 1.22). The PI synthase, PgsA (*Rv2612c*) catalyses the transfer of *myo*-inositol to diacylglycerol (DAG), from the cytidine diphosphate-diacylglycerol (CDP-DAG) nucleotide donor in the last step to generate the PI anchor. Both enzymes, the PI

synthase, PgsA and inositol phosphate synthase Ino1, are essential for the growth and viability of mycobacteria (Jackson *et al.*, 2000; Movahedzadeh *et al.*, 2004a). Interestingly, several ORFs such *suhB* (*Rv2701c*), *impA* (*Rv1604*), *cysQ (Rv2131c)* and *impC* (*Rv3137*), have been implicated as putative inositol-monophosphatases responsible for the synthesis of *myo*-inositol, of which only ImpC was determined to be essential for the growth of MTB and *M. smegmatis* (Movahedzadeh *et al.*, 2010), indicating a possible involvement as a phosphatase for *myo*-inositol production.

1.4.5.3.3 Biosynthesis of PIMs

The PI anchor undergoes a series of mannosylations that follow the order: PI → PIM_2 → PIM_4 → PIM_6 (Figure 1.23) to generate PI-based mannosides, a crucial component of the mycobacterial cell envelope. The synthesis of early PIM species is initiated by transfer of Man*p* from GDP-Man*p* to position *O*-2 of the inositol ring of PI, catalysed by an α-mannosyltransferase PimA (*Rv2610c*) to yield PIM_1 (Guerin *et al.*, 2007; Kordulakova *et al.*, 2002; Kordulakova *et al.*, 2003). The second step in the pathway is the generation of a crucial metabolite PIM_2 on which the higher PIMs, LM and LAM are synthesised (Besra *et al.*, 1997; Khoo *et al.*, 1995b). PIM_2 is commonly found in mono- and di-acylated forms in MTB (Kordulakova *et al.*, 2003) and two separate hypotheses have been suggested for the formation of these acylated PIM species. According to the first hypothesis, acylation of PIM_1 by an acyltransferase, encoded by *Rv2611c*, at the 6^{th} position of the Man*p* precedes the mannosylation step catalysed by an α-D-mannose-α-(1→6) phosphatidyl *myo*-inositol-mannopyranosyltransferase PimB' (*Rv2188c*). The second mannosylation occurs at position *O*-6 of the inositol ring (Kordulakova *et al.*, 2002; Kordulakova *et al.*, 2003). Evidence for this hypothesis was provided by recent genetic studies conducted in *C. glutamicum* where $AcPIM_1$ was

observed to accumulate in a deletion mutant of *pimB'* (Kordulakova *et al.*, 2003; Lea-Smith *et al.*, 2008; Mishra *et al.*, 2008). The second hypothesis favoured co-acylation of both PIM_1 and PIM_2. However, cell free experiments conducted in *M. smegmatis* demonstrated that acylaytion of PIM_2 occurs only after its synthesis (Guerin *et al.*, 2009a), thus ruling out the co-acylation hypothesis. The acyltransferase encoded by *Rv2611c* and the mannosyltransferase PimB' encoded by *Rv2188c* are essential for growth in mycobacteria. (Guerin *et al.*, 2009a; Kaur *et al.*, 2007; Kordulakova *et al.*, 2003). The function of *Rv2188c* was initially assigned to *Rv0557,* earlier designated as PimB. However, genetic experiments in *M. tuberculosis* identified no changes to PIM biosynthesis due to disruption of the gene. The results obtained implied that the role of PimB, could either be substituted by complementary genes or the function of PimB is different to that of PimB' (Torrelles *et al.*, 2009). In addition, recent investigations in *C. glutamicum* have identified *Rv2188c* as the mannopyranosyltransferase involved in the second mannosylation step for the generation of $AcPIM_2$ (Lea-Smith *et al.*, 2008; Mishra *et al.*, 2008; Mishra *et al.*, 2009) and caused *Rv0557* to be renamed as MgtA, due to the α-mannosyl-glucopyranosylglucuronic acid transferase activity responsible for production of Cg-LM-B, a glucuronic acid based LM variant and $ManGlcAGroAc_2$, a glucuronic acid diacylglycerol based glycolipid found in *C. glutamicum* (Mishra *et al.*, 2009).

The synthesis of $AcPIM_4$ is the next crucial step in the PIM biosynthesis pathway. The less abundant intermediary PIM forms, such as Ac_1PIM_3 or Ac_2PIM_3 also exist in mycobacteria. Ac_1PIM_3 and Ac_2PIM_3 are synthesised by mannosyltransferase PimC (RvD2-ORF1) identified in *M. tuberculosis* strain CDC1551. However, no strong homologues of *pimC* were found to be present in *M. tuberculosis* H37Rv and *M.*

smegmatis. In addition, homologues of *pimC* in *M. bovis* BCG when deleted, exhibited normal PIM, LM and LAM levels, indicating the presence of other homologues or compensatory pathways (Kremer *et al.*, 2002b) to compensate for the loss of gene function. Generation of Ac_1/Ac_2PIM_4 by mannosylation of Ac_1/Ac_2PIM_3 at the non-reducing end is catalysed by an unidentified α(1→6) mannosyltransferase hypothesised to be either PimC or the unidentified putative 'PimD' protein (Guerin *et al.*, 2010). This step marks the point of divergence as the pathway now splits into two branches, with one branch leading to the formation of polar PIM species, such as Ac_1/Ac_2PIM_5 and Ac_1/Ac_2PIM_6 by two consecutive additions of α(1→2) Man*p*, probably by PimE (*Rv1159*), and the second branch leading to the formation of LM and LAM (Morita *et al.*, 2004; Morita *et al.*, 2006). An unknown flippase translocates Ac_1/Ac_2PIM_4 across the membrane to the periplasm for subsequent glycosylation.

Subsequent glycosylations of Ac_1/Ac_2PIM_4 are now mediated by the GT-C superfamily of glycosyltransferases that utilise polyprenylphosphate based sugar donors, PPM and DPA (Liu and Mushegian, 2003). Whilst the steps for the biosynthesis of the final product Ac_1/Ac_2PIM_6 are yet to be deduced, PimE an α(1→2) mannopyranosyltransferase of the GT-C superfamily is likely to be responsible for addition of one or more mannose residues to Ac_1/Ac_2PIM_4 (Morita *et al.*, 2006). The higher PIM species have prominent structural and physiological roles as PIM_4 forms the structural basis for LM and LAM, while PIM_6 is required for maintaining the integrity of the plasma membrane (Jankute *et al.*, 2012).

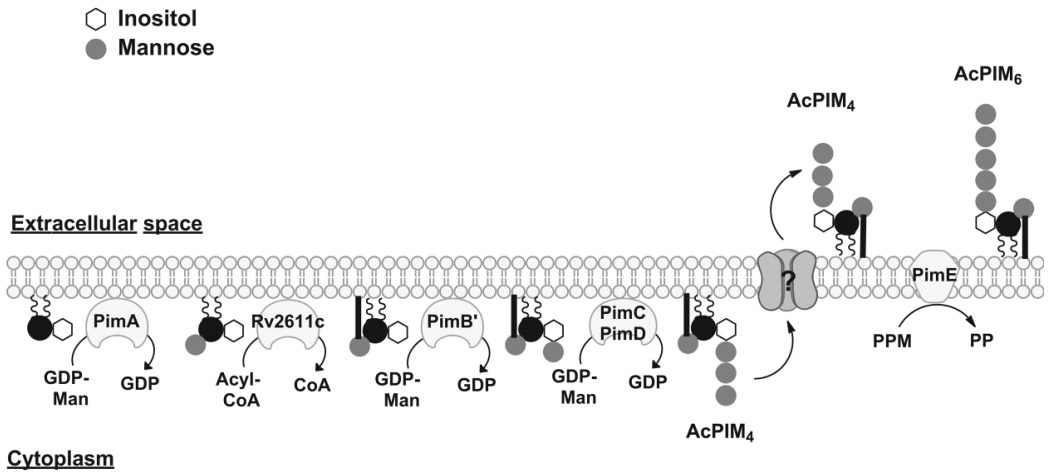

Figure 1.23: Pathway for biosynthesis of PIMs. Biosynthesis of PIMs is initiated by transfer of mannose residue from GDP-Man donor to PI by mannosyl transferase PimA. PIM_1 thus produced is acylated by acyltransferase Rv2611 to afford Ac_1/Ac_2PIM_1 which is subsequently mannosylated by PimB', unknown PimC or PimD to generate PIM_4. PIM_4 serves as the scaffold on which polar PIMs such as PIM_6 and lipoglycans such as LM and LAM are built. – Adapted from Grover S. and Jankute M. *et. al.*, Genetics of Arabinogalactan and Lipoarabinomannan, Molecular Genetics of Mycobacteria, 2nd Ed. (In Press).

1.4.5.3.4 Biosynthesis of LM and LAM

The intermediary PIM species Ac_1/Ac_2PIM_4 undergoes extensive modifications such as mannosylations and arabinosylations to yield LM and LAM. Since synthesis of Ac_1/Ac_2PIM_4 marks the branching point in lipoglycan and polar PIMs biogenesis, the channelling of the intermediate to either of the branches is regulated *via* a regulatory protein LpqW (*Rv1166*) (Crellin *et al.*, 2008; Kovacevic *et al.*, 2006). The regulator LpqW drives Ac_1/Ac_2PIM_4 into LM and LAM biosynthesis by interacting with a mannosyltransferase MptB, to promote the synthesis of the mannan core of LM and LAM (Crellin *et al.*, 2008; Rainczuk *et al.*, 2012). The mannan core in LM/LAM consists of approximately 25-30 linearly linked α(1→6) mannose residues with occasional branching at C-2 with single α(1→2) linked mannose units in *M. tuberculosis, M. leprae* and *M. smegmatis.* However, in case of *M. chelonae* single Man*p* units are substituted at position C-3 in the α(1→6) mannan core. Synthesis of

the linear α(1→6) mannan backbone is mediated by mannosyltransferases MptA (*Rv2174*) and MptB (*Rv1459c*) (Figure 1.24). Recent studies in *C. glutamicum* have highlighted that whilst MptB mediates the synthesis of the proximal end through the addition of 12-15 Man*p* residues to the backbone (Mishra *et al.*, 2008), MptA is responsible for the synthesis of distal end of the core (Kaur *et al.*, 2007; Mishra *et al.*, 2007). However, orthologues of MptB from *M. tuberculosis* and *M. smegmatis* when examined for their glycosyltransfease activity were unable to complement the *C. glutamicum*Δ*mptB* mutant, indicating that either differences in substrate specificity or redundancy of the gene function are responsible for the contradictory observations.

Branching in the α(1→6) mannan core is introduced by MptC (*Rv2181*) by the addition of α(1→2) Man*p* residues to the linear mannan backbone (Kaur *et al.*, 2006; Mishra *et al.*, 2011b) (Figure 1.24). A knockout of *MSMEG_4250*, the *M. smegmatis* orthologue of MptC synthesises a truncated version of LAM with a reduced number of (1→2) Man*p* branching residues. The mutant also lacked the ability to synthesise LM. Complementation of the mutant with the corresponding orthologue of MTB (*Rv2181*) restored normal LM/LAM synthesis indicating Rv2181 as the putative branching enzyme of the mannan core. However, regulation of LM and LAM biosynthesis in *M. smegmatis* appears to differ somewhat with *M. tuberculosis*, as *M. tuberculosis*Δ*Rv2181* produced truncated versions of LM and Man-LAM (Kaur *et al.*, 2008).

The arabinan domain in LAM is generated by further elaboration of LM with 55-70 Ara*f* units (Fig 1.24) (Besra and Brennan, 1997). The arabinan domain in AG and LAM share a high degree of similarity in both structure and biosynthesis. The addition

of Ara*f* residues to the mannan core is mediated by several Ara*f*Ts; of which EmbC (*Rv3793*), AftC (*Rv2673*) and AftD (*Rv0236c*) have been well characterised (Alderwick *et al.*, 2006b). Priming of the mannan core in LM with Ara*f* residues to generate the arabinan core is mediated by an unidentified Ara*f*T. The primed LM is subjected to sequential addition of 12-16 α(1→5) Ara*f* residues, exclusively catalysed by an α(1→5) Ara*f* transferase, EmbC (Alderwick *et al.*, 2011a; Birch *et al.*, 2010; Shi *et al.*, 2006). The linear arabinan polymer comprising α(1→5) Ara*f* residues in LAM is branched by addition of α(1→3) Ara*f* residues akin to AG.

The branching of the arabinan domain in both AG and LAM is mediated by the same branching enzyme, AftC (Birch *et al.*, 2010; Birch *et al.*, 2008). However, other branching enzymes with α(1→3) Ara*f* transferase activity have been suggested, such as AftD. AftD is hypothesised to be responsible for extension of the arabinan core by addition α(1→3) Ara*f* residues to the branched core. The evidence was provided by *in vitro* assays using artificial chemical acceptors and cell-free extracts from *M. smegmatis* and *C. glutamicum*. These experiments demonstrated that AftD was able to add α(1→3) Ara*f* residues to the linear α-1,5-linked neoglycolipid acceptor resulting in branching of the linear arabinan core, thus designating itself as a second branching enzyme (Skovierova *et al.*, 2009). The branched Ara-motif is further elaborated with Ara*f* residues into distinct tetra-arabinoside and hexa-arabinoside motifs. The enzyme AftB (*Rv3805c*) adds the terminal β(1→2) Ara*f* residues to both tetra and hexa-motifs and is common to both AG and LAM biosynthesis (Birch *et al.*, 2010).

The arabinose domains in AG and LAM are highly similar but harbour certain key differences; notably in the modification of the terminal Ara*f* residues. Whilst the terminal and penultimate residues in the arabinan domain in AG are attached to mycolates (Mcneil *et al.*, 1991), the terminal Ara*f* residue in LAM are instead modified with α-mannose units in all pathogenic strains of mycobacteria. Additionally, LAM consists of both tetra-arabinoside and hexa-arabinoside motifs in contrast to AG, where the highly branched arabinan domain terminates in hexa-arabinoside motifs (Daffe *et al.*, 1990) The mannose capped LAM in pathogenic strains of mycobacteria are referred to as Man-LAM and consist of one, two or three Man*p* residues with di-mannose cap being the most abundant (Chatterjee *et al.*, 1992; Chatterjee *et al.*, 1993). Synthesis of mannose caps is mediated in a two step-reaction catalysed by two distinct mannosyltansferases CapA (*Rv1635c*) and MptC (*Rv2181*) (Dinadayala *et al.*, 2006) (Kaur *et al.*, 2008) with α(1→2) mannosyltransferase activity (Figure 1.24). The GT-C enzyme CapA (*Rv1635c*) recognises the fully synthesised arabinan domain and catalyses the addition of the first Man*p* residue, while elongation of the cap with a second α(1→2) mannose unit is mediated by MptC (*Rv2181).*

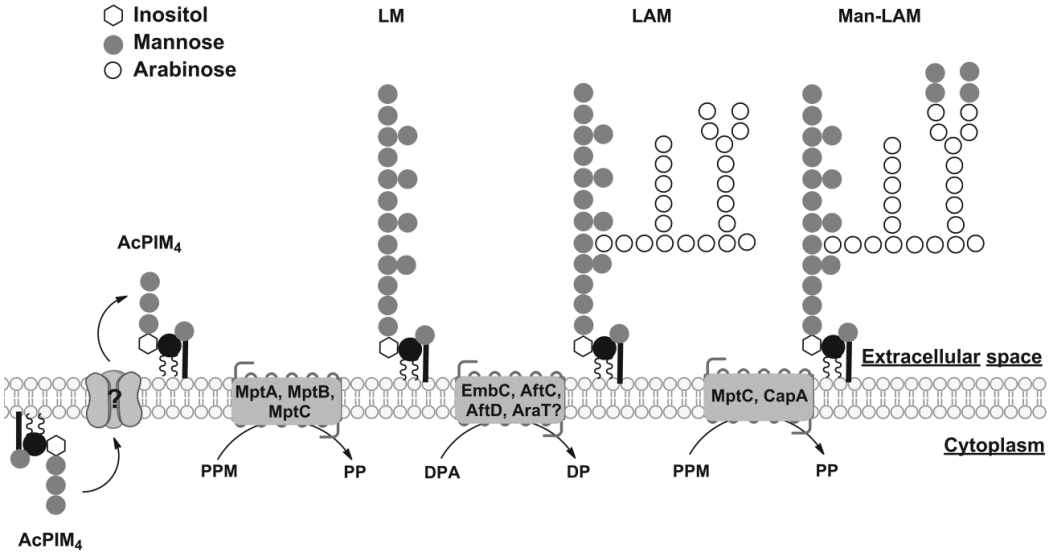

Figure 1.24: Biosynthesis of LM and LAM. Extensive glycosylation of $AcPIM_4$ generates LM and LAM. The mannan core is synthesised by GT-C superfamily mannosyltransferases MptB, MptA and MptC which utilise PPM as the mannose donor. The arabinan domain in LAM is synthesised by addition of 55-70 arabinose residues to LM by EmbC, AftC, AftD and an unknown transferase. The enzymes, MptC and CapA, synthesise the mannose cap in *M. tuberculosis.* –Adapted from Grover S. and Jankute M. *et. al.*, Genetics of Arabinogalactan and Lipoarabinomannan, Molecular Genetics of Mycobacteria, 2nd Ed. (In Press).

1.4.6 Decaprenyl phosphate

The poly-prenylphosphates, carriers for activated sugars, are the most important lipid molecules involved in cell wall biosynthesis. Since they are larger, these molecules are less abundant and their availability in cellular processes is limited. Of all the intracellular polyprenols, ω,di-E-poly-Z-undecaprenyl phosphate is the principal molecule in all bacterial species except *M. tuberculosis* and *M. smegmatis*, where ω,E-poly-Z-decaprenyl phosphate is predominant (Crick *et al.*, 2000). In case of *M. tuberculosis,* a single polyprenol pool is responsible for generating the carriers for activated sugars while in *M. smegmatis,* heptaprenyl diphosphate and decaprenyl diphosphate form the polyprenol pool (Crick *et al.*, 2000).

Although the major steps of the decaprenyl diphosphate biosynthesis have been elucidated, much of the information is still unknown. In mycobacteria, synthesis of polyprenylphosphate is initiated by sequential condensation of isopentenyl phosphate (IPP) with allylic prenyl diphosphates to generate longer allylic diphosphates. The condensation reactions are catalysed by prenyl diphosphate synthases, which are specific for E/Z type of stereochemistry of the allylic double bond. The allylic diphosphates thus generated are dephosphorylated to give the appropriate polyprenol phosphates. The genes *Rv1086* and *Rv2361c* encode the enzymes, E,Z-Farensyl-pyrophposphate (FPP) synthase and decaprenyl pyrophosphate synthase, respectively (Kaur *et al.*, 2004; Schulbach *et al.*, 2001). The first step of the pathway is the condensation of dimethyl allylic pyrophosphate (DMAPP) with isopentenyl pyrophosphate (IPP) to generate geranyl pyrophosphate (GPP). This reaction is catalysed by a previously unknown GPP synthase. However, a recent study employing purified Rv0989 for biochemical assays demonstrated that Rv0989 could efficiently condense IPP and DMAPP to generate FPP thus identifying Rv0989 as the 'missing GPP synthase'(Mann *et al.*, 2011). In addition, the enzyme could also afford moderate quantities of FPP from GPP indicating non-specificity of substrates for these prenyltransferases. The condensation of GPP with IPP by FPP synthase to yeild ω-E,E-FPP, is considered as the first committed step in the pathway. Subsequent condensation of seven IPP units with FPP, catalysed by decaprenyl phosphate synthase yields decaprenyl pyrophosphate as the ultimate product. The enzyme decaprenyl diphosphatase encoded by *Rv2136c*, dephosphorylates decaprenyl pyrophosphate to generate decaprenyl phosphate, which is channelled for PG, AG and LAM biosynthesis in mycobacteria.

1.4.7 Mycolic acids

Attached to the non reducing terminus in AG are the long chain α-alkyl, β-hydroxy fatty acids (Asselineau and Lederer, 1950), which are 70-90 carbon atoms in length in mycobacteria (Goodfellow and Minnikin, 1981) and referred to as mycolic acids. However, in Corynebacteria, these mycolic acids are shorter, upto 22-38 carbons in length and are referred to as corynomycolic acids (Collins *et al.*, 1982a; b; Puech *et al.*, 2001). Mycolic acids form the major bulk of the mycobacterial cell envelope and also impart resistance to common anti-mycobacterial agents. The general structure of mycolates includes a meromycolate chain of up to 56-carbon atoms and a saturated α-side chain, which is C_{24}-C_{26} in length.

The cell wall of mycobacteria comprises of three predominant types of mycolates, which differ from each other in the modifications of the fatty acyl chains. These include: non-oxygenated version containing two cyclopropane rings termed α-mycolates (Minnikin *et al.*, 1982; Qureshi *et al.*, 1978; Yuan *et al.*, 1995), methoxymycolates that are oxygenated with $–OCH_3$ groups and contain a single cyclopropane ring (George *et al.*, 1995), and the keto-mycolates that are oxygenated with a keto group and contain a single cyclopropane ring (George *et al.*, 1995). Whilst the majority of the mycolates are complexed with AG, free mycolates are prevalent in the outer layer of cell wall. These mycolates are glycosylated with either glucose or trehalose and are solvent extractable (Asselineau and Lederer, 1950; Minnikin *et al.*, 2002; Minnikin *et al.*, 1982). Trehalose esterified to a single mycolic acid residue is referred to as trehalose monomycolate (TMM) and to two mycolates as trehalose dimycolate (TDM), whilst a mycolate with esterified glucose is known as glucose monomycolate (GMM). The ‘cord factor’ in mycobacteria is TDM, which is only

present on the outer surface of mycobacteria and mediates the host immune response (Noll and Bloch, 1953; Noll *et al.*, 1956).

Synthesis of TDM is linked to TMM as TMM is first dephosphorylated and then transported to the periplasm with the aid of unknown mycolate transporters where it is further mycolated by three mycolyltransferases Ag85A, Ag85B and Ag85C to generate TDM (Belisle *et al.*, 1997). Biosynthesis of mycolic acids in mycobacteria is mediated by two multi-enzyme proteins FAS-I encoded by a single gene *fas* (*Rv2524c*) and FAS-II which consists of several enzymes including InhA, the primary target of INH (Marrakchi *et al.*, 2000), KasA, KasB, FabG1 and HadABC. FAS-I is common to eukaryotes, whilst FAS-II is found in bacteria. However, mycobacteria are an eeption as they harbour both FAS-I and FAS-II (Dover *et al.*, 2004). The two systems are linked *via* the enzyme mtFabH, a β-ketoacyl-ACP synthase III encoded by *Rv0533c* (Choi *et al.*, 2000) that channels acyl-CoA derivatives generated by FAS-I for condensation with the malonyl-acyl carrier protein-(AcpM) (*Rv2244*) to synthesise thioesters which are then directed to FAS-II for extension (Dover *et al.*, 2004; Scarsdale *et al.*, 2001). The enzymes KasA and KasB in FAS-II initially extend these thioesters by condensing them with malonyl-AcpM and the FAS-II cycle is completed by FabG1, HadABC and InhA (Kremer *et al.*, 2002a; Schaeffer *et al.*, 2001). The shorter mycolic acid chains in the corynebacterial counterparts are due to the absence of FAS-II orthologues (Dover *et al.*, 2004).

1.5 Aims

The primary objective of this thesis was to determine new targets for TB drug development and explore novel mechanisms for resistance in mycobacteria. In addition, this work also tested new strategies that can be implemented for effective targeting by anti-tubercular compounds. The pathway for LAM biosynthesis formed the nerve center of the study.

The first chapter of this thesis focuses on the pathway for decaprenyl phosphate recycling and its role in imparting resistance to the recently discovered class of anti-tubercular compounds, Benzothiazinones. Since benzathiazinones stall the synthesis of arabinose donor, DPA, which is involved in production of arabinan domains in cell wall components LAM and AG, these components were thoroughly analysed. To investigate the role of decaprenyl phosphate recycling in imparting resistance to the drug, the gene Z-prenyl diphosphate synthase was over-expressed and the effect of drug was re-examined on the cell wall components. This study was performed using *C. glutamicum* as the model organism.

The second chapter describes the regulation of mycothiol and phosphatidyl inositol based lipoglycan biosynthesis by the newly identified transcriptional regulator, IpsA. For this purpose, an *ipsA* deletion mutant was constructed in *C. glutamicum* and its function was characterised using genetic complementation and cell wall analysis.

The new approaches for design of therapeutic compounds such as ‘co-targeting of interacting proteins’ and ‘polar hydrophobicity in design of enzyme inhibitors’ were tested in chapter 3 and 4. The ‘co-targeting’ approach, as described in Chapter 3 focused on identifying interacting partners from the proteins involved in LAM

biosynthesis. An *E. coli* based two-hybrid system was utilised for this purpose. These interacting partners could serve as attractive targets for future drug development.

In Chapter 4, substrate analogues with strategically replaced fluorine atoms in the sugar ring were tested for their ability to inhibit the function of glycosyltransferases. The activity of these analogues was tested *in vitro* using the membrane preprations from *M. smegmatis* that served as the source of glycosyltransferases.

Chapter 2

2 Benzothiazinones mediate killing of *Corynebacterineae* by blocking decaprenyl phosphate recycling involved in cell wall biosynthesis

2.1 Introduction

The nitro-based sulphur containing benzothiazinones are a new class of highly potent anti-TB drug candidates that display very low MICs for both pathogenic, slow growing *M. tuberculosis* H37Rv (1 ng/mL) and for non pathogenic, fast-growing *Mycobacterium* species, such as *M. smegmatis* (4 ng/mL) (Makarov *et al.*, 2009). In addition, BTZs exhibit very high efficacy against both sensitive and drug resistant TB strains (Pasca *et al.*, 2010). The whole genome sequencing studies of *M. smegmatis*, *M. bovis* (BCG), and *M. tuberculosis* mutants with high resistance to BTZ revealed DprE1 (*Rv3790*), which is a FAD-containing oxidoreductase as the target, which was further validated using biochemical studies (Manina *et al.*, 2010; Trefzer *et al.*, 2010). The enzyme DprE1 functions in concert with a NADH-dependent reductase DprE2 (*Rv3791*) to catalyse the epimerisation of decaprenylphosphoryl-D-ribose (DPR) to decaprenylphosphoryl-D-arabinose (DPA) (Makarov *et al.*, 2009; Mikusova *et al.*, 2005). DPR is first oxidised to a keto intermediate, DPX *via* DprE1 and then reduced to DPA by DprE2.

BTZs are said to function in a similar manner to EMB as they both target the same pathway responsible for the synthesis of cell wall components, LAM and AG (Makarov *et al.*, 2009). Whilst EMB targets the *embCAB* encoded arabinofuranosyl transferases that utilises DPA as the sole arabinose donor, BTZs surpress the synthesis of this donor, thus inhibiting the formation of LAM and AG that are crucial for maintaining cellular integrity. However, BTZ is different to EMB in terms of potency as it displays a 1000-fold more activity against *M. tuberculosis* (Makarov *et al.*, 2009).

Since BTZs target the generation of DPA, a crucial metabolic intermediate, the oxido-reductase DprE1/E2 responsible for its synthesis has been tested for essentiality in several species of *Corynebacterineae.* Attempts to knock-out or knock-down the chromosomal copy of *dprE1* in *M. smegmatis* (*MSMEG_6382*) and its *C. glutamicum* orthologue (*NCgl0187)* have been successful only in presence of a plasmid-encoded copy (Crellin *et al.*, 2011; Meniche *et al.*, 2008). Interestingly, the DPPR phosphatase (*Rv3807c*) , which catalyses dephosphorylation of DPPR to yield the DprE1 substrate DPR is not essential in *M. tuberculosis* (Sassetti *et al.*, 2003) and redundancy is observed for DprE2 in both *M. smegmatis* and *C. glutamicum* (Crellin *et al.*, 2011; Meniche *et al.*, 2008). These experiments illustrate that the production of DPA and its utilisation in arabinan biosynthesis are a pre-requisite for formation of a complete cell wall in *Corynebacterineae* (Wolucka, 2008).

The two-step process for generation of DPR utilises a ribosyltransferase UbiA that condenses pRPP with decaprenyl phosphate to yield DPPR, a phosphatase (*Rv3807*) subsequently dephosphorylates DPPR to afford DPR. Since UbiA catalyses the first committed step in this pathway, its activity should thus be critical for survival. However, inactivation of *ubiA* in *C. glutamicum* produced a viable mutant devoid of cell wall arabinan. As expected, this mutant had lost its ability to synthesise DPA, an otherwise important metabolite suggesting that neither DPA production nor synthesis of cell wall arabinan are required for viability of *C. glutamicum* (Alderwick *et al.*, 2005; Tatituri *et al.*, 2007). These contrasting findings established a paradigm that even though BTZs target DprE1 and block DPA biosynthesis, the action of the drug is insufficient to cause a lethal effect on the bacilli. Therefore, to deduce an alternative

explanation for BTZ's lethal action, we examined the biochemical effects of BTZ inhibition on *C. glutamicum* and the DPA deficient strain, *C. glutamicum::ubiA*.

The data revealed that BTZ clearly inhibits growth and DPA production in wild type *C. glutamicum* but fails to have any deleterious effects on the *Cg*-UbiA mutant with a functional DprE1. Additionally, the effect of BTZ was also examined on growth and cell wall arabinan biosynthesis by over-expressing *C. glutamicum Z*-decaprenyl diphosphate synthase, encoded by *NCgl2203* (UppS) in *C. glutamicum*. The results demonstrated that over-expression of UppS could rescue the wild type strain (BTZ MIC 20 µg/mL) and shift its MIC to >40 µg/mL and restore arabinan biosynthesis that is otherwise blocked by BTZ treatment. Therefore, our results suggest that BTZ causes a lethal effect by blocking the recycling of decaprenyl phosphate as in its presence; the cell continually synthesises DPR, a toxic intermediate that renders decaprenyl phosphate unavailable for other macromolecules, such as peptidoglycan, LAM and AG. However, the over-expression of a prenylsynthase supplements enough decaprenyl phosphate to aid in cell wall biosynthesis hence evading the lethal effect of the drug.

2.2 Material and Methods

2.2.1 Bacterial strains and growth conditions

E. coli Top 10 cells were cultured in Luria-Bertani broth (LB, Difco) at 37°C. *C. glutamicum* ATCC 13032, *C. glutamicum*-pVWEx2 and *C. glutamicum*-pVWEx2-*uppS* (10 µg/mL tetracycline) was grown on rich Brain Heart Infusion medium (BHI, Difco) and *C. glutamicum*::*ubiA* (25 µg/mL kanamycin) on BHI containing 9.1% sorbitol (BHIS) supplemented with appropriate antibiotics for selection.

2.2.2 Construction of plasmids and strains

C. glutamicum-uppS (NCgl2203) was amplified from genomic DNA using the primers, 2203vwex_Fwd: 5' GCATGTCTAGAAGGAGATATAGATGTGAGTGAATTCCA AGTA 3' and 2203vwex_Rev 5' ATTAGGATCCTTATGCGCTTCCGAATCTGCG 3' (restriction sites underlined) and cloned in pVWEx2 under the isopropyl-β-D-thiogalactopyranoside (IPTG) inducible P_{tac} promoter. The vector and PCR product were digested using XbaI and BamHI and ligated to generate the *C. glutamicum*-pVWEx2-*uppS* construct. The pVWEx2-*uppS* plasmid thus obtained was confirmed by sequencing by Eurofins MWG Operon. The *C. glutamicum*::*ubiA* strain was obtained as described previously (Tatituri *et al.*, 2007). The empty pVWEx2 and pVWEx2-*uppS* plasmids were electroporated into *C. glutamicum* using a standard protocol as shown in General Materials and Methods, section 7.3.8 and 7.3.9.

2.2.3 Expression of UppS in *C. glutamicum*

Overnight cultures (5 mL BHI containing tetracycline) of selected *C. glutamicum*-pVWEx2-*uppS* colonies were used to inoculate 50 mL BHIS with 10 µg/mL tetracycline (30°C, 180 rpm). The cultures were induced with 0.5 mM IPTG at OD_{600}

0.6 and incubated at 30°C for 24 hours. Cells were harvested (7000 x *g*, 15 minutes), washed twice with phosphate buffered saline and resuspended in lysis buffer (50 mM MOPS (pH 7.9), 0.2 mg/mL lysozyme). The resuspended cell pellets were incubated at 37°C for 1 hour to allow cell lysis. The suspension was centrifuged (27000 x *g*, 20 minutes) and supernatant was checked for presence of protein on 12 % SDS PAGE gel.

2.2.4 Effect of BTZ043 on growth and viability of *C. glutamicum* strains

To determine the MIC of BTZ043 for *C. glutamicum* and *C. glutamicum* pVWEx2, approximately 10^8 cells were used to inoculate 2 mL of BHI broth containing 0 to 20 µg/mL BTZ043 in a step-wise gradient and the OD_{600} was measured up to 48 hours. To determine the effect of increasing concentrations of BTZ043 on growth of *C. glutamicum*::*ubiA* and *C.glutamicum*-pVWEx2-*uppS*, approximately 10^8 cells were used (30°C, BHIS, 200 rpm) to inoculate 2 mL BHIS containing 0 and 20 µg/mL BTZ043 and the OD_{600} was measured up to 48 hours. The cultures were also grown for 48 hours as above and the viability count was determined by spotting 10 µL of serially diluted cultures (up to dilution 10^{-8}) on BHIS plates for *C. glutamicum*::*ubiA* and BHI plates *C.glutamicum*-pVWEx2-*uppS.* The MIC was defined as the minimal concentration required to completely inhibit 99% of the growth.

2.2.5 Effect of BTZ043 on DPA synthesis in *C. glutamicum* strains

To characterise the effect of BTZ043 on DprE1, p[^{14}C]Rpp was synthesised as described in General Material and Methods, section 7.4.7 and supplemented as a substrate for the *in vitro* synthesis of DPA. Accumulation of DPR in the presence of BTZ043 was chosen as a parameter to monitor the effect of BTZ043. Cell membranes from *C. glutamicum* and *C. glutamicum*::*ubiA* were prepared as described in the General Materials and Methods, section 7.4.6 and assayed for DPA biosynthesis (Pathak *et al.*, 2002).

Briefly, decaprenyl phosphate (50 µg, 5 mg/mL stored in ethanol, 1 µL) was dried under nitrogen and was resuspended in buffer A (50 mM MOPS, 10 mM $MgCl_2$ pH 8.0). The mixture was sonicated until a colloidal suspension was visible. The basic assay mix consisted of 400 µg of membranes and a P60 fraction (Besra *et al.*, 1997), 25 mM ATP, 25 mM FAD, 25 mM NAD and 25 mM NADP, BTZ043 (stock concentration 20 µg/mL in DMSO) in a final volume of 55 µL of buffer A and initiated by the addition of p[^{14}C]Rpp (65,000 cpm), as described in the General Materials and Methods section 7.4.7. The reactions were incubated at 30°C for 1 hour and quenched by the addition of 110 µL of chloroform/methanol (1:1, v/v) and 55 µL of water, mixed for 15 minutes on a rotating mixer. The assay mixture was then centrifuged at 26,000 x *g* for 10 minutes and the lower organic phase was recovered and dried under nitrogen. The resulting products were resuspended in 20 µL of chloroform/methanol (2:1, v/v) and an aliquot was subjected to scintillation counting using 5 mL scintillation fluid, and a second aliquot was subjected to TLC analysis using silica gel plates (5735 silica gel 60F254, Merck) developed in chloroform/methanol/water/ammonium

hydroxide/ammonium acetate (180:140:23:9:9 v/v/v/v/v) and visualised by phosphor imaging by exposing the TLCs to a phosphor imaging screen (Kodak) for 24 hours.

2.2.6 Function of DprE1 in *C. glutamicum* and *C. glutamicum*::*ubiA*

To characterise the effect of BTZ043 on DprE1, DP[^{14}C]R was supplemented as a substrate for the *in vitro* synthesis of DP[^{14}C]A (Scherman *et al.*, 1996). Cell membranes from *C. glutamicum* and *C. glutamicum::ubiA* were assayed for DPA biosynthesis activity using p[^{14}C]Rpp as a substrate by previously described protocol (section 2.2.5). For estimating the activity of DprE1 in *C. glutamicum::ubiA*, reactions were initiated with DP[^{14}C]R that was prepared using p[^{14}C]Rpp with a few modifications to the protocol. To prepare DP[^{14}C]R, the reactions were supplemented with decaprenyl phosphate, buffer A containing all the co-factors, 400 µg membranes and P60, which was pre-incubated with BTZ043 and initiated by addition of p[^{14}C]Rpp (65,000 cpm). The resulting DP[^{14}C]R was extracted using 110 uL of 2:1 chloroform/MeOH and 55 µL water. The lower organic phase was recovered by centrifugation (26,000 x *g*, 10 minutes), transferred to a fresh tube and dried under a stream of nitrogen. The assay products were resuspended in 20 µL of chloroform/methanol (2:1, v/v) and an aliquot was subjected to TLC analysis using silica gel plates (5735 silica gel 60F254, Merck) developed in chloroform/methanol/water/ammonium hydroxide/ammonium acetate (180:140:23:9:9 v/v/v/v/v) and visualised by autoradiography by exposure of TLCs to X-ray film (Kodak X-Omat).

The DP[^{14}C]R was used as a substrate for determining the functionality of DprE1 in *C. glutamicum* and *C. glutamicum*::*ubiA.* The basic assay mixture consisted of DP[^{14}C]R

(20,000 cpm) dried and resuspended in buffer A, 500 µg membranes and P60 fraction, co-factor mix and BTZ043 (20 µg/mL in DMSO) in a final volume of 55 µL of Buffer A. The extractions were performed using the previously mentioned protocol (section 2.2.5). The recovered organic phase was dried and resuspended in 20 µL of chloroform/methanol (2:1, v/v). Equal counts (10,000 cpm) from these extracts were subjected to TLC analysis using silica gel plates (5735 silica gel 60F254, Merck) developed in chloroform/methanol/water/ammonium hydroxide/ammonium acetate (180:140:23:9:9 v/v/v/v/v) and visualised by phosphor imaging by exposing the TLCs to a phosphor screen (Kodak) for 24 hours.

2.2.7 Estimation of decaprenyl phosphate synthesis in *C. glutamicum*-pVWEx2-*uppS*

To characterise the effect of over-expression of the *C. glutamicum* decaprenyl phosphate synthase (UppS) on decaprenyl phosphate synthesis, the reactions were supplemented with [4-^{14}C]-isopentenyl pyrophosphate (IPP) triammonium salt (40-60 mCi/mmol, PerkinElmer Inc.) as a substrate. Cell membranes from *C. glutamicum*-pVWEx2 and *C. glutamicum*-pVWEx2-*uppS* were prepared as described in the General Materials and Methods, section 7.4.6 and assayed for decaprenyl phosphate synthesis activity.

For the reactions, the substrate [^{14}C]IPP (30 µM stored in ethanol) was dried and resuspended in appropriate volume of buffer A (50 mM MOPS, 10 mM $MgCl_2$ pH 8.0) and supplemented with 400 µg of membranes, 100 µM geranyl diphosphate (GPP, 1 mg/mL in methanol), 100 µM dimethyl allyl diphosphate (DMAPP, 1 mg/mL in methanol) as primers and BTZ043 (20 µg/mL in DMSO), where required in a final

volume of 80 µL of buffer A. The reactions were incubated at 30°C for 1 hour and quenched by the addition of 1 mL of water saturated NaCl. The mixture was partitioned into an aqueous and organic phase by adding 1 mL of butanol saturated with water. The lower organic phase of butanol was recovered and the process was repeated twice. The butanol fraction was dried under nitrogen and resuspended in 1mL 0.1 N HCl in 50% ethanol. Mild acid hydrolysis was performed by incubating the suspension at 37°C for 12 hours. To recover the radiolabeled dephosphorylated products, equal volume of chloroform was added to the hydrolysed fraction and mixed on the rotator for 15 minutes. The lower organic phase containing the dephosphorylated products were recovered and washed twice with water. The organic phase was recovered, dried and resuspended in 20 µL of chloroform/methanol (2:1, v/v). An aliquot was taken for liquid scintillation counting and equal counts (20,000 cpm) were subjected to TLC analysis using reverse phase silica gel plates (silica gel 60 RP-18 $F_{254}S$, Merck) developed in methanol/acetone (8:2, v/v) and visualised by autoradiography by exposing the TLCs to X-ray film (Kodak X-omat) for 24 hours.

For product analysis and comparision, known standards were spotted on a separate reverse phase silica gel plate (silica gel 60 RP-18 $F_{254}S$, Merck) developed in methanol/acetone (8:2, v/v), stained with ethanolic molybdophosphoric acid and heated gently using a heat-gun. Densitometric analysis was performed by scanning the autoradiogram in Bio-Rad GS-800 imaging densitometer and spots were quantified using the Quantity One software.

2.2.8 Analysis of AG and LAM biosynthesis in *C. glutamicum*-pVWEx2 and *C. glutamicum*-pVWEx2-*uppS* treated with BTZ043

To analyse the effect of over-expression of decaprenyl phosphate synthase on the cell wall component AG in *C. glutamicum,* overnight cultures of *C. glutamicum*-pVWEx2 and *C. glutamicum*-pVWEx2-*uppS* were used to sub-culture 20 mL of BHI media and grown to OD_{600} 0.4-0.6 (30ºC, 200 rpm, 4-5 hours), induced with 0.5 mM IPTG and split into two separate cultures of equal volume (10 mL each). To monitor the effect of the drug on arabinose incorporation in AG, one half of the culture was treated with BTZ043 at 0.75 x MIC (15 µg/mL) for 2 hours (30°C, 200 rpm). Both treated and untreated cultures were labelled with 1.0 µCi/mL of [^{14}C]-glucose (250-360 mCi/mmol, PerkinElmer Inc.) and grown for 48 hours (30°C, 200 rpm). The mAGP complex was isolated and sugar hydrolysis was performed on all the samples using the protocols described in General Materials and Methods, section 7.4.3 and 7.4.4. The radioactive sugar samples were analysed by loading equal counts (20,000 cpm) on aluminium backed HPTLC-cellulose plates (Merck) developed thrice in formic acid/water/tertiary-butanol/methylethyl ketone (3:3:8:6) and visualised by autoradiography by exposing the TLC to X-ray film (Kodak X-omat) for 4 days.

To analyse the effect of over-expression of decaprenyl phosphate synthase on the cell wall component LAM/LM in *C. glutamicum,* overnight cultures of *C. glutamicum*-pVWEx2 and *C. glutamicum*-pVWEx2-*uppS* were used to sub-culture 40 mL of BHI media and grown to OD_{600} 0.4-0.6 (30ºC, 200 rpm, 4-5 hours). The cultures were induced with 0.5 mM IPTG and labelled with 1.0 µCi/mL of [^{14}C]-glucose (250-360 mCi/mmol, PerkinElmer Inc.) and grown for 1 hour (30°C, 200 rpm) to allow its incorporation in cell wall. The effect of drug on LAM biogenesis was analysed in a

time dependant manner. At time 0 hour, the culture was split into 5 mL aliquots and BTZ043 (20 µg/mL) was introduced into half of the aliquots to afford treated and untreated cultures. The cultures were then sampled every 2 hours by taking 5mL aliquots, centrifuged and snap frozen using liquid nitrogen. The components LAM/LM were extracted from all the samples using previously described protocols as mentioned in the General Materials and Methods, section 7.4.5. The [^{14}C]LAM/LM samples were analysed by loading equal counts (3000 cpm) on 12% SDS-PAGE gels and visualised by autoradiography by exposing the gels to X-ray film (Kodak X-omat) for 14 days.

2.3 Results

2.3.1 Effect of benzothiazinone on *C. glutamicum* wild type and *C. glutamicum::ubiA*

The lead compound of the BTZ series BTZ043 targets DprE1, a FAD-containing oxidoreductase that is highly conserved across the *Corynebacterineae* (Batt *et al.*, 2012). The amino acid sequences of MTB DprE1 (*Rv3790*) and its orthologue in *C. glutamicum* (*NCgl0187*) when aligned display 65% identity (Meniche *et al.*, 2008) and a remarkable conservation of the active site residues, including Cys414, which corresponds to Cys387 in *Mt*-DprE1. The Cys387 residue in *Mt*-DprE1 forms a covalent semimercaptal linkage with the activated nitroso-group of BTZ043 which inactivates the enzyme (Manina *et al.*, 2010; Trefzer *et al.*, 2010; Trefzer *et al.*, 2012).

In this study, we have attempted to analyse the effect of BTZ043 on the synthesis of cell wall components using *C. glutamicum* as a model system. *C. glutamicum* has extensively been used in our previous studies to understand the molecular genetics of mycobacterial cell wall biosynthesis (Mishra *et al.*, 2007; Mishra *et al.*, 2009; Tatituri

et al., 2007). Both. *C. glutamicum* and *M. tuberculosis* are members of the same family *Corynebacterineae* with similar cell wall ultra-structure and biosynthetic machinery (Dover *et al.*, 2004). However, the faster growth rate, lesser complexity, ease of genetic manipulation and ability to tolerate mutations better than other mycobacterial species makes *C. glutamicum* an excellent model to study the function of otherwise essential genes in mycobacteria. (Cerdeno-Tarraga *et al.*, 2003; Seidel *et al.*, 2007b).

The drug BTZ043 stalls arabinan biosynthesis by targeting DprE1 and leads to production of arabinose deficient cell wall components. The effect produced by BTZ043 is functionally equivalent to the phenotype exhibited by *C. glutamicum::ubiA,* as the strain is completely devoid of arabinan in its cell wall. Therefore, to establish this equivalency and determine the effect of BTZ043, we cultured *C. glutamicum* (wild type) and *C. glutamicum*::*ubiA* in liquid media over a 48 hour period and examined their susceptibility to BTZ043 at a range of concentrations. The MIC of BTZ043 for *C. glutamicum* wild type was determined to be 20 µg/mL (Figure 2.1).

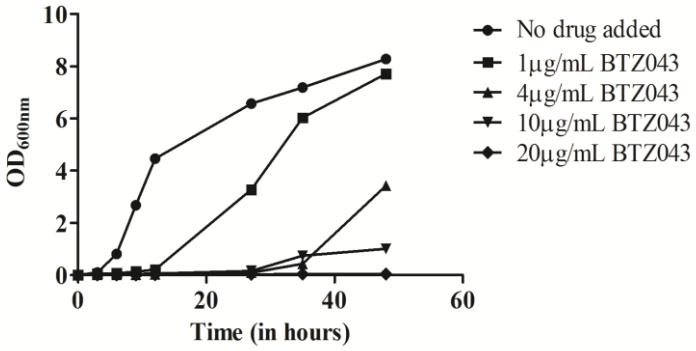

Figure 2.1: Effect of BTZ043 on growth of *C. glutamicum ATCC 13032*. The wild type *C. glutamicum* was tested for susceptibility to BTZ043 in liquid media at a range of concentrations (0, 1, 4, 10, 20 µg/mL). The maximum inhibition in growth (99%) was observed at [BTZ043] of 20 µg/mL and was chosen as the MIC for *C. glutamicum.* The data is representative of two separate experiments.

The *C. glutamicum*::*ubiA* strain was inherently slow-growing, and the effect of BTZ043 was tested on the growth rate of *C. glutamicum::ubiA* at the concentration that corresponds to the MIC (Figure 2.2) of the wild type strain. The results demonstrate that the arabinan deficient mutant is resistant to BTZ043 as no change was observed in growth rate for the mutant.

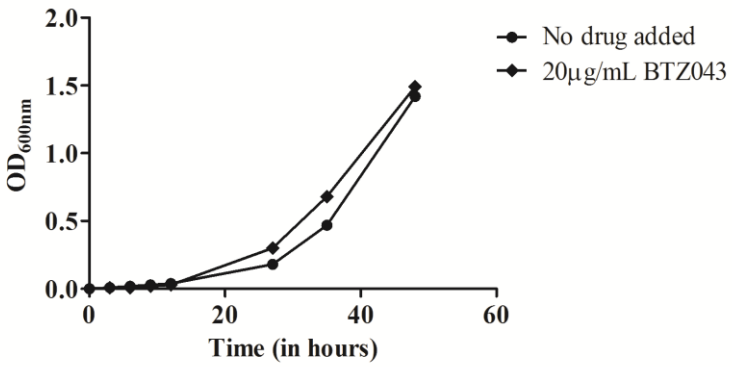

Figure 2.2: *C. glutamicum::ubiA* is resistant to BTZ043. *C. glutamicum::ubiA* was examined for its susceptibility to BTZ043 in liquid media at a final concentration of 20 µg/mL (MIC for *C. glutamicum*). The data is representative of two separate experiments.

The growth rate of *C. glutamicum::ubiA* mutant was also compared to that of wild type at different concentrations of BTZ043 (Figure 2.3). In comparison to wildtype, *C. glutamicum::ubiA* is a slow growing strain (Figure 2.3A) with an approximately five-fold lesser growth rate. When BTZ043 is added at concentrations of 1 µg/mL (Figure 2.3B), 4 µg/mL (Figure 2.3C), 10 µg/mL (Figure 2.3D) and at 20 µg/mL (Figure 2.3E), a shift in the growth rate is observed for wild type. An increase in drug concentration causes a sharp decrease in growth for the wild type and completely inhibits the strain at MIC whereas the growth of *C. glutamicum::ubiA* remains unaffected at all concentrations.

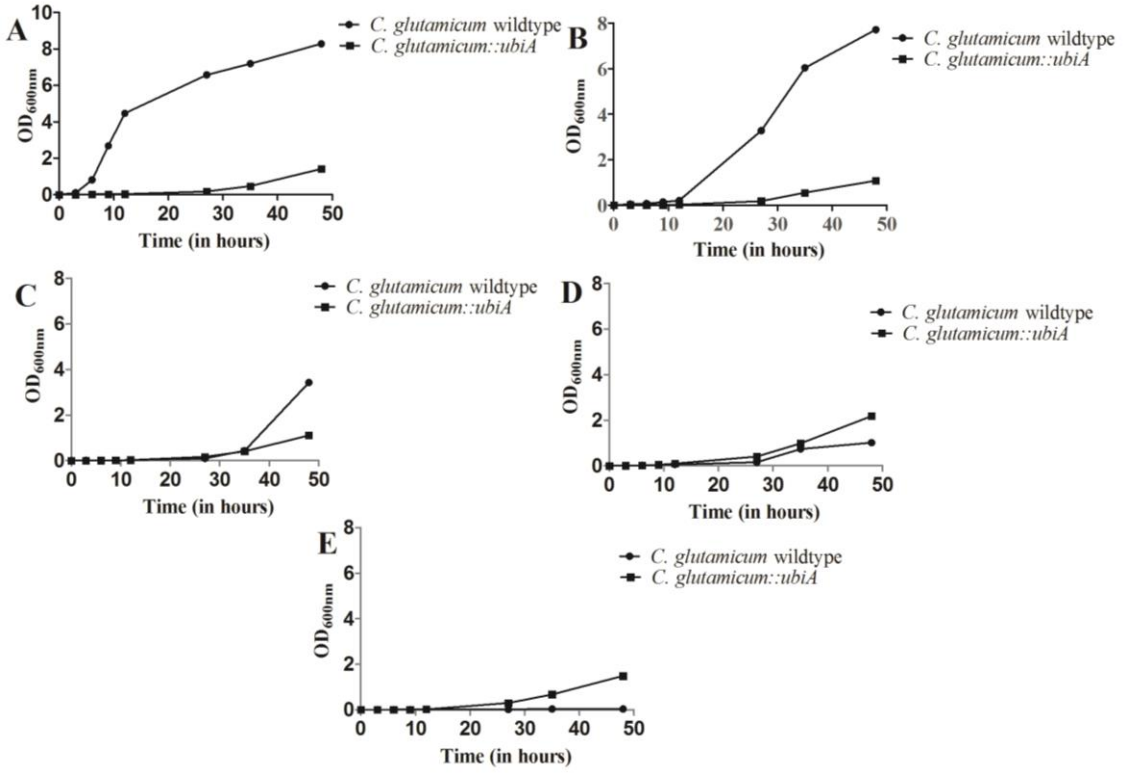

Figure 2.3: Comparison of growth rate and susceptibility to BTZ043 of *C. glutamicum* wild type and *C. glutamicum::ubiA*. A. *C. glutamicum::ubiA* is a slow growing strain in comparison to wild type. A decrease in growth rate of *C. glutamicum* wild type was observed for concentrations **B.** 1 µg/mL, **C.** 4 µg/mL, **D.** 10 µg/mL until the growth completely stalled at **E.** 20 µg/mL. The data is representative of two separate experiments.

Since OD_{600} is a measure of both viable and non-viable cells, cell viability assays were performed for *C. glutamicum* and *C. glutamicum*::*ubiA* against increasing concentrations of BTZ043 to estimate the viable population for each strain (Figure 2.4). The results demonstrate that BTZ043 elicits a 1000-fold decrease in cell viability against *C. glutamicum* in comparison to *C. glutamicum*::*ubiA* with no observable effect on cell viability. Therefore, *C. glutamicum::ubiA* was determined to be resistant to BTZ043 in comparison with the sensitive wild type *C. glutamicum* strain.

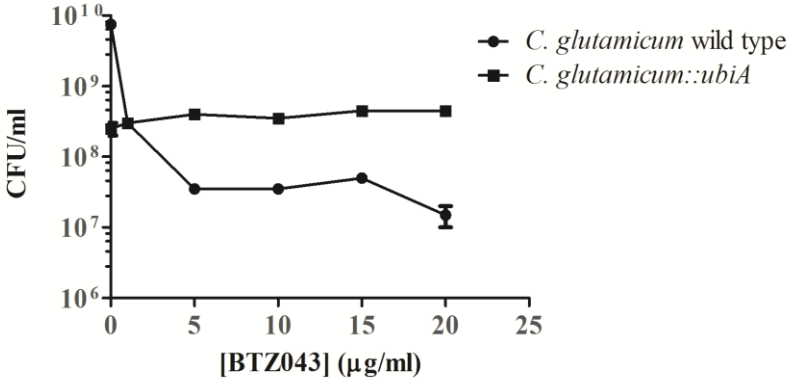

Figure 2.4: Effect of BTZ043 on of viability of *C. glutamicum* and *C. glutamicum::ubiA*. The cell viability of *C. glutamicum* and *C. glutamicum::ubiA* was tested at a range of BTZ043 concentrations (0, 1, 5, 10, 15, 20 µg/mL) by spotting approximately 10^8-10^9 cells on BHI agar plates incubated at 30°C for 48 hours after treatment with 20 µg/mL BTZ043. The data is representative of three biological replicates.

2.3.2 BTZ043 inhibits DPA synthesis in *C. glutamicum* and *C. glutamicum::ubiA* with a functional DprE1

The *C. glutamicum::ubiA* though defective in DPA biosynthesis retains a functional copy of the BTZ target, DprE1. To biochemically evaluate the effect of BTZ043 on DprE1, membrane extracts were prepared from *C. glutamicum* and *C. glutamicum::ubiA* and were examined for their ability to generate DPA in absence and presence of BTZ043. In the initial experiments, p[^{14}C]Rpp was supplemented as an exogenous substrate with extracts to monitor the conversion of p[^{14}C]Rpp to DP[^{14}C]R and DP[^{14}C]A. The reaction products were analysed using thin-layer chromatography (TLC) followed by phosphorimaging (Figure 2.5). Analysis of the radiolabelled products by TLC clearly demonstrates that *C. glutamicum* is able to utilise p[^{14}C]Rpp as a substrate and synthesise DP[^{14}C]A (Figure 2.5, lane 3). However, this conversion to DP[^{14}C]A is inhibited when reaction mixtures are incubated with BTZ043, affording only DP[^{14}C]R (Figure 2.5, lane 2). As expected, no [^{14}C]-products were evident when reactions were carried out using membranes prepared from *C. glutamiucm*::*ubiA* either

in the absence or presence of BTZ043 (Figure 2.5, lane 4 and 5). This inability of *C. glutamiucm*::*ubiA* to synthesise DPR/DPA is attributed to the absence of decaprenylphosphoryl-5-phosphor-β-D-ribose synthase UbiA, that is required for transfer of ribose-5-phosphate from p[^{14}C]Rpp to decaprenyl phosphate, and marks the first step in DPR/DPA biosynthesis (Alderwick *et al.*, 2011b).

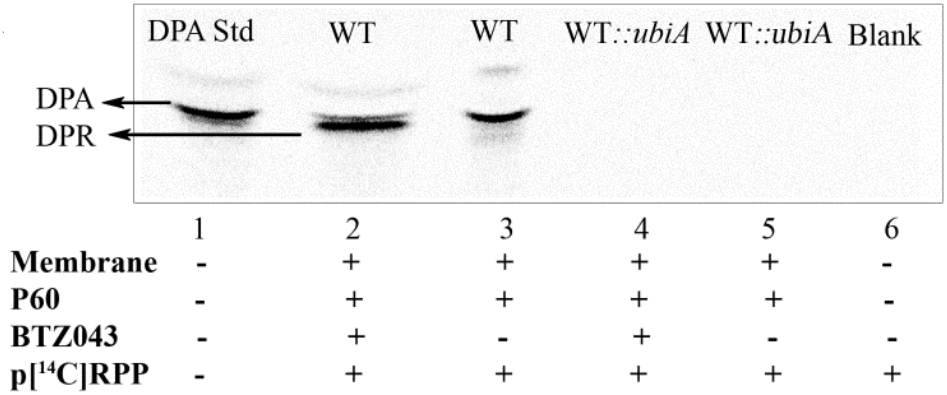

Figure 2.5: *C. glutamicum::ubiA* is deficient in DPA synthesis. Membrane and "P60" extracts prepared from *C. glutamicum* (WT) and *C. glutamicum::ubiA* (WT*::ubiA*) were examined for their ability to generate DP[^{14}C]A from p[^{14}C]Rpp in the absence and presence of BTZ043 (20 µg/mL). Preparations from *C. glutamicum* were capable of synthesising DP[^{14}C]A (lane 3) and inhibited in assays that included BTZ043 (lane 2). No [^{14}C]-products were apparent in preparations from *C. glutamicum::ubiA* (lane 4 and 5).

The strains *C. glutamicum* and *C. glutamicum*::*ubiA* were biochemically examined for their endogenous DprE1 activity by exogenously supplying DP[^{14}C]R as a substrate in the absence and presence of BTZ043. Extracted reaction products were separated by TLC and analysed by phosphorimaging. The results highlight that membrane extracts from *C. glutamicum* and *C. glutamicum*::*ubiA* strains are equally capable of synthesising DP[^{14}C]A (Figure 2.6 lane 2 and 4). However in presence of BTZ043, no DP[^{14}C]A is produced by either of the strains indicating that both *C. glutamicum* and

C. glutamicum::*ubiA* express a functional copy of DprE1 that is effectively inhibited by BTZ043 (Figure 2.6 lane 3 and 5).

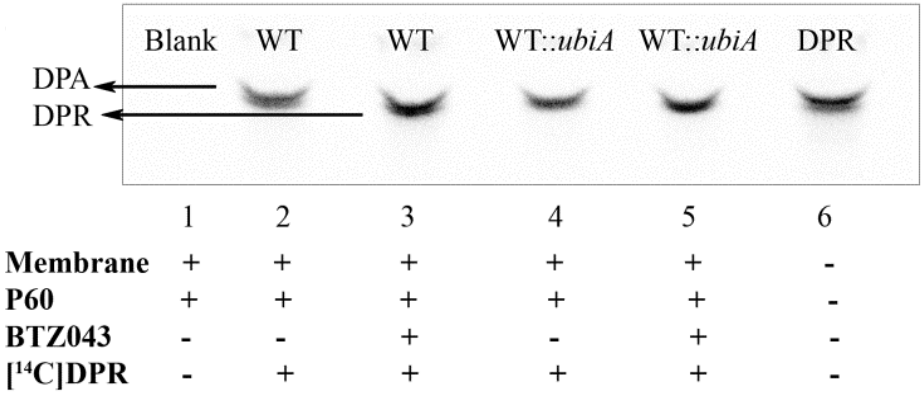

	1	2	3	4	5	6
Membrane	+	+	+	+	+	-
P60	+	+	+	+	+	-
BTZ043	-	-	+	-	+	-
[^{14}C]DPR	-	+	+	+	+	-

Figure 2.6: DprE1 is effectively inhibited by BTZ043 in *C. glutamicum* and *C. glutamicum::ubiA*. Membrane and "P60" extracts prepared from *C. glutamicum* (WT) and *C. glutamicum::ubiA* (WT*::ubiA*) were examined for their ability to generate DP[^{14}C]A from exogenously supplied DP[^{14}C]R in the absence and presence of BTZ043 (20 µg/mL). Formation of DP[^{14}C]A was observed for both the strains in absence of BTZ043 (lane 2 and 4), whilst complete inhibition was apparent when extracts were supplemented with BTZ043 (lane 3 and 5), indicating the presence of a fully functional DprE1 in *C. glutamicum::ubiA*.

These findings highlight a stark contrast in the ability of BTZ043 to have an effect on viability of *C. glutamimcum* and *C. glutamicum::ubiA* in liquid media even though the target enzyme DprE1 is functionally intact in both the strains. As evident, this synthetic viable phenotype is a result of interruption of *ubiA* that renders *C. glutamicum* insensitive to BTZ043. These results also suggest that DprE1 inhibition by BTZ043 may not be the sole cause of cell death.

Alternatively, we hypothesise that BTZ043 primarily causes an accumulation of DPR in *C. glutamicum* that subsequently results in a failure by the cell to recycle decaprenyl phosphate. Inhibition of decaprenyl phosphate recycling and its limited availability for other cellular process severely disrupts growth in *Corynebacterianane*. The lethal effect of BTZ043 is removed in *C. glutamicum*::*ubiA* as the strain does not produce

DPPR as a precursor to DPR, thus allowing for the recycling of decaprenyl phosphate to occur. This recycling is critical for other major cellular processes that employ decaprenyl phosphate based donors, such as the peptidoglycan biosynthesis.

2.3.3 Over-expression of Cg-*uppS*, a prenylphosphate synthase in *C. glutamicum*

The protein BLAST search revealed NCgl2203 as the *C. glutamicum* orthologue of MTB Z-decaprenyl diphosphate synthase with 65% identity between the sequences. The gene *NCgl2203* was amplified, cloned in expression vector pVWEx2 and transformed into *C. glutamicum* wild type. The gene expression was induced by 0.5mM IPTG and cell pellets were used to prepare membrane and cytosolic fractions. The fractions were resolved on 12% SDS-PAGE gels (Figure 2.7). The membrane (Lane 3) and cytosol (Lane 4) preparations from *C. glutamicum* pVWEx2-*uppS* revealed a concentrated band at 28.23 kDa corresponding to Cg-UppS.

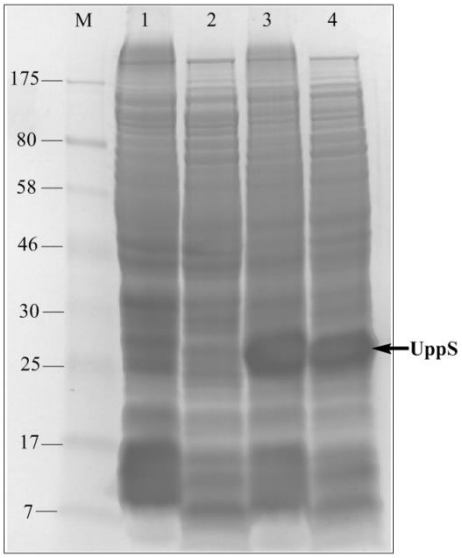

Figure 2.7: Over-expression of Cg-UppS. NCgl2203 (UppS) was cloned in pVWEx2 and over-expressed in *C. glutamicum* wild type. UppS expression was checked in wild type (Lane 1 & 2) and in over-expressed strain (Lane 3 & 4). Both membrane (Lane 3) and cytosolic (Lane 4) of *C. glutamicum* pVWEx2_*uppS* showed over-expression of UppS (28.23 kDa).

2.3.4 Over-expression of Cg-*uppS* protects *C. glutamicum* from inhibition by BTZ043

From the data it is apparent that distribution of decaprenyl phosphate into the pathways for DPA and lipid II formation which are employed in AG and peptidoglycan biosynthesis is highly equilibrated. To determine the role of decaprenyl phosphate in cell wall biosynthesis, decaprenyl phosphate synthase *uppS* (*NCgl2203*) was over-expressed by transforming *C. glutamicum* with pVWEx2-*uppS*. Since decaprenyl phosphate is synthesised in regulated amounts in a healthy cell, the over-expressed strain was examined for any growth defects when compared to wild type (Figure 2.8). The over-expressed strain showed growth kinetics akin to wild type and eliminated the possibility of any toxicity resulting from increased decaprenyl phosphate synthesis.

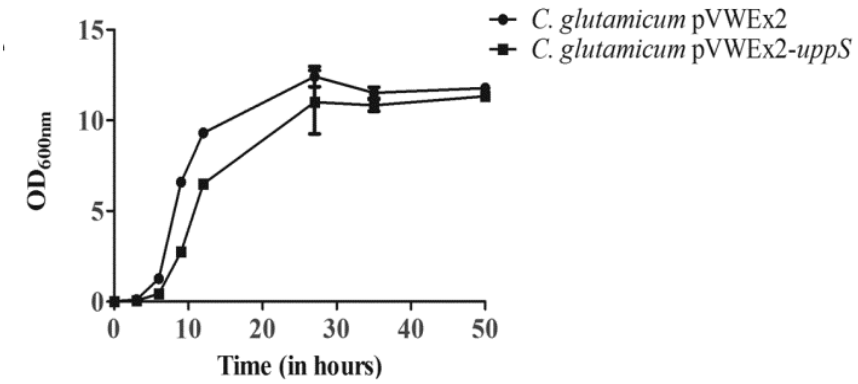

Figure 2.8: Over-expression of Cg-*uppS* is non toxic. The growth rates of both *C. glutamicum* and *C. glutamicum*-pVWEx2-*uppS* were monitored in BHI liquid media for 48 hours to check the effect of over-expression. The strains exhibited comparable growth rates with no visible harmful effects. The data is representative of three biological replicates.

The growth and viability of both *C. glutamicum*-pVWEx2 and *C. glutamicum*-pVWEx2-*uppS* was also examined by exposing the strains to BTZ043 at 1 x MIC and 2 x MIC in liquid media for 48 hours and the end-point readings for optical density

(Figure 2.9) and cell viability (Figure 2.10) were measured. As expected, BTZ043 inhibits the growth of *C. glutamicum*-pVWEx2 at a concentration of 1 x MIC and 2 x MIC. The decaprenyl phosphate over-expressing strain *C. glutamicum*-pVWEx2-*uppS* on the other hand displayed a significantly increased resistance to BTZ043 with a MIC >40 µg/mL (Figure 2.9).

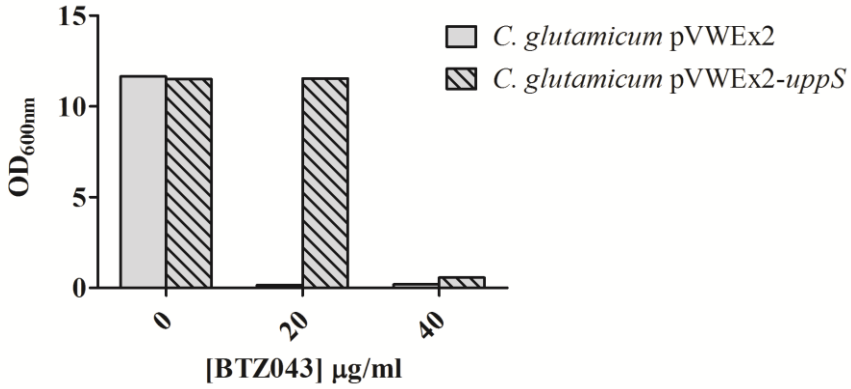

Figure 2.9: Effect of BTZ043 on growth of *C. glutamicum*-pVWEx2 and *C. glutamicum*-pVWEx2-*uppS*. The growth of *C. glutamicum*-pVWEx2 and *C. glutamicum*-pVWEx2-*uppS* was measured in the presence of BTZ043 at 1 x MIC (20 µg/mL) and 2 x MIC (40 µg/mL). The optical density (OD_{600}) obtained for *C. glutamicum*-pVWEx2-*uppS* was higher than *C. glutamicum*-pVWEx2 at both 1 x MIC and 2 x MIC, indicating increased tolerance to BTZ043. The data is representative of three biological replicates.

To estimate the proportion of viable cells for each strain, the cultures were pre-treated with BTZ043 at MIC (20 µg/mL) and 2 x MIC (40 µg/mL) incubated for 48 hours, serially diluted and spotted on BHI plates with tetracycline (10 µg/mL) and the colony forming units were determined. As expected, the viable counts for *C. glutamicum*-pVWEx2-*uppS* were 10^4-fold higher than *C. glutamicum*-pVWEx2 at the MIC (20 µg/mL) and 10^6 fold higher at 2 x MIC (40 µg/mL) of BTZ043, respectively (Figure 2.10). These results indicate that Cg-UppS prenylphosphate synthase, when over-expressed could rescue *C. glutamicum*-pVWEx2 from inhibition by BTZ043.

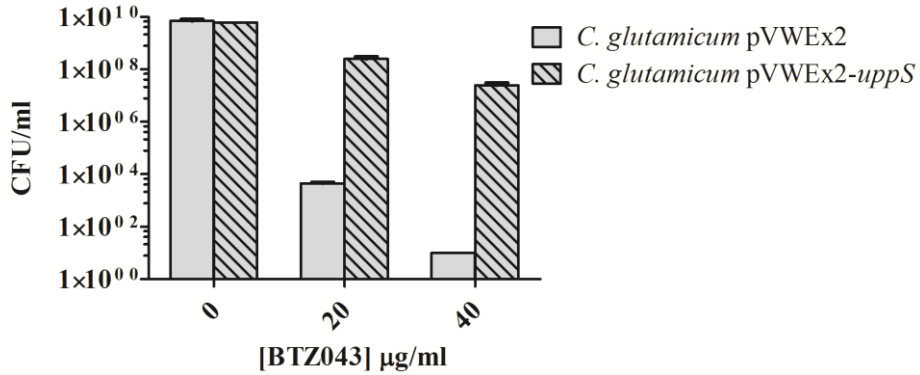

Figure 2.10: Effect of BTZ043 on viability of *C. glutamicum*-pVWEx2 and *C. glutamicum*-pVWEx2-*uppS*. Cell viability counts were determined for *C. glutamicum*-pVWEx2 and *C. glutamicum*-pVWEx2-*uppS* treated with BTZ043 at 1x MIC and 2x MIC after plating on BHI agar plates incubated at 30ºC for 48 hours. The data is representative of three biological replicates.

2.3.5 UppS over-expression increases decaprenyl phosphate synthesis in *C. glutamicum*

To biochemically determine the effect of UppS over expression on *C. glutamicum*, membrane and cytosol extracts from *C. glutamicum*-pVWEx2 and *C. glutamicum*-pVWEx2-*uppS*, were examined for their ability to synthesise decaprenyl phosphate in the absence and presence of BTZ043. The isoprenyl pyrophosphate synthases in mycobacteria and corynebacteria use allylic diphosphates to generate the decaprenyl phosphate lipid carrier. To initiate the pathway, DMAPP functions as an allylic primer to which IPP is repeatedly added by these isoprenyl pyrophosphate synthases until a prenyl diphosphate of a defined length and stereochemistry is generated. Therefore, to estimate the activity of the decaprenyl phosphate synthase UppS, [^{14}C]-isopentenyl pyrophosphate ([^{14}C]-IPP) was supplied as an exogenous substrate with membrane and cytosolic extracts to monitor the conversion of [^{14}C]-IPP to [^{14}C]-decaprenyl phosphate. The products were evaluated using TLC followed by phosphor imaging (Figure 2.11). Analysis of the [^{14}C]-products by TLC clearly demonstrates that *C.*

glutamicum is able to utilise [^{14}C]-IPP and generate [^{14}C]-decaprenyl phosphate as the product (Figure 2.11).

Densitometric analysis of the bands migrating on the TLC that correspond to decaprenyl phosphate was performed for *C. glutamicum*-pVWEx2 and *C. glutamicum*-pVWEx2-*uppS*. The proportion of counts for [^{14}C]-decaprenyl phosphate was calculated from a total of 20,000 cpm loaded *per* reaction as apparent on the TLC and from the total cpm value as returned by the assay. The strain *C. glutamicum* produced 481±72 cpm/µg protein whlist the amount of [^{14}C]-decaprenyl phosphate increased by 77% (853±16 cpm/µg of protein) when *uppS* was over-expressed. These results are illustrated by an increase in density of the decaprenyl phosphate on the TLC for *C. glutamicum*-pVWEx2-*uppS* (Figure 2.11). When reactions were performed with membrane and cytosol extracts, pre-treated with 20 µg/mL of BTZ043, a reduction in the synthesis of the decaprenyl phosphate pool was apparent in wild type *C. glutamicum*-pVWEx2 whilst no significant change could be observed for *C. glutamicum*-pVWEx2-*uppS*, when compared to assays conducted in the absence of BTZ043 (Figure 2.11). To estimate the actual proportion of counts incorporated into decaprenyl phosphate *per* reaction, the fraction of decaprenyl phosphate turn over as estimated from the TLC were applied to the total counts recovered for each reaction. These estimates highlighted a small, yet significant increase in the synthesis of decaprenyl phosphate for BTZ043 treated reactions, which equates to 8% and 10% for *C. glutamicum*-pVWEx2 and *C. glutamicum*-pVWEx2-*uppS*, respectively. These results suggest that BTZ043 inhibits DprE1 activity and results in a block in DPA biosynthesis, which prevents decaprenyl phosphate to be recycled back into the cellular

pool. In absence of this recycling, synthesis of other decaprenyl phosphate-linked intermediates such as PPM and lipid II, required for cell wall biosynthesis is affected.

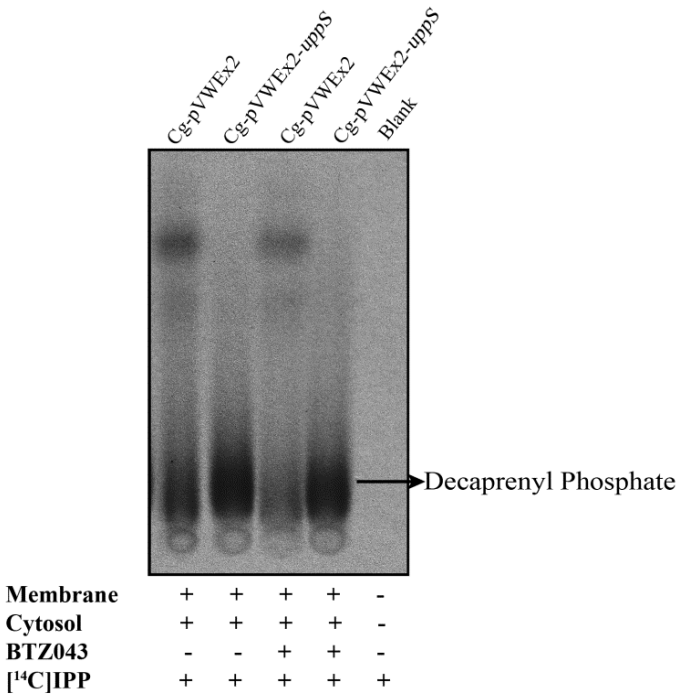

Figure 2.11. Over-expression of *uppS* in *C. glutamicum* elicits an increase in decaprenyl phosphate synthesis. Cell free extracts prepared form *C. glutamicum*-pVWEx2 (Cg-pVWEx2) and *C. glutamicum*-pVWEx2-*uppS* (Cg-pVWEx2-*uppS*) were examined for any increased biosynthesis of decaprenyl phosphate in the presence and absence of BTZ043 (20 μg/mL), by supplementing assay mixtures with exogenous [^{14}C]IPP. Assays were quenched after 1 hour incubation at 30°C and reaction products were extracted with organic solvent. Equal counts (20,000 cpm) were loaded onto a reverse phase silica gel plates (silica gel 60 RP-18 $F_{254}S$, Merck) developed in methanol/acetone (8:2, v/v) and visualised by phosphor imaging.

2.3.6 Over-expression of UppS restores AG biosynthesis in *C. glutamicum* treated with BTZ043

Since BTZ043 targets DPA biosynthesis, the sole arabinose donor for cell wall arabinan synthesis, arabinose containing cell wall components AG and LAM were assessed for incorporation of arabinose in the presence of BTZ043 in strains *C. glutamicum*-pVWEx2 and *C. glutamicum*-pVWEx2-*uppS* (Figure 2.12). The cultures were labelled with [^{14}C]-glucose and mAGP complex was prepared from samples collected at 48 hours from BTZ043 (15 µg/mL) treated and non-treated cultures. Mild acid treatment of the mAGP complex was performed and the distribution of radioactivity between [^{14}C]-arabinose, [^{14}C]-mannose and [^{14}C]-galactose was estimated after separation by TLC followed by autoradiography. Chromatographic analysis show a reduced incorporation of arabinose in AG for *C. glutamicum*-pVWEx2 treated with BTZ043. However, no significant changes were observed in the level of arabinose being incorporated in *C. glutamicum*-pVWEx2-*uppS* upon exposure to BTZ043. The TLC analysis of hydrolysed cell wall preparations also showed presence of mannose, which we apportion to being an impurity coming from LM and LAM contaminants. The galactan levels remain unchanged for both *C. glutamicum*-pVWEx2 and *C. glutamicum*-pVWEx2-*uppS* either treated or untreated with BTZ043 (Figure 2.12). Thus, *C. glutamicum*-pVWEx2-*uppS* was able to synthesise AG unhindered in the presence of BTZ043 at 0.75 x MIC.

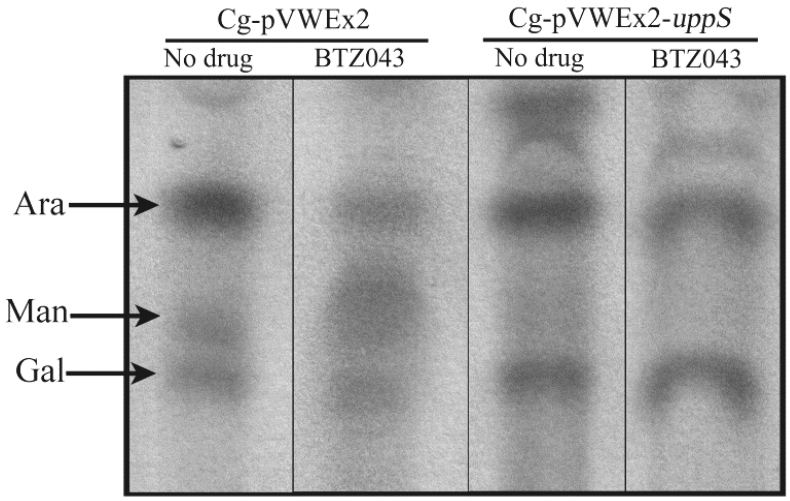

Figure 2.12: Effect of BTZ043 on AG biosynthesis in *C. glutamicum*-pVWEx2 and *C. glutamicum*-pVWEx2-*uppS*. Radioactive mAGP extracts were prepared from 0.75 x MIC BTZ043 (15 µg/mL) treated and untreated cultures of *C. glutamicum*-pVWEx2 (Cg-pVWEx2) and *C. glutamicum*-pVWEx2-*uppS* (Cg-pVWEx2-*uppS*) after 48 hours of treatment and were analysed for their sugar content. The [^{14}C]-arabinose content decreased in Cg-pVWEx2 treated with BTZ043 but remained unchanged for Cg-pVWEx2-*uppS*.

2.3.7 Over-expression of UppS restores LAM biosynthesis in *C. glutamicum* treated with BTZ043

Aside AG, LAM also utilises DPA for synthesis of the arabinan component. The strains *C. glutamicum*-pVWEx2 and *C. glutamicum*-pVWEx2-*uppS* were assessed for their ability to synthesise LAM in presence of BTZ043 (20 µg/mL) (Figure 2.13). The cultures of *C. glutamicum*-pVWEx2 and *C. glutamicum*-pVWEx2-*uppS* were labelled with [^{14}C]-glucose followed by treatment with BTZ043. The samples were removed every 2 hours from BTZ043 treated as well as non-treated cultures and lipoglycan extraction was performed. The presence of [^{14}C]-LAM was detected in SDS PAGE gels by autoradiography (Figure 2.13). The results demonstrate a significant reduction over time in LM and LAM synthesis for *C. glutamicum*-pVWEx2 cultures treated with BTZ043 (20 µg/mL), when compared to untreated cultures of *C. glutamicum*-pVWEx2 (Figure 2.13 A, B). However, the strain *C. glutamicum*-pVWEx2-*uppS* displayed

modest levels of LM and LAM when exposed to BTZ043 (20 µg/mL), as shown at 6 hours when compared to both *C. glutamicum*-pVWEx2 and *C. glutamicum*-pVWEx2-*uppS* treated with BTZ043 (Figure 2.13 C and D). Thus, *C. glutamicum*-pVWEx2-*uppS* was able to continually synthesise LAM in the presence of BTZ013 at 2 x MIC.

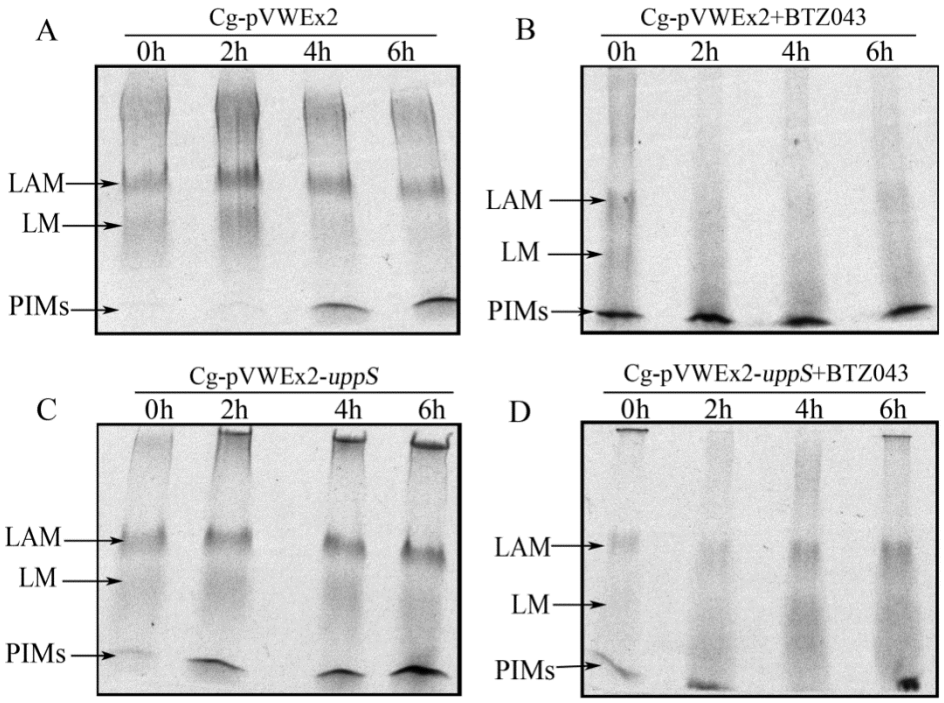

Figure 2.13: SDS PAGE analysis of lipoglycans extracts from A. *C. glutamicum*-pVWEx2 (Cg-pVWEx2), **B.** Cg-pVWEx2 treated with BTZ043, **C.** ***C****. glutamicum*-pVWEx2-*uppS* (Cg-pVWEx2-*uppS*) and **D.** Cg-pVWEx2-*uppS* treated with BTZ043. The cultures were grown in liquid media to an OD_{600} of 0.5 before the addition of [^{14}C]-glucose and BTZ043 (20 µg/mL). The growth was continued for upto 6 hours and lipoglycan extractions were performed for all samples.

2.4 Discussion

Benzothiazinones are newly discovered class of nitro-compounds with very high anti-tubercular activity (Makarov *et al.*, 2009). The lead compound of this series, BTZ043, was shown to target DprE1, a FAD-containing oxidoreductase that catalyses the conversion of DPR to DPX (Figure 2.14). The structural basis for DprE1 inhibition was recently determined using X-ray crystallography studies of the enzyme DprE1 in complex with BTZ043. These studies highlighted the importance of Cys387 residue in the active site which is responsible for forming a covalent semimercaptal linkage with the nitroso group in BTZ thus providing the basis for suicide inhibition by BTZ (Batt *et al.*, 2012; Neres *et al.*, 2012). DprE1 works in conjunction with a NADH-dependant reductase DprE2 that reduces DPX to DPA (Mikusova *et al.*, 2005). DPA is the sole arabinose donor that is utilised by an array of membrane embedded arabinofuranosyl transferases (Ara*f*Ts) that are employed for forming the D-arabinan, attached to LM and galactan and subsequently generating LAM and AG, respectively. Of the several Ara*f*Ts found in mycobacteria, EmbA, EmbB and EmbC, that are partly responsible for synthesis of the arabinan motif are targets for ethambutol, a front-line drug currently in use for TB treatment (Belanger *et al.*, 1996; Telenti *et al.*, 1997).

The high potency of BTZ043 and several other recently discovered unrelated compounds that target DprE1 have added onto its druggability factor and designated DprE1 as a ‘magic drug target’. Efforts are underway to develop new approaches for drug design and to identify other targetable characteristics of this enzyme. Whilst unlinking the PG layer from the outer layer of mycolic acids by targeting D-arabinan biosynthesis is a credible approach, it still doesn’t justify DprE1 as the ‘Achilles’ heel of MTB’. In this study, the enzyme DprE1 was thoroughly evaluated for its

susceptibility as a drug target and attempts were made to clarify its 'highly druggable' status.

The high degree of similarity in cell wall for MTB and *C. glutamicum* in terms of structure, biochemical processes and genetic make-up renders *C. glutamicum* as an excellent model organism for studying the molecular genetics of cell wall biogenesis in MTB (Alderwick *et al.*, 2006b; Dover *et al.*, 2004; Minnikin, 1978; Seidel *et al.*, 2007a; Varela *et al.*, 2012). Several mutants of *C. glutamicum* defective in cell wall arabinan biosynthesis have aided in understanding the processing of DPA. *C. glutamicum*::*ubiA* is one such mutant that displays an extremely intriguing phenotype of a cell wall completely devoid of arabinan and corynomycolates (Alderwick *et al.*, 2006a; Alderwick *et al.*, 2005; Tatituri *et al.*, 2007). This mutant when tested for its susceptibility to BTZ043 displayed no deleterious effects and was resistant to action of BTZ043 whilst high bactericidal activity was evident for *C. glutamicum* (MIC = 20 µg/mL). This stark contrast in findings questions the very basis of BTZ043 mediated killing by blocking D-arabinan biosynthesis in members of *Corynebacterineae.* To investigate the underlying cause of BTZ043 induced lethality, the enzyme UppS, a decaprenyl phosphate synthase, was over-expressed in *C. glutamicum* and its effect on bactericidal activity of the drug was monitored. The *Cg*-UppS over-expressed strain demonstrated increased tolerance to BTZ043 (Figure 2.9 and 2.10) ensuing upon augmented synthesis of decaprenyl phosphate which is required primarily for the production of lipid II, an essential intermediate involved in PG biosynthesis. These findings form the basis of an alternative hypothesis for BTZ's mechanism of action and suggest acute toxicity due to DPR accumulation and consequent halting of decaprenyl phosphate recycling as the primary cause for death (Figure 2.14). Accumulation of

DPR in cell membrane represents a metabolic 'dead end' in pathway for cell wall biogenesis. This data is in accordance with our previous observations that although *C. glutamicum* has a cell wall with enough plasticity to dispense with D-arabinan, it still requires PG to protect against the internal osmotic stress across the cytoplasmic membrane (Moker *et al.*, 2004; Radmacher *et al.*, 2005).

Interestingly, osmotic stress is apparent on BTZ treatment in *M. tuberculosis* H37Rv as demonstrated by swelling and ultimately bursting of the cells due to a weakened cell wall (Makarov *et al.*, 2009). In addition, the increase in susceptibility to many late-acting cell wall antibiotics, such as β-lactams and to the PG inhibitors fosfomycin and D-cycloserine, as a consequence of a decrease in the expression of *uppS* has already been reported in *Bacillus subtilis.* The enzyme UppS *in B. subtilis* generates undecaprenyl phosphate (C_{55}-P), the major polyprenyl carrier for PG and teichoic acid synthesis (D'elia *et al.*, 2009; D'elia *et al.*, 2006; Lee and Helmann, 2013). Furthermore, similar effects have also been reported in *Staphylococcus aureus*, whereby Targocil, a teichoic acid biosynthesis inhibitor, results in accumulation of undecaprenyl-linked intermediates, thus preventing recycling of the undecaprenyl-phosphate lipid carrier (Campbell *et al.*, 2012). The cell wall deficient bacteria, such as Mycoplasma, lack the necessary enzymes for synthesis and condensation of IPP, the precursor molecule for prenyl phosphate synthesis (Henrickson, 1966; Lange *et al.*, 2000). Whilst L-forms such as *Rickettsia prowazekii* is lacking in enzymes for IPP synthesis (Andersson *et al.*, 1998), the other member *Borrelia burgdorferi* contains highly divergent and uncharacterized genes encoding enzymes in IPP synthesis *via* the mevalonate pathway (Lange *et al.*, 2000).

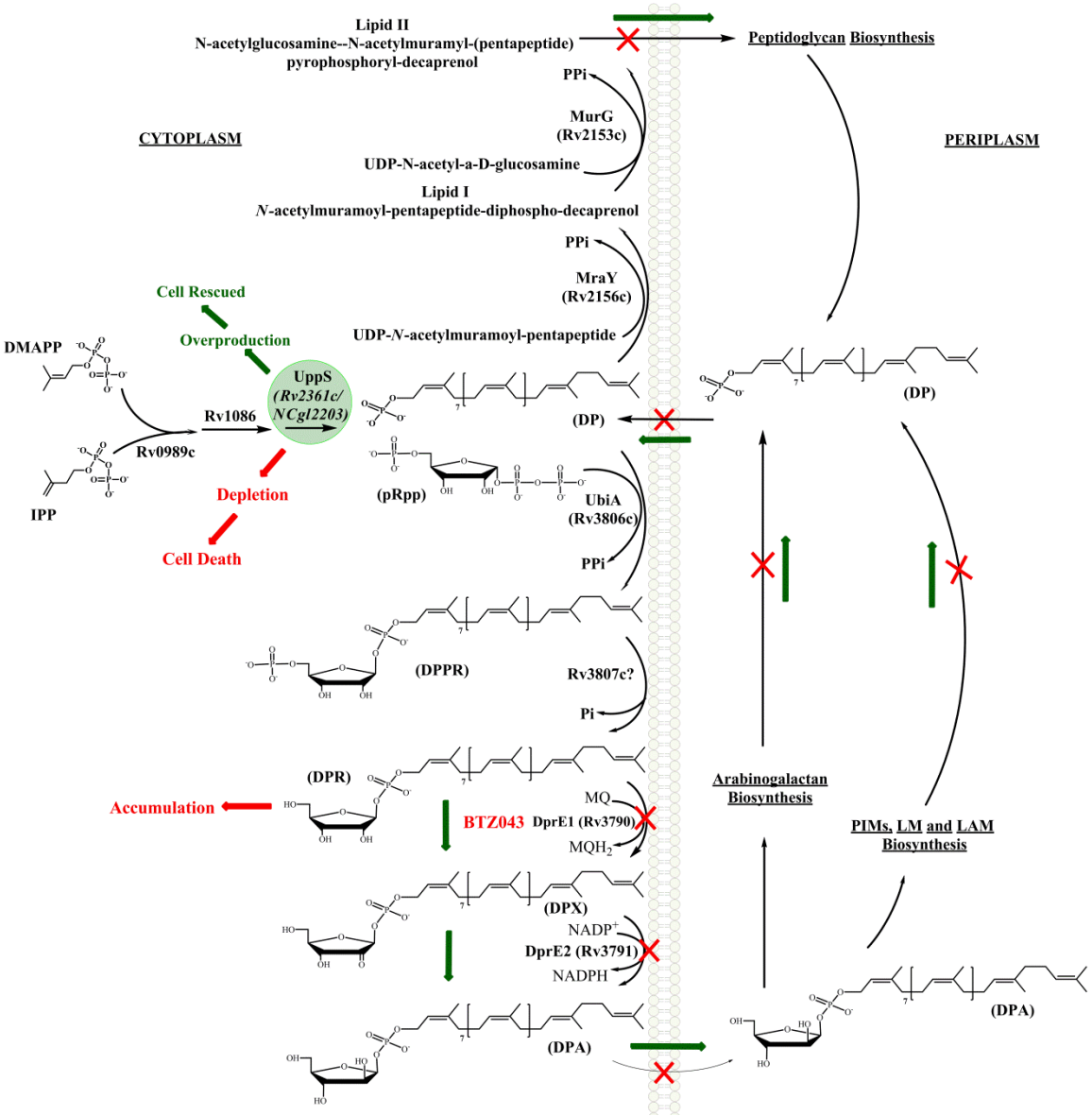

Figure 2.14. A schematic representation of the proposed mechanism of decaprenyl phosphate recycling. The lipid carrier decaprenyl phosphate is employed in biogenesis of peptidoglycan (PG), lipoarabinomannan (LAM) and arabinogalactan (AG) pathways in the form of Lipid II and DPA. Synthesis of DPA is crucial for producing the arabinan component of LAM and AG and is initiated by transfer of ribose phosphate from pRPP to decaprenyl phosphate and follows the pathway (black) where DprE1/E2 generates DPA from DPR. Treatment with BTZ043 (red) results in accumulation of DPR, thus stalling LAM and AG biosynthesis and blocking the decaprenyl phosphate recycling. This block interrupts the channelling of decaprenyl phosphate for Lipid II formation, thus affecting PG biosynthesis. The weakened cell wall is unable to bear osmotic stress arising from DPR toxicity and leads to cell lysis. Over-expression of UppS, the prenyl synthase (green) restores the recycling by supplementing enough decaprenyl phosphate for synthesis of cell wall components.

In addition to Lipid II, members of *Corynebacterineae*, such as *M. tuberculosis* and *C. glutamicum,* employ decaprenyl phosphate for generating the sugar donors, DPA and decaprenyl phosphomannose (DPM). Whilst DPA is directed for formation of D-arabinan in AG and LAM, DPM is utilised for synthesis of mannan in LM and LAM. Therefore, the effect of *uppS* overexpression was examined on these polysaccharides upon exposure to BTZ043 (15 µg/mL). The total sugar content from mAGP fractions prepared from *C. glutamicum*-pVWEx2 was analysed for distribution of radioactivity in sugars. As expected, an overall reduction in arabinose content was evident for BTZ043 treated samples mainly due to BTZ mediated inhibition of DPA synthesis. However, by over-expressing *uppS*, the effect of the drug on *C. glutamicum* could be evaded as [^{14}C]-arabinose was effectively incorporated into mAGP (Figure 2.12). Similarly, when lipoglycans were isolated from BTZ043 treated *C. glutamicum*-pVWEx2, a sharp decrease in radioactivity was observed for both LM and LAM. However, when *uppS* was overexpressed, LM and LAM were unaffected (Figure 2.13). These results demonstrate the ability of UppS to restore arabinan and mannan synthesis in the cell wall components by evading the action of the drug and challenge the prevailing notion on BTZ's mechanism of action.

Since BTZ is a newly discovered class of anti-tubercular compounds, our understanding of the mechanisms of resistance to this drug is fairly superficial. Natural resistance to BTZ is prevalent in mycobacterial species, such as *M. avium* and *M. aurum* and is attributed to the occurrence of a single mutation, Cys387 in DprE1 that substitutes Cys with an Ala in *M. avium* or Ser in *M. aurum* (Makarov *et al.,* 2009). Furthermore, BTZ043's activation requires reduction of the nitro-group to an electrophilic nitroso-derivative in order to react with the Cys387 residue in the active

site of DprE1 (Batt *et al.*, 2012). The activation of BTZ043 is catalysed either by DprE1 itself or by other oxygen sensitive nitroreductases (Manina *et al.*, 2010). This property of BTZ has also revealed an alternative mechanism for resistance to the drug mediated by bacterial nitroreductases such as NfnB that reduce the nitro group to the corresponding amine as observed in case of *M. smegmatis* (Manina *et al.*, 2010).

The results obtained from this study imply that increased expression of decaprenyl phosphate synthase (*uppS*) might provide a unique mechanism for *Corynebacterineae,* to become resistant to BTZ. Over-expression of prenylphosphate synthase, UppS generates DprE1 substrate DPR in increased amounts that out-competes BTZ043 at the active site of the enzyme. Consequently, accumulation of DPR is impeded and DPA synthesis is restored. Restoration of DPA synthesis imparts integrity to the cell wall whilst ensuring continuous recycling of decaprenyl phosphate pool. In this regard, UppS might also serve as an effective drug target since its role is crucial in synthesis of a variety of mycobacterial cell wall components.

Chapter 3

3 IpsA, a novel LacI-type regulator, is required for inositol-derived lipid formation in Corynebacteria and Mycobacteria

3.1 Introduction

The cell envelope of the human pathogens *M. tuberculosis* and *Corynebacterium diphtheriae*, of the order *Corynebacteriales,* play an important role in virulence and also confer resistance against current therapies (Mishra *et al.*, 2011c). The development of new drugs against tuberculosis and diphtheria infections is focused on enzymes and regulatory mechanisms involved in the biogenesis of the cell envelope. The plasma membrane of mycobacteria and corynebacteria are rich in phospholipids, such as PI that plays a role in the biosynthesis of glycolipids and lipoglycans. The PI anchors the PIMs together with LM and LAM to the plasma membrane and also serves as the scaffold for these components. Inositol, an essential polyol in eukaryotes, is present only in the order *Corynebacteriales* where it forms a constituent of structural components of the cell wall and serves as a building block of mycothiol (MSH), the major antioxidant in mycobacteria (Fahey, 2013).

In mycobacteria, the three step process for synthesis of PI is initiated by cyclisation of glucose-6-phosphate to *myo*-inositol-1-phosphate, catalysed by inositol phosphate synthase InO1 (*Rv0046c*) (Bachhawat and Mande, 1999a). In the second step, *myo*-inositol-1-phosphate is dephosphorylated by inositol mono-phosphatase (IMP) (Nigou and Besra, 2002), to yield *myo*-inositol. The transfer of DAG from CDP-DAG to *myo*-inositol by PI synthase, PgsA (*Rv2612c*) forms the third step of the pathway (Movahedzadeh *et al.*, 2010). The enzymes, inositol phosphate synthase, PI synthase, Ino1 and PgsA, are essential for viability of mycobacteria (Jackson *et al.*, 2000;

Movahedzadeh *et al.*, 2004a). In addition, an *ino1* mutant of *M. tuberculosis* could only survive in high concentrations of inositol and was no longer virulent in SCID mice (Haites *et al.*, 2005b). Therefore, Ino1 has been proposed as a target for developing new antibiotics (Hernick, 2013; Movahedzadeh *et al.*, 2004b).

In contrast to the wealth of knowledge about the biogenesis of the Corynebacterium cell wall, little is known about the regulatory circuits that control these processes (Morita *et al.*, 2011). In this study, we have examined the function of a novel transcriptional regulator IpsA, encoded by *Cg2910 (NCgl2538)* in *C. glutamicum.* We propose IpsA, as a novel LacI-type regulator that acts as an inositol-dependent transcriptional activator of the *myo*-inositol-phosphate synthase, *ino1*. Its function is conserved throughout corynebacteria and mycobacteria, including the prominent pathogenic species *C. diphtheria* and *M. tuberculosis*. The transcriptional regulators of Lac-I family are characterised by a distinct helix-turn-helix motif in the DNA binding N-terminal domain. The central region binds the sugar inducer whilst C-terminus aids in formation of a tetramer. The regulators in this class can function either as repressors such as, LacI in lac operon, CcpB in several operons in *B. subitilis* or as activators of gene transcription for example DegA in degradation of pRPP amidotransferase in *B. subitils* (Bussey and Switzer, 1993; Nguyen and Saier, 1995) . LacI family of transcriptional regulators also includes transcriptional factors with dual activity such as CcpA in *B. subtilis* and FruR in *E. coli* that functions both as a repressor and as an activator to direct carbon metabolism (Henkin, 1996; Ramseier *et al.*, 1995). The structure of IpsA (PDB:3H5T) from *C. glutamicum* was resolved recently. Structual analysis of IpsA revealed a helix-turn-helix motif in the DNA binding domain that designated it as a regulator of LacI family.

In this study, we have characterised the *ipsA* deletion mutant of *C. glutamicum* and its possible homologues in *C. diphtheria* (*DIP1969*) and in *M. tuberculosis* (*Rv3575c*). Targets of IpsA with putative functions in cell wall biogenesis were identified and a conserved palindromic motif within the corresponding promoter regions was designated as the binding site. *Myo*-inositol was identified as an effector for IpsA as it led to dissociation of the IpsA-DNA complex *in vitro*. The deletion mutant showed growth defects when cultured on glucose and presented elongated cell morphology. Analysis of the cell wall lipid composition revealed the absence of ionsitol-derived lipids including PI, PIMs and LAM. The cells were completely devoid of any mycothiol.

This work was performed in collaboration with Meike Baumgart, Kerstin Luder, Cornelia Gätgens and Julia Frunzke at Institut für Bio- und Geowissenschaften, IBG-1: Biotechnologie, Forschungszentrum Jülich, Jülich, Germany. MB designed and coordinated the study, constructed the mutant, performed the microarray experiments and fluorescence microscopy and prepared the figures. KL and CG carried out the recombinant DNA work, EMSAs, protein purification, promoter fusion studies and growth experiments. SG and GSB performed and analysed the cell wall lipid studies. This work has been published in BMC Biology, 2013 (Baumgart *et al.*, 2013a).

3.2 Materials and Methods

3.2.1 Bacterial strains, plasmids and growth media

All *C. glutamicum* strains used in this study unless specified were grown in Brain Heart Infusion broth (BHI, Sigma-Aldrich) at 30°C. *E. coli* DH5α was grown in Luria-Bertani broth (LB, Difco) at 37°C. The wild type *C. glutamicum* strain ATCC 13032 was used for construction of mutants. All cloning experiements were performed in *E coli* DH5α cultivated at 37 °C in LB broth, (Sambrook and Russell, 2001) supplemented with 50 µg/mL kanamycin.

3.2.2 Growth experiments

For growth experiments, 5 mL of BHI broth (Difco Laboratories) was inoculated with a colony from a fresh BHI agar plate and incubated for 6-8 hours at 30°C and 220 rpm. Cells from this pre-culture were washed once in phosphate buffered saline (PBS, 137 mM NaCl, 2.7 mM KCl, 4.3 mM Na_2HPO_4, 1.4 mM KH_2PO_4, pH 7.3) and used to inoculate a second pre-culture, consisting of 20 mL CGXII minimal medium (Keilhauer *et al.*, 1993) supplemented with 3,4-dihydroxybenzoate (30 mg/L) as an iron chelator and 2 % (w/v) glucose as a carbon source, to an OD_{600} of about 1. For sequential cultivation, the cells from this culture were diluted in fresh medium to a starting OD_{600} of 1 and incubated overnight at 30°C and 120 rpm. These cultures were then used to set up main cultures that were inoculated to an OD_{600} of about 1 and incubated at 30°C and 120 rpm in a Biolector (m2p-labs, Baesweiler, Germany) in 48-well FlowerPlates containing 750 µL CGXII minimal medium and different carbon sources, as specified in the results section. For induction of the expression of genes under the control of the P_{tac}-promoter, IPTG was used at the concentrations specified.

Where appropriate, the medium was supplemented with 25 µg/mL kanamycin. All the strains constructed and utilised in this study are listed in Table 3.1.

Table 3.1: Strains and plasmid constructs used in this study (Data provided by Baumgart *et al*.)

Strain or plasmid	Relevant characteristics	Source or Reference
M. tuberculosis H37Rv	wild-type laboratory strain, DNA used as PCR template	ATCC 25618
C. diphtheriae ATCC 27010	wild-type laboratory strain, DNA used as PCR template	DSM 44123
E. coli DH5α	F^- Φ80*dlac*Δ(*lacZ*)M15 Δ(*lacZYA-argF*) U169 *endA1 recA1 hsdR17* (r_K^- , m_K^+) *deoR thi-1 phoA supE44* λ^- *gyrA96 relA1*; strain used for cloning procedures	(Hanahan, 1983)
BL21(DE3)	F- *ompT hsdS*$_B$ (r_B-, m_B-) *gal dcm* (DE3); host for protein production	(Studier and Moffatt, 1986)
C. glutamicum ATCC13032	Biotin-auxotrophic wild type	(Kinoshita *et al.*, 1957)
ATCC13032 Δ*ipsA*	ATCC13032 with an in-frame deletion of *cg2910*	This work
ATCC13032::pK18int		This work
ATCC13032 Δ*ipsA*::pK18int		This work
ATCC13032::pK18int-*ipsA*		This work
ATCC13032 Δ*ipsA*::pK18int-*ipsA*		This work
ATCC13032 Δ*mshC*	ATCC13032 with a deletion of *cg1709*, defect in mycothiol biosynthesis	(Feng *et al.*, 2006)

Plasmids		
pK19*mobsacB*	Kan^R.; plasmid for allelic exchange in *C. glutamicum*; (pK18 *ori*$V_{E.c.}$, *sacB*, *lacZ*α)	(Schafer *et al.*, 1994)
pK19*mobsacB-ΔipsA*	Kan^R; pK19*mobsacB* derivative containing a PCR product covering the up- and downstream regions of *ipsA* (*cg2910*)	This work
pK18-int	Kan^R; plasmid for integration of foreign DNA into the intergenic region between *cg1121-cg1122* (*ori*$V_{E.c.}$, *sacB*, *lacZ*α)	(Baumgart *et al.*, 2013b)
pK18int-*ipsA*	Kan^R; plasmid for integration of the *ipsA* enconding region including the native promoter into the intergenic region between *cg1121-cg1122*	This work
pEKEx2-*eyfp*	Kan^R, pEKEx2 containing *eyfp* with artificial RBS, under control of P_{tac}	(Hentschel *et al.*, 2013)
pAN6	Kan^R; *C. glutamicum*/*E. coli* shuttle vector for regulated gene expression, derivative of pEKEx2	(Frunzke *et al.*, 2008)
pAN6-*ipsA*-STREP	Kan^R; pAN6-derivative for overproduction of IpsA with a C-terminal STREP-tag under control of the P_{tac} promoter	This work
pAN6-*Rv3575c*	Kan^R; pAN6-derivative for expression of Rv3575c (IpsA homolog from *M. tuberculosis*) under control of the P_{tac} promoter	This work
pAN6-*DIP1969*	Kan^R; pAN6-derivative for expression of DIP1969 (IpsA homolog from *C. diphtheriae*) under control of the P_{tac} promoter	This work
pAN6-*cg3323*	Kan^R; pAN6-derivative for expression of *ino1* under control of the P_{tac} promoter	This work

pET-TEV	Kan^R; pET28b derivative for over-expression of genes in *E. coli*, adding an N-terminal decahistdine tag and a TEV protease cleavage site to the target protein (pBR322 *ori*$V_{E.c.}$, PT7, *lacI*)	(Bussmann *et al.*, 2010)
pET-TEV-*ipsA*	Kan^R; pET-TEV derivative for overproduction of IpsA with an N-terminal decahistidine tag which can be cleaved off using TEV protease	This work
pJC1	Kan^R, Amp^R; *C. glutamicum/E. coli* shuttle vector	(Cremer *et al.*, 1991)
pXVENC-2	Kan^R, *oriT oriV*, P*xyl*, *venus*	(Thanbichler *et al.*, 2007)
pJC1-venus-term	Kan^R, pJC1 derivative carrying the venus coding sequence and additional terminators.	This work
pJC1-P*cg3323*-eYFP	Kan^R; pJC1-venus-term derivative carrying the promoter of *ino1* (*cg3323*) fused to *eyfp* for promoter activity studies.	This work

3.2.3 Recombinant DNA work

The *C. glutamicum* Δ*ipsA* mutant was constructed via a two-step homologous recombination protocol as described previously (Niebisch and Bott, 2001). For the construction of the deletion plasmid, the up- and downstream regions (~500 bp) of *ipsA* were amplified using the primer pairs Δ_*cg2910*_1(XmaI)/ Δ_*cg2910*_2 and Δ_*cg2910*_3/Δ_*cg2910*_4 (XbaI), respectively. The resulting PCR products were used as templates for overlap extension PCR using the oligonucleotide pair Δ_*cg2910*_1(XmaI)/ Δ_*cg2910*_4 (XbaI). The DNA fragment thus obtained was digested with XmaI and XbaI and cloned into recombination vector pK19*mobsacB.* The sequenced plasmid pK19*mobsacB-ΔipsA* was transformed into *C. glutamicum* and screened for the first and second recombination event using previously described protocols (Niebisch and Bott, 2001). The transformants were selected for kanamycin-sensitivity and sucrose-resistance and screened for the deletion of *cg2910* by colony PCR analysis with the primer pair Δ_*cg2910*_for/Δ_*cg2910*_rev.

To generate the vector constructs pET-TEV-*ipsA*, pAN6-*ipsA* and pAN6-*ipsA*-STREP, the *ipsA*-coding region was amplified from genomic DNA of *C. glutamicum* using the primer pairs *cg2910*-NdeI-fw/*cg2910*-EcoRI-rv (for pET-TEV-*ipsA* and pAN6-*ipsA*) and *cg2910*-NdeI-fw/*cg2910*-NheI-rv-nostop (for pAN6-*ipsA*-STREP). The PCR products were cut with the respective enzymes provided in the oligoname and ligated into pET-TEV and pAN6 double digested with same enzymes.

The plasmid pAN6-*cg3323* was constructed by amplifying the *cg3323* coding region using the primer pair *cg3323*-NdeI-fw/*cg3323*-NheI-rv using genomic DNA of *C. glutamicum* as template. The PCR product was cut with the NdeI-NheI and ligated into

pAN6 double digested with the same enzymes. For plasmid pJC1-venus-term, the *venus* coding region was amplified using the primer pair eYFP-Bam-NdeI-fw/Venus-term2-rv and plasmid DNA of pXVENC-2 as template. The terminator-encoding region was amplified using the primer pair Venus-term3-fw/Term4-SalI-rv and plasmid DNA of pAN6 as template. The fragments were joined by overlap extension PCR, cut with BamHI and SalI and ligated into pJC1 cut with the same enzymes.

To construct plasmid pJC1-P*cg3323*-eYFP, promoter region of *cg3323* was amplified from genomic DNA of *C. glutamicum* using the primer pair Prom*cg3323*-rv-YFP/Prom*cg3323*-fw-BamHI. The *eyfp*-coding sequence was amplified from plasmid DNA of pEKEx2-*eyfp* using the primer pair eYFP-SpeI-rv/eYFP-fw. The fragments were joined by overlap extension PCR, digested with BamHI and SpeI and ligated into pJC1-venus-term double digested with the same enzymes. Since SpeI site is located between *venus* and the terminator, *venus* is thus removed from the plasmid and only the *eyfp* reporter is available for use.

All primers used in this study were synthesised by Eurofins MWG Operon (Ebersberg, Germany). All constructs have been sequenced by Eurofins MWG Operon (Ebersberg, Germany). The oligo nucleotides used in this study are summarised in Table 3.2.

Table 3.2: Oligonucleotides used in this study. (Data provided by Baumgart et. al., Julich)

Oligonucleotide	Sequence (5' → 3') and properties[a]
Deletion of *ipsA* (*cg2910)* and PCR-analysis of the resulting mutants	
Δ_*cg2910*_1(XmaI)	TATATACCCGGGAATGCGTGGATGATGCGATCATC
Δ_*cg2910*_2	**CCCATCCACTAAACTTAAACA**TTGTTTCCTACCCATAATCATTTC
Δ_*cg2910*_3	**TGTTTAAGTTTAGTGGATGGG**GGTTCCACGGTTGCGCCAATCTAG
Δ_*cg2910*_4(XbaI)	TATATATCTAGAATTCGTGGAGATCAAGCCTTTCC
Δ_*cg2910*_for	GTGATCATCATGCTCGCTGTGG
Δ_*cg2910*_rev	GCCAAGATTGAAGCAGATCTGG
Construction of IpsA expression plasmid	
cg2910-NdeI-fw	GCGCCATATGATTATGGGTAGGAAACAACAATAC
cg2910-Nhe-rv-nostop	GCGCGCTAGCGATTGGCGCAACCGTGGAACC
Construction and PCR-verification of the chromosomal complementation with *ipsA*	
cg2910+Prom-MfeI-fw	GCGCCAATTGAATTGGATCCGGCAGCGTTG
cg2910+Prom-XhoI-rv	GCGCCTCGAGCTAGATTGGCGCAACCGTGGA
pK18-IGR-fw	CTTGGTTCGAATATGCAGTTCGG
cg2911-fw	ATCACCCTTGGCAACGGAG
int-reg-fw	AGCACCTTCGGCAAGAAGTA
int-reg-rv	CATCGAAGGTGTCGCAAAC
M13-rv	AGCGGATAACAATTTCACACAGGA
Construction of pAN6-*cg3323*	
cg3323-NdeI-fw	GCGCCATATGAGCACGTCCACCATCAG
Δ-NheI-rv	GCGCGCTAGCTTACGCCTCGATGATGAATGCC

Construction of pJC1-*venus*-term	
eYFP-Bam-NdeI-fw	CGCGGATCCGCGGATATCCCATATGGTGAGCAAGGGCGAGGAGCTG
Venus-term2-rv	**AAAACGACGGCCAGTACTAGTTTACTTGTACAGCTC**GTCCATGC
Venus-term3-fw	**GAGCTGTACAAGTAAACTAGTACTGGCCGTCGTTTT**
Term4-SalI-rv	ACGCGTCGACCAAAAGAGTTTGTAGAAACGCAA
Construction of the *cg3323* promoter fusion plasmid pJC1-P*cg3323*-eYFP	
Prom*cg3323*-rv-YFP	**CTCGCCCTTGCTCACCAT**CTAAAATTTCTCCTCTTAAAAAGATAACGGC
Prom*cg3323*-fw-BamHI	GCGCGGATCCGGAAATCTCCCGAACATCAGAAG
eYFP-SpeI-rv	GGACTAGTTTATCTAGACTTGTACAGCTCGTCCATG
eYFP-fw	ATGGTGAGCAAGGGCGAGGAG
Oligonucleotides for the expression plasmids of IpsA homologs of *M. tuberculosis* and *C. diphtheriae*	
DIP1969-NdeI-fw	GCGCCATATGGTGGTGCCTATGGCTTCC
DIP1969-NheI-rv	GCGCGCTAGCCTAGCCTCGCCGATGCTC
Rv3575c-NdeI-fw	GCGCCATATGAGTCCCACACCGCGGAGG
Rv3575c-NheI-rv	GCGCGCTAGCTTACGCCGGCGGACCCGC
PCR products used in gel shift assays (~500 bp fragments)	
cg0044-fw	GCAGATTGCAACATCGTGGAC
cg0044-rv	GATTAACAGCGCAGCACCAATG
cg0043-fw	TAGTGATGCCGTGGCTACTC
cg0043-rv	GCGATTTCTGGCACAAGGTTG
cg0326-fw	GCTTCGATAAGCTCCTGGTTG
cg0326-rv	CAAGGCAAACTTGACGTCGAC
cg0404-fw	CGCAATAAGTTTCGCCTTACAGG
cg0404-rv	GGAGCTTCATCGGTGTATTTGC
cg0508-fw	CGACCACCCTCTCAACAGGTG

cg0508-rv	GAGTGCAAAAACAGTAACGGCAG
cg3405-fw	TCGATTTCACCGCTGTCGAG
cg3405-rv	CTTGAATACGAACCTGACCTGG
cg2911-fw	ATCACCCTTGGCAACGGAG
cg2911-rv	CAGTTGAGCAGCCAGCTAG
cg3323-fw	GGAAATCTCCCGAACATCAGAAG
cg3323-rv	AATGGCAACCCTGATGGTGG
cg3195-fw	TCGTCACATGGTGGTTTCCTAC
cg3195-rv	GGCCAAGGTGGTTAAGTCTTG
cg0623-fw	ACTGCTGAGGTAAACCCTGAG
cg0623-rv	CACAACCAGCAATACCCAACG
cg2896-fw	CGTTCTACGCAATCGCTGTAG
cg2896-rv	AAGCCGTCACCACGGCGGTAA
cg0625-fw	GTCGCAGGAGATAACGAAGC
cg0625-rv	CACGGTTGCAGCAGACCA
cg2870-fw	AACCGGTGGAGAATTCCTTCTG
cg2870-rv	TTGACCTCAACACTTGAAGATTCTG
cg1421-fw	==
cg1421-rv	GATTGCGGTGCCCATGTTG
cg1055-fw	ATCATCCGAACCAGGGAAACG
cg1055-rv	AGGTCTGCGGTGGCAATG
cg0727-fw	GAAGCATTGGAAACTACTTTAGCGC
cg0727-rv	CTCTTGGGTCTTTAGTGAATCGAG
cg3389-fw	GAGCTATTCCAACACTTGGACG
cg3389-rv	CGGGTGGGTGATGCCTAG
cg0534-fw	GCTGGTGGTGCGTTATGATTC
cg0534-rv	CCAAGAGGATACGTGCGATG
cg2181-fw	CACGCGAATTAACGCTTATCGAC
cg2181-rv	GGTTACAGCGAGAGACTTCTTC
cg1918-fw	ATAAGCATCAGAGCCATGCTCG

cg1918-rv	GTTGCGGGTGAGGGTCTGA
cg3138-fw	GCAGTCGATGAGAACAGGAATC
cg3138-rv	TCCAGGAGTGCGCTCTTCTA
cg1290-fw	AACCACACGTCACCGCGTTGC
cg1290-rv	AGCGACAGTGGAAGAAAAGTTGG
cg2061-fw	AGCTTGATGATGTAGAAGCGAAAG
cg2061-rv	GACGCCTGCAGCCTTGGA
cg0936-fw	CCGGAAAGTTACATCGCTACC
cg0936-rv	GGAGCTAGTCTTAGTGGAGTG
cg3107-fw	CTATCTAGTAGGTACGGCGC
cg3107-rv	GGTAAATTCTTGGGGTGCAGC
cg3286-fw	CGGTGTGCGGTCAGCCAT
cg3286-rv	CGTGAGGGCGAGGGTAAG
cg1580-fw	GCTTGTGGCGACTCTGAG
cg1580-rv	CATAGTTACACCATACACGTTATGC
cg0753-fw	ACCAAGCAGACAAGCTAGTACAG
cg0753-rv	GTGGTAGCAAAAGCGCCAG
cg1476-fw	GCTCTAACAACCGCCAAAAGAAGAAC
cg1476-rv	CGGGTGGATCTCATTTTGGG
cg0998-fw	TGGATTGGAAACTGCTGGGC
cg0998-rv	CGGGTTCTCACCGTTGTTTG
cg2906-fw	GCTGCGATTGCTGCAACAG
cg2906-rv	GGACGAGTGTCCGTGATTTTG
cg2909-fw	CGTGGAAATGACAGATTCCACC
cg2909-rv	GTCTTGGCGATTTCCTCAATAGTC
PCR products and oligonucleotides used for the determination of the IpsA binding sites in the *cg3323* promoter	
cg3323-3	GAATGGTATGTCCGTACCCTG
cg3323-4	CAGGGTACGGACATACCATTC
cg3323-5	CGTTCCAAAATGTGGGGATTCC

cg3323-6	GGAATCCCCACATTTTGGAACG
cg3323-7	CATTACCCCCATTCGGGAGTG
cg3323-8	CACTCCCGAATGGGGGTAATG
cg3323-30er-A-fw	AATGGGGGTAATGCTTGATCGATCAATTGA
cg3323-30er-A-rv	TCAATTGATCGATCAAGCATTACCCCCATT
cg3323-30er-B-fw	TGCTTGATCGATCAATTGAGTTGCTTGATCGATCAGG
cg3323-30er-B-rv	CCTGATCGATCAAGCAACTCAATTGATCGATCAAGCA
cg3323-30er-C-fw	GTTGCTTGATCGATCAGGTCTGATTTCTGC
cg3323-30er-C-rv	GCAGAAATCAGACCTGATCGATCAAGCAAC
cg3323-30er-D-fw	AGGTCTGATTTCTGCTGGGAATCCCCACAT
cg3323-30er-D-rv	ATGTGGGGATTCCCAGCAGAAATCAGACCT
PCR products and oligonucleotides used for the determination of the IpsA binding site in the *cg0044* promoter	
cg0044-3	GTGGTTCCTTGGTTGCGTTG
cg0044-4	CAACGCAACCAAGGAACCAC
cg0044-5	CACAGCGCAAAGCCACTGAATC
cg0044-6	GATTCAGTGGCTTTGCGCTGTG
cg0044-7	GCAGATCAGATTATCGCCTTGGA
cg0044-8	ACGATCTTGATCAAGCACATCAAGC
cg0044-9	GCTTGATGTGCTTGATCAAGATCGT
cg0044-10	CAAGTCAACGCAGGTCAGAG
cg0044-11	CTCTGACCTGCGTTGACTTG
cg0044-30er-E-fw	AGCCACTGAATCAATAAAGAAGCGTTAATA
cg0044-30er-E-rv	TATTAACGCTTCTTTATTGATTCAGTGGCT
cg0044-30er-F-fw	AAAGAAGCGTTAATAAAGTTTGACTTGTGC
cg0044-30er-F-rv	GCACAAGTCAAACTTTATTAACGCTTCTTT
cg0044-30er-G-fw	AAGTTTGACTTGTGCCTCTGACCTGCGTTG
cg0044-30er-G-rv	CAACGCAGGTCAGAGGCACAAGTCAAACTT

PCR products and oligonucleotides used for the investigation of putative IpsA binding sites in other promoters	
cg3195-3	GATGGATCCTGTGGTTGAACC
cg3195-4	GGTTCAACCACAGGATCCATC
cg2896-3	CTAGTAAGCAACCCACCAAGC
cg2896-4	GCTTGGTGGGTTGCTTACTAG
cg3195-5	AATCTGTGCACCGTGGGTAC
cg3195-6	GTACCCACGGTGCACAGATT
cg3195-7	CCGTTTGTAATTCTTGCAAAGTGGG
cg3195-8	CCCACTTTGCAAGAATTACAAACGG
cg3389-3	CAATGCTCAGAGGGGTTACC
cg3389-4	GGTAACCCCTCTGAGCATTG
cg3210-30er-fw	GCTCACTTCTTGATTGATGCGGTGGCTTTT
cg3210-30er-rv	AAAAGCCACCGCATCAATCAAGAAGTGAGC
cg3195-30er-A-fw	TTCAACCACAGGATCCATCCAGTTTTCCGT
cg3195-30er-A-rv	ACGGAAAACTGGATGGATCCTGTGGTTGAA
cg1421-3	GACTTTTAGCAGCTCAACGGC
cg1421-4	GCCGTTGAGCTGCTAAAAGTC
cg0534-3	CTCGATTGCCAGGGTTCCAAC
cg0534-4	GTTGGAACCCTGGCAATCGAG
cg1918-3	CTACTGCGTCGTGTCCAC
cg1918-4	GTGGACACGACGCAGTAG
cg1918-30er-fw	TTTAATGACTTTAGCTATACTTCTATCTTG
cg1918-30er-rv	CAAGATAGAAGTATAGCTAAAGTCATTAAA
cg0534-30er-fw	CATTCTAGCTTTAGTGACCATGTCAACTAC
cg0534-30er-rv	GTAGTTGACATGGTCACTAAAGCTAGAATG
cg1421-30er-A-fw	ACTAATTACTTGACACGTCAAGTAATTAGG
cg1421-30er-A-rv	CCTAATTACTTGACGTGTCAAGTAATTAGT
cg1421-30er-B-fw	GTTGTGTTCATGATCAAAGAACTGCTCAAC
cg1421-30er-B-rv	GTTGAGCAGTTCTTTGATCATGAACACAAC

cg3195-30er-B-fw	CCAATTCATTCGATAGATCCTCGCAAAAAG
cg3195-30er-B-rv	CTTTTTGCGAGGATCTATCGAATGAATTGG
cg0534-30er-B-fw	GCTGAGCTGCTTCCAGATCCAGTTTCTGAG
cg0534-30er-B-rv	CTCAGAAACTGGATCTGGAAGCAGCTCAGC
cg0534-30er-C-fw	TTATCAAACTTTCCCGGCTGAGCTGCTTCC
cg0534-30er-C-rv	GGAAGCAGCTCAGCCGGGAAAGTTTGATAA
cg0534-30er-D-fw	CCCCAATAGTTGACACGGAAACTAATTCAT
cg0534-30er-D-rv	ATGAATTAGTTTCCGTGTCAACTATTGGGG
Oligonucleotides for the mutational analysis of the DNA binding site in the *cg3323* promoter	
cg3323-WT-fw	TTGAGTTGCTTGATCGATCAGGTCTGATTT
cg3323-WT-rv	AAATCAGACCTGATCGATCAAGCAACTCAA
cg3323-M1-fw	TTGAGTGTATTGATCGATCAGGTCTGATTT
cg3323-M1-rv	AAATCAGACCTGATCGATCAATACACTCAA
cg3323-M2-fw	TTGAGTTGCGGTATCGATCAGGTCTGATTT
cg3323-M2-rv	AAATCAGACCTGATCGATACCGCAACTCAA
cg3323-M3-fw	TTGAGTTGCTTGCGAGATCAGGTCTGATTT
cg3323-M3-rv	AAATCAGACCTGATCTCGCAAGCAACTCAA
cg3323-M4-fw	TTGAGTTGCTTGATCTCGCAGGTCTGATTT
cg3323-M4-rv	AAATCAGACCTGCGAGATCAAGCAACTCAA
cg3323-M5-fw	TTGAGTTGCTTGATCGATACTGTCTGATTT
cg3323-M5-rv	AAATCAGACAGTATCGATCAAGCAACTCAA
cg3323-M6-fw	TTGAGTTGCTTGATCGATCAGTGATGATTT
cg3323-M6-rv	AAATCATCACTGATCGATCAAGCAACTCAA
PCR products and oligonucleotides used for the determination of the IpsA binding site in promoters of genes of *C. diphtheriae* and *M. tuberculosis*	
Rv0046c-P-fw	AACGCCGGGAAGGCTTGC
Rv0046c-P-rv	GGTAACGACTGGTGCTCACTCAT
DIP-0115-P-fw	CCTCAAAGTGGGGAGGCTT
DIP-0115-P-rv	GGCAACACGAATAGCAGACAC

DIP0115-30er-A-fw	TTTTGTAGCTGCATGATCCATCTGTACCGA
DIP0115-30er-A-rv	TCGGTACAGATGGATCATGCAGCTACAAAA
DIP0115-30er-B-fw	ATTTACTTAACCGATTAACCAGCAGTTTTA
DIP0115-30er-B-rv	TAAAACTGCTGGTTAATCGGTTAAGTAAAT
DIP0021-30er-A-fw	TGGGTCAACTTGATCAAGCAATTTCTCTTC
DIP0021-30er-A-rv	GAAGAGAAATTGCTTGATCAAGTTGACCCA
DIP0021-30er-B-fw	AACCCCACTGAATCGGTAAAGATGCAGGTC
DIP0021-30er-B-rv	GACCTGCATCTTTACCGATTCAGTGGGGTT
Rv0483-30er-fw	GTGCGCGATGGGGTCCATGATGTGTTTGGT
Rv0483-30er-rv	ACCAAACACATCATGGACCCCATCGCGCAC
Rv0047-A-fw	GAGCAAATTCGATGCGAAGACC
Rv0047-A-rv	ATTTGCGACAACATCACCGCGTC
Rv0047-B-fw	GTTGTCGTTGTCGTTGTATGTCTC
Rv0047-B-rv	TAGCCATGCATCGGTGACTC
Rv0047-30er-A-fw	CGCAGGTGACGGCACCATCAAGCACGTCAG
Rv0047-30er-A-rv	CTGACGTGCTTGATGGTGCCGTCACCTGCG
Rv0047-30er-B-fw	TGTCGCAAATATATCGAGGCGATACGATGA
Rv0047-30er-B-rv	TCATCGTATCGCCTCGATATATTTGCGACA
Rv0047-30er-C-fw	AAAAGGAGGTGACTCGATGCTGGAGCTCGC
Rv0047-30er-C-rv	GCGAGCTCCAGCATCGAGTCACCTCCTTTT
Rv0047-30er-D-fw	CTGGGTCTGTTGATCGAGTCACCGATGCAT
Rv0047-30er-D-rv	ATGCATCGGTGACTCGATCAACAGACCCAG
PCR products for the control EMSA with AcnR	
acn-Prom-5-for	ACATCACGCACGTACCCATTTCG
acn-Prom-3-rev	TAGTCATAGGACTTGTCGCC

[a]In some cases oligonucleotides were designed to introduce recognition sites for restriction endonucleases(recognition sites underlined). Complementary sequences used for overlap extension PCR are written in bold letters. Red letters indicate mutated bases.

3.2.4 DNA microarrays

For transcriptome analysis, *C. glutamicum* wild type and Δ*ipsA* cells were grown in 5 mL BHI (Brain Heart Infusion, Difco) for about 6 hours at 30°C and were then used to inoculate CGXII minimal medium containing 2% (w/v) glucose as carbon source. The main cultures were inoculated using the pre-inoculum to an OD_{600} of 0.5 in CGXII minimal medium with 2% (w/v) glucose. The cells were harvested at an OD_{600} of 5 by centrifugation (4120 x *g*, 10 minutes and 4°C). The cell pellet was subsequently frozen in liquid nitrogen and stored at -70°C. Total RNA was prepared with the RNeasy Kit (Qiagen) using the previously described protocols (Möker *et al.*, 2004). Fluorescently-labeled cDNA was synthesised as described previously (Lange *et al.*, 2003; Möker *et al.*, 2004). Purified cDNA samples to be compared were pooled and the prepared two-color samples were hybridised at 65°C while rotating for 17 hours using Agilent's Gene Expression Hybridisation Kit, hybridisation oven and hybridisation chamber. After hybridisation the arrays were washed using Agilent's Wash Buffer Kit according to the manufacturer's instructions. Fluorescence signals from hybridised DNA microarrays was measured at 532 nm (Cy3) and 635 nm (Cy5) at 5 µm resolution with a GenePix 4000B laser scanner and GenePix Pro 6.0 software (Molecular Devices, Sunnyvale, CA, USA). Fluorescence images were saved as raw data files in TIFF format (GenePix Pro 6.0). Quantitative TIFF image analysis was carried out using GenePix image analysis software and results were saved as GPR-file (GenePix Pro 6.0). For background correction of spot intensities, ratio calculation and ratio normalisation, GPR-files were processed using the BioConductor R-packages limma and marray (http://www.bioconductor.org). Array data was deposited in the GEO database (ncbi.nlm.nih.gov/geo) under the accession number GSE50210.

3.2.5 Overproduction and purification of IpsA

Overnight cultures of *E. coli* BL21(DE3) cells harbouring the expression plasmids pET-TEV-*ipsA* or pAN6-*ipsA*-STREP were set up in 1L LB medium at 37°C and 120 rpm. For expression analysis, cultures were induced by addition of 50 µM IPTG and transferred to 16°C for 20 hours before the cells were harvested by centrifugation. The protein was purified from lysates using Nickel chelate and StrepTactin affinity chromatography as described previously (Garcia-Nafria *et al.*, 2010; Niebisch *et al.*, 2006). To further purify the protein preparation and determine the molecular weight, gel filtration was performed using a Superdex™ 200 10/300 GL column (GE Healthcare, Munich, Germany) in Tris buffer (50 mM Tris-HCl pH 8, 250 mM NaCl, 1 mM DTT). Fewer aggregates were obtained for IpsA-variant with the C-terminal STREP-tag in comparison to the His_{10}-tag. SDS-PAGE analysis of the eluted fraction revealed a band for IpsA at 79 kDa suggesting dimer formation. The protein was concentrated, flash frozen in liquid nitrogen and stored in the gel filtration buffer at -70˚C.

3.2.6 Electrophoretic mobility shift assays (EMSAs)

Unless otherwise stated, EMSAs were performed with purified STREP-tag variant of IpsA and DNA fragments of the predicted target genes using previously described protocols (Heyer *et al.*, 2012) with the stated modifications. The purified protein was incubated with DNA fragments (30-500 bp, final concentration 0.028-1 µM) in bandshift buffer (50 mM TRIS-HCl pH 7.5, 40 mM KCl, 5 mM $MgCl_2$) in a total volume of 10 µL. The DNA-protein complex was resolved on 10-15% non-denaturing polyacrylamide gels at room temperature run at 150 or 180 V for 45-60 minutes (varied *w. r. t.* DNA fragments being analysed). To determine the effector molecules, purified

IpsA was pre-incubated with the effector for 20 minutes at room temperature. The pre-incubated effector-protein mix was then incubated with target DNA for 20 minutes and electrophoresed as described above. AcnR protein and the *acn* promoter fragment was used as experimental control (Garcia-Nafria *et al.*, 2013). ImageQuant TL software (GE Heathcare) was used for quantifying the shifted DNA.

3.2.7 Fluorescence microscopy

DAPI and nile red staining was performed on the previously cultured strains for flouresence microscopy analysis. The cells were centrifuged and resuspended in phosphate buffered saline (PBS, 137 mM NaCl, 2.7 mM KCl, 4.3 mM Na_2HPO_4, 1.4 mM KH_2PO_4, pH 7.3) containing 200 ng/mL 4',6-diamidino-2-phenylindole (DAPI) and 300 ng/mL nile red and incubated for 5-10 minutes at room temperature. For analysis, the cells were mounted on agar pads and analysed using Zeiss Axioplan 2 imaging microscope with an AxioCam MRm camera and a Plan-Apochromat 100x, 1.40 Oil DIC oil-Immersion objective. Digital images were acquired and analysed with AxioVision 4.6 software (Zeiss, Göttingen, Germany).

3.2.8 Promoter fusion studies

The effect of IpsA as a regulator on the *ino1* promoter *in vivo* was analysed using promoter-reporter fusion constructs. For this purpose, a DNA fragment containing the *cg3323* promoter region was fused to the *eyfp*-coding sequence and cloned into pJCI to generate the pJC1-P*cg3323*-eYFP construct. The resulting plasmid was then transformed into wild type and Δ*ipsA* cells and analysed for fluorescence output on minimal medium supplemented with 2% (w/v) glucose or *myo*-inositol in the Biolector system.

3.2.9 Growth of bacteria for [^{14}C]-labelled lipid analysis

Overnight cultures of *C. glutamicum* wild type ATCC 13032, *C. glutamicum ΔipsA*, *C. glutamicum ΔipsA::*pK18int_*ipsA*, and *C.glutamicum ΔipsA* harbouring *cg3323* (*NCgl2894), Rv3575c* and *DIP1969* in plasmid pAN6 were pre-grown in 20 mL of 3.7% BHI (Sigma) containing kanamycin (25 µg/mL). The cells were washed once with phosphate buffered saline (137 mM NaCl, 2.7 mM KCl, 4.3 mM Na_2HPO_4, 1.4 mM KH_2PO_4, pH 7.3, PBS) and were used to inoculate a second pre-culture to an OD_{600} of 1 in 50 mL CGXII minimal medium (50mL) supplemented with 2% glucose and incubated with gentle shaking overnight at 30°C. The cells of the second pre-culture were washed once with PBS and used to inoculate the main cultures to an OD_{600} of 0.1 in 10 mL CGXII minimal medium (10 mL), supplemented with either 2% glucose or 2% *myo*-inositol and grown until early log phase. At early log phase, the cells were labelled with 1 µCi/mL of [1,2-^{14}C]-acetate (1.66-2.22 GBq/mmol, PerkinElmer Inc.) and incubated overnight at 30ºC with gentle shaking. The cells were recovered following centrifugation at 3,500 x *g* and dried.

3.2.10 Analysis of polar lipids

Polar and apolar lipid extracts were prepared from the dried cell pellets using established procedures (Dobson G., 1985) as mentioned in General Materials and Methods, section 7.4.2. Briefly, the dried polar lipid extracts were re-suspended in chloroform:methanol (100 µL, 2:1, v/v) and the incorporation of [1,2-^{14}C]-acetate in lipid extracts was determined by counting an aliquot (5%) using scintillation fluid (5 mL). To analyse the lipid profiles, equal counts of polar lipid extracts (20,000 cpm) were applied to silica thin layer chromatography (silica gel 60 F_{254} Merck 5554, TLC plates) and developed using the solvent system: chloroform/methanol/water (60:30:6,

v/v/v) in the first dimension and chloroform/acetate/methanol/water (40:25:3:6, v/v/v/v) in the second dimension. The autoradiograms were obtained by exposing the TLCs to X-ray films (Kodak-Biomax MR) for 48 hours.

3.2.11 Extraction and purification of lipoglycans

Lipoglycans were extracted using previously described protocols (Ludwiczak *et al.*, 2001) as described in General Materials and Methods, section 7.4.5. Briefly, dried cell pellets from a 10 mL volume culture were resuspended in water and refluxed five times with equal volume of 50% aqueous ethanol at 85°C, for 6 hour intervals. The suspension was centrifuged and the supernatant recovered between each extraction following centrifugation. The combined supernatant fractions were dried and subjected to hot phenol-water treatment at 65°C. The aqueous phase containing the crude lipoglycan fraction was recovered and dialyzed (MWCO 3.5 KDa) against water. The dialyzed fraction was dried and 20 µg of lipoglycans were loaded on a 15% SDS-PAGE gel. The lipoglycans were visualised using Pro-Q emerald glycoprotein stain (Life Technologies).

3.2.12 Mycothiol extraction and analysis.

The extraction of mycothiol was carried out using previously published protocols (Newton *et al.*, 1996) with a few modifications. Briefly, relevant strains were cultured in BHI medium for 6 hours and then sub-cultured twice in CGXII minimal medium supplemented with 4% glucose (w/v) as carbon source and grown at 30 °C and 120 rpm for 16 hours and 24 hours, respectively. For extraction, 200 mg of wet cells were resuspended in 1 mL of warm (60°C) acetonitrile containing 20 mM Tris-HCl, pH 8.0 and 2 mM bromobimane (Sigma) and sonicated for 20 seconds. The resuspended cells

were further incubated in dark at 60°C for 15 minutes. The samples were then treated with 5 µL of 5 M methanesulfonic acid and centrifuged at 16000 x *g* for 10 minutes to remove debris. The supernatant was separated, filtered and diluted 5-fold in 10 mM methanesulfonic acid. To block thiol groups, the control sample from wild type was pre-incubated with 5 mM N-methylmaleimide (NMM) and then derivatised with bromobimane. For HPLC analysis, the samples were loaded onto a C_{18} column (LiChrospher RP 18, 125 × 4 mm) and eluted using the solvents A (100 mM sodium acetate buffer pH 7.2) and B (100% methanol) at a flow rate of 0.7 mL/minutes at a gradient: 0 minutes, 15% B; 1 minutes, 15% B; 1.5 minutes, 35% B; 11 minutes, 80% B; 12 minutes, 95% B; 13 minutes 100% B. To identify the peak for mycothiol (5.61 minutes) wild type chromatogram was compared to that of Δ*mshC* strain and the NMM treated sample. In addition, previously published chromatograms for glutathione (5.14) obtained using similar methods also indicated the peak at 5.61 minutes to correspond to mycothiol (Anderberg *et al.*, 1998).

3.3 Results

3.3.1 IpsA is a novel LacI-type regulator conserved in the *Corynebacteriales*

The genomic loci of IpsA from *C. glutamicum* wild type was compared across the *Corynebacteriales* and the homologues for the protein were identified using BLAST search. The comparison of genome loci from species of this order revealed a high degree of conservation (Figure 3.1). The crystal structure (PDB ID: 3H5T) and sequence homology have designated IpsA as a member of LacI family of transcriptional regulators (Swint-Kruse and Matthews, 2009).

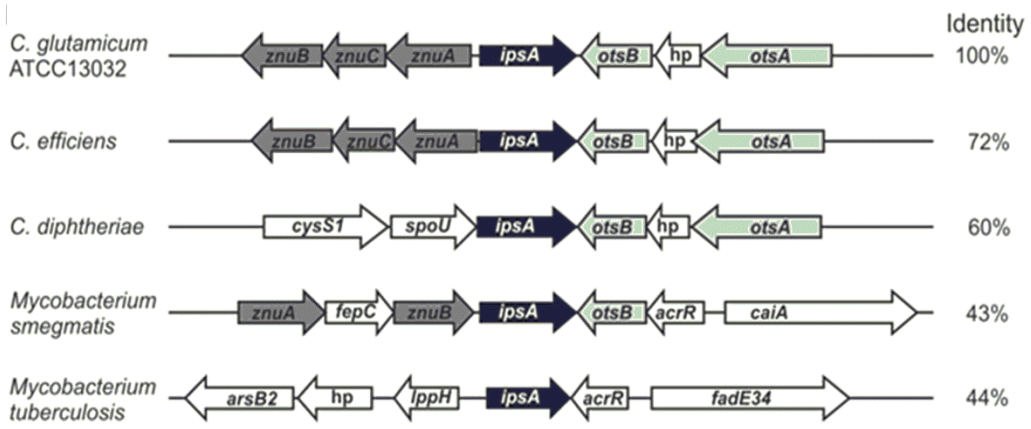

Figure 3.1: Conservation of IpsA in *Corynebacteriales*. The organization of genome locus harbouring *ipsA* in *C. glutamicum* and related species revealed a remarkable degree of conservation across the species, IpsA homologues are depicted in black. Data was obtained from www.microbesonline.org (Alm *et al.*, 2005). (The figure and data was provided by Baumgart *et. al*., Julich)

3.3.2 Effect of IpsA deletion on cell shape and growth

An in-frame deletion mutant of *ipsA* was constructed to study the function and determine possible target genes that are regulated by IpsA. The growth rate of Δ*ipsA* was measured in cells cultured in minimal media supplemented with glucose. These cells were also checked for backscatter. The growth rate and backscattering of Δ*ipsA* strain was significantly below the control levels. These deficiencies were enhanced with successive sub-cultivation (Figure 3.2).

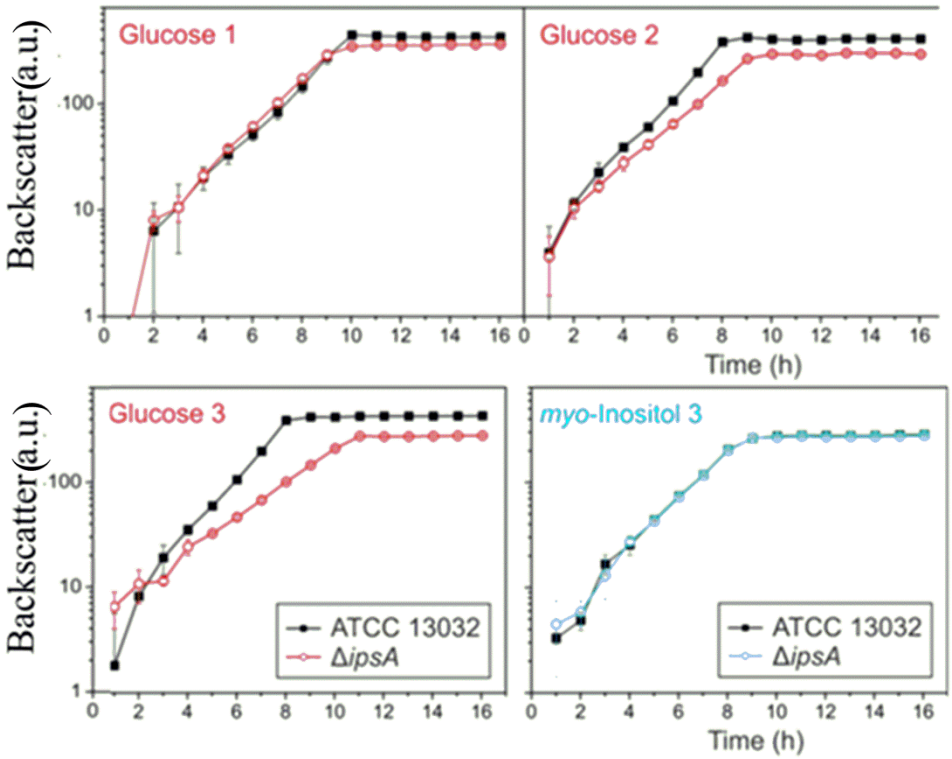

Figure 3.2: Growth of *C. glutamicum* wild type and *ΔipsA*. A. The growth curves for *C. glutamicum* wild type and *C. glutamicum* Δ*ipsA* from sequential cultures in minimal medium supplemented either with glucose (1, 2, 3) or with *myo*-inositol (3) as carbon source revealed a decrease in backscatter with subsequent cultivations for glucose while no change was observed with *myo*-inositol. The data is representative of three biological replicates. (Figure and data were provided by Baumgart *et. al*., Julich)

Fluorescence microscopy analysis of DNA (DAPI) and membranes (nile-red) from Δ*ipsA* revealed an alerted morphology as the mutant cells demonstrated formation of chain-like structures, failure of cell division and an intact cell septa in several unshaped cells. Uneven distribution was observed for the DNA and its frequent presence in extracellular space was suggestive of a highly fractured cell envelope (Figure 3.3).

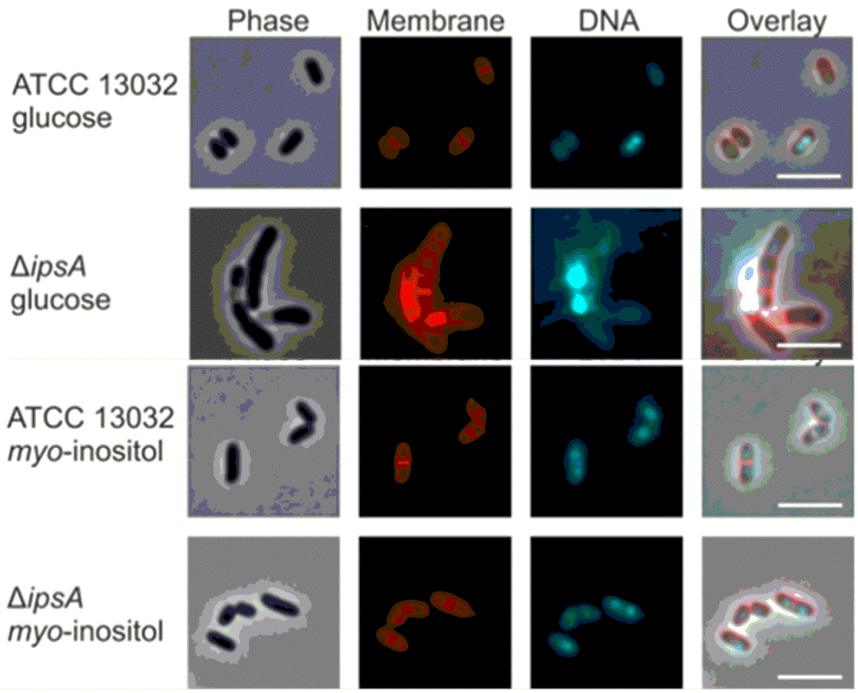

Figure 3.3: Cell shape of *C. glutamicum* wild type and *ΔipsA*. Fluorescence microscopic images of membrane and DNA preparations from wildtype and Δ*ipsA* strains depict abnormal phenotype for the mutant. The Δ*ipsA* cells cultured in minimal media with glucose were elongated in shape with intact septa whilst those cultured in minimal media with *myo*-inositol as carbon source were normal and identical to wild type. The scale bar is 5 µm. (Figure and data were provided by Baumgart *et. al*., Julich)

Attempts were made to complement the mutant with plasmid-encoded *ipsA* with an inducible promoter, plasmid encoded putative target *ino1* (*cg3323*) and by genomic reintegration of *ipsA* into the intergenic region between *cg1121-cg1122*. Whilst controlled expression of IpsA under the inducible promoter could partially restore growth, full complementation was achieved only in case of an integrated copy of *ipsA* under the control of native promoter (Figure 3.4A). The growth defects were also overcome in a Δ*ipsA* strain containing the plasmid encoded copy of target gene *ino1* under an inducible promoter (Figure 3.4B).

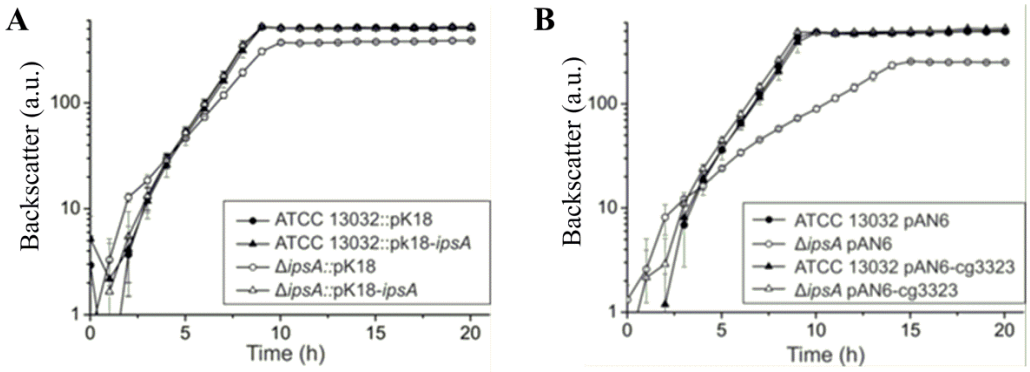

Figure 3.4: Complementation of the Δ*ipsA* phenotype with *ipsA* and the target gene *ino1* (*cg3323*). A. Growth curves obtained for mutant strain complemented with the integrated copy of the gene *ipsA* cultured in minimal media with glucose as carbon source. **B.** The growth curves obtained for mutant strain with plasmid encoded copy of the target gene *ino1* (*cg3323*) depicting full restoration of phenotype. The data is representative of three biological replicates. (Data and figure provided by Baumgart *et. al.*, Julich)

Fluorescence microscopy analysis of the mutant and the complemented strains showed full complementation in mutant strain with integrated copy of *ipsA* (Figure 3.5).

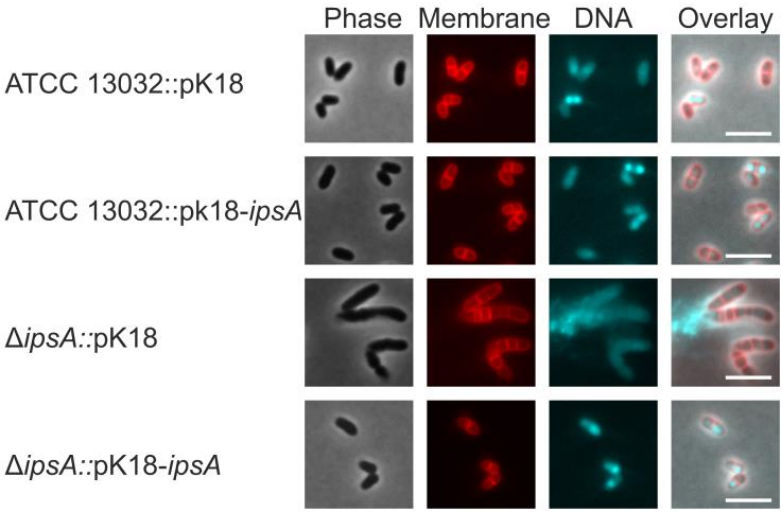

Figure 3.5: Flouresence microscopy depicting complementation of the Δ*ipsA* phenotype with *ipsA*. Fluorescence microscopy images of stationary phase cells of the cultures depicting full restoration of phenotype in the complemented strain. The data is representative of three biological replicates. (Data and figure provided by Baumgart *et. al.*, Julich)

3.3.3 Transcriptome analysis of *ipsA* deletion mutant

Global transcriptional profiling was performed to study the transcriptional changes introduced by *ipsA* deletion. DNA microarray analysis of cells in exponential phase (OD_{600}=5) cultured in minimal media supplemented with glucose, revealed increased transcription for more than 450 genes (mRNA level greater than a factor of two). Some of the relevant genes are summarised in Table 3.3 and full data for the study was deposited in GEO database (ncbi.nlm.nih.gov/geo) under accession number GSE50210.

Table 3.3: Gene loci with more than four-fold regulation in Δ*ipsA* mutant in comparison to wild type. (Data provided by Baumgart *et. al.*, Julich)

Locus tag	Gene	Annotated function	Ratio	n	p-value
cg3323	*ino1*	*myo*-inositol-phosphate synthase	0.047	3	0.011
cg0044	*rbsB*	ABC transporter/periplasmic D-ribose-binding protein	0.082	3	0.004
cg2896		putative secreted protein, hypothetical endoglucanase	0.114	3	0.003
cg2181		ABC-type peptide transport system, secreted component	0.128	3	0.005
cg0446	*sdhA*	succinate dehydrogenase	0.138	3	0.003
cg0045		probable ABC transport protein, membrane component	0.138	3	0.028
cg2636	*catA1*	catechol 1,2-dioxygenase	0.143	3	0.003
cg0622		duplicated ATPase component SCO2324 of energising module of predicted cobalamine ECF transporter	0.160	3	0.003
cg2182		ABC-type peptide transport system, permease component	0.167	3	0.022
cg1918		putative secreted protein	0.169	3	0.005
cg3138	*ppmA*	putative membrane-bound protease modulator	0.171	3	0.004
cg2910	*ipsA*	transcriptional regulator, LacI family	0.173	3	0.030
cg3195		flavin-containing monooxygenase (FMO)	0.178	3	0.010
cg0447	*sdhB*	succinate dehydrogenase	0.185	3	0.002
cg0621		substrate-specific component SCO2325 of predicted cobalamine ECF transporter	0.187	3	0.006
cg0445	*sdhC*	succinate dehydrogenase	0.189	3	0.005
cg0623		transmembrane component SCO2323 of energising module of predicted cobalamine ECF transporter	0.194	3	0.004
cg3048	*pta*	phosphate acetyltransferase	0.202	2	0.082
cg0601	*rpsC*	30S ribosomal protein S3	0.212	3	0.007
cg3139		hypothetical protein cg3139	0.213	3	0.002
cg0599	*rpsS*	30S ribosomal protein S19	0.215	3	0.009
cg0600	*rplV*	50S ribosomal protein L22	0.216	3	0.007
cg0598	*rplB*	50S ribosomal protein L2	0.217	3	0.011
cg1487	*leuC*	isopropylmalate isomerase large subunit	0.218	3	0.035
cg0624		secreted oxidoreductase	0.219	3	0.005
cg0602	*rplP*	50S ribosomal protein L16	0.226	3	0.005
cg1290	*metE*	5-methyltetrahydropteroyltriglutamate-	0.226	3	0.017

		homocysteine methyltransferase			
cg0594	*rplC*	50S ribosomal protein L3	0.233	2	0.085
cg0593	*rpsJ*	30S ribosomal protein S10	0.237	2	0.064
cg2061	*psp3*	putative secreted protein	0.244	3	0.000
cg0936	*rpf1*	resuscitation promoting factor	0.247	2	0.098
cg3107	*adhA*	Zn-dependent alcohol dehydrogenase	0.251	3	0.033
cg3210		cell envelope-related transcriptional regulator	0.411	2	0.024
cg2870	*dctA*	Na+/H+-dicarboxylate symporter	3.948	3	0.004
cg3286		putative secreted protein	4.073	2	0.013
cg0527	*glyR*	transcriptional regulator of glyA	4.578	2	0.021
cg1580	*argC*	N-acetyl-gamma-glutamyl-phosphate reductase	4.798	3	0.003
cg3391	*oxiD*	*myo*-Inositol dehydrogenase	4.979	3	0.018
cg1421		putative dinucleotide-binding enzyme	5.214	3	0.000
cg0533	*menE*	O-succinylbenzoic acid-CoA ligase	5.467	3	0.001
cg0753		secreted protein	5.507	3	0.000
cg2797		hypothetical protein cg2797	5.517	3	0.023
cg3389	*oxiC*	*myo*-Inositol dehydrogenase	5.528	3	0.006
cg0471	*htaC*	secreted heme transport-associated protein	5.553	3	0.003
cg1476	*thiC*	thiamine biosynthesis protein ThiC	5.554	3	0.000
cg0534		putative integral membrane protein	5.597	3	0.000
cg0998		trypsin-like serine protease	5.798	3	0.001
cg2311		SAM-dependent methyltransferase	6.217	2	0.032
cg1120	*ripA*	transcriptional regulator of iron proteins, AraC family	6.983	3	0.005
cg3390		*myo*-Inositol catabolism, sugar phosphate isomerase/epimerase	7.674	3	0.012
cg0470	*htaA*	secreted heme transport-associated protein	8.972	3	0.008
cg3156	*htaD*	secreted heme transport-associated protein	9.695	3	0.002
cg2796		MMGE/PRPD family protein	11.215	3	0.021

Significant alteration was observed in mRNA level for genes which are the components of DtxR/RipA-regulon (shaded in grey, Table 3.3) that is required for iron homeostasis in *C. glutamicum* (Wennerhold and Bott, 2006; Wennerhold *et al.*, 2005). These alterations could manifest from impaired iron uptake resulting from a damaged cell wall. IpsA is not part of the DtxR-stimulon as no conserved DtxR motif is present in the *ipsA* or *ino1* promoter regions. The genes that encode ribosomal proteins (shaded in grey, Table 3.3) were also not included for analysis. More than ten-fold decrease in gene expression levels was observed for *cg3323*, which encodes a *myo*-inositol-phosphate synthase (*ino1)*, and of the operon (*cg0044-46*), which encodes an uncharacterised ABC transporter in the mutant strain (Table 3.3). Other down-regulated genes include a flavin-containing monooxygenase (*cg3195*), a hypothetical endoglucanase (*cg2896*), and two further transporters (*cg0621-23* and *cg2181-84*) (Table 3.3). Strong upregulation was evident for genes clusters with enzymes for inositol catabolism (*cg3389-92*), *menE* and a putative integral membrane protein (*cg0533-34*) and a putative dinucleotide binding enzyme (*cg1421*). On the basis of gene expression analysis, all genes that were either up-regulated or down-regulated by a factor of four and were not a part of DtxR-stimulon or encode for ribosomal proteins were selected for EMSA studies.

3.3.4 Identification of direct IpsA target promoter, binding site and effecter molecules

The promoter regions of the putative target genes of IpsA, as implicated by microarray experiments were tested for direct regulation by IpsA using electrophoretic mobility shift assays (EMSAs) and mutational analysis. DNA fragments (~30 & 500 bp) harboring the promoter regions of predicted target genes were incubated with

increasing concentrations of IpsA and analysed for formation of IpsA-DNA complex. EMSA analysis revealed high affinity binding of IpsA to the promoter regions of *cg0044* and *ino1* (*cg3323*) lower affinity for the promoter regions of *cg0534*, *cg1421*, *cg1476 (thiC)*, *cg3210*, and *cg3195* (Figure 3.6 and 3.7). The EMSA results for all the targets hits are summarised in Figure 3.7.

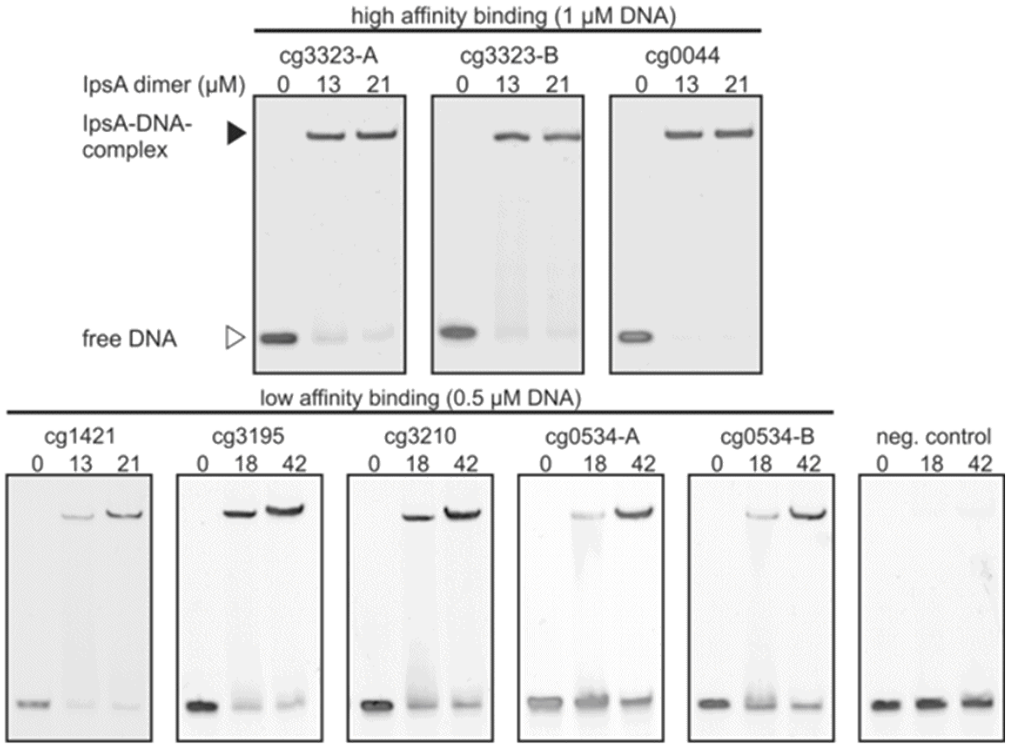

Figure 3.6: Binding efficiency of IpsA to promoter regions of putative target genes. The 30bp sequence located immediately downstream of *IpsA* binding site in *cg3323* was used as a negative control. (Figure and data were provided by Baumgart *et. al.*, Julich)

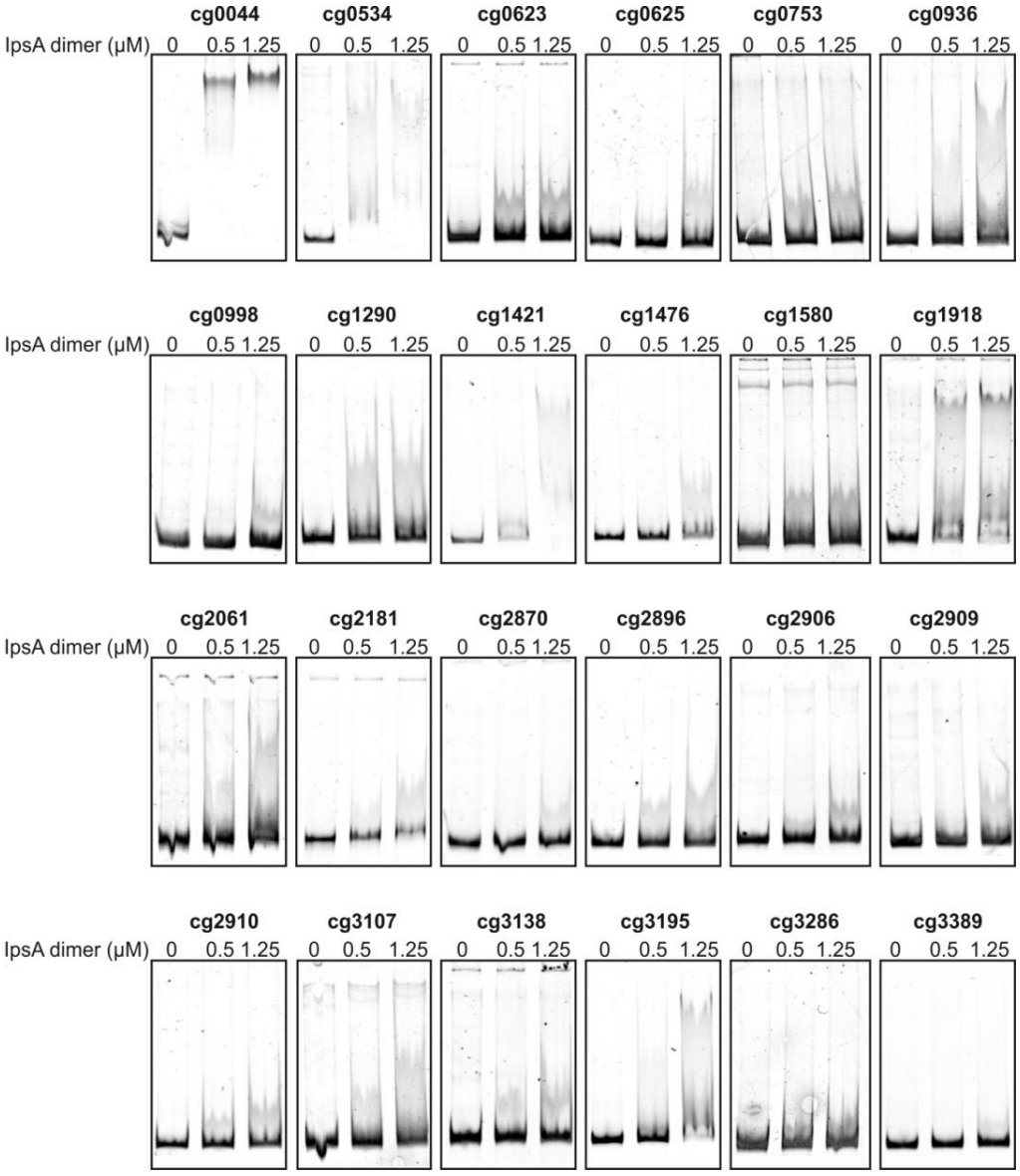

Figure. 3.7: IpsA binding with promoter regions of predicted target genes. 30bp DNA fragments containing promoter regions of putative target genes were incubated with IpsA at mentioned concentrations and analysed on 10% native polyacrylamide gels, stained with SYBR green for bandshift due to DNA-IpsA formation. (Figure and data were provided by Baumgart *et. al.*, Julich)

The high affinity binding sites from promoter regions of *ino1* (*cg3323*) and *cg0044* as identified by EMSA (Figure 3.6) were subjected to motif based sequence analysis tool MEME, (http://meme.ebi.edu.au/meme/) to generate a preliminary palindrome motif

(Figure 3.8) that was further verified using mutational analysis.Three nucleotides of the proposed motif were substituted in DNA fragment containing *ino1* promoter and EMSA was performed (Figure 3.8). The results highlighted central six base pairs to be important as high degree of conservation was evident among these.

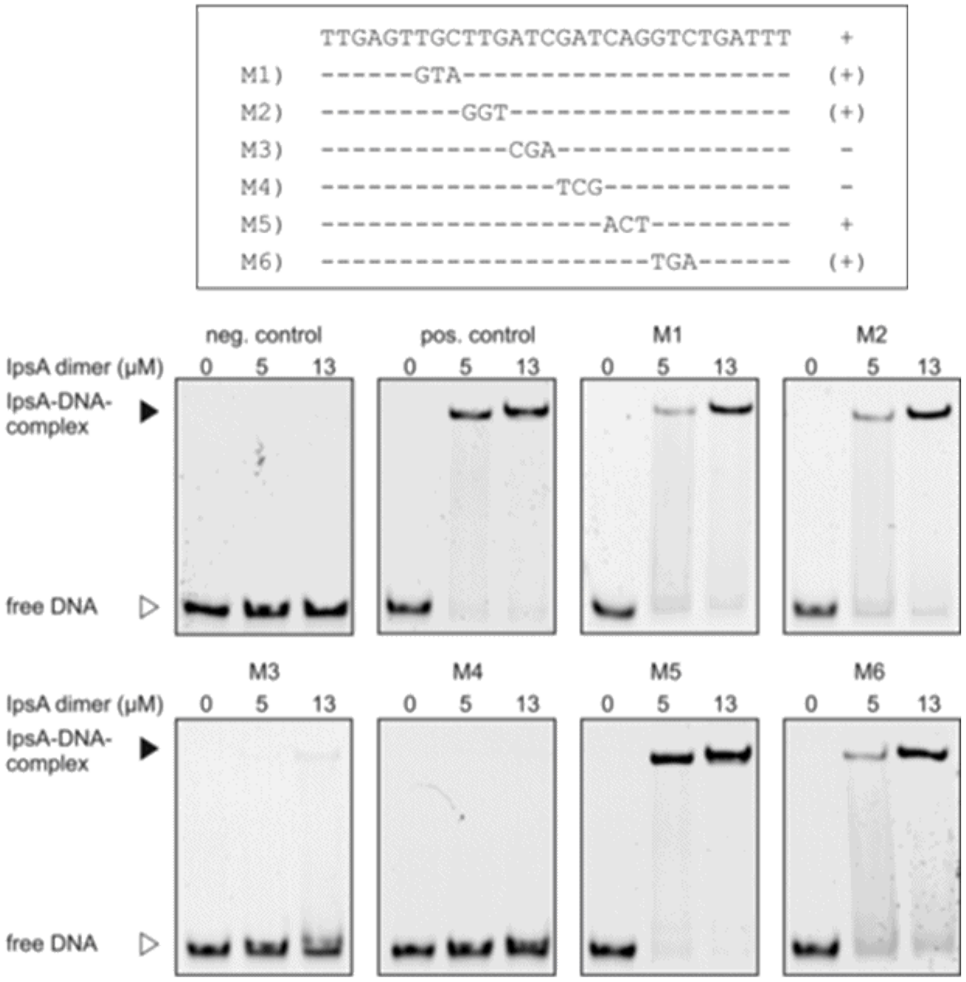

Figure 3.8: Mutational analysis of IpsA binding site in the *ino1* promoter. The mutated DNA fragments marked with + exhibited same affinity for binding as the wild type fragment (pos. control); while those with (+) showed reduced binding affinity. The fragments marked with - indicate loss of binding such as in case of M3 and M4 highlighting the importance of central six base pairs in IpsA binding. (Figure and data were provided by Baumgart *et. al.*, Julich)

The binding site information thus generated from EMSA analysis of promoter regions of *cg3323, cg0044, cg1421, cg3195, cg3210* and *cg0534* and the mutational analysis of the predicted motif were used to define a consensus palindromic motif depicted in Figure 3.9.

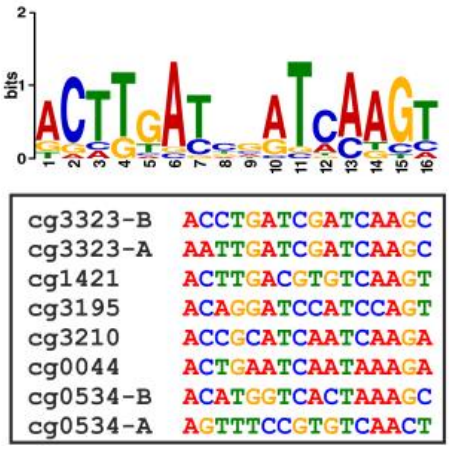

Figure 3.9: Consensus motif for IpsA binding as defined by MEME and EMSA analysis (Figure and data were provided by Baumgart *et. al.*, Julich)

Since EMSA analysis revealed a very high affinity of IpsA for *ino1*, that encodes a *myo*-inositol phosphate synthase (Bachhawat and Mande, 1999b), metabolites generated in *myo*-inositol biosynthesis pathway were chosen as prime candidates for effector molecules that influence IpsA-DNA complex formation. The purified IpsA was pre-incubated with effector molecules to be tested and then subjected to EMSA. Electrophoresis highlighted backshift only for *myo*-inositol whilst no differences were observed for 1D-*myo*-inositol-1-phosphate, 1D-*myo*-inositol-3-phosphate or glucose-6-phosphate (Figure 3.10).

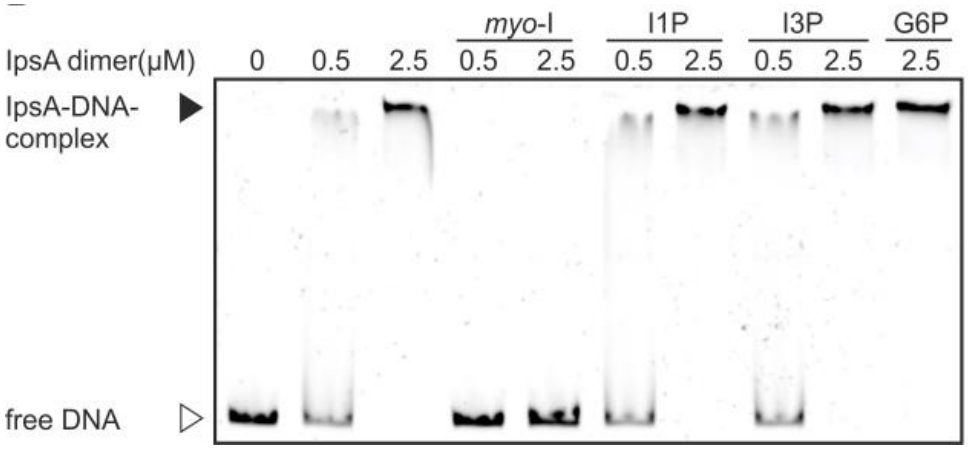

Figure 3.10: Effect of metabolites inositol metabolism on IpsA- *ino1* promoter complex. (Figure and data were provided by Baumgart *et. al.*, Julich)

3.3.5 Inositol-dependent regulation of *ino1* by IpsA

The results obtained so far suggest involvement of IpsA in regulation of *myo*-inostiol synthesis by activating *ino1* in absence of exogenous inositol. This initial observation was made from complementation studies with a plasmid encoded functional copy of *ino1* in C. *glutamicum* Δ*ipsA* where constitutive expression of Ino1 could successfully restore the wild type phenotype (Figure 3.4). To test the effect of IpsA and *myo*-inositol on *ino1* promoter, promoter-reporter fusion constructs were generated where *ino1* promoter was fused to *eyfp* (enhanced yellow fluorescent protein). The fluorescence output was recorded from wild type and Δ*ipsA* strain grown in minimal media supplemented with either glucose or *myo*-inositol (Figure 3.11). High *eyfp* expression was observed for wild type strain cultured using glucose as a carbon source. However, the gene expression levels for Δ*ipsA* strain were significantly low when the mutant was cultured in glucose. Both the strains showed highly reduced YFP levels when *myo*-inositol was used as the carbon source.

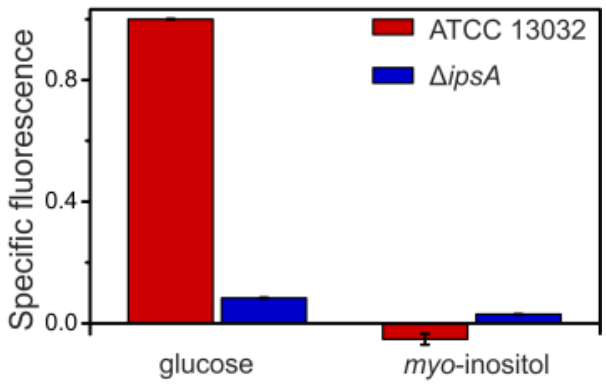

Figure 3.11: Promoter-fusion studies using the promoter of *ino1* fused to *eyfp* (pJC1-P*cg3323-eyfp*). The specific fluorescence of ATCC 13032 on glucose was set to 1 and the other values were calculated accordingly. (Figure and data were provided by Baumgart *et. al.*, Julich)

3.3.6 Function of IpsA in *C. diphtheria* and *M. tuberculosis*

IpsA homologues were identified in members of *Corynebacteriales* and a high degree of conservation was observed for the gene loci (Figure 3.1). This implicated its role in the pathogenic species of the order such as *C. diphtheria* and MTB. To deduce the function of *ipsA* in pathogens, homologues of IpsA in *M. tuberculosis* (Rv3575) and *C. diphtheriae* (DIP1969) were tested for restoration of wild type phenotype in *C. glutamicum* Δ*ipsA*. The expression of IpsA homologues from pathogenic species could partially restore the wild type phenotype in the mutant as slight retardation in growth (Figure 3.12 A and B) and shorter chain-clusters were evident in the complemented strains (Figure 3.12 C). IpsA homologue from *C. diphtheria* (DIP1969) could complement the loss of phenotype to a greater extent than the *M. tuberculosis* (Rv3575) homologue.

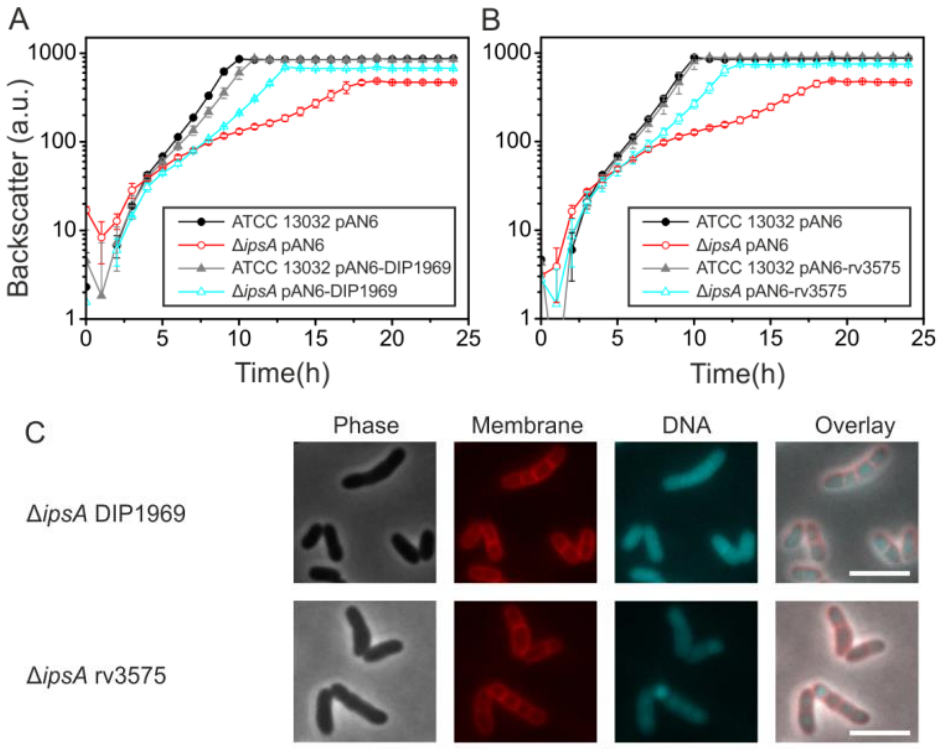

Figure 3.12: Complementation of phenotype of IpsA homolgues in *C. diphtheria* and *M. tuberculosis*. Growth curves for *C. glutamicum* Δ*ipsA* with plasmids pAN6, pAN6-*DIP1969* (**A**) or pAN6-*Rv3575c* (**B**) and *C. glutamicum* wild type with pAN6 as control in CGXII with glucose without IPTG (**A**) or with 50 µM IPTG (**B**). **C**. Morphology of the complemented strains with DAPI stained DNA (cyan) and nile red stained membrane regions (red), scale bar 5 µm. The data is respresentative of three biological replicates. (Figure and data were provided by Baumgart *et. al.*, Julich)

The IpsA binding site analysis for *cg3323* and *cg0044* homologues in *C. diphtheriae* and MTB revealed strong binding affnity of IpsA for *C. diphtheriae* promoters DIP0115 and DIP0021 (Figure 3.13A) and a binding site within the orf of *Rv0047c*, located upstream of *Rv0046c* in *Rv0047c-46* operon in MTB. The binding sites as revealed by MEME and EMSA analysis are summarised in Figure 3.13 B. The complex location of identified binding site within the gene highlights the possibility of presence of an alternative promoter upstream of *ino1*.

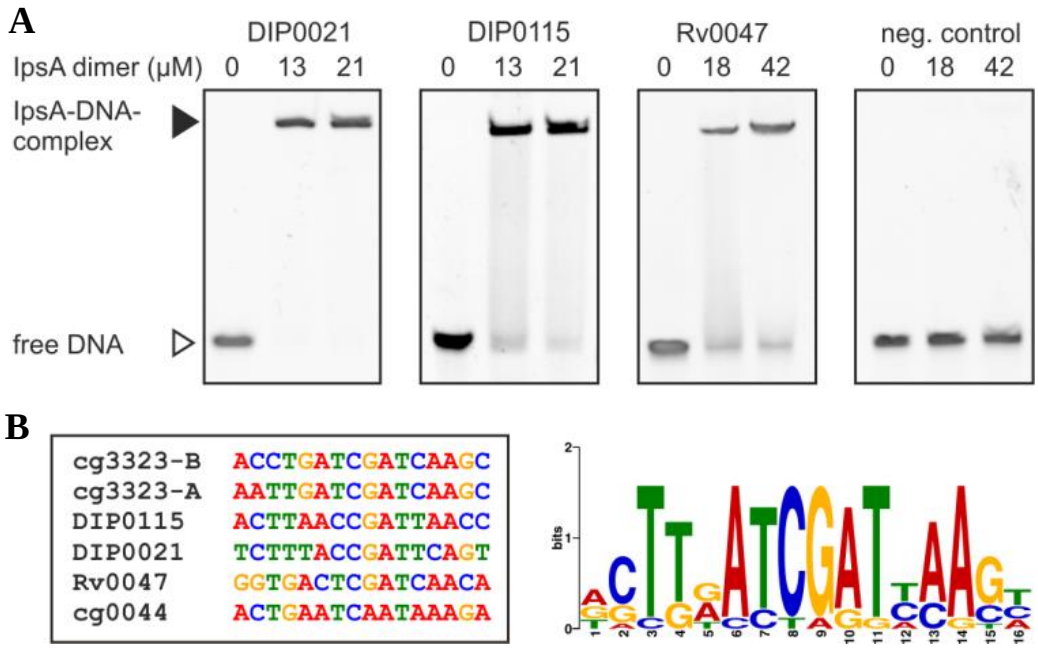

Figure 3.13: Binding affinity and motif for IpsA homologues in *C. diphtheria* and *M. tuberculosis*. **A**. EMSA analysis for predicted IpsA binding sites of DIP0021, DIP0115, Rv0047 and the neg. control. **B**. IpsA binding motif as generated by MEME analysis of IpsA binding sites in *C. diphtheriae* and *M. tuberculosis* target genes. (Figure and data were provided by Baumgart *et. al*., Julich)

3.3.7 Chromatographic analysis of polar lipid extracts from *C. glutamicum* Δ*2910* and complemented strains.

Since *myo*-inostiol is implicated in synthesises of PI, the building block of PIMs, LM and LAM, the effect of IpsA deletion was also studied on these cell wall components. For this purpose, [^{14}C]-labelled polar lipids were extracted from the wild type, *C. glutamicum* Δ*ipsA* and the complemented strains grown on glucose (Figure 3.14) and inositol (Figure 3.15) and the respective glycolipid profiles were examined using 2D-TLC. The wild-type strain showed spots corresponding to $AcPIM_2$, PI, Gl-A ($GlcAGroAc_2$) and Gl-X ($ManGlcAGroAc_2$) in lipid extracts (Figure 3.14A and 3.15A). Since Gl-A and Gl-X are phosphorous free lipoglycans based on

glucopyranosyl uronic acid, incorporation of [^{14}C]-acetate label was evident and weak spots were obtained for both Gl-A and Gl-X. The predominant spot on the TLCs migrating at the same position as Gl-X corresponds to PI. Interestingly, no $AcPIM_2$ was observed in lipid extracts isolated from the mutant *C. glutamicum* Δ*ipsA* (Figure 3.14B) when cultured in minimal media supplemented with glucose indicating absence of PI based glycolipid synthesis in the mutant. Successful complementation of the loss of gene function was observed for Δ*ipsA* complemented with *cg3323* (Figure 3.14C), *cg2910* (Figure 3.14D), *DIP1969* (Figure 3.14F) with an exception of *Rv3575c* (Figure 3.13E), as none of the components were stained with phosphate specific stain. The lipid extracts isolated from the mutant and complemented strains cultured in minimal media supplemented with inositol were similar to wildtype with distinct $AcPIM_2$ and PI (Figure 3.15 A-F)

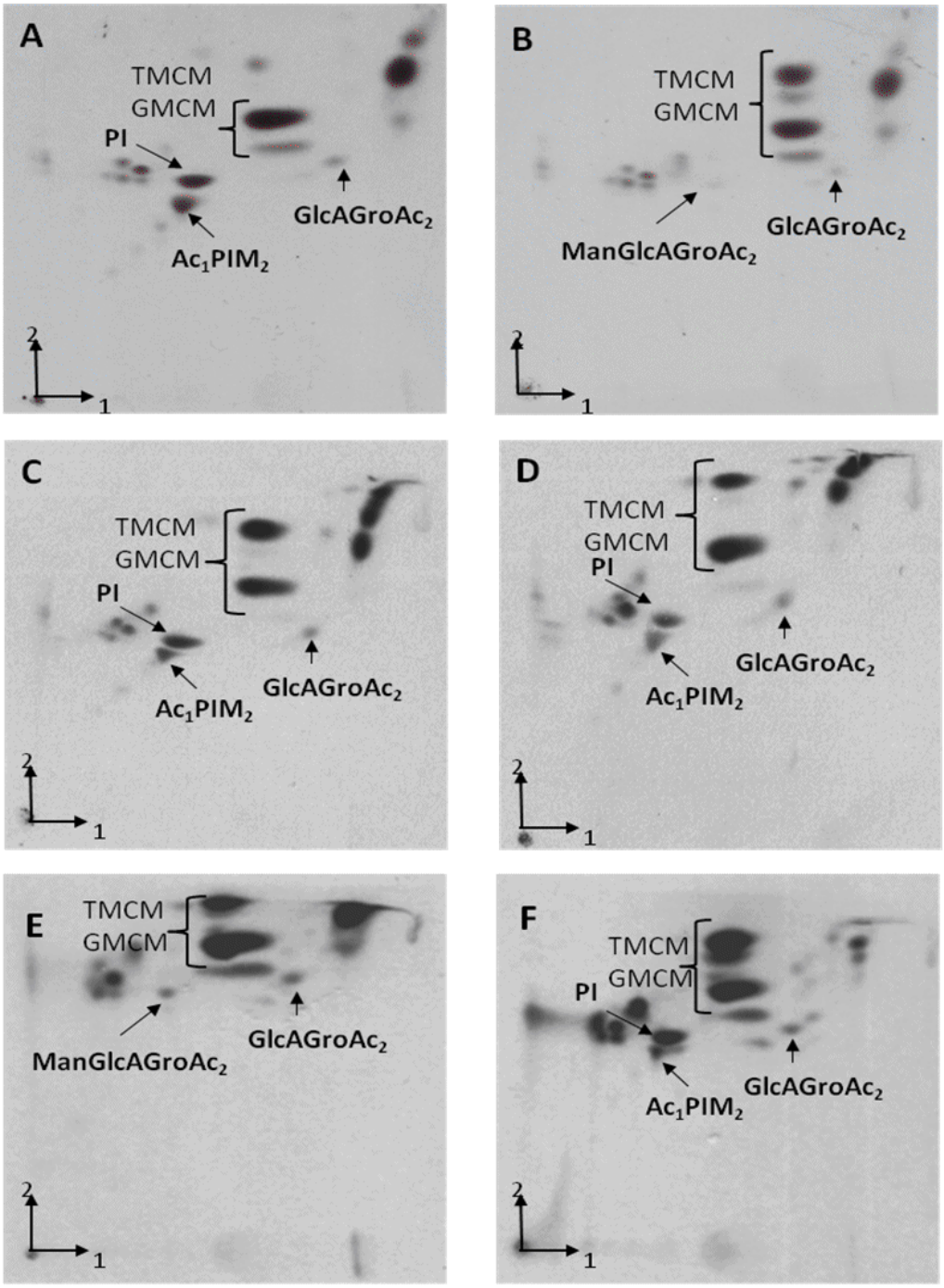

Figure 3.14. 2D-TLC analysis of [^{14}C]-labelled polar lipids from glucose grown cells. A. *C. glutamicum* ATCC 13032, **B.** ATCC 13032 Δ*ipsA*, **C**. ATCC 13032 Δ*ipsA* pAN6-*cg3323*, **D.** ATCC 13032 Δ*ipsA*::pK18int-*ipsA*, **E.** ATCC 13032 Δ*ipsA* pAN6-*Rv3575c* and **F.** ATCC 13032 Δ*ipsA* pAN6-*DIP1969*, cultured in CGXII supplemented with 2% (w/v) glucose. The polar lipids extracts were loaded on silica gel 60 TLCs and developed in the solvent system: chloroform/methanol/water (60:30:6, v/v/v) in direction 1 and chloroform/acetate/methanol/water (40:25:3:6, v/v/v/v) in direction 2.

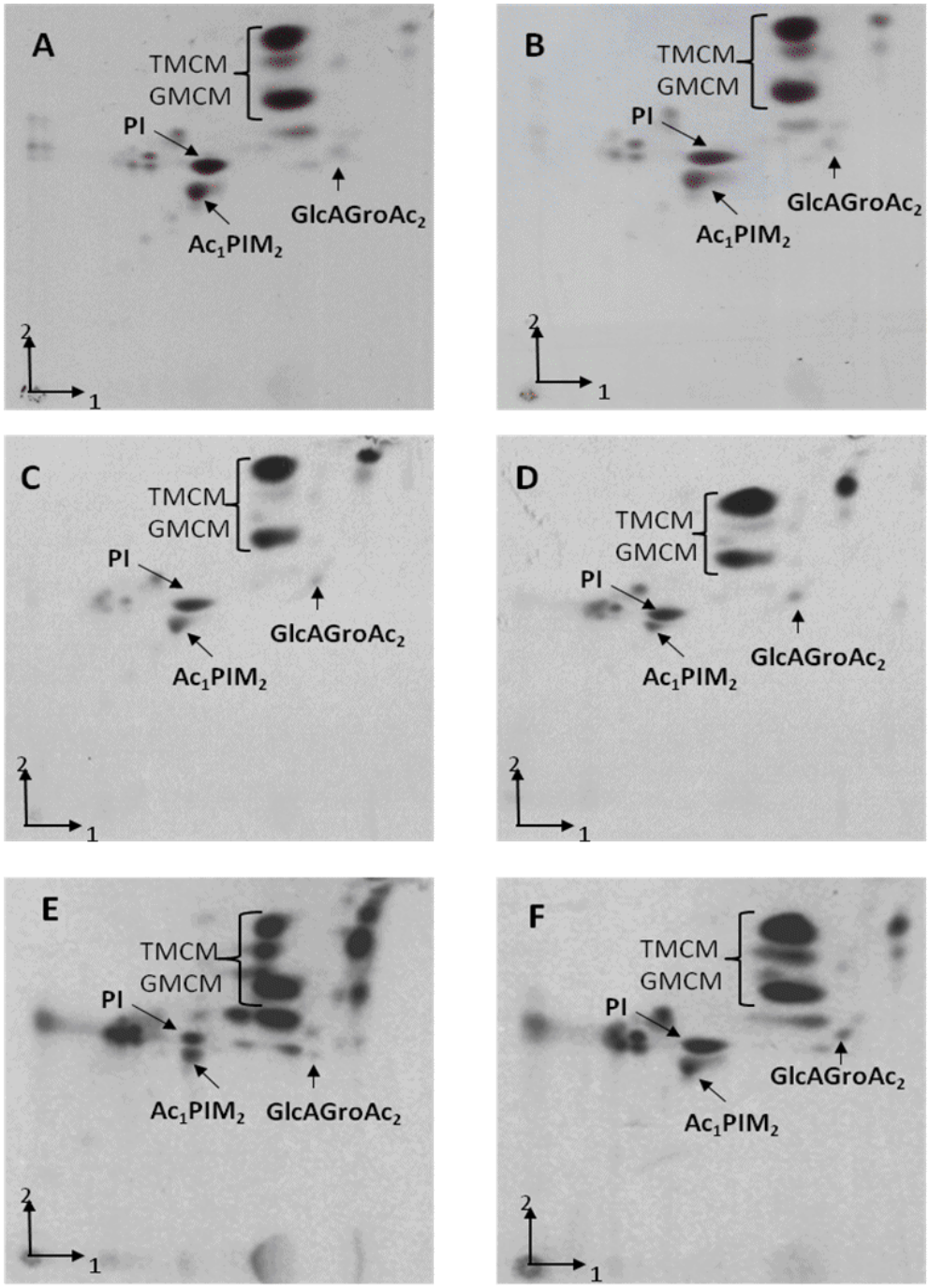

Figure 3.15. 2D-TLC analysis of [^{14}C]-labelled polar lipids from myo-inositol-grown cells. **A.** *C. glutamicum* ATCC 13032, **B.** ATCC 13032 Δ*ipsA*, **C.** ATCC 13032 Δ*ipsA* pAN6-*cg3323*, **D.** ATCC 13032 Δ*ipsA*::pK18int-*ipsA*, **E.** ATCC 13032 Δ*ipsA* pAN6-*Rv3575c* and **F.** ATCC 13032 Δ*ipsA* pAN6-*DIP1969*, cultured in CGXII supplemented with 2% (w/v) inositol. The polar lipids extracts were loaded on silica gel 60 TLCs and developed in the solvent system: chloroform/methanol/water (60:30:6, v/v/v) in direction 1 and chloroform/acetate/methanol/water (40:25:3:6, v/v/v/v) in direction 2.

3.3.8 Analysis of lipoglycan extracts.

Since the lipoglycans LM and LAM are built on PIMs which are mannosylated products of PI, effect of transcriptional regulator IpsA was also studied on these lipoglycans extracted from the wild type, mutant strain *C. glutamicum* Δ*ipsA* and the complemented strains cultured in minimal media supplemented with glucose or inositol and analysed by 15% SDS-PAGE gels stained using Pro-Q emerald stain specific for glycoproteins (Figure 3.16 A and B). The lipoglycan extracts from the wildtype cultured in glucose or inositol showed clear presence of LAM and Cg-LM-A/B. However, the lipoglycan extracts from the mutant *C. glutamicum* Δ*ipsA* grown on minimal media supplemented with glucose revealed no LAM while a band corresponding to Cg-LM-B could be observed (Fig 3.16A). The complemented strains *C. glutamicum ΔipsA::*pK18int-*ipsA* and *C.glutamicum ΔipsA* containing *cg3323* and *DIP1926* in plasmid pAN6 grown in minimal media supplemented with glucose exhibited lipoglycan profiles identical to the wildtype (Figure 3.16A). However, no band corresponding to LAM was observed in lipoglycan extracts of *C.glutamicum ΔipsA* complemented with *Rv3575c* in pAN6 plasmid grown in minimal media supplemented with glucose (Fig 3.16A). Instead, a band corresponding to Cg-LM-B was evident. Absence of LAM in lipoglycan isolates from the mutant strain complemented with Rv3575 was a result of partial complementation of phenotype by Rv3575c in *C.glutamicum ΔipsA*. The lipoglycans isolated from the mutant and complemented strains cultured in minimal media supplemented with inositol were similar to wildtype with distinct LM and LAM (Fig 3.16B).

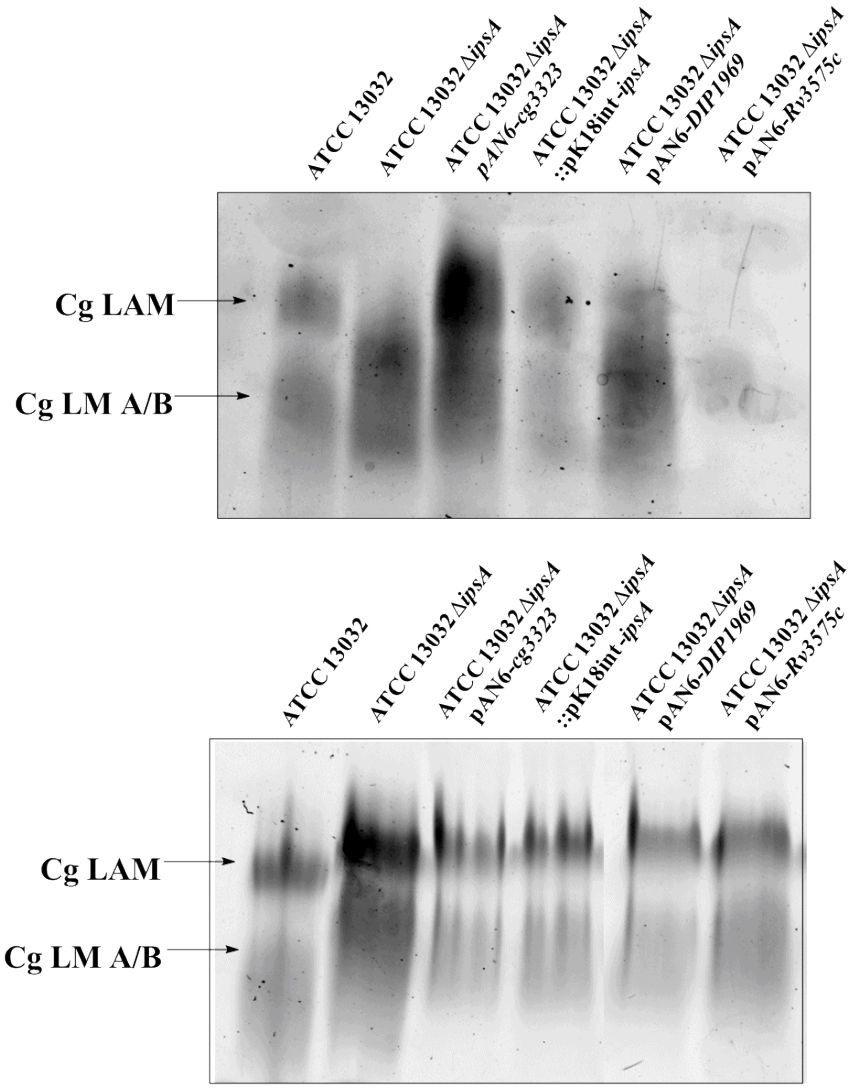

Figure 3.16: Lipoglycan profiles of *C. glutamicum* ATCC 13032, ATCC 13032 Δ*ipsA*, ATCC 13032 Δ*ipsA* pAN6-*cg3323*, ATCC 13032 Δ*ipsA*::pK18int-*ipsA*, ATCC 13032 Δ*ipsA* pAN6-*DIP1969* and ATCC 13032 Δ*ipsA*, pAN6-*Rv3575c* **A**. cultured in CGXII supplemented with 2% (w/v) glucose and **B.** in CGXII supplemented with 2% (w/v^{-}) inositol. Lipoglycans were analysed on 15% SDS-PAGE and visualised using Pro-Q emerald glycoprotein stain. The two major bands represented by Cg-LAM and Cg-LM-A/B are highlighted. The mutant *C. glutamicum* Δ*ipsA* was not complemented with pAN6-*Rv3575c* and produced Cg-LM-B in minimal media supplemented with glucose.

3.3.9 Effect of IpsA on mycothiol synthesis

As implicated from previous results, the Δ*ipsA* strain loses its ability to synthesise *myo*-inositol. Therefore, the effect of loss of *ipsA* gene function should also be evident on mycothiol biosynthesis. To test this hypothesis, intracellular levels of mycothiol were measured in wild type, deletion mutant and the complemented strains (Figure 3.17) using a previously described protocol (Feng *et al.*, 2006). To identify the peak corresponding to Mycothiol, chromatograms obtained for the wild type, IpsA deletion mutant and complemented strains were compared to those of mutant lacking mycothiol (Δ*mshC*) and to a control sample from wild type pre-treated with NMM (N-methyl-maleimide) that served as standards. The largest peak in wild type sample at ≈5 minutes was absent in control samples thus implying it as mycothiol. The Δ*ipsA* strain showed no peak corresponding to mycothiol but full complementation was seen for mutant with plasmid-encoded copy of IpsA (Figure 3.17). However, only partial complementation of mycothiol biosynthesis was observed in IpsA homologs from *C. diphtheriae* and *M. tuberculosis* consistent with the growth and morphology phenotypes. The mutant strain *C. glutamicum* Δ*mshC* exhibited a slow growth particularly during the pre-culture, consistent with previous studies (Feng *et al.*, 2006; Newton *et al.*, 2008). It is likely that MSH may have an important role to play in initiation of cell metabolism in an oxygen rich environment (Newton *et al.*, 2008). However, in this study the *C. glutamicum* Δ*mshC* strain was not analysed for any defects in cell wall biosynthesis.

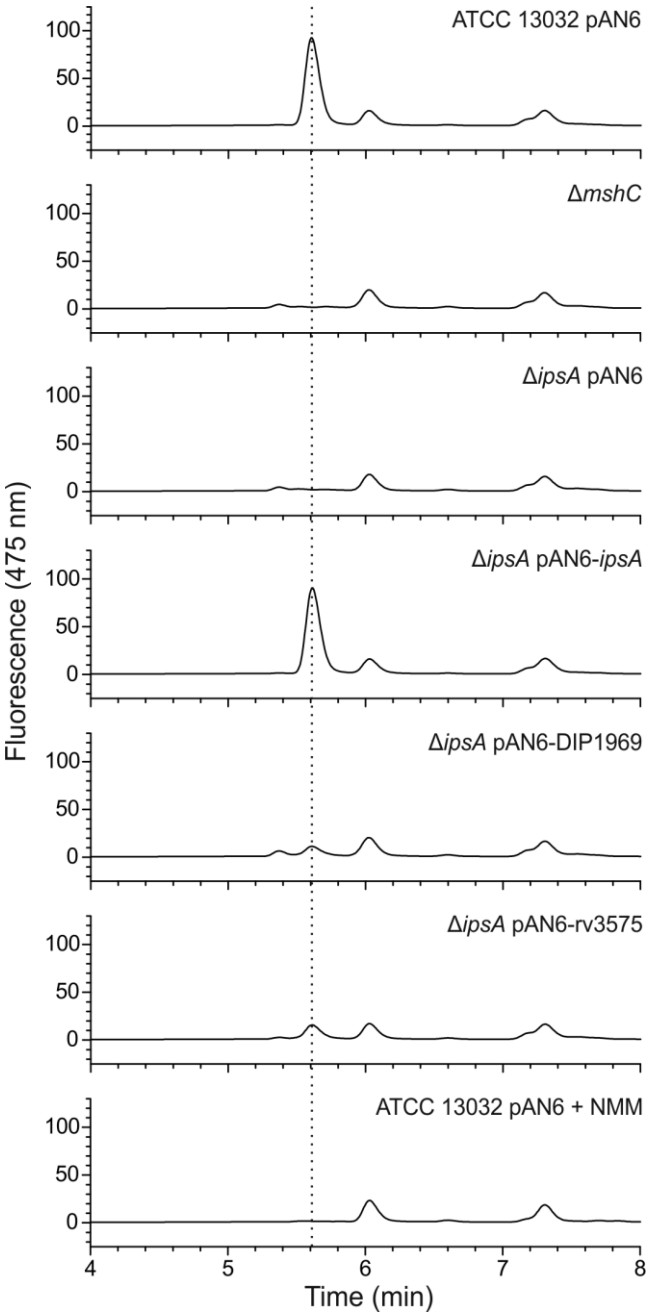

Figure 3.17: Analysis of mycothiol biosynthesis in *C. glutamicum* wild type, IpsA mutant and complemented strains. Mycothiol was extracted from relevant strains, derivatised and subjected to HPLC. The eluted fractions were checked using a fluorescence detector (390 nm excitation and 475 nm emission) for presence of mycothiol. Based on the chromatograms from mycothiol lacking Δ*msh* strain and NMM treated wild type samples as standards, the corresponding peak for mycothiol (marked with the dotted line) was identified and analysed for all strains. **(**Figure and data were provided by Baumgart *et. al*., Julich).

3.4 Discussion

The pathways for biogenesis of the cell wall components are well characterised in mycobacteria and corynebacteria with few missing pieces. However the regulation of biosynthesis of these components in both the organisms remains poorly understood. In an attempt to understand the regulation of biosynthesis of these cell wall components, we have identified a novel transcriptional regulator, named IpsA in corynebacteria and mycobacteria that functions as an activator of *ino1*, an inositol monophosphate synthase which is responsible for *myo*-inositol synthesis in *Corynebacteriales.* Inositol is an important component in mycobacteria and corynebacteria as it functions as a key component in synthesis of cell wall lipogycans and the antioxidant MSH (Fahey, 2013; Mishra *et al.*, 2011c). Disruption in inositol or mycothiol biosynthesis in MTB can lead to serious growth defects (Movahedzadeh *et al.*, 2004b; Vilcheze *et al.*, 2008), thus highlighting its significance in development of new drugs and its potential as a putative target. In this study, we have demonstrated that deletion of *ipsA* in *C. glutamicum* leads to a complete loss of mycothiol, PI and its derived lipids thus suggesting the significance of IpsA in these biosynthetic pathways. The two genes *ino1* and *cg0044*, were identified as major targets of IpsA that are activated in an inositol-dependant manner (Klaffl *et al.*, 2013; Krings *et al.*, 2006). Our findings are consistent with previous studies that have identified tranporters, regulators and enzymes for inostiol catabolism and suggested *myo*-insoitol to function as an alternative carbon source in *C. glutamicum* (Turner *et al.*, 2002).

The bioinformatic analysis of genomic loci of *ipsA* and its homologues in other corynebacteria and mycobacteria revealed a high degree of conservation of this gene among these species (Figure 3.1). In the genomes analysed, *ipsA* was found to be

situated downstream to *znuACB*, that encodes a putative zinc transport system (Krings *et al.*, 2006). Interestingly, zinc ion is required as a co-factor for catalytic function of IpsA target, Ino1 along with NAD^+ (Norman *et al.*, 2002). Downstream region of *ipsA* shows variability in terms of genetic arrangement dominated by genes encoding for proteins in trehalose biosynthesis (*otsAB*) (Schröder *et al.*, 2010).

DNA microarray analysis revealed several targets of IpsA whose promoters were subsequently tested for their binding efficiency with purified IpsA using EMSA. These results suggested *ino1* as the primary target which was further confirmed with genetic complementation studies. Whilst *ino1* may serve as the major target for IpsA, it is likely that other target genes, as suggested by DNA microarray and binding assays can also function as secondary targets, but the effect of IpsA on regulation of these genes is only important in specific stress conditions like shortage of carbon source, nutrients, metal ions etc. Majority of the targets as revealed by microarray and EMSA analysis are uncharacterised but might be important for regulation of cell wall and MSH biosynthesis with a potential to serve as drug targets for development of therapeutics. Some of the suggested functions for the possible targets are summarised in Table 4.

Table 3.4: IpsA targets with probable link to cell wall and MSH biosynthesis. (As suggested by Baumgart *et. al*., Julich)

Target gene	Protein attributes	Possible function
cg0044-0046	ABC-transporter of unknown function	Uptake of inositol (-derived) carbohydrates for cell wall biogenesis
cg3210	Cell envelope-related transcriptional regulator of the LytR type	Regulation of cell envelope biogenesis
cg1421	putative dinucleotide-binding enzyme similar to coenzyme F420-dependent NADP oxidoreductases	Supply or regeneration of co-factor for MSH-dependent detoxification
cg3195	flavin-containing monooxygenase with NAD(P) binding domain	

Interestingly, information about regulation of target genes by IpsA, as generated from microarray analysis suggested a strong correlation between the location of IpsA binding site and the -35 region of promoter sequences. The analysis of these regions highlighted that the IpsA binding site is located upstream of the -35 region in the target genes which are up-regulated (*cg3323*, c*g0044*, *cg3210*, and *cg3195*) in Δ*ipsA* strain while the for the down-regulated genes (*cg1421* and *cg0534*), the sites show overlapping with the -35 and/or the -10 region indicating a direct correlation between gene expression levels and IpsA deletion (Figure 3.18).

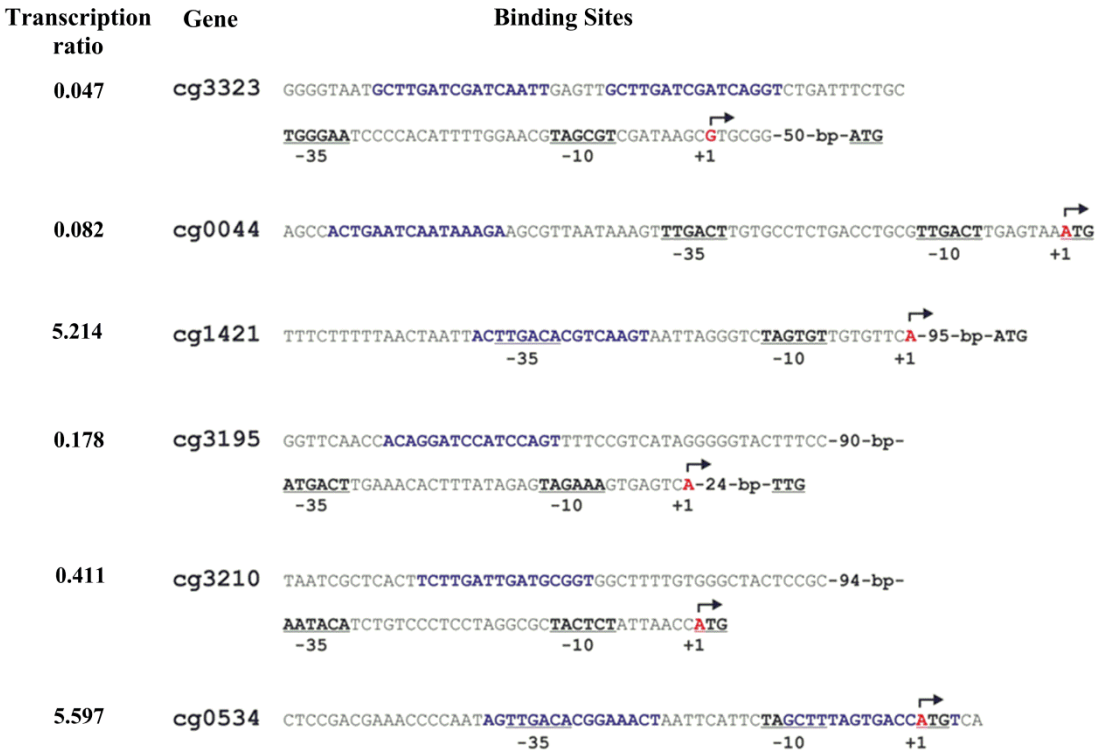

Figure 3.18: Transcription start sites, IpsA binding sites and promoter regions of the IpsA target genes in *C. glutamicum*. Transcriptional start sites for target genes (red) and binding sites for IpsA (blue) in the target genes and their location in the promoter including the -35 and -10 regions and transcription ratio as obtained from microarray of IpsA mutant. IpsA binds the -35 regions in *cg1421* and *cg0534* that prevents ribosome from translating the genes. **(**Figure and data were provided by Baumgart *et. al*., Julich).

The data obtained from microarray, EMSA, growth and morphology studies identified IpsA as a transcriptional regulator of *ino1*, inositol monophosphate synthase that catalyses the conversion of glucose-6-phosphate to inositol-1-monophosphate, the first step of PI biosynthesis. Since PI serves as the scaffold on which the cell wall components such as PIMs, LM and LAM are built, the mutant and the complemented strains were analysed for polar lipids and lipoglycans. The chromatographic analysis of radiolabelled polar lipids extracts of the mutant *C. glutamicum* Δ*ipsA* grown in minimal media supplemented with glucose displayed deficiency of $AcPIM_2$ and PI whilst Gl-A and Gl-X remained unaffected. In addition, the mutant strain grown on minimal media supplemented with glucose failed to produce PI based LAM and

instead, GL-X based LM, Cg-LM-B was apparent on SDS-PAGE analysis of lipoglycans. The loss of phenotype in *C. glutamicum* Δ*ipsA* was checked for self complementation in *C. glutamicum::*pK18int-*ipsA*. The polar lipid and lipoglycan extracts from this strain grown on minimal media supplemented with glucose displayed adequate $AcPIM_2$, PI, LM and LAM biosynthesis and profiles akin to wild type suggesting that the deletion of this putative transcriptional regulator in *C. glutamicum* abolishes the capacity of the bacteria to synthesise $AcPIM_2$ and PI based LM and LAM thus implying its involvement in early stages of PI biosynthesis.

To validate *ino1* as the effector target for IpsA, *C. glutamicum* Δ*ipsA* was checked for reversal of mutant phenotype when complemented with plasmid harbouring *ino1*. The polar and lipoglycan extracts obtained from the complemented strain grown in glucose when analysed, displayed profiles identical to that of wild type due to restoration of PI biosynthesis. The results obtained strongly imply that in absence of IpsA , PI based PIMs, LM and LAM are not synthesised as the mutant strain no longer produces the inositol monophosphate synthase (*ino1*) required for synthesis of *myo*-inositol, a substrate for PI production. These findings supplement the possibility of IpsA to function as a transcriptional activator of inositol monophosphate synthase, Ino1. Furthermore, the polar lipid and lipoglycan extract of *C. glutamicum* Δ*ipsA* complemented with its *C. diphtheria* homologue (*DIP1926*) exhibited lipid profiles akin to wildtype indicating DIP1926 to be a functional equivalent of IpsA and can be designated as a transcriptional activator of *ino1* (*DIP0115*) in this pathogen. The IpsA homologue in *M. tuberculosis* (Rv3575) demonstrated partial complementation in terms of growth, morphology and mycothiol biosynthesis, no PI based lipids or lipogylcans were identified on the TLCs. It is possible that any inositol generated in

this state is diverted for mycothiol biosynthesis probably due to higher affinity of the enzyme at this step than for PgsA. This diversion of inostiol away from PI biosynthesis pathway could result in generation of low quantities of PI and its derived lipids, sufficient enough for growth but not for detection by TLC. Additionally, the strategic placement of PadR like transcriptional regulator, upstream of *ino1* in the genomic loci of *M. tuberculosis* and its co-transcription with IpsA target, *ino1* (Norman *et al.*, 2002) hint towards its involvement as an extra regulator in *ino1* expression. Further studies are required to confirm the function of IpsA in mycobacteria.

This study has identified IpsA, as a novel LacI based transcriptional regulator for inositol biosynthesis in *Corynebacteriales.* The function of IpsA and its regulatory mechanism highlights the fine control of cell wall biogenesis by interplay of various enzymes. Since disruption of any of these pathways could drastically affect cell wall, the first line of defense in species of mycolata taxon, these pathways thus generate novel targets for therapy and drug development. In addition, identification and characterisation of this novel regulator could prove as a stepping-stone for further exploration the regulatory mechanisms in cell wall biosynthesis.

Chapter 4

4 Mapping the protein-protein interactions between mycobacterial glycosyltransferases for LAM biosynthesis using adenylate cyclase based bacterial two hybrid system and its potential applications in drug discovery

4.1 Introduction

The availability of whole genome sequence data for MTB has helped the research community make major advancements into tackling the problems of high-level TB drug resistance. The advent of the genomic era triggered a change in experimentation and helped researchers shift their focus towards identifying and characterising the gene products of mycobacteria that play an important role in virulence, immunity and survival of this pathogen. This approach enabled the mycobacterial research community to recognise several genes in mycobacteria with a potential to serve as drug targets. Numerous new compounds are generated each year but fail to translate into future drugs. In an attempt to bridge this gap, the post-genomic era in TB research has made use of data from sequencing, microarrays and other high-throughput methods, and successfully applied it to the fairly new field of proteomics. In this regard, protein-protein interactions has emerged as a valuable tool in drug discovery. Protein-protein interactions (PPI) has been employed to study protein dimerisation (Mai *et al.*, 2011), formation of enzymatic complexes (Veyron-Churlet *et al.*, 2005; Veyron-Churlet *et al.*, 2004), signal transduction (Cui *et al.*, 2009; Lee *et al.*, 2012a), and transport systems (Raman and Chandra, 2008) in mycobacteria. In addition, PPI studies at the proteome-level have aided in dissecting the pathways to drug resistance (Cui *et al.*, 2009; Raman and Chandra, 2008). This information can be exploited to assess druggablity of the interacting protein partners and hence aid in development of novel inhibitors against MTB.

The cell wall of mycobacteria has always served as a very attractive target for developing anti-tubercular compounds. The free lipids in the mycobacterial cell wall, such as PIMs, LM, and LAM are important structural components, that play a central role in the pathogen's viability and the modulation of host immune responses (Mishra *et al.*, 2011a). Therefore, the pathways for the biogenesis of these components provides a valuable system to discover new anti-tubercular agents. The arabinan and mannan motifs in LAM are extensively branched and require a series of glycosylation reactions which are mediated by numerous mannopyranosyl transferases (ManTs) and arabinofuranosyl transferases (AraTs) that are tightly regulated. For this purpose, a rapid and efficient flux of the metabolic intermediates from one catalytic site to another is necessary and can likely be achieved if the intermediates are channeled through the pathway. Therefore, these AraTs, ManTs and other associated enzymes of LAM biosynthesis can possibly exist in metabolons that are dependent on protein-protein interactions to aid in the channeling process. This hypothesis is further strengthened by blue native poly-acrylamide gel electrophoresis (BN-PAGE) studies on the proteome of *M. bovis* BCG that identified several proteins clustered together in multi-enzyme complexes, which included the AraTs EmbA, EmbB and EmbC (Zheng *et al.*, 2011). In addition, the genetic organisation of the *emb* operon, reveals a high degree of similarity between the Emb proteins (61% - 68%) (Wolucka, 2008), similar catalytic activities and their contribution to EMB resistance all favour the possibility of EmbA (*Rv3794*), EmbB (*Rv3795*) and EmbC (*Rv3793*) to exist as a metabolon in *M. tuberculosis.*

The BN-PAGE study also identified the regulatory protein LpqW (*Rv1166*) to be associated with the probable Emb complex as a soluble functional partner of these AraTs (Zheng *et al.*, 2011). The function of LpqW is critical as it mediates the flux of

PIM_4, to polar PIMs and LAM (Kovacevic *et al.*, 2006; Rainczuk *et al.*, 2012). Synthesis of PIM_4 serves as a branch point in the pathway as it can either be flipped towards the extra-cytoplasmic side by unknown flippases (Berg *et al.*, 2007) and subsequently mannosylated by the GT-C superfamily glycosyltransferases MptB, MptA and MptC (Besra *et al.*, 1997) or be directed towards PIM_6 formation that is catalysed by another GT-C superfamily glycosyltransferase, PimE (Haites *et al.*, 2005a; Morita *et al.*, 2004). The relative distribution of PIM_4 is determined by regulating the competing mannosyltransferases PimE (*Rv1159*) and MptB (*Rv1459c*) by LpqW (Berg *et al.*, 2007), that is possibly dependent on PimE-LpqW, MptB-LpqW interactions.

Therefore, in this study, we have attempted to deduce the critical homotypic and heterotypic interactions between the glycosyltransferases and accessory proteins of the lipoglycan biosynthesis pathway using a Bacterial Two Hybrid system based on the reconstitution of adenylate cyclase (Karimova *et al.*, 1998b). This system relies on functional complementation between the two fragments (T25: residues 1-224 and T18: residues 225-399) of the catalytic domains in adenylate cyclase (AC) enzyme (*cyaA*) from *Bordetella pertussis* to reconstruct the cAMP signalling cascade in *E. coli.* The individual proteins in LAM biosynthesis were fused to the T25 and T18 fragments and co-expressed in Cya^- *E. coli*. Positive interactions result in heterodimerisation of chimeric T25 and T18 that confers a Cya^+ phenotype that is detected using indicator/selective media. The degree of interaction between the proteins was also assessed using β-galactosidase assays. The principle and methodology of the procedure is outlined in Figure 4.1 and 4.2 respectively.

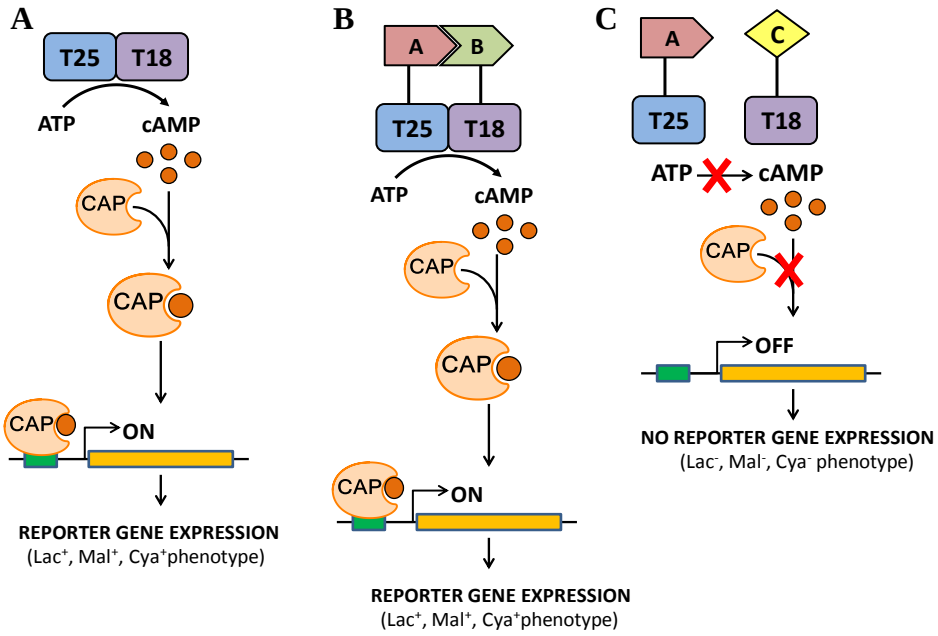

Figure 4.1: Principle of detecting protein-protein interactions using two-hybrid system. A. The interaction between the two domains (T18 and T25) is necessary for reconstitution of a functional adenylate cyclase (AC). AC synthesises the regulatory molecule cAMP that has a pleiotroipc effect on transcription in *E. coli* by binding to the catabolite activator protein (CAP). The cAMP-CAP complex controls the expression of many genes involved in catabolism of carbohydrates, including the *lac* or *mal* genes of lactose and maltose catabolism. The strains used for selecting the positive clones lack the endogenous adenylate cyclase (*cya*) and thus are unable to ferment these carbohydrates. When adenylate cyclase is reconstituted in Cya^- *E.coli*, it drives the synthesis of cAMP to give a Cya^+ phenotype that can be distinguished from Cya^- on indicator media such as LB supplemented with X-Gal, MacConkey or on selective media such as M63. **B.** The fusion of the T25 and T18 domains with proteins of interest (A and B) would result in a Cya^+ phenotype only when the proteins interact. **C.** In absence of any interaction between the proteins of interest (A and C) would not synthesise adenylate cyclase and fail to exhibit reporter gene expression.

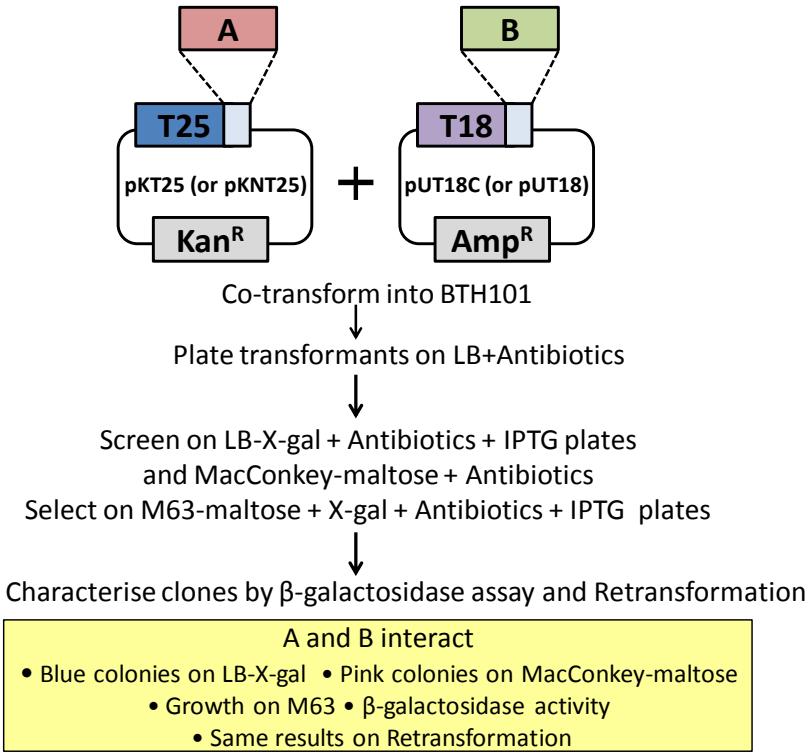

Figure 4.2: Methodology for detecting protein-protein interactions using two-hybrid system based on reassembly of adenylate cyclase. The proteins of interest (A and B) are cloned into the IPTG inducible vectors with an N or C-terminal T25 (pKT25/pKNT25) or T18 domain (pUT18C/pUT18) and co-transformed into Cya^- *E. coli* strain (BTH101). The transformants are selected on LB agar plates with antibiotics and overnight cultures are set up in LB broth with antibiotics. The cultures are also induced with 0.5 mM IPTG for expression of the hybrid proteins. The overnight cultures are screened for Cya^+ or Cya^- phenotype by spotting or streaking on LB agar plates with 40 µg/mL X-gal and MacConkey agar plates with 1% maltose. The plates are supplemented with 0.5 mM IPTG and antibiotics. The colonies are also tested for growth on minimal M63 agar plates with 0.2% maltose. For characterisation, β-galactosidase assays are performed to assay the activity of the enzyme and the extent of interaction. Additionally, the plasmids are retransformed into BTH101 and put through the same procedure to confirm the interaction. A true positive interaction is characterised by blue colonies on LB-X-gal, red colonies on MacConkey-maltose, growth on M63-maltose, detectable β-galactosidase activity and consistent results on retransformation.

4.2 Materials and Methods

4.2.1 Chemicals, reagents and enzymes

All chemicals and solvents were bought from Sigma-Aldrich (Dorset, UK), Bio- Rad (Ca, USA) and Fisher Chemicals (UK) unless otherwise stated, and were of AnalR grade or equivalent. Plasmids were propagated during cloning in E. coli XL-1 Blue cells (Invitrogen). All restriction enzymes, T4 DNA ligase and Phusion DNA polymerase enzyme were sourced from New England Biolabs. Oligonucleotides were from MWG Biotech Ltd and PCR fragments were purified using the QIAquick gel extraction kit (Qiagen). Plasmid DNA was purified using the QIAprep purification kit (Qiagen).

4.2.2 Bacterial strains, plasmids and growth conditions

The vector plasmids were propagated in *E. coli* XL-1 Blue cells using the protocol mentioned in General Materials and Methods section 7.3.6 and 7.3.7. The strain BTH101 **(**F^-, *cya-99, araD139, galE15, galK16, rpsL1 (Str* ^{r}*), hsdR2, mcrA1, mcrB1*) was used as the host organism for detection of protein-protein interactions (Claessen *et al.*, 2008; Karimova *et al.*, 1998a). The strains were routinely grown in Luria-Bertani broth (LB, Difco) at 37°C (Sambrook *et al.* 1989) unless otherwise stated. Appropriate antibiotics were added for selection of required strains.

Plasmids were isolated using the QIAprep Spin Miniprep Kit. The *E. coli* cells were transformed using rubidium chloride method as mentioned in the General Materials and Methods, section 7.3.6 and 7.3.7

4.2.3 Construction of plasmids and strains

The plasmids used in this work are IPTG inducible *E. coli* expression vectors. To generate C-term and/or N-term T25 and/or T18 fused proteins, pUT18 (T18 fusion in N-terminus), pUT18C (T18 fusion in C-terminus), pKT25 (T25 fusion in C-terminus) and pKNT25 (T25 fusion in N-terminus) vectors were used for cloning the gene of interest. The genes for LAM biosynthesis pathway in *M. tuberculosis* were amplified from genomic DNA of *M. tuberculosis* H37Rv. The primers and the restriction sites used for the study are listed in Table 4.1. The BACTH system kit (Karimova *et al.*, 1998b) comprising of vectors, positive controls and relevant strains required for analysis of complementation were obtained from Euromedex. All the constructs were confirmed by sequencing by Eurofins DNA Ltd. using the standard M13 reverse primer (29mer) and gene specific internal primers where necessary.

4.2.4 Control plasmids

The plasmid pKT25-zip is a derivative of pKT25 in which the leucine zipper of eukaryotic transcriptional activiator GCN4 is genetically fused in frame to the T25 fragment (cloned within the *KpnI* site of pKT25) of adenylate cyclase enzyme. The vector construct pUT18C-zip is a derivative of pUT18C in which the leucine zipper of GCN4 is genetically fused in frame to the T18 fragment (cloned between the restriction sites, *KpnI* and *EcoRI* of pUT18C). The constructs pKT25-zip and pUT18C-zip function as positive controls for complementation analysis as the T25-zip and T18-zip fusion proteins expressed by these plasmids interact due to dimerization of the leucine zipper motifs attached to the T25 and T18 fragments. When pKT25-zip and pUT18C-zip are co-transformed into BTH101, they restore the characteristic Cya^+ phenotype that

is detected by red colonies on MacConkey, blue colonies on LB-X-gal and growth on M63 minimal media plates.

4.2.5 Screening of protein-protein interactions using the bacterial two hybrid system

The screening of potential protein-protein interactions relies on reverting Cya^- *E. coli* strain to Cya^+ by co-expressing the fusion constructs. The reversion of mutant phenotype happens only during a positive interaction as in this case the adenylate cyclase is successfully reconstituted, thus resulting in expression of resident reporter genes that confer β-galactosidase activity, ability to utilise lactose and maltose as a carbon source to the mutant.

The genes encoding the glycosyltransferases and accessory proteins of the LAM biosynthesis pathway (Table 4.1) were amplified from genomic DNA of *M. tuberculosis* H37Rv by PCR using suitable primer pairs (Table 4.1) and were ligated in frame with the T25 and T18 fragment of pKT25 (or pKNT25) and pUT18 (or pUT18C) vectors linearised *via* appropriate restriction enzymes (Table 4.1). The ligation reactions were performed using T4 DNA ligase. Since the vectors do not encode the LacI repressor, to avoid accumulation of mutations in the constructs, the vectors and recombinant plasmids were commonly propagated at 30°C in standard *E. coli* strain, such as XL1-Blue with $lacI^q$. Plasmid DNA was routinely purified using the QIAgen miniprep kit used for mini-preparation of DNA, according to the manufacturer's instructions. Positive clones were subsequently verified by sequencing using M13 reverse primer (5'-CAGGAAACAGCTATGACC-3') and internal primer where necessary. The two recombinant plasmids encoding the N or C-terminal T25 domain and N or C-terminal

T18 domain tagged hybrid proteins were transformed into competent BTH101 reporter cells. Transformants were plated on LB agar plates supplemented with antibiotics (100 µg/mL Amp, 50 µg/mL Kan) for selection of both plasmids and incubated at 30°C for 24 hours. A positive control using the pKT25-zip and pUT18C-zip was subjected through the same process and was employed for detecting the interactions. The combinations pKT25-pUT18, pKT25-pUT18C, pKNT25-pUT18, pKNT25-pUT18C were used as negative experimental controls. To eliminate false positives due to sticky proteins, the fusion constructs were transformed with empty vector with the second interacting domain (For eg. A-pKT25 was tested with pUT18 and pUT18C) and analysed using the same method.

For screening, 2-3 colonies of the co-transformants were used to initiate overnight cultures (200 rpm, 30ºC, 16 hours) in 2 mL LB broth supplemented with antibiotics (100 µg/mL Amp, 50 µg/mL Kan, 50 µg/mL Strep) and 0.5 mM IPTG to induce protein expression. To analyse the expression of the β-galactosidase (*lacZ*) in co-transformants, 3-5µL of the overnight cultures were spotted on LB agar plates with 40 µg/mL X-gal (5-bromo-4-chloro-3-indolyl-β-d-galactopyranoside), 0.5 mM IPTG and antibiotics (100 µg/mL Amp, 50 µg/mL Kan, 50 µg/mL Strep). The plates were incubated at 30ºC for 48 hours and the colour change was noted. As a second screening procedure, the co-transformants were also spotted on MacConkey agar plates with 1% maltose, 0.5 mM IPTG and antibiotics (100 µg/mL Amp, 50 µg/mL Kan, 50 µg/mL Strep) and incubated at 30ºC for 2-3 days. The phenotype of the colonies on indicator plates was compared to that of the positive control. The blue colonies on LB-X-gal plates and red colonies on MacConkey-maltose plates were indicative of positive interactions.

Table 4.1: Oligonucleotides and plasmid constructs used in this study.

Construct	Oligonucleotide Sequence (5' → 3')	Properties
pKT25	-	Kan^R, pSU40 derivative with T25 domain of CyaA under *lac* promoter, MCS at 3' end of T25
pKNT25	-	Kan^R, pSU40 derivative with T25 domain of CyaA under *lac* promoter, MCS at 5' end of T25
pUT18	-	Amp^R, pUC19 derivative with T18 domain of CyaA under *lac* promoter, MCS at 5' end of T18
pUT18C	-	Amp^R, pUC19 derivative with T18 domain of CyaA under *lac*promoter, MCS at 3' end of T18
pKT25-zip	-	Kan^R, pSU40 derivative with T25 domain of CyaA fused in frame with leucine zipper of GCN4 within *KpnI* site under *lac*promoter
pUT18C-zip	-	Amp^R, pUC19 derivative with T18 domain of CyaA fused in frame with leucine zipper of GCN4 within *KpnI* and *EcoRI* site under *lac*promoter
pKNT25-PimA	fw:AACTCCTGCAGCATGCGGATCGGCATGATTTG rv:TTAATCTAGAGTGCTGGCCACCTGAACCTTG	Kan^R, *Rv2610* fused in frame with T25 domain of CyaA at N-terminus within *XbaI* and *PstI* site under *lac* promoter
pUT18C-PimA	fw:AACTCCTGCAGCATGCGGATCGGCATGATTTG rv:TTAATCTAGAGTGCTGGCCACCTGAACCTTG	Amp^R, *Rv2610* fused in frame with T18 domain of CyaA at C-terminus within *XbaI* and *PstI* site under *lac* promoter
pKT25-PimB'	fw:AATTCTGCAGAGTGAGCCGGGTCCTGTTG rv:AATTGGTACCCGACGGGCCGCATCGTCG	Kan^R, *Rv2188c* fused in frame with T25 domain of CyaA at C-terminus within *PstI* and *KpnI* site under *lac* promoter
pKNT25-PimB'	fw:AATTCTGCAGAGTGAGCCGGGTCCTGTTG rv:AATTGGTACCCGACGGGCCGCATCGTCG	Kan^R, *Rv2188c* fused in frame with T25 domain of CyaA at N-terminus within *PstI* and *KpnI* site under *lac* promoter

pUT18-PimB'	fw:AATTCTGCAGAGTGAGCCGGGTCCTGTTG rv:AATTGGTACCCGACGGGCCGCATCGTCG	Amp^R, *Rv2188c* fused in frame with T18 domain of CyaA at N-terminus within *PstI* and *KpnI* site under *lac* promoter
pUT18C-PimB'	fw:AATTCTGCAGAGTGAGCCGGGTCCTGTTG rv:AATTGGTACCCGACGGGCCGCATCGTCG	Amp^R, *Rv2188c* fused in frame with T18 domain of CyaA at C-terminus within *PstI* and *KpnI* site under *lac* promoter
pKT25-Rv2611	fw:AACCTCTAGAAGTGATTGCCGGCCTTAAG rv:AATTGGTACCCGCTCTGGACCTCAGTTGC	Kan^R, *Rv2611c* fused in frame with T25 domain of CyaA at C-terminus within *XbaI* and *KpnI* site under *lac* promoter
pKNT25-Rv2611	fw:AACCTCTAGAAGTGATTGCCGGCCTTAAG rv:AATTGGTACCCGCTCTGGACCTCAGTTGC	Kan^R, *Rv2611c* fused in frame with T25 domain of CyaA at N-terminus within *XbaI* and *KpnI* site under *lac* promoter
pUT18C-Rv2611	fw:AACCTCTAGAAGTGATTGCCGGCCTTAAG rv:AATTGGTACCCGCTCTGGACCTCAGTTGC	Amp^R, *Rv2611c* fused in frame with T18 domain of CyaA at C-terminus within *XbaI* and *KpnI* site under *lac* promoter
pKNT25-LpqW	fw:AATTTCTAGAAATGGGCGTGCCCAGCCCAG rv:CCAAGGTACCCGTTGCCCGGTCTTCACC	Kan^R, *Rv1166* fused in frame with T25 domain of CyaA at N-terminus within *XbaI* and *KpnI* site under *lac* promoter
pUT18C- LpqW	fw:AATTTCTAGAAATGGGCGTGCCCAGCCCAG rv:CCAAGGTACCCGTTGCCCGGTCTTCACC	Amp^R, *Rv1166* fused in frame with T18 domain of CyaA at C-terminus within *XbaI* and *KpnI* site under *lac* promoter
pUT18C-PimE	fw:AGGATCTAGAAATGTGCCGCACCCTGATCGACG rv:ATTAGAATTCCTAATTGGCCATGCGCCGCGGCC	Amp^R, *Rv1159* fused in frame with T18 domain of CyaA at C-terminus within *XbaI* and *EcoRI* site under *lac* promoter
pKT25-MptA	fw:AGGCTCTAGAAATGACTACTCCGAGCCATGCTCC rv:CAACGAATTCTGTGGCGTATTGACCACCGGGGTTG	Kan^R, *Rv2174* fused in frame with T25 domain of CyaA at C-terminus within *XbaI* and *EcoRI* site under *lac* promoter

pKNT25-MptB	fw:ATTATCTAGACATGGCAGCCCGCCACCATACGCT rv:ATTAGGTACCGTCGTGGAATCAGCGTAGGCGTC	Kan^R, *Rv1459c* fused in frame with T25 domain of CyaA at N-terminus within *XbaI* and *KpnI* site under *lac* promoter
pUT18C-MptB	fw:ATTATCTAGACATGGCAGCCCGCCACCATACGCT rv:ATTAGGTACCTCACGTGGAATCAGCGTAGGCGTC	Amp^R, *Rv1459c* fused in frame with T18 domain of CyaA at C-terminus within *XbaI* and *EcoRI* site under *lac* promoter
pKT25-MptC	fw:ATTACTGCAGACATGAGTGCATGGCGGGCGC rv:ATTATCTAGAGCTGGCCGTCGGCGCCGGGGT	Kan^R, *Rv2181* fused in frame with T25 domain of CyaA at C-terminus within *PstI* and *EcoRI* site under *lac* promoter
pKNT25-MptC	fw:ATTATCTAGAAATGAGTGCATGGCGGGCGCCCG rv:ATTAGAATTCGTTCAGCTGGCCGTCGGCGCCG	Kan^R, *Rv2181* fused in frame with T25 domain of CyaA at N-terminus within *XbaI* and *EcoRI* site under *lac* promoter
pUT18-MptC	fw:ATTATCTAGAAATGAGTGCATGGCGGGCGCCCG rv:ATTAGAATTCGTTCAGCTGGCCGTCGGCGCCG	Amp^R, *Rv2181* fused in frame with T18 domain of CyaA at N-terminus within *XbaI* and *EcoRI* site under *lac* promoter
pKT25-EmbA	fw:AGACTCTAGAAGTGCCCACGACGGTAATG rv:ATAAGAGCTCTGGCAGCGCCCTGATCGGTCCT	Kan^R, *Rv3794* fused in frame with T25 domain of CyaA at C-terminus within *XbaI* and *SacI* site under *lac* promoter
pKNT25-EmbB	fw:AGACTCTAGAAATGACACAGTGCGCGAGCAGACGC rv:ATAAGAGCTCTGGACCAATTCGGATCTTGCCCGG	Kan^R, *Rv3795* fused in frame with T25 domain of CyaA at N-terminus within *XbaI* and *SacI* site under *lac* promoter
pUT18C-EmbB	fw:AGACTCTAGAAATGACACAGTGCGCGAGCAGACGC rv:ATAAGAGCTCCTATGGACCAATTCGGATCTTGGCCGG	Amp^R, *Rv3795* fused in frame with T18 domain of CyaA at C-terminus within *XbaI* and *SacI* site under *lac* promoter

pKNT25-EmbC	fw:AGACTCTAGAAATGG CTACCGAAGCCGCCCC rv:ATAAGAGCTCGCCGC GGCGCAACGGC	Kan^R, *Rv3793* fused in frame with T25 domain of CyaA at N-terminus within *XbaI* and *SacI* site under *lac* promoter
pUT18C-EmbC	fw:AGACTCTAGAAATGG CTACCGAAGCCGCCCC rv:ATAAGAGCTCCTAGC CGCGGCGCAACGG	Amp^R, *Rv3793* fused in frame with T18 domain of CyaA at C-terminus within *XbaI* and *SacI* site under *lac* promoter
pKNT25-AftC	fw:ATTCTCTAGAAGTGT ACGGTGCGCTGG rv:ATTAGAATTCCTCCG CTGGCCCTCCC	Kan^R, *Rv2673* fused in frame with T25 domain of CyaA at N-terminus within *XbaI* and *EcoRI* site under *lac* promoter
pUT18C-AftC	fw:ATTCTCTAGAAGTGT ACGGTGCGCTGG rv:ATTAGAATTCTCACC GCTGGCCCTCCCG	Amp^R, *Rv2673* fused in frame with T18 domain of CyaA at C-terminus within *XbaI* and *EcoRI* site under *lac* promoter
pKNT25-AftD	fw:ATTCTCTAGAAGTGG CGCCGTTGTCTC rv:TCCAGAATTCTTGCA TGCGGTCTTGAC	Kan^R, *Rv0236c* fused in frame with T25 domain of CyaA at N-terminus within *XbaI* and *EcoRI* site under *lac* promoter
pUT18-AftD	fw:ATTCTCTAGAAGTGG CGCCGTTGTCTC rv:ATCCGATTCTGTTGC ATGCGGTCTTGAC	Amp^R, *Rv0236c* fused in frame with T18 domain of CyaA at N-terminus within *XbaI* and *EcoRI* site under *lac* promoter
pKNT25-CapA	fw:ATTATCTAGAATGCA TGCCAGTCGTCCCGGCG C rv:AGGAGAATTCCCGCG TTGACTTGACCACCTG	Kan^R, *Rv1635c* fused in frame with T25 domain of CyaA at N-terminus within *XbaI* and *EcoRI* site under *lac* promoter
pUT18C-CapA	fw:ATTATCTAGAATGCA TGCCAGTCGTCCCGGCG C rv:ATTAGAATTCTTACC GCGTTGACTTGACCACC TGCG	Amp^R, *Rv1635c* fused in frame with T18 domain of CyaA at C-terminus within *XbaI* and *EcoRI* site under *lac* promoter

4.2.6 Selection of positive interactions as determined by the screening procedure

The transfomants screened for a Lac^+ phenotype were further selected for Mal^+ by spotting the co-transformants on M63-maltose plates. For this purpose, the co-transformants previously cultured on the LB-X-gal plates were used to inoculate 2 mL of LB broth supplemented with antibiotics (100 µg/mL Amp, 50 µg/mL Kan, 50 µg/mL Strep) and 0.5 mM IPTG to induce protein expression. The cultures were grown overnight at 30ºC, 200 rpm and harvested by centrifugation at 4000 rpm, 10 minutes. The pellets were washed twice with 2 mL of M63 minimal media (2 g $(NH_4)_2SO_4$, 13.6 g KH_2PO_4, 0.5 mg $FeSO_4.7H_2O$, 1 mg vitamin B1, pH 7.0 adjusted with KOH) in order to remove all traces of the rich medium and were resuspended in 2 mL of M63 minimal medium with 0.2 % maltose, 0.5 mM IPTG and antibiotics (50 µg/mL Amp, 25 µg/mL Kan, 25 µg/mL Strep). The suspension volume of 3-5 µL was used to spot M63 agar plates with 0.2 % maltose, 40 µg/mL X-gal, 0.5 mM IPTG and antibiotics (50 µg/mL Amp, 25 µg/mL Kan, 25 µg/mL Strep) and incubated at 30ºC for 2-7 days. The plates were examined for growth of Mal^+ colonies after 3-7 days of incubation at 30°C. Since plates were supplemented with X-gal, any blue colonies arising on the plates would be both Lac^+ and Mal^+.

4.2.7 Characterisation of selected positive interactions using β-galactosidase activity assay

The co-transformants that were tested positive were analysed for β-galactosidase activity due to restoration of Cya^+ phenotype in the Cya^- BTH101. Freshly co-transformed cells, selected on LB plates with antibiotics (100 µg/mL Amp, 50 µg/mL Kan) were cultured in 2 mL LB broth supplemented with antibiotics (100 µg/mL Amp,

50 µg/mL Kan, 50 µg/mL Strep) and 0.5 mM IPTG at 200 rpm, 30ºC for 16 hours to induce protein expression. The cultures were spotted on LB agar plates with 40 µg/mL X-gal, 0.5 mM IPTG and antibiotics (100 µg/mL Amp, 50 µg/mL Kan, 50 µg/mL Strep) and the plates were incubated at 30ºC for 2 days. These co-transformants were then used to inoculate 2 mL of LB broth supplemented with antibiotics (100 µg/mL Amp, 50 µg/mL Kan, 50 µg/mL Strep) and 0.5 mM IPTG to induce protein expression. The cultures were grown overnight at 30ºC, 200 rpm and harvested by centrifugation at 3219 x *g*, 10 minutes. The pellets were washed twice with 2 mL of M63 minimal media in order to remove all traces of the rich medium and resuspended in 2 mL of M63-maltose (M63 minimal medium with 0.2% maltose), 0.5 mM IPTG and antibiotics (50 µg/mL Amp, 25 µg/mL Kan, 25 µg/mL Strep).

For the assay, the overnight cultures were diluted four-fold (0.5 mL cell culture in 1.5 mL M63-maltose) in M63-maltose with antibiotics and 0.5 mM IPTG. The optical density at 600 nm was measured for 1 mL of the diluted cultures. The cells in remaining 1 mL of the diluted cultures were permeabilised with a few drops (20-30 µL) of toluene and 1% SDS solution and were rigorously vortexed for 10 seconds to allow thorough mixing of the components. The traces of toluene were removed by incubating the cultures at 37ºC for 30 minutes. To assess the enzyme activity, 100 µL of permeabilised cells were added to 900 µL of PM2 buffer (70 mM $Na_2HPO_4.12H_2O$, 30 mM $NaH_2PO_4.H_2O$, 1 mM $MgSO_4$, 0.2 mM $MnSO_4$, 100 mM β-mercaptoethanol, pH 7) and the reaction was initiated by addition of 250 µL of 0.4 % ONPG (*o*-nitrophenol-galactoside, prepared in PM2 buffer without 100 mM β-mercaptoethanol). A reaction containing all assay components but lacking in the cells was used as a blank. The assay mixture was incubated at 28ºC for 15 minutes and stopped by addition of 1 mL of 1 M

aqueous Na_2CO_3 solution. The optical density at 420 nm was measured for the samples and the extent of β-galactosidase activity was calculated in terms of Miller Unit (in units/mL) values using Miller's formula, Miller Units = (OD_{420} X 1000) / (Reaction time X Volume of culture assayed X OD_{600}) and Activity Units (in units/mL) using the formula, Activity Units = 200 X OD_{420} / (Reaction time) X dilution factor (i.e. dilution factor 10 for 100 µL cells in 900 µL PM2 buffer). The readings were expressed in Activity Units/mg protein. The concentration of the protein was determined considering the Euromedex prescribed conversions i.e 1mL of culture with OD_{600} = 1 corresponds to 300µg of dry weight of bacteria.

The positive control of pKT25-zip and pUT18C-zip, negative controls from combinations pKT25-pUT18, pKT25-pUT18C, pKNT25-pUT18, pKNT25-pUT18C and the fusion constructs were transformed with empty vector with the second interacting domain were assayed for β-glactosidase activity to eliminate false positives.

4.2.8 Validation of the positive interactions by re-transformation

The plasmid pairs that were screened positive were validated as true positives by re-transforming into BTH101 and re-checking on indicator plates (MacConkey-maltose and M63-maltose) using the afore-mentioned protocols. The co-transformants of the pairs that showed consistent Cya^+ phenotype were designated as true interactors in this study.

4.3 Results

Adenylate cyclase based bacterial two-hybrid system relies on reconstitution of the cAMP triggered signal transduction pathway in *E. coli.* Calmodulin binding adenylate cyclase (AC) of *Bordetella pertussis* is a 1706 amino acid with a catalytic domain residing in the first 400 amino acid residues. The catalytic site is further divided into two sub-domains, a 25kDa fragment (1-224 residues) which is responsible for catalysis, and a 18kDa fragment (225-399 residues) that binds calmodulin. The enzyme AC that synthesises cAMP from ATP is re-assembled in advent of protein-protein interaction when the plasmids bearing the T25 and T18 domains of the enzyme are co-expressed in Cya$^-$ *E. coli*. Expression and reassembly of AC in Cya$^-$ *E. coli* restores the cAMP cascade which further drives the expression of the endogenous genes of the *lac* and *mal* operon, that is easily detected on indicator plates. When the proteins of interest are fused to the T25 and T18 domains of AC, their interaction serves the purpose of calmodulin in bringing the two domains together, thus restoring the enzyme function.

4.3.1 Screening and selection of protein-protein interactions using the bacterial two-hybrid system

To identify the potential protein-protein interactions in the LAM biosynthesis pathway, the genes encoding the enzymes of the pathway were cloned in T25 and T18 domain bearing plasmids (summarised in Table 4.1) and co-expressed in BTH101, a Cya$^-$ *E. coli* strain. The co-transformants, thus obtained were examined for expression of *lac* operon and *mal* operon on LB-X-gal or MacConkey-maltose and on M63-maltose plates after 48 hours of incubation at 30ºC to enable accumulation of cAMP. Inability of Cya$^-$ *E. coli* to use X-gal or lactose due to absence of β-galactosidase activity results in white colonies on LB-X-gal and MacConkey-maltose. In addition, since no cAMP-CAP

complex is formed in these cells, expression of *mal* operon is completely inhibited. Consequently, these cells are unable to utilise maltose and cease to grow on M63 minimal media plates supplemented with maltose as the sole carbohydrate. These attributes of Cya^- *E. coli* are reversed in the case of an interaction between the proteins fused to the T25 and T18 domains and is characterised by blue colonies on LB-X-gal, red colonies on MacConkey-maltose and growth on M63-maltose plates. The strains that produced blue colonies on LB-X-gal and/or red colonies on MacConkey-maltose were designated to have a Lac^+ phenotype and the ones with an ability to grow on M63-maltose were conferred to have a Mal^+ phenotype. Since, M63-maltose plates were also supplemented with X-gal, any blue colonies on these plates are also Lac^+.

The genes were cloned into the vectors with T25 and T18 tags either at the N-terminus or at the C-terminus, such that the hybrid protein with either an N or a C-terminal tag could be generated. However, despite several attempts at cloning, a few genes such as PimE, MptA, EmbA could only be tagged with either of the two domains at only one terminus. An interaction can only be detected in case of synthesis of a full-length protein which is properly folded. In addition, for a membrane protein to show interaction, the protein should correctly be inserted into the membrane with both T25 and T18 tags facing either the peripasmic or cytoplasmic side at the same instance. The corresponding phenotypes obtained for the various prey and bait combinations tested are summarised in Table 4.2.

Table 4.2: Probable interacting partners in LAM biosynthesis pathway and their phenotypes on indicator plates.

Prey - T25 fusion construct	Bait - T18 fusion construct	Indicator phenotype			Interaction
		LB-X-gal	Mac Conkey - maltose	M63-maltose	
Vector controls					
pKT25-Zip	pUT18C-Zip	Lac^{-}*	Lac^{-}*	Mal^{-}	Positive
pKT25	pUT18	Lac^{-}	Lac^{-}	Mal^{-}	Negative
pKT25	pUT18C	Lac^{-}*	Lac^{-}*	Mal^{-}	Negative
pKNT25	pUT18	Lac^{-}*	Lac^{-}*	Mal^{-}	Negative
pKNT25	pUT18C	Lac^{-}	Lac^{-}	Mal^{-}	Negative
Proteins tested for probable interactions					
pKNT25-PimA	pUT18-PimB	Lac^{-}	Lac^{-}	Mal^{-}	Negative
pKNT25-PimA	pUT18C-PimB	Lac^{-}	Lac^{-}	Mal^{-}	Negative
pKNT25-PimA	pUT18C-Rv2611	Lac^{-}	Lac^{-}	Mal^{-}	Negative
pKNT25-PimA	pUT18C-PimA	Lac^{+}	Lac^{+}	Mal^{+}	Positive
pKT25-PimB	pUT18C-PimA	Lac^{-}	Lac^{-}	Mal^{-}	Negative
pKNT25-PimB	pUT18C-PimA	Lac^{-}	Lac^{-}*	Mal^{-}*	Negative
pKT25-PimB	pUT18-PimB	Lac^{-}	Lac^{-}	Mal^{-}	Negative
pKNT25-PimB	pUT18-PimB	Lac^{-}	Lac^{-}	Mal^{-}	Negative
pKT25-PimB	pUT18C-PimB	Lac^{-}	Lac^{-}	Mal^{-}	Negative
pKNT25-PimB	pUT18C-PimB	Lac^{-}	Lac^{-}	Mal^{-}	Negative
pKT25-PimB	pUT18C-Rv2611	Lac^{-}	Lac^{-}	Mal^{-}	Negative
pKNT25-PimB	pUT18C-Rv2611	Lac^{-}*	Lac^{-}*	Mal^{-}*	Negative
pKT25-PimB	pUT18C-PimE	Lac^{-}	Lac^{-}	Mal^{-}	Negative
pKNT25-PimB	pUT18C-PimE	Lac^{-}	Lac^{-}	Mal^{-}	Negative
pKT25-PimB	pUT18C-LpqW	Lac^{-}	Lac^{-}	Mal^{-}	Negative
pKNT25-PimB	pUT18C-LpqW	Lac^{-}	Lac^{-}	Mal^{-}	Negative
pKT25-Rv2611	pUT18C-PimA	Lac^{-}	Lac^{-}	Mal^{-}	Negative
pKNT25-Rv2611	pUT18C-PimA	Lac^{-}	Lac^{-}	Mal^{-}	Negative
pKNT25-Rv2611	pUT18-PimB	Lac^{-}	Lac^{-}	Mal^{-}	Negative
pKT25-Rv2611	pUT18-PimB	Lac^{-}	Lac^{-}	Mal^{-}	Negative
pKT25-Rv2611	pUT18C-PimB	Lac^{-}	Lac^{-}	Mal^{-}	Negative

pKNT25-Rv2611	pUT18C-PimB	Lac^-	Lac^-	Mal^-	Negative
pKT25-Rv2611	pUT18C-PimE	Lac^-	Lac^-	Mal^-	Negative
pKNT25-Rv2611	pUT18C-PimE	Lac^-	Lac^-	Mal^-	Negative
pKT25-Rv2611	pUT18C-Rv2611	Lac^-	Lac^-	Mal^-	Negative
pKNT25-Rv2611	pUT18C-Rv2611	Lac^-	Lac^-	Mal^-	Negative
pKT25-LpqW	pUT18-PimB	Lac^-	Lac^-	Mal^-	Negative
pKT25-LpqW	pUT18C-PimB	Lac^-	Lac^-	Mal^-	Negative
pKNT25-LpqW	pUT18-PimB	Lac^-	Lac^-	Mal^-	Negative
pKNT25-LpqW	pUT18C-PimB	Lac^-	Lac^-	Mal^-	Negative
pKT25-LpqW	pUT18C-PimE	Lac^-	Lac^-	Mal^-	Negative
pKNT25-LpqW	pUT18C-PimE	$Lac^{+/-}$*	$Lac^{+/-}$*	$Mal^{+/-}$*	Positive/ Negative
pKNT25-LpqW	pUT18C-MptB	Lac^-	Lac^-	Mal^-	Negative
pKT25-LpqW	pUT18C-MptB	Lac^-	Lac^-	Mal^-	Negative
pKNT25-LpqW	pUT18-MptC	Lac^-*	Lac^-	Mal^-	Negative
pKT25-LpqW	pUT18-MptC	Lac^-	Lac^-	Mal^-	Negative
pKT25-LpqW	pUT18C-LpqW	Lac^+	Lac^-*	Mal^+	Positive/ Negative
pKNT25-LpqW	pUT18C-LpqW	Lac^-	Lac^-	Mal^-	Negative
pKT2- MptA	pUT18C-PimE	Lac^-	Lac^-	Mal^-	Negative
pKT25-MptA	pUT18C-LpqW	Lac^-	Lac^-	Mal^-	Negative
pKT25- MptA	pUT18C-MptB	Lac^-	Lac^-	Mal^-	Negative
pKT25-MptA	pUT18C-MptB	Lac^-	Lac^-	Mal^-	Negative
pKT25- MptA	pUT18-MptC	Lac^-	Lac^-	Mal^-	Negative
pKT25-MptA	pUT18C-EmbC	Lac^-	Lac^-	Mal^-	Negative
pKT25-MptA	pUT18C-AftC	Lac^-	Lac^-	Mal^-	Negative
pKT25-MptA	pUT18-AftD	Lac^-	Lac^-	Mal^-	Negative
pKNT25-MptB	pUT18C-PimE	Lac^-	Lac^-	Mal^-	Negative
pKNT25-MptB	pUT18C-LpqW	Lac^-	Lac^-	Mal^-	Negative
pKNT2- MptB	pUT18C-MptB	Lac^-	Lac^-	Mal^-	Negative
pKNT25-MptB	pUT18-MptC	Lac^-	Lac^-	Mal^-	Negative
pKT25-MptB	pUT18C-EmbC	Lac^-	Lac^-	Mal^-	Negative
pKNT25-MptB	pUT18C-EmbC	Lac^-	Lac^-	Mal^-	Negative
pKT25-MptB	pUT18C-AftC	Lac^-	Lac^-	Mal^-	Negative
pKNT25-MptB	pUT18C-AftC	Lac^-	Lac^-	Mal^-	Negative
pKT25-MptB	pUT18-AftD	Lac^-	Lac^-	Mal^-	Negative
pKNT25-MptB	pUT18-AftD	Lac^-	Lac^-	Mal^-	Negative

pKT25-MptC	pUT18C-PimE	Lac$^-$*	Lac$^-$*	Mal$^-$*	Negative
pKNT25-MptC	pUT18C-PimE	Lac$^-$	Lac$^-$	Mal$^-$	Negative
pKT25-MptC	pUT18C-LpqW	Lac$^+$	Lac$^+$	Mal$^+$	Positive
pKNT25-MptC	pUT18C-LpqW	Lac$^-$	Lac$^-$	Mal$^-$	Negative
pKT25-MptC	pUT18C-MptB	Lac$^-$	Lac$^-$	Mal$^-$	Negative
pKNT25-MptC	pUT18C-MptB	Lac$^-$	Lac$^-$	Mal$^-$	Negative
pKT25-MptC	pUT18-MptC	Lac$^-$	Lac$^-$	Mal$^-$	Negative
pKNT25-MptC	pUT18-MptC	Lac$^-$	Lac$^-$	Mal$^-$	Negative
pUT18-MptC	pKT25-MptC	Lac$^-$	Lac$^-$	Mal$^-$	Negative
pUT18-MptC	pKNT25-MptC	Lac$^-$	Lac$^-$	Mal$^-$	Negative
pKT25-MptC	pUT18C-EmbC	Lac$^-$	Lac$^-$	Mal$^-$	Negative
pKNT25-MptC	pUT18C-EmbC	Lac$^-$	Lac$^-$	Mal$^-$	Negative
pKT25-MptC	pUT18C-AftC	Lac$^-$	Lac$^-$	Mal$^-$*	Negative
pKNT25-MptC	pUT18C-AftC	Lac$^-$	Lac$^-$	Mal$^-$	Negative
pKT25-MptC	pUT18-AftD	Lac$^-$	Lac$^-$	Mal$^-$	Negative
pKNT25-MptC	pUT18-AftD	Lac$^-$	Lac$^-$	Mal$^-$	Negative
pKT25-MptC	pUT18C-CapA	Lac$^-$	Lac$^-$	Mal$^-$	Negative
pKNT25-MptC	pUT18C-CapA	Lac$^-$	Lac$^-$	Mal$^-$	Negative
pKT25-EmbA	pUT18C-EmbB	Lac$^-$	Lac$^-$	Mal$^-$	Negative
pKT25-EmbA	pUT18C-EmbC	Lac$^-$	Lac$^-$	Mal$^-$	Negative
pKNT25-EmbB	pUT18C-EmbC	Lac$^-$	Lac$^-$	Mal$^-$	Negative
pKNT25-EmbB	pUT18C-EmbB	Lac$^-$	Lac$^-$	Mal$^-$	Negative
pKNT25-EmbC	pUT18C-EmbB	Lac$^-$	Lac$^-$	Mal$^-$	Negative
pKNT25-EmbC	pUT18C-EmbC	Lac$^-$*	Lac$^-$*	Mal*	Negative
pKNT25-EmbC	pUT18C-MptB	Lac$^+$	Lac$^+$	Mal$^+$	Positive
pKNT25-EmbC	pUT18-MptC	Lac$^-$	Lac$^-$	Mal$^-$	Negative
pKNT25-EmbC	pUT18C-AftC	Lac$^-$	Lac$^-$	Mal$^-$	Negative
pKNT25-EmbC	pUT18-AftD	Lac$^-$	Lac$^-$*	Mal$^-$*	Negative
pKNT25-AftC	pUT18C-MptB	Lac$^-$	Lac$^-$	Mal$^-$	Negative
pKNT25-AftC	pUT18-MptC	Lac$^+$	Lac$^+$	Mal$^+$	Positive
pKNT25-AftC	pUT18C-EmbC	Lac$^-$	Lac$^-$	Mal$^-$	Negative
pKNT25-AftC	pUT18C-AftC	Lac$^-$	Lac$^-$	Mal$^-$	Negative
pKNT25-AftC	pUT18-AftD	Lac$^-$	Lac$^-$	Mal$^-$	Negative
pKNT25-AftC	pUT18C-CapA	Lac$^-$	Lac$^-$	Mal$^-$	Negative
pKNT25-AftD	pUT18C-MptB	Lac$^-$	Lac$^-$	Mal$^-$	Negative
pKNT25-AftD	pUT18-MptC	Lac$^+$	Lac$^+$	Mal$^+$	Positive

pKNT25-AftD	pUT18C-EmbC	Lac^+	Lac^+	Mal^+	Positive
pKNT25-AftD	pUT18-AftD	Lac^-	Lac^-	Mal^-	Negative
pKNT25-AftD	pUT18C-CapA	Lac^-	Lac^-	Mal^-	Negative
pKNT25-CapA	pUT18-MptC	Lac^-*	Lac^-*	Mal^-*	Negative
pKNT25-CapA	pUT18C-AftC	Lac^-	Lac^-	Mal^-	Negative
pKNT25-CapA	pUT18-AftD	Lac-	Lac^-	Mal^-	Negative
pKNT25-CapA	pUT18C-CapA	Lac-	Lac^-	Mal^-	Negative
Empty vector controls to detect sticky proteins					
pKNT25-PimA	pUT18	Lac^-	Lac^-	Mal^-	Negative
pKNT25-PimA	pUT18C	Lac^-	Lac^-*	Mal^-*	Negative
pKT25	pUT18C-PimA	Lac^-	Lac^-	Mal^-	Negative
pKNT25	pUT18C-PimA	Lac^-	Lac^-	Mal^-	Negative
pKT25-PimB	pUT18	Lac^-	Lac^-	Mal^-	Negative
pKT25-PimB	pUT18C	Lac^-	Lac^-	Mal^-	Negative
pKNT25-PimB	pUT18	Lac^-	Lac^-	Mal^-	Negative
pKNT25-PimB	pUT18C	Lac^-	Lac^-	Mal^-	Negative
pKT25	pUT18-PimB	Lac^-	Lac^-	Mal^-	Negative
pKT25	pUT18C-PimB	Lac^-	Lac^-	Mal^-	Negative
pKNT25	pUT18-PimB	Lac^-	Lac^-	Mal^-	Negative
pKNT25	pUT18C-PimB	Lac^-	Lac^-	Mal^-	Negative
pKT25-Rv2611	pUT18	Lac^-	Lac^-*	Mal^-*	Negative
pKT25- Rv2611	pUT18C	Lac^-	Lac^-	Mal^-	Negative
pKNT25-Rv2611	pUT18	Lac^-	Lac^-	Mal^-	Negative
pKNT25-Rv2611	pUT18C	Lac^-	Lac^-	Mal^-	Negative
pKT25	pUT18C-PimE	Lac^-	Lac^-	Mal^-	Negative
pKNT25	pUT18C-PimE	Lac^-	Lac^-	Mal^-	Negative
pKT25-LpqW	pUT18	Lac^-	Lac^-	Mal^-	Negative
pKT25-LpqW	pUT18C	Lac^-	Lac^-	Mal^-	Negative
pKNT25-LpqW	pUT18	Lac^-	Lac^-	Mal^-	Negative
pKNT25-LpqW	pUT18C	Lac^-	Lac^-	Mal^-	Negative
pKT25	pUT18C-LpqW	Lac^-	Lac^-	Mal^-	Negative
pKNT25	pUT18C-LpqW	Lac^-	Lac^-	Mal^-	Negative
pKT25-MptA	pUT18	Lac^-	Lac^-	Mal^-	Negative
pKT25-MptA	pUT18C	Lac^-	Lac^-	Mal^-	Negative
pKNT25-MptB	pUT18	Lac^-	Lac^-	Mal^-	Negative
pKNT25-MptB	pUT18C	Lac^-	Lac^-	Mal^-	Negative

pKT25	pUT18C-MptB	Lac^-	Lac^-	Mal^-	Negative
pKNT25	pUT18C-MptB	Lac^-	Lac^-	Mal^-	Negative
pKT25-MptC	pUT18	Lac^-	Lac^-	Mal^-	Negative
pKT25-MptC	pUT18C	Lac^-	Lac^-	Mal^-	Negative
pKNT25-MptC	pUT18	Lac^-	Lac^-	Mal^-	Negative
pKNT25-MptC	pUT18C	Lac^-	Lac^-	Mal^-	Negative
pKT25	pUT18-MptC	Lac^-	Lac^-	Mal^-	Negative
pKNT25	pUT18-MptC	Lac^-	Lac^-	Mal^-	Negative
pKT25-EmbA	pUT18	Lac^-	Lac^-	Mal^-	Negative
pKT25-EmbA	pUT18C	Lac^-	Lac^-	Mal^-	Negative
pKNT25-EmbB	pUT18	Lac^-	Lac^-	Mal^-	Negative
pKNT25-EmbB	pUT18C	Lac^-	Lac^-	Mal^-	Negative
pKT25	pUT18C-EmbB	Lac^-	Lac^-	Mal^-	Negative
pKNT25	pUT18C-EmbB	Lac^-	Lac^-	Mal^-	Negative
pKNT25- EmbC	pUT18	Lac^-	Lac^-	Mal^-	Negative
pKNT25-EmbC	pUT18C	Lac^-	Lac^-	Mal^-	Negative
pKT25	pUT18C- EmbC	Lac^-	Lac^-	Mal^-	Negative
pKNT25	pUT18C-EmbC	Lac^-	Lac^-	Mal^-	Negative
pKNT25-AftC	pUT18	Lac^-	Lac^-	Mal^-	Negative
pKNT25-AftC	pUT18C	Lac^-	Lac^-	Mal^-	Negative
pKT25	pUT18C-AftC	Lac^-	Lac^-	Mal^-	Negative
pKNT25	pUT18C-AftC	Lac^-	Lac^-	Mal^-	Negative
pKNT25-AftD	pUT18	Lac^-	Lac^-	Mal^-	Negative
pKNT25-AftD	pUT18C	Lac^-	Lac^-	Mal^-	Negative
pKT25	pUT18-AftD	Lac^-	Lac^-	Mal^-	Negative
pKNT25	pUT18-AftD	Lac^-	Lac^-	Mal^-	Negative
pKNT25-CapA	pUT18	Lac^-	Lac^-	Mal^-	Negative
pKNT25-CapA	pUT18C	Lac^-	Lac^-	Mal^-	Negative
pKT25	pUT18C-CapA	Lac^-	Lac^-	Mal^-	Negative
pKNT25	pUT18C-CapA	Lac^-	Lac^-	Mal^-	Negative

*accumulation of Lac^+ and Mal^+ revertants on indicator plates

Several of the interactions analysed in the screening revealed occasional Lac^+ revertants (Table 4.2) that clustered in a few small colonies in culture spots. These revertants could mainly arise in response to stress, such as over-expression of a protein that imparts a significant growth disadvantage. To overcome this defect, mutations can be introduced in sites that promote growth (Quinones-Soto and Roth, 2011), consequently reverting the phenotype to Lac^+. Additionally, introduction of the plasmid can augment the rate of spontaneous mutations in the strain, thus conferring it a mutator phenotype. This phenomenon is resultant of defective DNA repair machinery that causes the strain to accumulate mutations over time in highly susceptible *rec*$^+$ BTH101.

The screening process identified eight putative interactions in the system that include, two homotypic interactions; PimA-PimA and LpqW-LpqW and six heterotypic interactions; LpqW-PimE, LpqW-MptC, EmbC-MptB, AftC-MptC, AftD-MptC, AftD-EmbC as characterised by Lac^+ and Mal^+ phenotypes on respective indicator plates (Figure 4.3). The colony morphologies and phenotypes of protein combinations that resulted in a positive signal (Figure 4.3) for interaction were further analysed and compared to the negative controls to adjudge their significance. The culture spots were homogenous for the afore-mentioned interactions, however sectoring due to revertants was evident on MacConkey-maltose in case of LpqW-LpqW (Figure 4.3B). This interaction showed a clear positive signal on LB-X-gal and M63-maltose plates. The LpqW-PimE pair on the other hand demonstrated a large number of sectors on all the plates. Both the interactions could neither be classified as a definite positive or a negative interaction and were analysed further.

Red papillae and sectoring were also a feature of negative vector controls comprising of pKT25 and pKNT25 vectors paired with pUT18C plasmid (Figure 4.3A). These revertants in negative controls arise upon introduction of pUT18C plasmid that renders a mutator phenotype to the BTH101 strain. The empty vector controls for all the positive interactions were also tested for Lac^+ and Mal^+ phenotype to eliminate false positives due to mis-folded or sticky proteins. All the empty vector controls except pKNT25-PimA + pUT18C were found to be Lac^- and Mal^-. The sectoring observed for the pKNT25-PimA + pUT18C combination was evident on both MacConkey-maltose and on M63-maltose. Over-expression of PimA could impart a growth disadvantage on nutrient deficient medium or lead to membrane overcrowding that results in a weak Lac^+ phenotype. However, none of the other negative controls presented a Mal^+ phenotype (Figure 4.3 A and C).

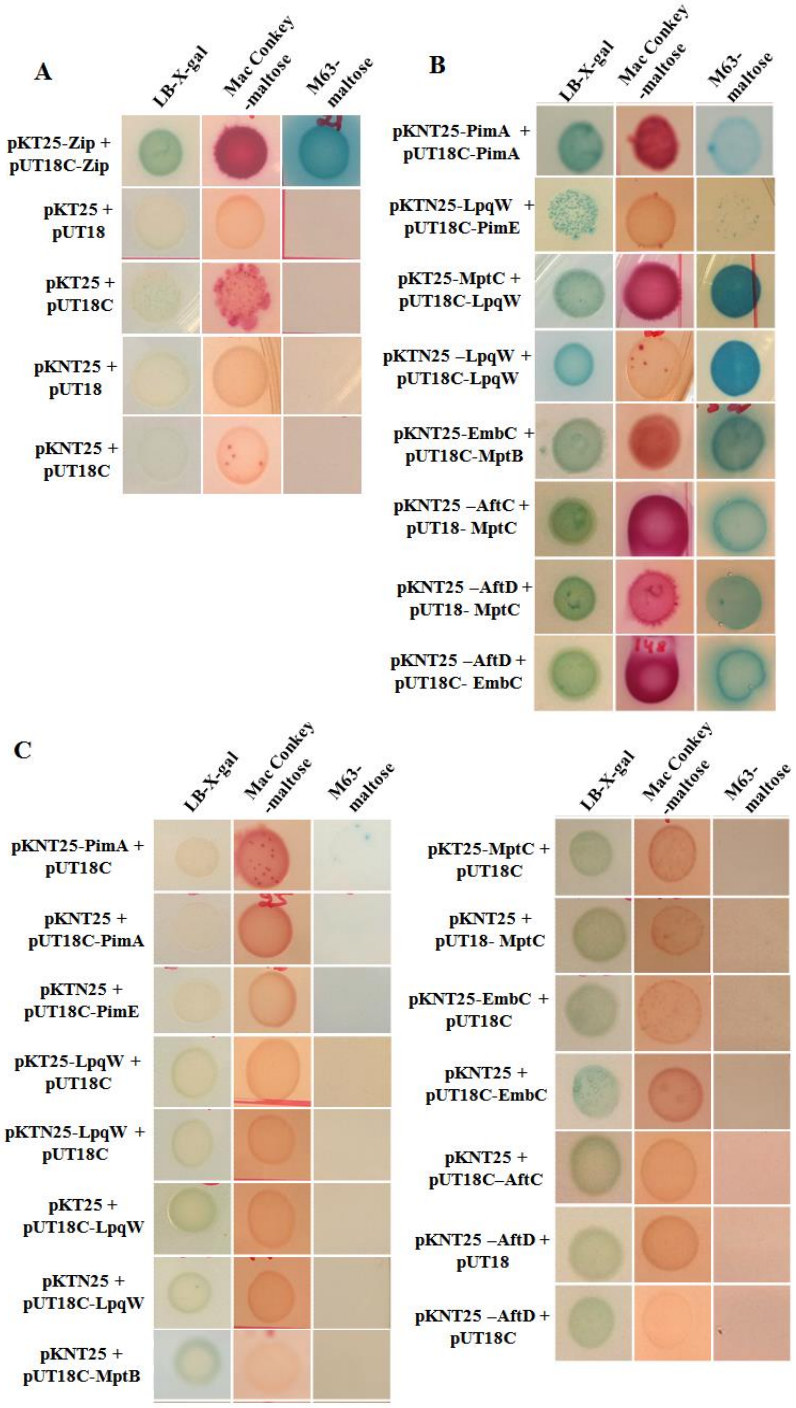

Figure 4.3: Screening of the putative interactions in LAM biosynthesis pathway. A. Vector controls for the two-hybrid system**. B**. Putative interactions from the array of interactions screened. The combinations listed in Table 4.1 were all screened for Lac^+ and Mal^+ phenotype and the resultant positive interactions are highlighted. **C.** Empty vector controls of the screened positive interactions**.** Blue colonies on LB-X-gal, pink colonies on MacConkey and growth on M63-maltose plates are indicative of a probable interaction between the listed prey and bait pairs.

4.3.2 Quantification of functional complementation between the hybrid proteins by measuring β-galactosidase activity

A successful interaction is characterised by reconstitution of a functional AC enzyme that drives the synthesis of cAMP. This leads to formation of cAMP-CAP complex, which switches on the expression of the *lac* operon including the enzyme β-glactosidase, encoded by *lacZ.* The activity of β-glactosidase in co-tranformants harbouring prey and bait constructs is therefore an indirect measurement of the protein-protein interaction between the expressed hybrid proteins. The pairs that were selected positive for interaction were also examined for β-galactosidase activity to quantify their degree of interaction. The enzyme activity was expressed in activity units (AU) per milligram of the dry weight of the cells and were compared to that of the positive control (pKT25-Zip + pUT18C-Zip) and negative experimental controls to establish the upper and lower limits. The base line activity as determined by negative controls was estimated between 75-110 AU/mg and highest enzyme activity as determined by positive controls was estimated between 3400-4400 AU/mg (Figure 4.4). The sectoring prominent for pUT18C controls had no significant contribution to the activity levels thus validating its status as a negative control.

The enzyme activity of interaction pairs was tested along with the respective empty vector controls to establish a true interaction. Of the pairs tested, highest activity was obtained for PimA-PimA pair estimated at 2482 ± 993 AU/mg (Figure 4.4A). The negative controls for this interaction had activities ranged between 42-58 AU/mg (Figure 4.4A). The sectoring and accumulation of revertants as observed in case of pKNT25-PimA + pUT18C (Figure 4.3C) did not affect the β-galactosidase activity levels thus rendering PimA-PimA as the true interaction pair with a significant degree of

complementation. The interaction pairs LpqW-PimE (Figure 4.4A) and AftD-EmbC (Figure 4.4B) recorded moderate β-galactosidase activity levels estimated at 812 ± 165 AU/mg and 1206 ± 116 AU/mg, respectively. Insignificant activity was observed for the corresponding controls, thus establishing LpqW-PimE and AftD-EmbC as a true complementation pair. The pairs MptC-LpqW and LpqW-LpqW recorded very low levels of β-glactosidase activity (Figure 4.4A) estimated at 327 ± 77 AU/mg and 209 ± 12 AU/mg, respectively. These values could result either from a weak interaction between the pairs or from instability of one of the plasmid constructs affording a false positive.

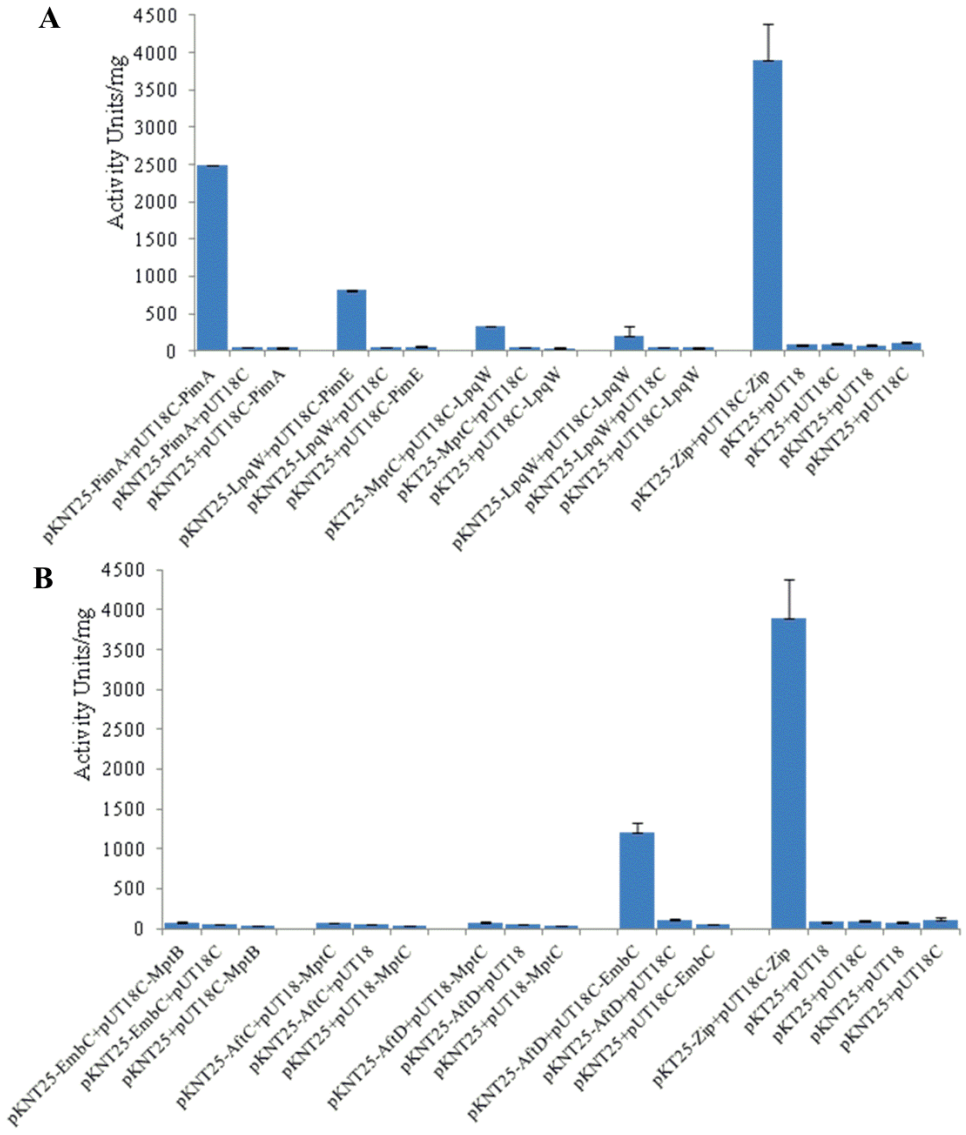

Figure 4.4: Quantification of functional complementation between the hybrid proteins by β-galactosidase assay. The positive interactions as determined by the screening process were evaluated for their ability to reconstitute adenylate cyclase using β-galactosidase assays. The values are representative of three independent assays performed. The error bars indicate the standard error as from the mean.

4.3.3 Validating the selected positive interactions

The prey and bait pairs predicted to interact by the screening and selection process were re-transformed into Cya$^-$ BTH101 cells and re-examined for their Lac$^+$ and Mal$^+$ phenotype to eliminate any possibility of a false positive to have been selected (Figure 4.5). The combinations with consistent results as obtained previously were designated

as true interactions. The pairs PimA-PimA, MptC-LpqW, AftD-EmbC consistently displayed Lac^+ and Mal^+ phenotypes while the results could not be replicated for LpqW-LpqW, EmbC-MptB, AftC-MptC and AftD-MptC. Interestingly, a stronger signal for interaction was evident in case of LpqW-PimE prey-bait pair. Amplification of signal for LpqW-PimE pair on retransformation could signify a weak interaction between the pair. In addition, a very weak signal was prominent for LpqW-LpqW pair on indicator plates. It is likely that expression of LpqW may have deleterious growth defects on BTH101which results in instability of this plasmid over generations. Sectoring was evident for LpqW-LpqW and EmbC-MptB on MacConkey plates.

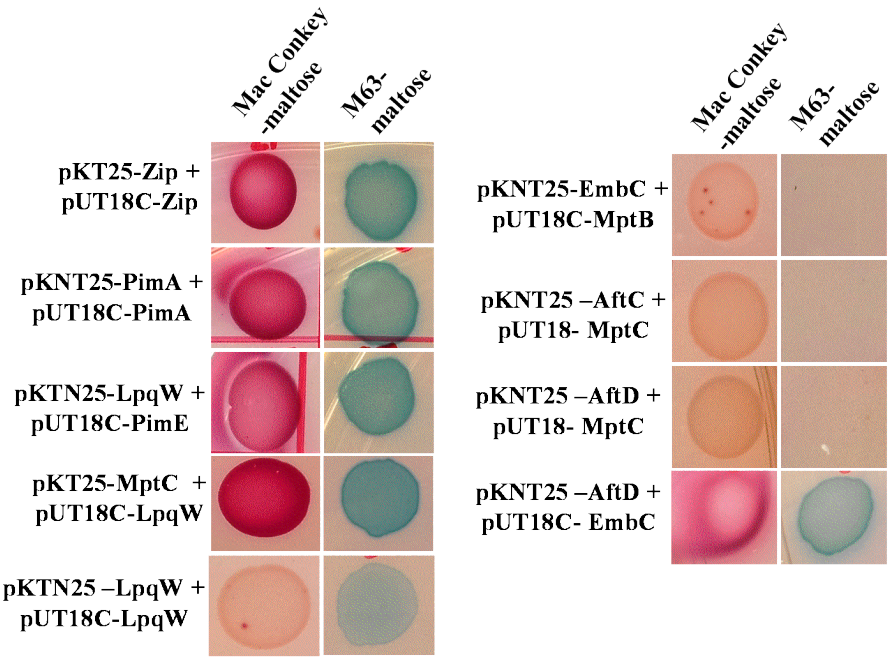

Figure 4.5: Validation of the interactions determined by the screening process. The interactions obtained from screening were re-evaluated for their Lac^+ and Mal^+ phenotype by plating on respective indicator plates. The pairs PimA-PimA, MptC-LpqW and AftD-EmbC were tested positive for the interaction while inconsistencies were apparent for LpqW-PimE, LpqW-LpqW, EmbC-MptB, AftC-MptC and AftD-MptC.

4.3.4 Discussion

The bacterial two-hybrid system based on reassembly of cAMP signaling pathway (Karimova *et al.*, 1998b) was employed to study protein-protein interactions between membrane and soluble proteins of the LAM biosynthetic pathway. The enzymes were tagged with domains T25 (prey) and T18 (bait) at either N-terminus or the C-terminus and tested for interactions. Following a stringent selection process, we identified four hybrid pairs that displayed consistent phenotypes on retransformation and also demonstrated significant β-galactosidase activity. These include; self-association between PimA, heterotypic association between LpqW and the mannosyl transferase PimE and a close involvement between the arabinosyltransferases EmbC and AftD.

The self-association of PimA as suggested by complementation of Cya^+ phenotype by PimA fused to T25 domain at C-terminus and PimA fused to T18 domain at N-terminus highlights a high possibility of PimA to function as a dimer. PimA catalyses the transfer of the first mannose residue from GDP-mannose to the PI anchor, thus affording the primary PIM species, PIM_1 (Besra *et al.*, 1997; Kordulakova *et al.*, 2002). Although, the crystal structure of *M. smegmatis* homologue of PimA in complex with donor substrate GDP-mannose provided no evidence for its dimerisation in solution, a multimer formation for catalysis is a prominent feature of several glycosyltransferases of the GT-B superfamily (Buschiazzo *et al.*, 2004; Horcajada *et al.*, 2006; Metzger and Raetz, 2009). These evidences hint towards a novel process of dimerisation of a glycosyltransferase facilitated by a ligand, such as phosphatidyl inositol (PI) to either mediate transfer of mannose from GDP-Mannose to the PI acceptor or aid in release of the synthesised phosphatidyl inositol mannoside (PIM_1) product. Ligand-mediated protein dimerisation has also been reported in Carbohydrate Binding Module (CBM)

with protein-carbohydrate interactions (Flint *et al.*, 2004). Self-association in case of CBMs contribute to the substrate specificity of these proteins. Conformational studies on *M. smegmatis* homologue of PimA bound to GDP-Mannose suggest a switch in conformation from the previously closed state to a relaxed state for the enzyme upon binding with PI (Giganti *et al.*, 2013; Guerin *et al.*, 2009b). Therefore, it is highly probable that oligomerisation of mannosyltransferase PimA could play an important role either in allosteric regulation or in determining the specificity of protein-lipoglycan interaction for this enzyme. Dimerisation of PimA can further be analysed using the same approach to map the essential domains that mediate the interaction. Furthermore, mutations can be introduced into the mapped domains to identify amino acid residues critical for this interaction. The information thus generated can aid in the design of novel compounds that inhibit this interaction.

The flux of intermediary PIM species PIM_4 for generation of LAM and polar PIM species requires LpqW to interact with the mannosyltransferases PimE and MptB (Crellin *et al.*, 2008; Kovacevic *et al.*, 2006; Rainczuk *et al.*, 2012). The heterotypic associations of LpqW with the mannosyltransferases PimE as determined by the two-hybrid study therefore support its involvement in regulation of LAM biosynthesis. Functional complementation between the LpqW fused to T25 domain at C-terminus and PimE fused to T18 domain at N-terminus as revealed in our study, provides a direct evidence for regulation of PimE by LpqW. Studies on LpqW in *C. glutamicum* have functionally linked the enzyme to mannosyltransferase MptB (Rainczuk *et al.*, 2012), but no evidence for the interaction was determined in our study with two-hybrid system. It is likely that the interaction between LpqW and MptB may occur in mycobacteria and be presented as a false negative by the two-hybrid system. The interactions responsible

for formation of these multi-enzyme complexes between the glycosyltransferases can serve as potential targets for anti-tubercular agents. Novel inhibitors against heterotypic interactions that prevent the metabolon formation would subsequently target two or more enzymes at the same time rendering it difficult for bacteria to develop resistance. Therefore, this 'co-target' approach offers a unique and an efficient alternative strategy for developing new and potent anti-TB compounds.

Furthermore, the arabinosyltransferases AftD and EmbC which function along with AftC to synthesise the arabinan domain in LAM were also indentified to have a high degree of interaction between them. The enzyme EmbC catalyses the formation of linear arabinan chain comprising α(1→5) linked arabinose residues (Alcaide *et al.*, 1997; Alderwick *et al.*, 2011a; Birch *et al.*, 2010; Shi *et al.*, 2006). The branching is introduced in this linear chain by addition of α(1→3) units by AftD (Skovierova *et al.*, 2009). Our results are consistent with the already established functional relationship between EmbC and AftD.

The two-hybrid approach based on reconstitution of AC is a powerful technique for analysis of protein-protein interactions that offers a few drawbacks when employed to study membrane proteins of mycobacteria. Since a positive interaction can only be obtained in a scenario where both the proteins of interest are sufficiently synthesised, correctly inserted into the membrane and not result in plasmid instability, the combinations tested negative for interactions may not be true negatives (Battesti and Bouveret, 2012; Karimova *et al.*, 1998b; Karimova *et al.*, 2000). These negative results may also result from non-expression of a fully functional protein, incorrect orientation in the membrane or mis-folding which results in cellular toxicity and plasmid instability

(Battesti and Bouveret, 2012; Karimova *et al.*, 1998b; Karimova *et al.*, 2000). Since the system is based on *E. coli*, expression of mycobacterial proteins in full is mostly a failure which increases the amount of false negatives generated (Battesti and Bouveret, 2012). Therefore, a western blotting procedure to detect a full expression of the protein and secondary techniques such as co-immunoprecipitation, BN-PAGE, or more specific systems such as mycobacterial two hybrid system or yeast two hybrid system can be employed to reconfirm the interactions. In addition, a few protein interactions may occur only in presence of an accessory protein and go undetected by this system. In the reverse situation where functional complementation due to a non-specific interaction initiated by endogenous protein that acts as a tethering agent can also result in false positives. Therefore, a three hybrid approach or use of mycobacteria based two hybrid systems can help identify the potential membrane protein complexes especially between LpqW, MptB and MptC and between EmbA, EmbB and EmbC which could not be recognised by this system.

Chapter 5

5 Tetrafluorinated galactofuranoside compounds as inhibitors of GlfT1 and GlfT2 in *Mycobacterium smegmatis*

5.1 Introduction

The mAGP complex is the target of many first line drugs including EMB with the target residing in the *embCAB* locus (Belanger *et al.*, 1996) and INH that targets the enoyl-ACP reductase, InhA (Banerjee *et al.*, 1994). Biosynthesis of the monosaccharides such as Rha, Gal*f* and Ara*f* which are the major constituents of the mycobacterial cell wall, that are lacking in humans and other mammals, constitute potential drug targets. The arabinan domain consists of approximately 30 Ara*f* residues with the majority of the residues being α(1→5) linked and branching introduced by 3,5-α-D-Ara*f* residues (Daffe *et al.*, 1990; Mcneil *et al.*, 1991). The synthesis of the arabinan domain requires several Ara*f*Ts of the GT-C superfamily with a distinct DDX motif (Berg *et al.*, 2007), which employ DPA as the arabinose donor (Liu and Mushegian, 2003; Wolucka *et al.*, 1994). A recently, solved crystal structure of the C-terminus of EmbC, an Ara*f*T, revealed the presence of ligand binding sites (Alderwick *et al.*, 2011a). The GlfTs, utilise UDP-Gal*f* as the galactofuranose donor for building the galactan core of AG (De Arruda *et al.*, 1989). The substrate UDP-Gal*f* is synthesised from UDP-Glc *via* an epimerisation step to yield UDP-Gal*p* that is subsequently converted to UDP-Gal*f* by an essential flavoenzyme UDP-Gal*p* mutase (UGM) (Pan *et al.*, 2001). The galactan core is assembled by galactofuranosyltransferases, GlfT1 and GlfT2, which are encoded by *Rv3782* and *Rv3808c*, respectively. GlfT2 is responsible for the synthesis of the bulk of galactan core, whilst GlfT1 initiates the synthesis by adding the first two sugar units. Both enzymes are recognised by the presence of a distinct DXD motif in the active site,

characteristic of the glycosyltransferases of the GT-A superfamily (Liu and Mushegian, 2003). The enzyme GlfT1 is said to exhibit β-D-Gal*f* (1→6) transferase activity (Alderwick *et al.*, 2008) and catalyses the transfer of the two first Gal*f* residues on to α-L-Rhap-(1→3)-GlcNAc-phosphate peptidoglycan anchor. Experimental evidences suggest that GlfT2 exhibits both β-D-Gal*f* (1→5) and β-D-Gal*f* (1→6) transferase activity (Kremer *et al.*, 2001; Wheatley *et al.*, 2012), transferring both β-D-Gal*f* (1→5) and β-D-Gal*f* (1→6) to the polyprenol-bound oligosaccharide. A recent crystal structure of *M. tuberculosis* GlfT2 (Wheatley *et al.*, 2012) has given much insight into the functioning of the catalytic core of the mycobacterial GlfTs. GlfT2 is a membrane bound protein with Asp256-Asp258 forming the DXD motif. GlfT2 binds Mn^{2+} in its active site, which probably functions as the co-factor for the enzyme. The possible explanation for dual activity of GlfT2 is provided by the ability of a narrow channel near loop 1 to accommodate trisaccharide substrates and the non-reducing ends of longer galactan substrates

Additional insight into the functioning of these glycosyltransferases has been provided by *in vitro* glycosyltransferase assays using synthetic acceptors that act on substrate analogues (Alderwick *et al.*, 2008; Lee *et al.*, 1997; Pathak *et al.*, 2001; Pathak *et al.*, 2007). These synthetic acceptor molecules have also been implicated in the design and evaluation of potential inhibitors of these enzymes (Cren *et al.*, 2004; Pathak *et al.*, 2009; Subramaniam *et al.*, 2005). At present, glycosyltransferase inhibitors are typically either donor or acceptor analogues with identical or lower K_m values to the natural donors or acceptors (Pesnot *et al.*, 2010). To design new inhibitors with higher binding affinities, a thorough insight into the protein-carbohydrate interactions is necessary. In this regard, a novel strategy of using "polar hydrophobicity" for

synthesising substrate analogues is lucrative and is currently being implemented to study protein-carbohydrate interactions (Ioannou *et al.*, 2011). This strategy employs the use of donor and acceptor analogues with selectively replaced hydroxyl or hydrogen groups to highly electrophilic fluorine atoms for interaction with the enzyme. These fluorinated compounds have a higher affinity for the enzyme when compared to their non-fluorinated counterparts (Biffinger *et al.*, 2004; Gao *et al.*, 1995). The presence of fluorine atoms near the anomeric position in disaccharides significantly affects the activity of glycosyltransferases in various ways that aids in its inhibitory effect. These include inactivation of enzyme by means of chemical reactions, inhibition of enzyme activity or slow reactivity of the enzyme with the substrate. Modified disaccharides with 2' deoxy-2' fluoro and 5'-fluoro substitutions are very potent inhibitors of glycosyltransferases. For example, UDP-Gal-2F inhibitor that is synthesised by replacement of a hydroxyl group at position 2 in α-D-galactopyranose with a fluorine atom is a reversible inhibitor of α-1, 3-GalT with sufficiently high binding affinity. The compound functions as a competitive inhibitor as it generates no reaction product (Jamaluddin *et al.*, 2007; Persson *et al.*, 2001). Similarly, compounds such as UDP-(5F)-GlcNAc shows marked competitive inhibition against the substrate UDP-GlcNAc for GalTs such as UDP-GlcNAc:GlcNAc-P-P-Dol *N*-acetylglucosaminyl transferase, chitobiosyl-P-P-lipid synthase and *N*-acetyllactosamine synthase and can be employed to study glycosyl transfer reactions at C-3 or C-6 position (Hartman *et al.*, 2007). In addition, these fluoride based inhibitors have found their use in determining the structure of glycosyl-enzyme intermediates by means of NMR spectroscopy or X-ray crystallography. For example, 2-acetamido-2-deoxy-β-D-glucopyranosyl-(1→4)-2-deoxy-2-fluoro-β-D-glucopyranosyl fluoride, an inhibitor of hen egg white lysozyme was used to determine the structure of glycosyl-enzyme

intermediate from X-ray crystallography (Vocadlo *et al.*, 2001) for both α- and β-glycosyltransferases (Davies *et al.*, 2003; Lovering *et al.*, 2005). These mechanistic studies reveal the transition state mechanisms of the fluorine based compounds that assist in designing of highly selective inhibitors with improved binding affinities (Gloster *et al.*, 2007).

In order to determine the residues essential for activity of GlfTs in the disaccharides for generation of the arabinan and galactan core, we tested a series of tetrafluorinated substrate analogues, synthesised by the Linclau group, University of Southampton, for their potential as acceptors or inhibitors. Table 5.1 summarises the structure and IUPAC names of the compounds utilised in the study. These synthetic compounds are designed to have a high degree of similarity with the natural substrates of GalTs and AraTs in mycobacteria and thus function as substrate analogues. The presence of fluorine atom in these compounds confers high electronegativity to the molecule and thus aids in their function as an acceptor. GlfTs and AraTs mediate a transglycosylation reaction by transfering Gal and Ara residues from the natural sugar donors UDP-Gal and DPA to afford the corresponding [^{14}C]-Gal*f*-acceptor and [^{14}C]-Ara*f*-acceptor product respectively. Both GalTs and AraTs are inverting enzymes that utilize carboxylate groups from Asp residues in the DXD motif in the active site. The synthetic acceptors initiate a nucleophilic attack at anomeric carbon of the sugar donor to afford a glycosyl enzyme intermediate that forms a glycosidic linkage with inversion of anomeric stereochemistry. In addition, the reaction regenerates the carriers UDP and decaprenyl phosphate (DP).The fluorine atoms in the substrate analogues can also engage in covalent binding with the enzyme. In this situation, inhibition of enzyme activity occurs due to loss of fluorine at or near the enzyme active site. The proposed

reaction scheme of the tested compounds along with the respective synthetic substrates is illustrated in Figure 5.1.

The compounds were tested for their acceptor and inhibitor activity using membrane and cell wall extracts from *M. smegmatis* by mixing the compounds with 0.4 mM Gal (1→5) (SRI20668) and Gal (1→6) (SRI20669) gal-gal disaccharide probes, which are known to exhibit excellent acceptor activities (Pathak *et al.*, 2007). Similarly, to test competitive inhibition of Ara*f*Ts, the test compound was mixed with 0.4 mM α-D-Ara*f*-(1→5)-α-D-Ara*f*-l-*O*-C_8H_{17} neoglycolipid acceptor with an established acceptor activity (Lee *et al.*, 1998; Pathak *et al.*, 2002).

Table 5.1: Tetra-fluorinated compound tested for their acceptor and inhibitor activity in *M. smegmatis*

Compound #	IUPAC Name	Strucure	Linkage
48	1-*O*-Octyl-5-*O*-(*β*-galactofuranosyl)-2,3-dideoxy-2,2,3,3-tetrafluoro-*β*-galactofuranose	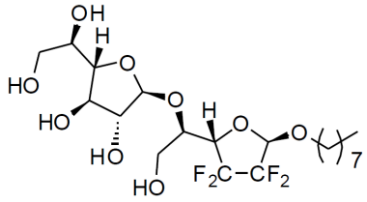	β (1→5)
83	1-*O*-Octyl-5-*O*-(*β*-galactofuranosyl)-2,3-dideoxy-2,2,3,3-tetrafluoro-*α*-galactofuranose	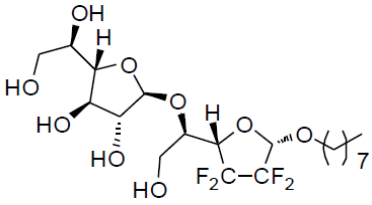	α (1→5)
84	1-*O*-Octyl-6-*O*-(*β*-galactofuranosyl)-2,3-dideoxy-2,2,3,3-tetrafluoro-*β*-galactofuranoside	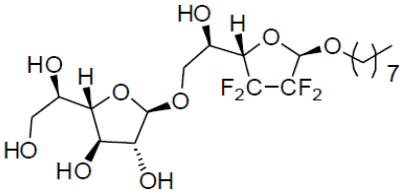	β (1→6)
85	1-*O*-Octyl-6-*O*-(*β*-galactofuranosyl)-2,3-dideoxy-2,2,3,3-tetrafluoro-*α*-galactofuranoside	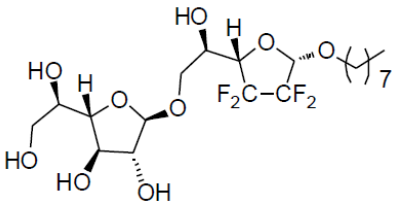	α (1→6)
87	1-*O*-Octyl-5-*O*-(*α*-arabinofuranosyl)-2,3-dideoxy-2,2,3,3-tetrafluoro-arabinofuranose	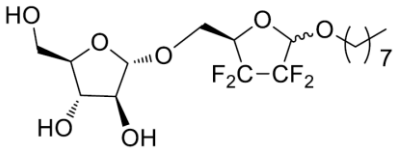	α (1→5)

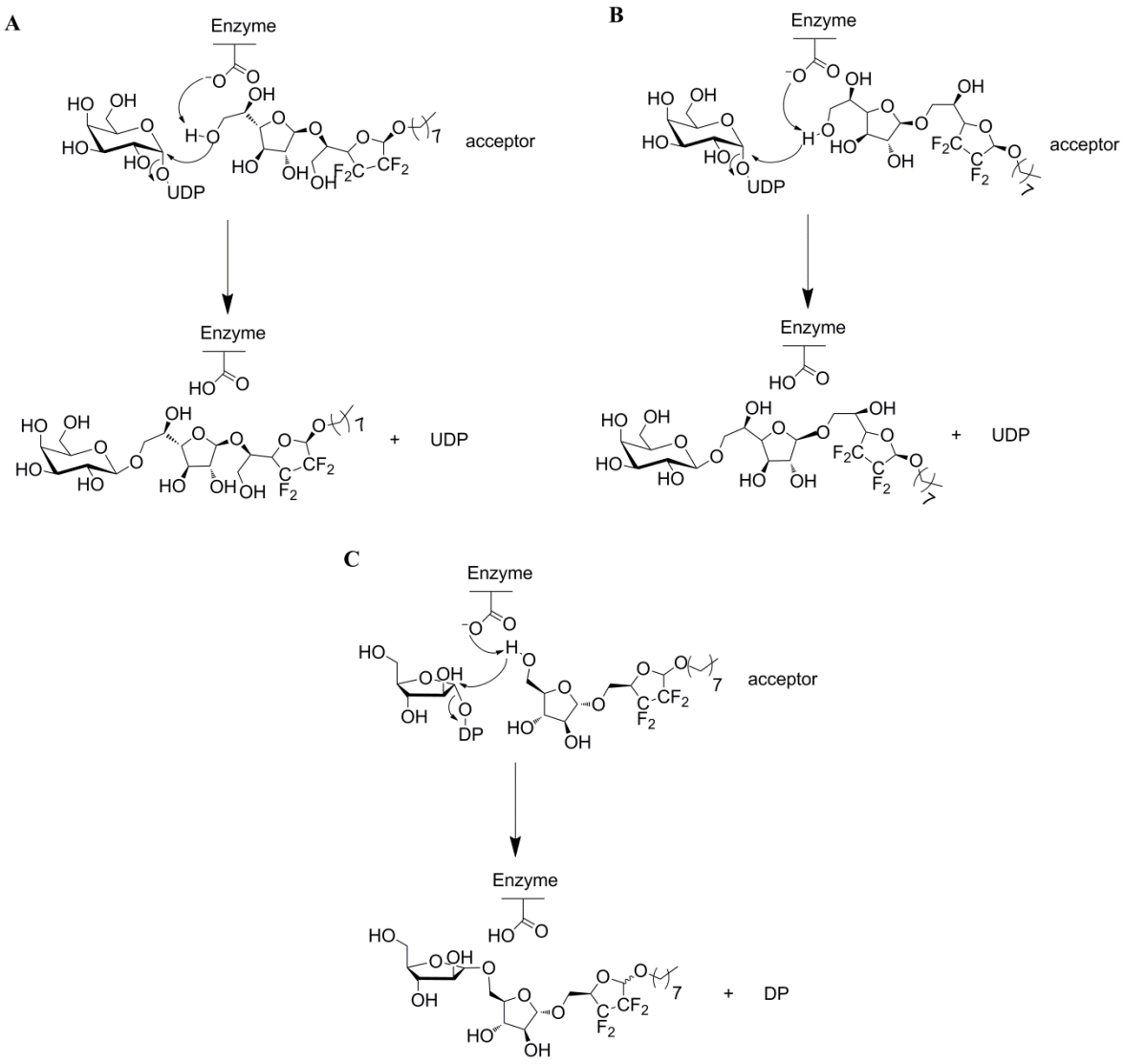

Figure 5.1: Proposed mechanism for transglycosylation reactions catalysed by A. GalTs for compounds 48 and 83, B. GalTs for compounds 84 and 85 and C. AraTs for compound 87.

5.2 Materials and Methods

5.2.1 GalT assay

The acceptor activity of all four compounds 48, 83-85 (20 mM stock, stored in ethanol) was performed using a step-wise concentration gradient of 0.1-2.0 mM. The required concentration of the compound and 0.25 µCi of [U-^{14}C]-UDP-Gal*p* (American Radiolabeled Chemicals Inc., 250-300 mCi/mmol) were dried under a stream of argon in a microcentrifuge tube (1.5 mL) to remove any solvent. The dried mixture was resuspended in buffer containing 50 mM MOPS (adjusted to pH 8 with KOH), 10 mM $MgCl_2$ and 1% IgePal (8 µL) and mixed with the remaining components of the assay; 1mM ATP (10 µL) and 100 mM NADH (8µL). The reaction was initiated by the addition of membranes (500 µg) and P60 fraction (200µg) resulting in a final reaction volume of 80 µL. The reaction mixtures were then incubated at 37^{o}C for 1 hour and stopped using chloroform:methanol (1:1, 533 µL). The contents of the tubes were centrifuged at 18, 000 x *g* and supernatant was recovered and dried under a stream of argon. The dried constituents were re-suspended in ethanol:water (1:1, 1 mL) and loaded onto a pre-equilibrated (ethanol:water [1:1]) 1 mL Whatman Strong Anion Exchange (SAX) cartridge washed with 3 mL of ethanol. The eluate was dried and the contents were partitioned between the aqueous and organic phase resulting from a mixture of *n*-butanol (2 mL) and H_20 (2 mL). The contents were centrifuged at 3,500 x *g* and the organic phase recovered. The remaining aqueous phase was re-extracted with 2 mL of *n*-butanol saturated water and the extracts pooled. The organic fraction of pooled extracts were back-washed twice with water saturated with *n*-butanol (2 mL). The *n*-butanol-saturated water fraction (4 mL) was then dried and re-suspended in 200 µL of *n*-butanol. The total cpm of radiolabeled material in *n*-butanol fraction was measured by scintillation

counting using 50% of the labeled material and 10 mL of EcoScintA (National Diagnostics, Atlanta). The counts present in control assays (reaction components lacking the test compound) were subtracted from the test samples to estimate the incorporation of [^{14}C]-Gal*f*. The remaining 50 % of the labeled material was subjected to thin-layer chromatography (TLC) in chloroform/methanol/ammonium hydroxide/water (65:25:0.5:3.6) on aluminium backed Silica Gel 60 F_{254} plates (E. Merck, Darmstadt, Germany). Autoradiograms were obtained by exposing TLC's to X-ray film (Kodak X-Omat) for 5 days. To estimate the inhibitor activity of the compounds, a step-wise gradient 0.1-2 mM was mixed alongside [U-^{14}C]-UDP-Gal*p* (0.25 µCi) with 0.4 mM SRI20668 and 0.4 mM SRI20669 acceptor (20 mM stock stored in ethanol), depending upon the activity to be assayed Gal (1→5) or Gal(1→6) and dried under the stream of argon in a microcentrifuge tube (1.5 mL).

5.2.2 AraT assay

The acceptor activity of compound 87 (20 mM stock, stored in ethanol) was estimated by using a step-wise concentration gradient of 0.1-2.0 mM. Compound 87 was dried under a stream of argon in a microcentrifuge tube (1.5 mL) and placed in a vacuum desiccator for 15 minutes to remove any residual solvent. The dried compound was resuspended in buffer containing 50 mM MOPS (adjusted to pH 8 with KOH), 10 mM $MgCl_2$, 10 mM ATP, 10 mM NADP, 10 mM NAD, 10 mM FAD. To initiate the reaction, p[^{14}C]RPP (140,000 cpm, stored in 1 M sodium acetate), membranes (250 µg) and P60 fraction (250 µg) extracts prepared from *M. smegmatis* using previously described protocols (Lee *et al.*, 1996) elaborated in General Materials and Methods, Section 7.4.6 were added to a final reaction volume of 80 µL. The reaction mixtures were then incubated at 37^{o}C for 2 hours and stopped using chloroform:methanol (1:1,

533 µL). The contents of the tubes were centrifuged at 18,000 x *g* and supernatant was recovered and dried under a stream of argon. The dried constituents were re-suspended in ethanol:water (1:1, 1 mL) and loaded onto a pre-equilibrated (ethanol:water, 1:1) 1 mL Whatman Strong Anion Exchange (SAX) cartridge and washed with 3 mL of absolute ethanol. The elute was dried and the contents were partitioned between aqueous and organic phase resulting from a mixture of *n*-butanol (2 mL) and water (2 mL). The contents were centrifuged at 3,500 x *g* and organic phase was recovered. The remaining aqueous phase was re-extracted with 2 mL of *n*-butanol saturated water and the extracts were pooled. The organic fraction of pooled extracts was back-washed twice with water saturated with *n*-butanol (2 mL). The *n*-butanol-saturated water fraction (4 mL) was then dried and re-suspended in 200 µL of *n*-butanol. The total cpm of radiolabeled material in *n*-butanol was measured by scintillation counting using 50% of the labeled material and 10 mL of EcoScintA (National Diagnostics, Atlanta). The counts present in control assays (reaction components lacking compound 87) were subtracted from the test samples to estimate the incorporation of [^{14}C]-Ara*f*. The remaining 50% of the labeled material was dried, resuspended in butanol and equal counts were loaded on aluminium backed Silica Gel 60 F_{254} plates (E. Merck, Darmstadt, Germany) and subjected to thin-layer chromatography (TLC) in chloroform/methanol/ammonium hydroxide/water (65:25:0.5:3.6). Autoradiograms were obtained by exposing TLC's to X-ray film (Kodak X-Omat) for 5 days. To estimate the inhibitor activity of the Compound 87, a step-wise gradient of 0.1-2 mM was mixed with 0.4 mM Ara (α1→5) acceptor (20 mM stock stored in ethanol) and dried under the stream of argon in a microcentrifuge tube (1.5 mL) and placed in a vacuum desiccator for 15 minutes to remove any residual solvent. The assay was performed as mentioned above. The total cpm of radiolabeled material in *n*-butanol

was measured by scintillation counting using 50% of the labeled material and 10 mL of EcoScintA (National Diagnostics, Atlanta). The counts present in control assays (reaction components lacking compound 87) were subtracted from the test samples to estimate the incorporation of [^{14}C]-Ara*f*. The remaining 50% of the labeled material was dried, resuspended in butanol and equal counts were loaded on aluminium backed Silica Gel 60 F_{254} plates (E. Merck, Darmstadt, Germany) and subjected to thin-layer chromatography (TLC) in chloroform/methanol/ammonium hydroxide/water (65:25:0.5:3.6). Phophor-imaging was performed by exposing TLCs to phosphor-screen (Bio-Rad) for 2 days.

5.3 Results

The tetrafluorinated compounds were evaluated for their acceptor and inhibitor activity using a cell free assay system comprising of membrane extracts and the cell wall enzymatic fraction P60 prepared from *M. smegmatis*. The compounds were analysed for their galactosyltransferase and arabinosyltransferase acceptor and inhibitor activity in a range of concentrations from 0.1 mM to 2.0 mM.

5.3.1 Acceptor activity analysis for galactofuranosyltransferases using *M. smegmatis* membrane extracts for compounds 48, 83, 84 and 85.

All compounds were analysed for their acceptor activity measured by the amount of radioactivity recovered. The radioactive counts recovered from the parent disaccharides were considered as one hundred percent and was used as a reference to estimate the percent recovery for the test compounds. The parent disaccharides Gal(β1→5)Gal (SRI20668) and Gal(β1→6)Gal (SRI20669) showed excellent incorporation of [^{14}C]-Gal*f* however, none of the compounds tested exhibited any significant acceptor activity, as very low amounts of radioactivity was recovered in the organic phase i.e. 1-9% (Table 5.2) when compared to the disaccharide analogues SRI20668 and SRI20669. The products were not analysed on TLC plates due to very low amounts of radioactivity recovered.

Table 5.2: Percent acceptor activity and radioactivity recovered for compounds 48, 83, 84 and 85.

Acceptor/ Compound	Concentration (mM)	Radioactivity (in CPM)	% Activity
0.4mM SRI20668	0.4	12017	100
0.1mM 48	0.1	1141	9.49
0.25mM 48	0.25	596	4.96
0.5mM 48	0.5	570	4.74
0.75mM 48	0.75	670	5.58
1.0mM 48	1	761	6.33
2mM 48	2	718	5.97
0.4mM SRI20668	0.4	12017	100
0.1mM 83	0.1	159	1.32
0.25mM 83	0.25	192	1.60
0.5mM 83	0.5	221	1.84
0.75mM 83	0.75	252	2.10
1.0mM 83	1	298	2.48
2.0mM 83	2	197	1.64
0.4mM SRI20669	0.4	15299	100
0.1mM 84	0.1	234	1.53
0.25mM 84	0.25	704	4.60
0.5mM 84	0.5	1397	9.13
0.75mM 84	0.75	1327	8.67
1.0mM 84	1	1856	12.13
2mM 84	2	870	5.69
0.4mM SRI20669	0.4	15299	100
0.1mM 85	0.1	207	1.35
0.25mM 85	0.25	506	3.31
0.5mM 85	0.5	359	2.35
0.75mM 85	0.75	475	3.10
1.0mM 85	1	634	4.14
2.0mM 85	2	823	5.38

5.3.2 Inhibitor activity analysis galactofuranosyltransferases using *M. smegmatis* membrane extracts for compounds 48, 83, 84 and 85.

Since the compounds showed poor acceptor activity, they were also tested as inhibitors and the activity was measured by the amount of radioactivity recovered when mixed with the disaccharide analogues SRI20668 (Gal-β(1→5)Gal) and SRI20669 (Gal-β(1→6)Gal). The inhibitor activity was estimated using densitometry analysis of the autoradiograms. The radioactive counts recovered from the parent disaccharides were considered as one hundred percent and was used as a reference to estimate the percent recovery for the test compounds. The TLC/autoradiography demonstrated the inhibitor activity of compounds 48 and 83 (Figure 5.2 and 5.3) with maximum inhibition of 82.26 and 74.25% respectively (Table 5.3), at a concentration of 2 mM, as a gradual decrease in conversion of Gal*f* (1→5) disaccharide to the corresponding trisaccharide and tetrasaccharide product. However, only moderate inhibition, 47.42 and 67.26% was observed for compounds 84 and 85, respectively (Table 5.3), at a concentration of 2 mM, rendering them less suitable as substrate analogues for enzyme inhibition studies. The TLC/autoradiography for compounds 84 and 85 (Figure 5.4 and 5.5) did not demonstrate a gradual decrease in conversion of Gal*f* (β1→6) disaccharide to the corresponding trisaccharide or tetrasaccharide product except at the highest concentration of 2 mM where a moderate decrease was observed. In addition, all compounds at their inhibitory concentrations showed an overall reduction in trisaccharide and tetrasaccharide product formation. The inhibitor activity for all the compounds with respect to the concentration is summarised in Table 5.3.

Table 5.3: Percent inhibitor activity and radioactivity recovered for compounds 48, 83, 84 and 85.

Acceptor/ Compound	Concentration (mM)	CPM	Density of tetra & trisaccharide	% Inhibiton
0.4mM SRI20668	0.4	2471	36.82	0
0.1mM 48	0.1	2475	39.71	~ 0
0.25mM 48	0.25	2202	33.37	9.37
0.5mM 48	0.5	1852	34.16	7.22
1.0mM 48	1	2027	31.01	15.78
2mM 48	2	317	6.53	82.26
0.4mM SRI20668	0.4	2471	38.53	0
0.1mM 83	0.1	4378	77.24	-100
0.25mM 83	0.25	1679	27.96	27.43
0.5mM 83	0.5	813	18.42	52.19
1.0mM 83	1	738	13.89	63.95
2.0mM 83	2	385	9.92	74.25
0.4mM SRI20669	0.4	34497.5	124.43	0
0.1mM 84	0.1	28904	118.68	5.17
0.25mM 84	0.25	32956	124.48	0
0.5mM 84	0.5	33298	117.64	5.46
1.0mM 84	1	30381	101.28	18.6
2mM 84	2	20105	65.42	47.42
0.4mM Gal SRI20669	0.4	34497.5	114.1	0
0.1mM 85	0.1	29281	88.13	22.76
0.25mM 85	0.25	33570	103.43	9.59
0.5mM 85	0.5	24790	72.8	36.19
1.0mM 85	1	28313	70.86	37.9
2.0mM 85	2	11781	37.35	67.26

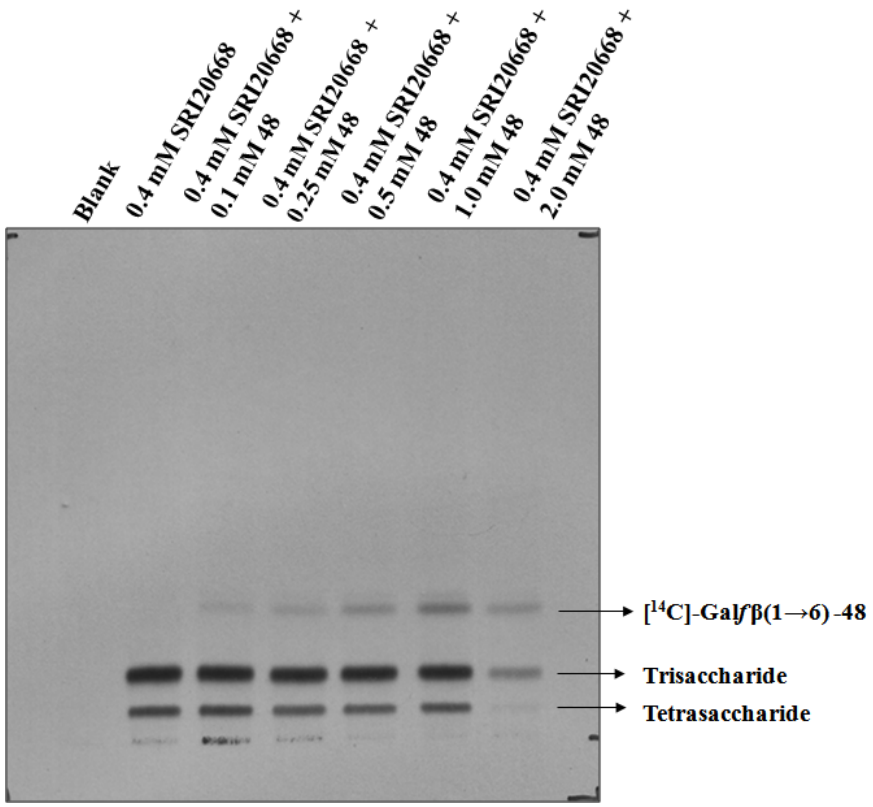

Figure 5.2: Autoradiogram for inhibitory activity of compound 48 with Gal-β(1→5)Gal acceptor. The assays were supplemented with 0.25 µCi [^{14}C-U]-UDP-Gal, 0.4 mM Gal-β(1→5)Gal acceptor (SRI20668) along with concentrations 0.1, 0.25, 0.5, 1.0 and 2.0 mM of compound 48 to check its inhibitory effect. The reactions supplemented with only 0.4 mM SRI20668 acceptor generated corresponding tri- and tetrasaccharide products. Addition of compound 48 at concentrations 0.1, 0.25. 05, 1.0 and 2.0 mM to reaction mixture with 0.4 mM SRI20688 led to a gradual decrease in synthesis of tri- and tetrasaccharide products. The compound was found to be a highly effective inhibitor at the concentration of 2.0 mM as an overall reduction by 82% in the tri- and tetrasaccharides was observed. The compound 48 reacted with [^{14}C-U]-UDP-Gal donor and generated [^{14}C] Gal*f* -β(1→6)-48 as a reaction product.

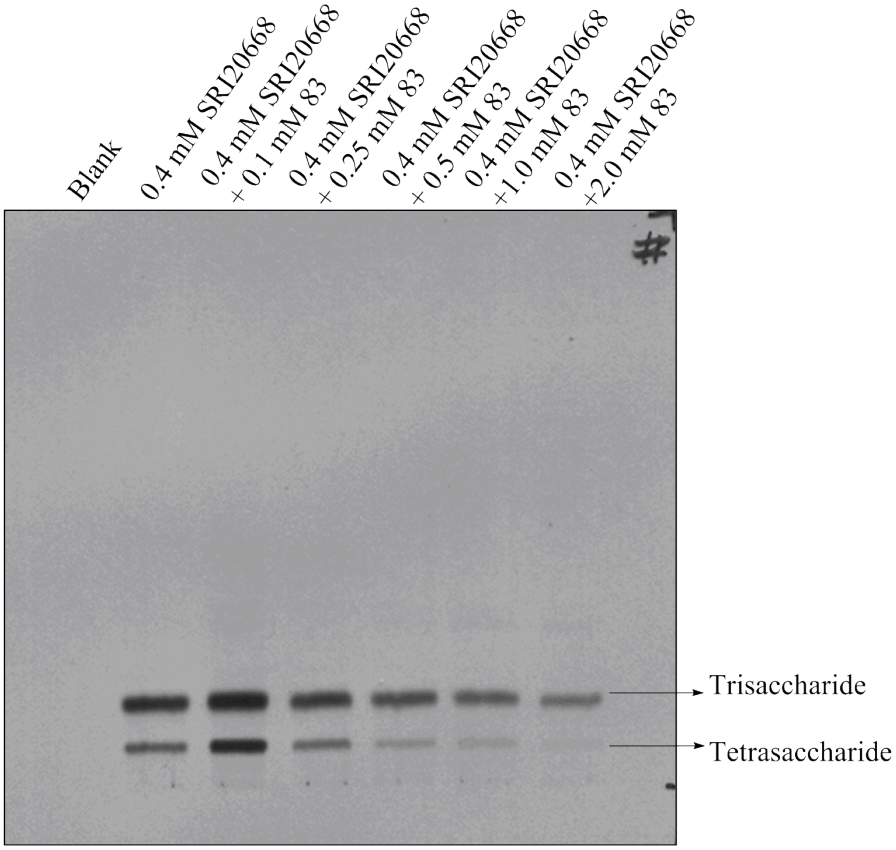

Figure 5.3: Autoradiogram for inhibitory activity of compound 83. The assays were supplemented with 0.25 µCi [^{14}C-U]-UDP-Gal, 0.4 mM Gal-β(1→5)Gal acceptor (SRI20668) along with concentrations 0.1, 0.25, 0.5, 1.0 and 2.0 mM of compound 83 to check its inhibitory effect. The reactions supplemented with only 0.4 mM SRI20688 acceptor generated corresponding tri- and tetrasaccharide products. Addition of compound 83 at concentrations 0.1, 0.25. 05, 1.0 and 2.0 mM to reaction mixture with 0.4 mM SRI20688 led to a gradual decrease in synthesis of tri and tetrasaccharide products. The compound was found to be an effective inhibitor at the concentrations of 0.5-2.0 mM with an overall reduction in the tri and tetrasaccharides due to a reduction in the activity of disaccharide analogue Gal-β(1→5)Gal by 52-74%.

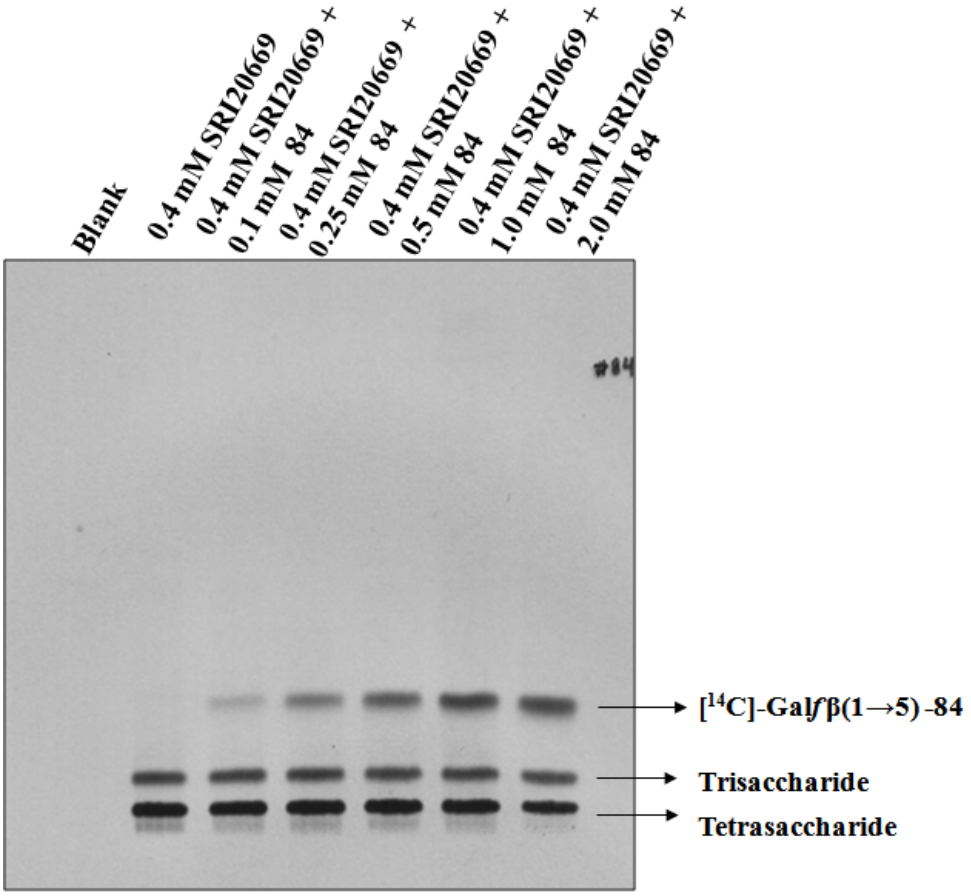

Figure 5.4: Autoradiogram for inhibitory activity of compound 84. The assays were supplemented with 0.25 µCi [^{14}C-U]-UDP-Gal, 0.4 mM Gal-β(1→6)Gal acceptor (SRI20669) along with concentrations 0.1, 0.25, 0.5, 1.0 and 2.0 mM of compound 84 to check its inhibitory effect. The reactions supplemented with only 0.4 mM SRI20669 acceptor generated corresponding tri- and tetrasaccharide products. Addition of compound 84 at concentrations 0.1, 0.25. 05, 1.0 and 2.0 mM to reaction mixture with 0.4 mM SRI20688 led to no significant reduction in synthesis of tri- and tetrasaccharide products. Modest amount of reduction i.e. 42.4% in radioactivity was observed for the compound at the concentration of 2.0 mM. The compound 84 reacted with [^{14}C-U]-UDP-Gal to generate [^{14}C] Gal*f* -β(1→5)-84 as a reaction product.

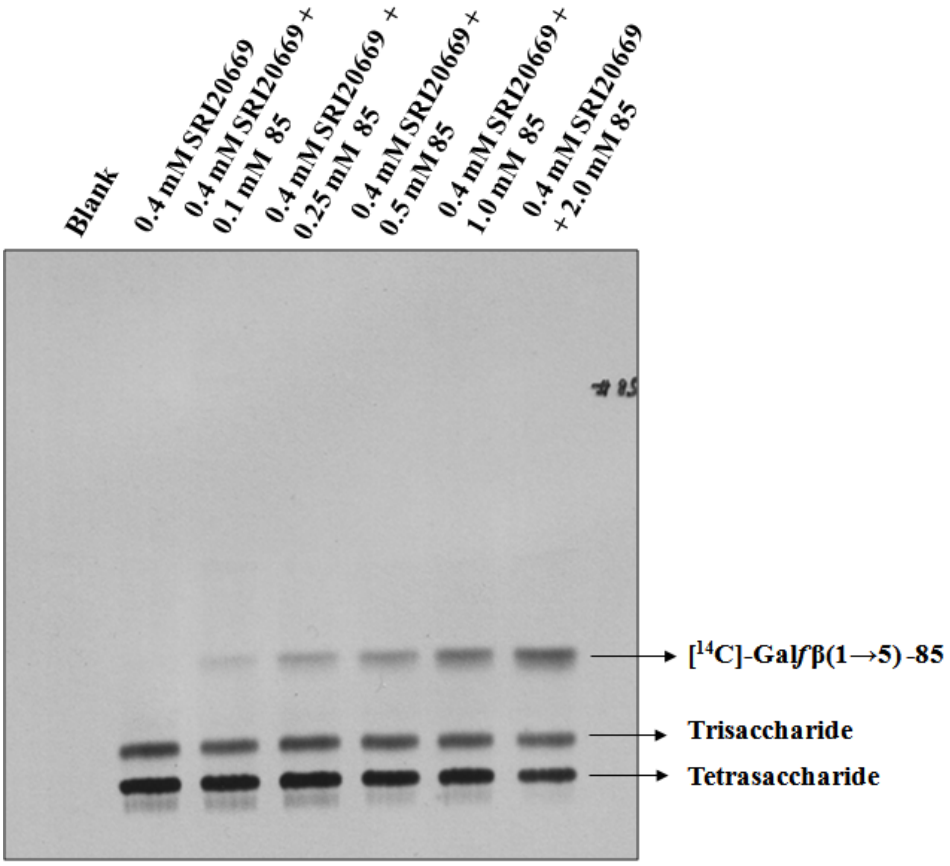

Figure 5.5: Autoradiogram for inhibitory activity of compound 85. The assays were supplemented with 0.25 µCi [^{14}C-U]-UDP-Gal, 0.4 mM Gal-β(1→6)Gal acceptor (SRI20669) along with concentrations 0.1, 0.25, 0.5, 1.0 and 2.0 mM of compound 85 to check its inhibitory effect. The reactions supplemented with only 0.4 mM SRI20669 acceptor generated corresponding tri- and tetrasaccharide products. Addition of compound 85 at concentrations 0.1, 0.25. 05, 1.0 and 2.0 mM to reaction mixture with 0.4 mM SRI20688 led to no significant reduction in synthesis of tri- and tetrasaccharide products. At a concentration of 2.0 mM, 67% radioactivity was recovered for compound 85 with an overall reduction in products formed. The compound 85 reacted with [^{14}C-U]-UDP-Gal and generated [^{14}C] Gal*f* -β(1→5)-85 as a reaction product.

5.3.3 Acceptor and inhibitor activity analysis for arabinofuranosyltransferases using *M. smegmatis* membrane extracts for compound 87.

Compound 87 was analysed either as an acceptor and/or inhibitor of DP[^{14}C]A and activity was measured by the amount of radioactivity recovered in organic extracts. The parent disaccharide Ara-α(1→5)Ara showed excellent incorporation of [^{14}C]-Ara*f* from the donor DP[^{14}C]A when assays were exogenously supplemented with p[^{14}C]RPP (Figure 5.6 & 5.7) as evident from the trisaccharide produced. However, compound 87 when tested as an acceptor in assays supplemented with p[^{14}C]RPP and compound 87 (0.1 mM-2 mM) yielded [^{14}C]-Ara*f*-(1→?)-87 and an unidentified product in very low quanities as evident from the autoradiogram (Figure 5.6).

In addition, the compound was also tested as an inhibitor of [^{14}C]-Ara*f* incorporation from p[^{14}C]RPP into Ara*f*-α(1→5)-Ara*f* acceptor at a concentration of 2 mM (Figure 5.7). Since the reaction supplemented with 0.4 mM Ara*f*-α(1→5)-Ara*f* and 2 mM 87 generated the trisaccaharide product, the compound was ineffective as an inhibitor. In addition, the radioactivity recovered from reactions containing 0.4 mM disaccharide acceptor supplemented with compound 87 was higher (7472 cpm) than the assays supplemented with 0.4 mM disaccharide acceptor alone (5274 cpm) implying its role as a detergent that enhances the activity of the disaccharide acceptor (Pathak *et al.*, 2002).

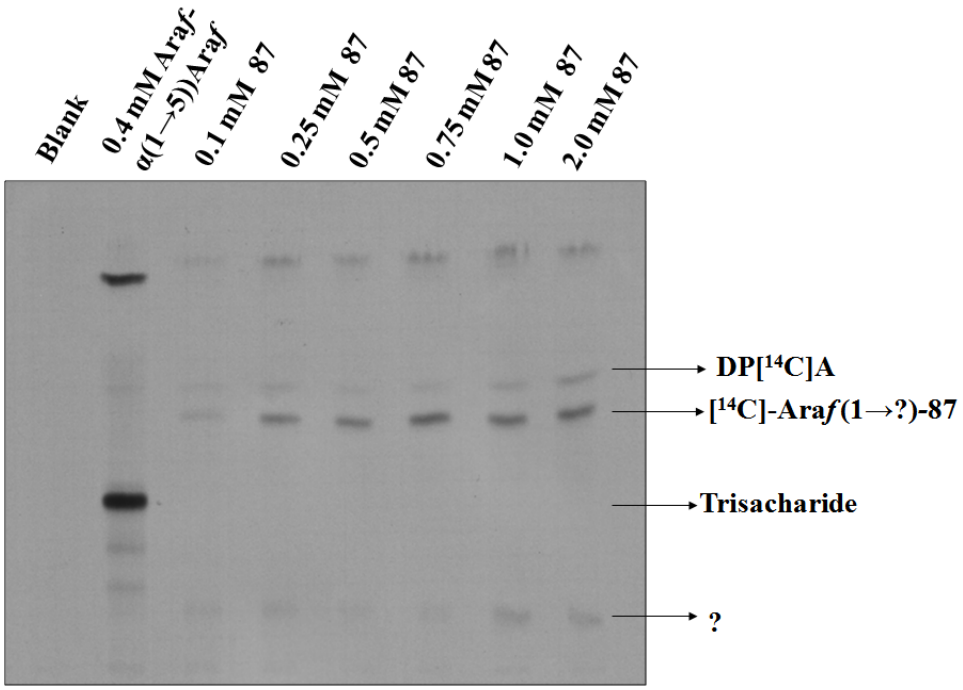

Figure 5.6: Autoradiogram for acceptor activity of compound 87. The assays were supplemented with 140,000 cpm of p[^{14}C]RPP, 0.4 mM Ara*f*-α(1→5)Ara*f* acceptor and compound 87 (0.1, 0.25, 0.5, 1.0 and 2.0 mM) to check its acceptor activity. The reactions supplemented with only 0.4 mM Ara*f*-α(1→5)Ara*f* acceptor generated corresponding trisaccharide product. Addition of compound 87 at concentrations 0.1, 0.25. 05, 0.75, 1.0 and 2.0 mM to reaction mixture with 140,000 cpm of p[^{14}C]RPP led to synthesis of [^{14}C]-Ara*f* – (1→?)-87 as a reaction product. The weak acceptor activity was evident for compound 87 as an unknown product (?) was also synthesised.

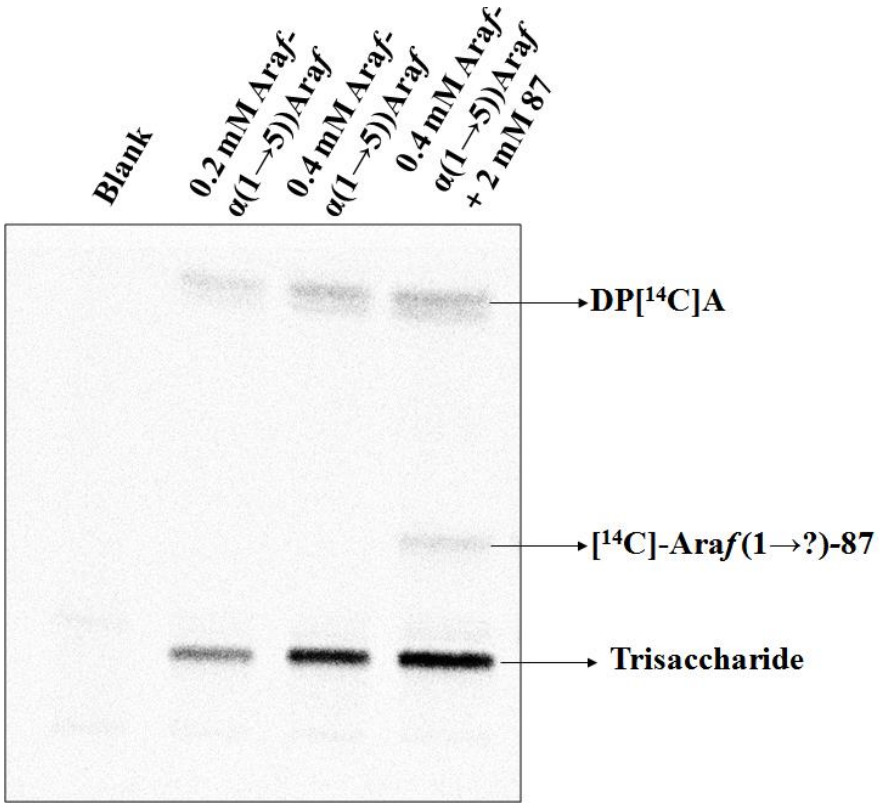

Figure 5.7: Phosphor-imaging scan for inhibitor activity of compound 87. The assays were supplemented with 140,000 cpm of p[^{14}C]RPP, 0.2 mM and 0.4 mM Ara*f*-α(1→5)Ara*f* acceptor, 0.4 mM Ara*f*-α(1→5)Ara*f* acceptor with 2 mM compound 87 to check its inhibitory activity. All the reactions supplemented with Ara*f*-α(1→5)Ara*f* acceptor generated corresponding trisaccharide product. Addition of compound 87 at 2.0 mM concentration to reaction mixture with 140,000 cpm of p[^{14}C]RPP and 0.4 mM Ara*f*-α(1→5)Ara*f* acceptor led to synthesis of corresponding trisaccharide and [^{14}C]-Ara*f* –(1→?)-87 as a reaction product implying no inhibitory effect of the compound.

5.4 Discussion

The analysis of the crystal structure of galactofuranosyltransferases have suggested three vital strategies for generation of GlfT inhibitors (Wheatley *et al.*, 2012). These include: modification of uridine base in substrate analogues with increased binding affinity to the enzyme in comparison to the natural substrate (Pesnot *et al.*, 2010); allosteric inhibition of the enzyme by donor substrates with bulky functional groups and higher affinity to the ribose binding pocket in the enzyme resulting in stearic hindrance in neighbouring pockets (Qasba *et al.*, 2005), and inhibitors that bind to the hydrophobic residues in the cytoplasmic face of the enzyme and prevent its interaction with the membrane, thus disallowing the catalysis to proceed adequately (Wheatley *et al.*, 2012). New inhibitors for arabinofuranosyl transferases can be developed based on similar strategies. Inhibition of Ara*f*Ts can be achieved by synthetic DPA analogs that either inhibit arabinan synthesis or interfere in its interaction with plasma membrane and its components. Since, the activity of these enzymes is crucial for mAGP complex formation, substrate analogs which compete with the natural disaccharides for binding with the galactosyltransferases and arabinofuranosyltransferases can give insights into the mechanism of function of these enzymes and also help generate drug-like molecules that inhibit transferase activity.

The four tetrafluorinated substrate analogues of naturally occurring disaccharides used in this study were found to be inhibitors for the galactosyltransferases GlfT1 and GlfT2, as they all showed some reduced incorporation of [^{14}C]-Gal*f* from the [U-^{14}C]-UDP-Gal*p* donor when mixed with the respective disaccharide analogues SRI20668 and SRI20669. The compounds 48; 1-*O*-Octyl-5-*O*-(*β*-galactofuranosyl)-2,3-dideoxy-2,2,3,3-tetrafluoro-*β*-galactofuranose and 83**;** 1-*O*-Octyl-5-*O*-(*β*-galactofuranosyl)-2,3-

dideoxy-2,2,3,3-tetrafluoro-*α*-galactofuranose, effectively inhibited the conversion of disaccharide analogue SRI20668 by 87 and 84% respectively at a concentration of 2 mM. The IC_{50} value of 1.0 mM, as approximated from the graph was found to be lowest for compound 83. Therefore, compound 83 can be used for inhibitory studies for the enzymes GlfT1 and GlfT2.

The compound 87; 1-*O*-Octyl-5-*O*-(*α*-arabinofuranosyl)-2,3-dideoxy-2,2,3,3-tetrafluoro-arabinofuranose; readily accepts Ara*f* residues to generate corresponding radioactive product and an unknown product. However, when tested as an inhibitor for Ara*f*-α(1→5)Ara*f* acceptor activity, compound 87 aided in [^{14}C]-Ara*f* uptake by the disaccharide acceptor, thus acting as a detergent. Therefore, compound 87 can be used in arabinofuranosyltransferase assays to enhance the efficiency of the reaction.

The selective replacement of a hydrogen atom or hydroxyl group in a biologically active molecule with small and highly electrophilic fluorine atoms can alter its stereochemistry to suit development of pharmacologically active compounds (Liu *et al.*, 2008). New drug candidates for therapy can be generated based on these fluoro-analogues (Peek *et al.*, 2001; Reyes and Heidelberger, 1965; Umeda and Heidelberger, 1969). The fluorine atom offers a selective advantage over other modifications as its small size atom doesn't distort the chemistry of the compound, imparts polar hydrophobicity and stability to the molecule, thus facilitating synthetic acceptor studies especially in case of glycosyltransferases where stability and weak binding of the synthetic acceptor to the enzyme is a persistent problem. These fluorinated analogues of Gal*f* and Ara*f* based disaccharides, substrates for Gal*f*Ts and Ara*f*Ts can not only be used to study enzyme function, metabolic pathways but can also be developed into potential drug candidates with significant pharmacological activity.

Chapter 6

6 Discussion and Future work

The problem of emergence of drug resistant forms of *M. tuberculosis* poses a huge threat in controlling its spread. Repeated misuse of drugs in DOTS therapy have contributed to mutations in several of the target genes leading to the rise of MDR and XDR strains that are resistant to currently available first and second line anti-TB drugs. Consequently, considerable emphasis is being placed on developing potent therapeutics that are unaffected by current resistance mechanisms. The extremely hydrophobic and unusual cell wall of mycobacteria functions as the first line of defence against the chemotherapeutic agents and the pathway for the biogenesis of cell wall components, such as PG, AG, PI-based lipoglycans, their precursors and regulators offer excellent target systems for generating new antimycobacterial drugs. In this regard, the recently discovered cell wall inhibitors BTZs represent a promising drug candidate. Its mechanism of action was further investigated in this work. BTZs target the FAD dependent oxidoreductase DprE1 that functions in concert with DprE2 to catalyse epimerisation of DPR into DPA (Makarov *et al.*, 2009). The end product DPA, is a prenyl based arabinose donor employed in the synthesis of the arabinan component in AG and LAM. In the presence of BTZ, the cell is unable to synthesise DPA which impairs the assembly of arabinan domains in AG and LAM, thus disrupting the cell wall (Makarov *et al.*, 2009). The enzyme DprE1 is established as an essential enzyme in *M. smegmatis* and *C. glutamicum* (Crellin *et al.*, 2011; Meniche *et al.*, 2008). These experiments indicate that generation of DPA and its utilisation in arabinan synthesis is important for the formation of a complete cell wall in both mycobacteria and corynebacteria. The pathway for DPA biogenesis is initiated by transfer of a ribose residue to decaprenyl diphosphate carrier and is catalysed by UbiA, a prenyl

transferase (Alderwick *et al.*, 2006a). Interestingly, inactivation of UbiA in *C. glutamicum* produced a viable mutant indicating that formation of DPA is not an essential reaction (Alderwick *et al.*, 2005).

The results reported in this thesis have explored the possible cause of death resulting from BTZ treatment of *C. glutamicum.* The effect of BTZ lead compound BTZ043 was examined on growth of *C. glutamicum* wild type and *C. glutamicum::ubiA* strains. Whilst the lethal effect of BTZ043 was evident in case of wild type, Cg-*ubiA* was resistant to the compound. Biochemical assays on membrane extracts from Cg-*ubiA* using DP[^{14}C]R as a substrate established that the strain retains a functional copy of DprE1 which is effectively inhibited by BTZ043. Ineffectiveness of BTZ in case of Cg-*ubiA* mutant hinted towards existence of a secondary mechanism responsible for cellular toxicity and lysis. To deduce the alternative basis of lethality, *C. glutamicum Z*-decaprenyl diphosphate synthase (*NCgl2203*), was over-expressed in *C. glutamicum* and the inhibitory effect of BTZ on cell wall arabinan biosynthesis was examined. Interestingly, over expression of *NCgl2203* in presence of BTZ, increased the tolerance of *C. glutamicum* wild type and restored arabinan biosynthesis in this strain. These results imply that the lethal effect of BTZ043 in corynebacteria and mycobacteria is a consequence of abated recycling of decaprenyl phosphate.

Whilst a dearth of knowledge cannot be available in terms of cell wall biosynthesis, the regulatory networks for its synthesis are still poorly understood. In this work, we have identified a novel Lac-I based transcriptional regulator named IpsA that functions as an inositol-dependent transcriptional activator of the *myo*-inositol-phosphate synthase, *ino1*. A series of deletion mutants constructed in *C. glutamicum* were analysed for their cell morphology. Significantly altered cell morphology displayed by the Cg-*ipsA*

mutant highlighted a possible defect in its cell wall biosynthesis. The growth defects displayed by Cg-*ipsA* mutant when cultured in glucose media could be overcome when the media was supplemented with inositol as the carbon source. Inositol was then established as an effector of IpsA by EMSA studies. The microarray analysis of Cg-*ipsA* revealed several downstream effectors including inositol-1-phosphate synthase Ino1 that was confirmed as a target from genetic complementation studies. Further analysis of cell wall lipids revealed complete absence of inositol-derived lipids including PI, PIMs and LAM and established IpsA to be a transcriptional activator, that facilitates transcription of *ino1* which generates inostiol-1-phosphate from glucose-6-phosphate.

The gycosyltransferases in AG biosynthesis pathway are very attractive targets for developing anti-TB compounds. Several synthetic donor or acceptor analogues have been tested as inhibitors of the transferase activity of these enzymes. Lower binding affinities of these compounds have rendered them as weak inhibitors (Cren *et al.*, 2004; Pathak *et al.*, 2009; Pesnot *et al.*, 2010; Subramaniam *et al.*, 2005). In this regard, a novel strategy of using "polar hydrophobicity" for synthesising substrate analogues with increased binding affinities offers a reliable solution (Ioannou *et al.*, 2011). Here in, we attempted to identify potential inhibitors of GlfTs by using tetrafluorinated substrate analogues. The four substrate analogues of naturally occurring disaccharides were deduced as inhibitors of the galactosyltransferases GlfT1 and GlfT2 with compound:1-*O*-Octyl-5-*O*-(*β*-galactofuranosyl)-2,3-dideoxy-2,2,3,3-tetrafluoro-*α*-galactofuranose as the most promising candidate for pharmacological studies. In addition, the protein-protein interactions between glycosyltransferases of LAM biosynthesis pathway was employed to assess the druggablity of the interacting

partners. The significant homotypic and heterotypic interactions between the glycosyltransferases and accessory proteins were identified using a Bacterial Two Hybrid system based on reassembly of cAMP signaling pathway (Karimova *et al.*, 1998b). This approach recognised four possible interaction pairs that include; self-associating PimA, heterotypic interactions between LpqW and the PimE and a significant association between EmbC and AftD. Whilst self-association of PimA implicated a novel process of dimerisation of a glycosyltransferase facilitated by PI ligand, the heterotypic associations of LpqW with the mannosyltransferases PimE strengthened the role of LpqW as a regulatory protein in LAM biosynthesis. The essential homotypic and heterotypic interactions as deduced offer a valuable target resource. Furthermore, the interacting partners as revealed by this study may also serve as 'co-targets' rendering it difficult for bacteria to develop resistance to inhibitors that prevent these interactions.

It is predicted that the studies reported herein could further be explored in future experiments concerning: i) effect of DPR toxicity in cells upon BTZ action, ii) developing drug candidates against the MTB UppS and IpsA, iii) pharmacodynamic studies on tera-fluorinated inhibitors iv) development of a high throughput screen platform to identify inhibitors of potential co-targets determined by PPI studies.

Chapter 7

7 General materials and methods

7.1 Culture media

7.1.1 Luria-Bertani (LB) Broth

25 g of LB powder (5 g/L sodium chloride; 10 g/L tryptone and 5 g/L yeast extract) was dissolved in 1 L of deionised water and sterilised by autoclaving at 121˚C for 15 minutes.

7.1.2 LB Agar

37 g of LB-agar powder (15 g/L agar, 10 g/L tryptone, 5 g/L yeast extract, 5 g/L sodium chloride) was dissolved in 1 L of deionised water and sterilised by autoclaving at 121˚C for 15 minutes.

7.1.3 MacConkey Agar

40 g of MacConkey agar powder (17 g/L pancreatic digest of gelatine, 3 g/L peptones (meat and casein), 10 g/L lactose, 1.5 g/L bile salts no. 3, 5 g/L sodium chloride, 13.5 g/L agar, 0.03 g/L neutral red, 1 mg/L crystal violet) was dissolved by boiling for 1 minute in 1 L deionised water. The media was sterilised by autoclaving at 121ºC for 15 minutes. MacConkey agar was purchased from Difco Laboratories.

7.1.4 M63 minimal media

15.6 g of M63 medium broth powder (2 g/L ammonium sulphate, 13.6 g/L potassium phosphate, monobasic, 0.5 mg/L ferrous sulphate heptahydrate) was dissolved in 1 L of deionised water and adjusted to pH 7.0 with potassium hydroxide and autoclaved at

121ºC for 15 minutes. The solution was allowed to cool to 50ºC and supplemented with 1 mL vitamin B_1 (50 mg in 10 mL deionised water, filter sterilised) and desired carbon source just before use. M63 medium broth powder was purchased from Amresco.

7.1.5 M63 minimal agar

15.6g M63 medium broth powder (2 g/L ammonium sulphate, 13.6 g/L potassium phosphate, monobasic, 0.5 mg/L ferrous sulphate heptahydrate) was dissolved in 1 L of deionised water and adjusted to pH 7.0 using potassium hydroxide. 15 g/L of agar was added to the salts mix and contents autoclaved at 121ºC for 15 minutes. The solution was allowed to cool to 50ºC and supplemented with 1 mL vitamin B_1 (50 mg in 10 mL deionised water, filter sterilised) and desired carbon source just before use. M63 medium broth powder was purchased from Amresco.

7.1.6 Tryptic Soy Broth (TSB)

30 g of TSB broth (17 g/L pancreatic digest of casein, 3 g/L papaic digest of soybean, 2.5 g/L dextrose, 5 g/L sodium chloride, 2.5 g/L dipotassium phosphate) was dissolved in 1 L of deionised water and sterilised by autoclaving at 121˚C for 15 minutes.

7.1.7 Tryptic Soy Agar

40 g of Tryptic Soy Agar (15 g/L pancreatic digest of casein, 5 g/L enzymatic digest of soybean meal, 5 g/L sodium chloride, 15 g/L agar) was dissolved in 1 L of deionised water and sterilised by autoclaving at 121˚C for 15 minutes.

7.1.8 Brain Heart Infusion (BHI) Broth

37 g of BHI broth (12.5 g/L calf brains, 5 g/L beef heart, 10 g/L peptone, 5 g/L sodium chloride, 2 g/L glucose, 2.5 g/L disodium hydrogen phosphate) was dissolved in 1 L of deionised water and sterilised by autoclaving at 121˚C for 15 minutes.

7.1.9 Brain Heart Infusion (BHI) Agar

37 g of BHI broth (12.5 g/L calf brains, 5 g/L beef heart, 10 g/L peptone, 5 g/L sodium chloride, 2 g/L glucose, 2.5 g/L disodium hydrogen phosphate) was dissolved in 1 L of deionised water. 15 g/L of agar was added to the mix and contents were sterilised by autoclaving at 121˚C for 15 minutes.

7.1.10 Brain Heart Infusion Sorbitol (BHIS) Broth

37 g of BHI broth (12.5 g/L calf brains, 5 g/L beef heart, 10 g/L peptone, 5 g/L sodium chloride, 2 g/L glucose, 2.5 g/L disodium hydrogen phosphate) was dissolved in 800 mL of deionised water. 91 g sorbitol was added to the prepared BHI and volume was adjusted to 1 L. The contents were sterilised by autoclaving at 121˚C for 15 minutes.

7.1.11 Brain Heart Infusion Sorbitol (BHIS) Agar

37 g of BHI broth (12.5 g/L calf brains, 5 g/L beef heart, 10 g/L peptone, 5 g/L sodium chloride, 2 g/L glucose, 2.5 g/L disodium hydrogen phosphate) was dissolved in 800 mL of deionised water. 91 g of sorbitol, 15 g/L of agar were added to the prepared BHI and contents were sterilised by autoclaving at 121˚C for 15 minutes.

7.1.12 CGXII minimal media

CGXII salts media was prepared by mixing 20 g ammonium sulphate, 5 g urea, 1 g potassium dihydrogen phosphate, 1 g dipotassium hydrogen phosphate, 0.25 g magnesium sulphate hepta hydrate, 42 g MOPS (3-[N-Morpholino] propanesulfonic acid) in 800 mL deionised water.

The prepared salt mix was mixed with 1 mL of trace elements solution (1 g ferric sulphate heptahydrate, 1 g manganese sulphate monohydrate, 0.1 g zinc sulphate heptahydrate, 0.02 g copper sulphate, 0.002 g nickel chloride hexahydrate prepared in 90 mL deionised water, adjusted to pH 1 using concentrated hydrochloric acid and filter sterilised), 1 mL calcium chloride solution (1 g in 100 mL deionised water, filter sterilised), 50 µL biotin solution (10 mg in 100 mL deionised water, filter sterilised), 8 mL protocatechuate (0.3 g in 8 mL deionised water, dissolved by addition of 1 mL 10 N sodium hydroxide, filter sterilised). The pH of the mixture was adjusted to 7 with 1 N sodium hydroxide and final volume was adjusted to 920 mL and filter sterilised. The required carbon source was added to the minimal medium just before use.

7.2 Antibiotic and Supplements

Table 7.1: Antibiotics and supplements used and their preparation

Accompaniments	Stock Concentration	Storage
Kanamycin	50 mg/mL	-20ºC, in water
Ampicillin	100 mg/mL	-20ºC, in water
Streptomycin	100 mg/mL	-20ºC, in water
Tetracycline	10 mg/mL	-20ºC, in 70% ethanol
BTZ043	10 mg/mL	-20ºC, in DMSO
Isopropyl β-D-1-thiogalactopyranoside (IPTG)	1 M/mL	-20ºC, in water
5-bromo-4-chloro-3-indolyl-β-D-galactopyranoside (X-gal)	40 mg/mL	-20ºC, in DMSO
Inositol	50 % w/v	4ºC, in water
Glucose	50 % w/v	4ºC, in water
Maltose	50 % w/v	4ºC, in water

7.3 Molecular biology techniques

7.3.1 Plasmid extraction

Plasmid DNA was purified using QIAGEN plasmid mini-prep kits. Overnight cultures of bacterial strains harbouring the required plasmids were pelleted and resuspended in RNase containing P1 resuspension buffer. The cells were lysed using sodium dodecyl sulphate based P2 lysis buffer, which aids in removal of proteins. The contents were mixed and treated with acetate-guanidine hydrocholoride containing neutralisation buffer N3 to separate chromosomal DNA from plasmid DNA. The plasmid DNA is recovered in soluble state by centrifuging the suspension. The supernatant is applied to the spin column and washed with ethanol containing PE buffer to remove any traces of

proteins. The purified plasmid DNA is eluted in deionised water or in 10 mM Tris-HCl (pH 8.5).

7.3.2 Polymerase Chain Reaction (PCR)

A standard PCR mix was set up and amplified at a temperature gradient to deduce best amplification conditions for each gene.

Table 7.2: PCR reaction mix conditions.

Components	Mix A	Mix B	Mix C	Mix D
100 pmol/µL 5' cloning primer	0.08 µL	0.08 µL	0.08 µL	0.08 µL
100 pmol/µL 3' cloning primer	0.08 µL	0.08 µL	0.08 µL	0.08 µL
5X GC buffer	4 µL	4 µL	4 µL	4 µL
10 mM dNTP mix	0.4 µL	0.4 µL	0.4 µL	0.4 µL
Template DNA	0.4 µL	0.4 µL	0.4 µL	0.4 µL
10 U/mL Phusion polymerase	0.2 µL	0.2 µL	0.2 µL	0.2 µL
DMSO	-	1.0 µL	-	1.0 µL
50 mM Magnesium chloride	-	-	0.4 µL	0.4 µL
deionised water	14.84 µL	13.84 µL	14.44 µL	13.44 µL

7.3.2.1 Two step PCR programme for gene amplification

Initial denaturation at 98ºC for 30 seconds

Denaturation at 98ºC for 10 seconds

Annealing at 72ºC ± 8ºC for 1 minute

} X 30 Cycles

Final extension at 72ºC for 10 minutes

Hold at 4ºC for 10 minutes

7.3.2.2 Three step PCR programme for gene amplification

Initial denaturation at 98ºC for 1.5 minutes

Denaturation at 98ºC for 10 seconds
Annealing at 66ºC ± 10ºC for 30 seconds
Extension at 72ºC for 2 minutes
} X 30 Cycles

Final extension at 72ºC for 10 minutes

Hold at 4ºC for 10 minutes

7.3.3 Gel Electrophoresis

7.3.3.1 Agarose gel elctrophoresis

To separate the different fragments of DNA, 0.8-1% agarose gel was prepared by dissolving agarose (Bioline) in 1X TAE buffer (50X stock: 242 g Tris-base, 57.1 mL acetate, 100 mL 0.5 M EDTA). The DNA samples to be analysed were loaded into the wells using 1X DNA loading dye (6X stock: 30% glycerol, 0.25% bromophenol blue in water) and electrophoresed at 100-120V. DNA was visualised by staining the gels with ethidium bromide and analysed under UV light using BioRad Gel Doc XR System.

7.3.3.2 Sodium dodecyl sulphate polyacrylamide gel electrophoresis (SDS-PAGE)

The levels of UppS were assessed in membrane and cytosolic fractions of *C. glutamicum* and *C. glutamicum* harbouring pVWEx2_*uppS* construct by 12% SDS PAGE. The LAM samples were also analysed by 15% SDS PAGE. The gels were prepared using the following components:

For resolving gel:

3.7 5 mL 4X Resolving gel buffer (1.5 M Tris-HCI, 0.4% SDS pH 8.8), 11.25 mL acrylamide/bis/water mix (30% 37.5:1 acylamide/bis-acrylamide:water, proportions were adjusted according to the percentage of acrylamide in the gel, 6 mL acrylamide-bis mix for 12%, 7.5 mL acrylamide-bis mix for 15%), 30 µL TEMED (N,N,N´,N´-tetramethylethylenediamine), 75 µL 10% ammonium persulphate were mixed in a 50 mL Falcon tube and poured immediately in the gel cast. The gels were allowed to set for 15-20 minutes at room temperature.

For stacking gel:

1.25 mL 4X stacking gel buffer (0.5 M Tris-HCI, 0.4% SDS pH 6.8), 0.65 mL acrylamide/bis mix, 3.05 mL water, 15 µL TEMED, 75 µL 10% ammonium persulphate solution were mixed in a 15 mL Falcon tube and poured over the resolving gel. The gels were allowed to set for 15-20 minutes at room temperature.

The protein samples to be analysed were mixed with 5X SDS loading buffer (360 mM Tris-HCI, pH 8.8, 9% (w/v) SDS, 0.9% (w/v) bromophenol blue, 15% (w/v) β-mercaptoethanol and 30% glycerol) and boiled for 5 minutes. The gels were run at 300V, 25 mA/gel until completion in running buffer (25 mM Tris, 190 mM Glycine, 4 mM SDS). The gels were stained with Instant Blue stain (Expedeon) for proteins and with ProQ emerald glycoprotein stain (Invitrogen) for lipoglycans according to manufacturer's instructions.

7.3.4 Restriction digestion

The plasmid DNA and PCR products were single or double digested based on required experimental conditions. For this purpose, 1-1.5 ug of DNA was mixed with 2 µL of

10X digestion buffer (as recommended by manufacturer), 2 µL of 10X BSA (if required by the enzyme), 50 units of enzyme and volume was adjusted to 20 µL with deionised water. The reaction mixture was incubated at 37°C for 2 hours. Following digestion, the enzymes were heat inactivated by incubating the reaction mixtures at 65°C for 20 minutes. The products were analysed on Agarose gels if required.

7.3.5 Ligation

The digested PCR products were ligated into the linearised vectors using T4 DNA ligase. For this purpose, the vector and the amplicon were mixed in a molar ratio of 1:3 with 2 µL of 10X Ligation buffer (50 mM Tris-HCl, 10 mM $MgCl_2$, 1 mM ATP, 10 mM DTT), 2000 units of T4 DNA ligase and volume was adjusted to 20 µL with deionised water. The mixture was incubated at 16°C for 30-60 minutes.

7.3.6 Preparation of competent *E. coli* cells

The plasmid construct pVWEx2_*uppS* was propagated in TOP10 *E. coli* cells. The plasmid constructs for two-hybrid system were propagated in *E. coli* XL-1 blue cells. For analysis of fusion proteins, the plasmids were tested in Cya^- BTH101 cells. A single colony of relevant strains was used to inoculate 5 mL of LB broth and incubated at 37°C, 200 rpm for overnight. The cultures were supplemented with a suitable antibiotic marker if required. The overnight cultures were then used to inoculate 250 mL LB in 1 L erlenmeyer flask and incubated at 37°C, 200 rpm until 0.4-0.6 OD_{600}. The cells were harvested by centrifugation (3129 x *g*, 10 minutes, 4°C) and resuspended in $1/4^{th}$ volume of ice-cold TFB1 buffer (30 mM potassium acetate, 100 mM $RbCl_2$, 10 mM $CaCl_2$, 50 mM $MnCl_2$, 15% glycerol, filter sterilised, stored at 4°C). The suspension was incubated on ice for 10 minutes and harvested by

centrifugation (3129 x *g*, 10 minutes, 4°C). The supernatant was discarded and the pellet was resuspended in 1/25th volume of ice-cold TFB2 (10 mM MOPS pH 6.5, 10 mM $RbCl_2$, 75 mM $CaCl_2$, 15% glycerol, filter sterilised, stored at 4°C). The suspension was incubated on ice for 1 hour. Aliquots of 200 µL were prepared, flash frozen and stored at -80°C for several days.

7.3.7 Transformation of chemically competent *E. coli* cells

Prepared competent cells of required *E. coli* strain were thawed on ice and mixed with 2 µL of the ligation mix. The mixture was further incubated on ice for 15 minutes. For heat shock, the cold mixture was incubated at 42°C for 45-60 seconds and immediately transferred to ice and incubated on ice for further 10 minutes. The transformation mixture was added to 1 mL LB broth and transferred to 37°C, 200 rpm for 45 minutes. This allows plasmid to settle and propagate in the freshly transformed cells. The required transfomants were obtained by plating 75 µL of the culture on suitable selection plates.

7.3.8 Preparation of electrocompetent *C. glutamicum* cells

Fresh *C. glutamicum* colonies were streaked out on BHI agar plates and incubated at 30°C overnight. A pre-culture was set up by inoculating a single colony from BHI plates in 50 mL BHIS in 500 mL Erlenmeyer flask and incubated overnight at 30°C, 200 rpm. On day 2, 2 mL of pre-culture was used to inoculate 100 mL BHIS medium in 500 mL Erlenmeyer flask and transferred to 30°C, 200 rpm until OD_{600} was 1.75 (approximately 2-4 hours). The cells were harvested by centrifugation at 3129 x *g*, 20 minutes, 4°C. The supernatant was discarded and pellet was resuspended in 2 mL ice cold TG buffer (1 mM Tris-HCl, pH 7.5, 12 g 87% glycerol per 100 mL prepared in

deionised water; filter sterilised and stored at 4°C. The cell suspension was transferred into a 50 mL Falcon tube and centrifuged as before. This step was repeated and cells were maintained on ice throughout. After a wash with TG buffer, the pellet was resuspended in 2 mL of 10% glycerol (60 mL 87% glycerol in 500 mL deionised water, filter sterilised, stored at 4°C) and centrifuged as before. The pellet thus obtained was resuspended in 1 mL of 10% glycerol and dispensed into 150 µL aliquots, flash frozen and stored at -80°C until further use.

7.3.9 Electroporation of plasmids into *C. glutamicum* cells

The pVWEx2_UppS plasmid construct was electroporated into *C. glutamicum* to generate *C. glutamicum* pVWEx2_UppS strain. For this purpose, an aliquot of prepared electrocompetent cells was thawed on ice and mixed with 2 µL of plasmid DNA (max. conc. 10 µg). The mixture was transferred into a 2 mm electroporation cuvette and carefully layered with 0.8 mL ice cold 10% glycerol. The cuvette was placed in the electroporator and electroporated at 25 µF, 200 Ω, 2,500 V and immediately transferred into 4 mL pre-warmed BHIS broth and incubated at 46°C for 6 minutes. The cells were now allowed to regenerate at 30°C, 200 rpm for 1 hour. The culture was harvested, resuspended in 75 µL BHIS and plated on BHIS plates with 5 µg/mL tetracycline. The plates were incubated at 30°C for 2 days.

7.4 Biochemical techniques

7.4.1 Thin layer chromatography

The samples for TLC analysis are applied onto the silica plates and developed in different solvent systems. The 2D-TLCs for polar and apolar lipid analysis are run in

specific solvent systems as described below. System A, B, C and D are used for separation of non-polar lipids. System D and E are utilised in separation of polar lipids. The TLCs are thoroughly dried after each run.

Table 7.3: Solvent systems for 1D and 2D TLC analysis of lipid extracts

System	Direction	Solvent	Proportions	No. of runs
A	1	petroleum ether 60-80°C/ethyl acetate	98:2 (v/v)	3
A	2	petroleum ether 60-80°C/acetone	92:8 (v/v)	1
B	1	petroleum ether 60-80°C/acetone	92:8 (v/v)	3
B	2	toluene/acetone	95:5 (v/v)	1
C	1	chloroform/methanol	96:4 (v/v)	1
C	2	toluene/acetone	80:20 (v/v)	1
D	1	chloroform/methanol/water	14:00.8 (v/v/v)	1
D	2	chloroform/acetone/methanol/water	50:60:2.5:3 (v/v/v/v)	1
E	1	chloroform/methanol/water	60:30:06 (v/v/v)	1
E	2	chloroform/acetone/methanol/water	40:25:3:6 (v/v/v/v)	1

7.4.2 Non polar and polar lipid extraction

Non-polar and polar lipid extracts were prepared from *C. glutamicum* cells and analysed by 2D TLC. For this purpose, cells from required cultures were harvested by centrifugation (3129 x *g*, 10 minutes) and resuspended in 2 mL of methanol/0.3% NaCl (100:10, v/v) and 2 mL of petroleum ether (60-80°C) and mixed on a rotator for 30 minutes. Addition of petroleum ether results in partitioning of the extracts into an upper organic and a lower aqueous phase. The mixture was centrifuged (3129 x *g*, 3 minutes) and the upper layer of petroleum ether was transferred into a separate tube. The lower layer with the cell debris was again treated with 2 mL of petroleum ether (60-80°C) and mixed on a rotator for 30 minutes. The mixture was centrifuged as

before and the upper layer was combined with the previously collected supernatant. The petroleum ether extracts thus obtained contained non-polar lipids, which were dried under nitrogen and analysed on TLC using appropriate systems.

The lower aqueous layer was then treated with 2.3 mL of chloroform/methanol/0.3 % NaCl (90:100:30, v/v/v) and the suspension was mixed on a rotator for 1 hour. The mixture was centrifuged as before and the supernatant was transferred into a fresh tube. The pellet was further treated with 0.75 mL of chloroform/methanol/0·3% NaCl (50:100:40, v/v/v) and mixed on a rotator for 30 minutes. The suspension was then centrifuged as before and the supernatant was pooled with the previously collected fraction. This step was repeated. The pellets were retained for further analysis and the combined supernatant fractions were processed with 1.3 mL of chloroform and 1.3 mL of 0.3 % NaCl. The suspension was mixed on a rotator for 10 minutes and centrifuged as before. The lower phase containing the polar lipids was recovered and dried under nitrogen. The extracts were analysed using appropriate TLC systems.

Thin layer chromatography (TLC) analysis for lipids for cold samples, 50-100 µg of extracts were loaded onto the TLC for analysis. In case of radiolabelled extacts, 10,000-50,000 cpm of each sample was used for lipid analysis using chromatography. The cold samples were stained with phosphomolybdic acid (MPA, 5% in ethanol) for lipids or Molisch reagent (6 g α-napthol in 25 mL H_2SO_4 and 450 mL ethanol) for carbohydrates and charred using a heat gun to reveal lipids on the TLC plates. To analyse phospholipids, Dittmer and Lester reagent was prepared by mixing solution A (40 g molybdenum VI oxide dissolved in 1 L of boiling sulfuric acid), solution B (1.7 g solid molybdenum dissolved in 0.5 L of solution A) and water in the ratio 1:1:4 and

used to stain the TLC plates. The stained plates were left at room temperature and the presence of blue spots on TLC corresponding to phospholipids was noted. Autoradiography was performed for radiolabelled lipid extracts.

7.4.3 Preparation of mAGP from *C. glutamicum*

The required cultures of *C. glutamicum* were cultivated as per the experimental conditions and cells were harvested by centrifugation at 3129 x *g*, 10 minutes. The pellet was extracted thrice with 50% ethanol at 85°C for 6 hours (in oil bath) to remove lipoarabinomannan. Following the hot ethanol extraction, cell pellets were resuspended in phosphate buffered saline with 20% Triton X-100 (pH 7.2) and treated with Proteinase K at 55°C for 3-4 hours. The debris were centrifuged at 3129 x *g* for 10 minutes and the pellet was resuspended in 2% SDS solution (prepared in PBS). The samples were incubated at 95°C for 1 hour to remove any residual proteins. This extraction step was repeated twice. De-proteinated pellet was washed with water to remove any residues. The pellet was further washed with 90% acetone (v/v, prepared in water) and dehydrated completely by washing with 100% acetone. The pellet was dried under a stream of nitrogen to yield a highly purified mAGP preparation

7.4.4 Acid hydrolysis of mAGP for carbohydrate analysis

The mAGP preparations were hydrolysed using 400 µl of 2 M trifluoroacetic acid (TFA) at 120°C for 3 hours. The acid was completely removed by drying the preparation under a stream of nitrogen. The carbohydrate residues were resuspended in 2 mL water. The suspension was partitioned into an aqueous and an organic phase by addition of 2 mL chloroform and mixed on the rotator for 10 minutes. The mixture was centrifuged at 3129 x *g*, 5 minutes; the upper aqueous phase was recovered and dried

under a stream of nitrogen. The samples were loaded on HP-Cellulose TLC (Merck) and developed thrice in pyridine/ethyl acetate/glacial acetic acid/water (5:5:1:3 v/v/v/v). The radiolabelled extracts were visualised by autoradiography and the cold samples were analysed using α-naphthol staining as described in section 4.2.

7.4.5 Preparation of cell wall lipoglycans from *C. glutamicum*

The cell cultures were grown as per the experimental conditions and analysed for their lipoglycans using hot ethanol extraction method. For this purpose, the cells were harvested from cultures by centrifugation (3129 x *g*, 10 minutes) and pellet was washed with 2 mL phosphate buffered saline. The washed pellet was resuspended in 2 mL 50% ethanol (prepared in water) and the mixture was refluxed at 85°C in hot-oil bath for 5-6 hours. Following the hot-ethanol treatment, the mixture was centrifuged as before and the supernatant was collected in a fresh tube. The remaining pellet was further extracted 3-4 times using the same procedure. The pooled supernatant was dried under a stream of nitrogen and the resulting pellet containg proteins, lipoglycans, neutral glycans was resuspended in 1.5 mL water by brief sonication. The suspension was treated with 95% phenol (w/v prepared in PBS) at 65°C for 1 hour. The mixture was cooled to room temperature and tubes were centrifuged at 3129 x *g* for 1 hour to obtain a clear bi-phase. The upper aqueous layer was recovered and transferred to a 1.5 inch low molecular weight cut off dialysis tubing, (Spectra/Por membrane 6, MWCO 3,500 kDA, Spectrum Labs) and dialysed overnight against water. The dialysed sample was recovered and dried under a stream of nitrogen. The extracts were resuspended in required volume of water and analysed using SDS-PAGE and visualised with ProQ emerald glycoprotein stain as described in section 7.3.3.2.

7.4.6 Preparation of enzymatically active membranes and cell envelope

The required strains of *C. glutamicum* and *M. smegmatis* were grown to 1 L and the cells were harvested by centrifugation (4˚C, 7000 x *g*, 10 minutes). The pellet was washed twice with phosphate buffered saline (4˚C, 7000 x *g*, 10 minutes) and resuspended in 35 mL BufferA (50 mM MOPS pH 7.9, 5 mM β-mercaptoethanol, 5 mM $MgCl_2$) and sonicated (60s on, 90s off, 10 cycles) on ice. The cell debris was pelleted (30,000 x *g*, 20 minutes, 4˚C) and the supernatant was used for membrane preparations. The pellet was resuspended in 24 mL BufferA and equally divided into two 40 mL centrifuge tubes. To each tube, 18 mL of cold Percoll solution was added and centrifuged (30,000 x *g*, 60 minutes, 4˚C). The particulate upper diffused band, containing both cell wall and cell membranes was collected and washed thrice in Buffer A. The pellet was resuspended in 1mL Buffer A and protein concentration was determined using BCA method (Pierce BCA Protein Assay Kit, Thermo Scientific) as per manufacturer's instructions. The supernatant collected previously was subjected to ultracentrifugation (100,000 x *g*, 90 minutes, 4˚C) and the pellet (containing the enzymatically active membranes) was resuspended in 400 µL BufferA. The protein concentration was determined using the BCA method (BCA Protein Assay Kit, Thermo Scientific) as per manufacturer's instructions.

7.4.7 Synthesis of pRPP

To characterise the effect of BTZ043 on *C. glutamicum*, the substrates pRPP and DPR were exogenously prepared and supplemented in the final assay. The recombinant Mt-PrsA was expressed in *Escherichia coli* C41 cells and the subsequently purified by IMAC at a concentration of 2 mg/mL. To synthesise pRPP *in vitro*, [^{14}C]-U-D-glucose (0.1 mCi, 500µL) was dried down and resuspended in 500 µL Buffer A (50 mM

KH_2PO_4, 5 mM $MgCl_2$) and the first three enzymic reactions of the pentose phosphate pathway were performed using commercially available enzymes (Roche and Sigma). To the radiolabelled glucose, 20 µL ATP (100 mM) and 50µL Hexokinse/Glucose-6-Phosphate Dehydrogenase mix (3 mg/mL) were added and the reaction was incubated at 37˚C for 20 minutes. To the mix, 10 µL ATP and 20 µL NADP (100 mM) were added and mixture was incubated at 37˚C for 10 minutes followed by addition of 50 µL 6-phosphogluconic dehydrogenase and incubation at 37˚C for 20 minutes. In the third step, 50 µL phosphoriboisomerase was added to the mix along with 20 µL NADP and incubated at 37˚C for 15 minutes. This resulted in purified [^{14}C]-U-α-D-Ribose-5-Phosphate as a substrate for p[^{14}C]Rpp synthetase, Mt-PrsA. In the last step, 0.2 mL purified Mt-PrsA was added twice in a step wise manner along with 20 µL ATP and each reaction was incubated at 37˚C for 30 minutes. The mixture was then transferred to protein concentrator to remove the enzymes. The flow-through was loaded on LC-SAX ion exchange columns and washed twice with water. The pure p[^{14}C]Rpp was eluted using a step gradient of sodium acetate (100 mM-2 M) and radioactivity was determined using the scintialltion counter for all the fractions. The fractions with highest counts were used for the assays.

8 Bibliography

A. R. Zink, E. M. R., N. Motamedi, G. Palfy, A. Marcsik and A. G. Nerlich (2007). Molecular History of Tuberculosis from Ancient Mummies and Skeletons. *International Journal of Osteoarchaeology*, 17, 380-391.

Aids Control and Prevention (Aidscap) Project of Family Health Internal, T. F.-X. B. C. F. P. H. a. H. R. O. T. H. S. O. P. H., Unaids (1996). The Status and Trends Of the Global HIV/AIDS Pandemic Official Satellite Symposium.

Alangaden, G. J., Kreiswirth, B. N., Aouad, A., Khetarpal, M., Igno, F. R., Moghazeh, S. L., Manavathu, E. K. and Lerner, S. A. (1998). Mechanism of resistance to amikacin and kanamycin in *Mycobacterium tuberculosis*. *Antimicrob Agents Chemother*, 42, 1295-1297.

Alangaden, G. J., Manavathu, E. K., Vakulenko, S. B., Zvonok, N. M. and Lerner, S. A. (1995). Characterization of fluoroquinolone-resistant mutant strains of *Mycobacterium tuberculosis* selected in the laboratory and isolated from patients. *Antimicrob Agents Chemother*, 39, 1700-1703.

Alcaide, F., Pfyffer, G. E. and Telenti, A. (1997). Role of embB in natural and acquired resistance to ethambutol in mycobacteria. *Antimicrob Agents Chemother*, 41, 2270-2273.

Alderwick, L. J., Dover, L. G., Seidel, M., Gande, R., Sahm, H., Eggeling, L. and Besra, G. S. (2006a). Arabinan-deficient mutants of *Corynebacterium glutamicum* and the consequent flux in decaprenylmonophosphoryl-D-arabinose metabolism. *Glycobiology*, 16, 1073-1081.

Alderwick, L. J., Dover, L. G., Veerapen, N., Gurcha, S. S., Kremer, L., Roper, D. L., Pathak, A. K., Reynolds, R. C. and Besra, G. S. (2008). Expression, purification and characterisation of soluble GlfT and the identification of a novel galactofuranosyltransferase Rv3782 involved in priming GlfT-mediated galactan polymerisation in *Mycobacterium tuberculosis*. *Protein Expr Purif*, 58, 332-341.

Alderwick, L. J., Lloyd, G. S., Ghadbane, H., May, J. W., Bhatt, A., Eggeling, L., Futterer, K. and Besra, G. S. (2011a). The C-terminal domain of the Arabinosyltransferase *Mycobacterium tuberculosis* EmbC is a lectin-like carbohydrate binding module. *PLoS Pathog*, 7, e1001299.

Alderwick, L. J., Lloyd, G. S., Lloyd, A. J., Lovering, A. L., Eggeling, L. and Besra, G. S. (2011b). Biochemical characterization of the *Mycobacterium tuberculosis* phosphoribosyl-1-pyrophosphate synthetase. *Glycobiology*, 21, 410-425.

Alderwick, L. J., Radmacher, E., Seidel, M., Gande, R., Hitchen, P. G., Morris, H. R., Dell, A., Sahm, H., Eggeling, L. and Besra, G. S. (2005). Deletion of Cg-*emb* in *corynebacterianeae* leads to a novel truncated cell wall arabinogalactan, whereas inactivation of Cg-*ubiA* results in an arabinan-deficient mutant with a cell wall galactan core. *J Biol Chem*, 280, 32362-32371.

Alderwick, L. J., Seidel, M., Sahm, H., Besra, G. S. and Eggeling, L. (2006b). Identification of a novel arabinofuranosyltransferase (AftA) involved in cell wall arabinan biosynthesis in *Mycobacterium tuberculosis*. *J Biol Chem*, 281, 15653-15661.

Alm, E. J., Huang, K. H., Price, M. N., Koche, R. P., Keller, K., Dubchak, I. L. and Arkin, A. P. (2005). The MicrobesOnline web site for comparative genomics. *Genome Research*, 15, 1015-1022.

Anderberg, S. J., Newton, G. L. and Fahey, R. C. (1998). Mycothiol biosynthesis and metabolism - Cellular levels of potential intermediates in the biosynthesis and degradation of mycothiol in *Mycobacterium smegmatis*. *Journal of Biological Chemistry*, 273, 30391-30397.

Anderson, R. (1983). The immunopharmacology of antileprosy agents. *Lepr Rev*, 54, 139-144.

Andersson, S. G., Zomorodipour, A., Andersson, J. O., Sicheritz-Ponten, T., Alsmark, U. C., Podowski, R. M., Naslund, A. K., Eriksson, A. S., Winkler, H. H. and Kurland, C. G. (1998). The genome sequence of Rickettsia prowazekii and the origin of mitochondria. *Nature*, 396, 133-140.

Andries, K., Verhasselt, P., Guillemont, J., Gohlmann, H. W., Neefs, J. M., Winkler, H., Van Gestel, J., Timmerman, P., Zhu, M., Lee, E., Williams, P., De Chaffoy, D., Huitric, E., Hoffner, S., Cambau, E., Truffot-Pernot, C., Lounis, N. and Jarlier, V. (2005). A diarylquinoline drug active on the ATP synthase of *Mycobacterium tuberculosis*. *Science*, 307, 223-227.

Arora, P., Venkataswamy, M. M., Baena, A., Bricard, G., Li, Q., Veerapen, N., Ndonye, R., Park, J. J., Lee, J. H., Seo, K. C., Howell, A. R., Chang, Y. T., Illarionov, P. A., Besra, G. S., Chung, S. K. and Porcelli, S. A. (2011). A rapid fluorescence-based assay for classification of iNKT cell activating glycolipids. *J Am Chem Soc*, 133, 5198-5201.

Asselineau, J. and Lederer, E. (1950). Structure of the mycolic acids of Mycobacteria. *Nature*, 166, 782-783.

Bachhawat, N. and Mande, S. C. (1999a). Identification of the *INO1* gene of *Mycobacterium tuberculosis* H37Rv reveals a novel class of inositol-1-phosphate synthase enzyme. *J Mol Biol*, 291, 531-536.

Bachhawat, N. and Mande, S. C. (1999b). Identification of the *INO1* gene of *Mycobacterium tuberculosis* H37Rv reveals a novel class of inositol-1-phosphate synthase enzyme. *Journal of Molecular Biology*, 291, 531-536.

Ballou, C. E. and Lee, Y. C. (1964). The structure of a *myo*inositol mannoside from *Mycobacterium tuberculosis* Glycolipid. *Biochemistry*, 3, 682-685.

Ballou, C. E., Vilkas, E. and Lederer, E. (1963). Structural studies on the *myo*-inositol phospholipids of *Mycobacterium tuberculosis* (var. bovis, strain BCG). *J Biol Chem*, 238, 69-76.

Banerjee, A., Dubnau, E., Quemard, A., Balasubramanian, V., Um, K. S., Wilson, T., Collins, D., De Lisle, G. and Jacobs, W. R., Jr. (1994). inhA, a gene encoding a target for isoniazid and ethionamide in *Mycobacterium tuberculosis*. *Science*, 263, 227-230.

Barry, V. C., Belton, J. G., Conalty, M. L., Denneny, J. M., Edward, D. W., O'sullivan, J. F., Twomey, D. and Winder, F. (1957). A new series of phenazines (rimino-compounds) with high antituberculosis activity. *Nature*, 179, 1013-1015.

Batt, S. M., Jabeen, T., Bhowruth, V., Quill, L., Lund, P. A., Eggeling, L., Alderwick, L. J., Futterer, K. and Besra, G. S. (2012). Structural basis of inhibition of *Mycobacterium tuberculosis* DprE1 by benzothiazinone inhibitors. *Proc Natl Acad Sci U S A*, 109, 11354-11359.

Battesti, A. and Bouveret, E. (2012). The bacterial two-hybrid system based on adenylate cyclase reconstitution in *Escherichia coli*. *Methods*, 58, 325-334.

Baulard, A. R., Betts, J. C., Engohang-Ndong, J., Quan, S., Mcadam, R. A., Brennan, P. J., Locht, C. and Besra, G. S. (2000). Activation of the pro-drug ethionamide is regulated in mycobacteria. *J Biol Chem*, 275, 28326-28331.

Baumgart, M., Luder, K., Grover, S., Gatgens, C., Besra, G. S. and Frunzke, J. (2013a). IpsA, a novel LacI-type regulator, is required for inositol-derived lipid formation in Corynebacteria and Mycobacteria. *BMC Biol*, 11, 122.

Baumgart, M., Unthan, S., Rückert, C., Sivalingam, J., Grünberger, A., Kalinowski, J., Bott, M., Noack, S. and Frunzke, J. (2013b). Construction of a prophage-free variant of *Corynebacterium glutamicum* ATCC 13032 - a platform strain for basic research and industrial biotechnology. *Applied and Environmental Microbiology*, 79, 6606-6015.

Belanger, A. E., Besra, G. S., Ford, M. E., Mikusova, K., Belisle, J. T., Brennan, P. J. and Inamine, J. M. (1996). The *embAB* genes of *Mycobacterium avium* encode an arabinosyl transferase involved in cell wall arabinan biosynthesis that is the target for the antimycobacterial drug ethambutol. *Proc Natl Acad Sci U S A*, 93, 11919-11924.

Belanger, A. E., Porter, J. C. and Hatfull, G. F. (2000). Genetic analysis of peptidoglycan biosynthesis in mycobacteria: characterization of a *ddlA* mutant of *Mycobacterium smegmatis*. *J Bacteriol*, 182, 6854-6856.

Belisle, J. T., Vissa, V. D., Sievert, T., Takayama, K., Brennan, P. J. and Besra, G. S. (1997). Role of the major antigen of *Mycobacterium tuberculosis* in cell wall biogenesis. *Science*, 276, 1420-1422.

Berg, S., Kaur, D., Jackson, M. and Brennan, P. J. (2007). The glycosyltransferases of *Mycobacterium tuberculosis* - roles in the synthesis of arabinogalactan, lipoarabinomannan, and other glycoconjugates. *Glycobiology*, 17, 35-56R.

Besra, G. S. and Brennan, P. J. (1997). The mycobacterial cell wall: biosynthesis of arabinogalactan and lipoarabinomannan. *Biochem Soc Trans*, 25, 845-850.

Besra, G. S., Khoo, K. H., Mcneil, M. R., Dell, A., Morris, H. R. and Brennan, P. J. (1995). A new interpretation of the structure of the mycolyl-arabinogalactan complex of *Mycobacterium tuberculosis* as revealed through characterization of oligoglycosylalditol fragments by fast-atom bombardment mass spectrometry and ^{1}H nuclear magnetic resonance spectroscopy. *Biochemistry*, 34, 4257-4266.

Besra, G. S., Morehouse, C. B., Rittner, C. M., Waechter, C. J. and Brennan, P. J. (1997). Biosynthesis of mycobacterial lipoarabinomannan. *J Biol Chem*, 272, 18460-18466.

Bhamidi, S., Scherman, M. S., Rithner, C. D., Prenni, J. E., Chatterjee, D., Khoo, K. H. and Mcneil, M. R. (2008). The identification and location of succinyl residues and the characterization

of the interior arabinan region allow for a model of the complete primary structure of *Mycobacterium tuberculosis* mycolyl arabinogalactan. *J Biol Chem*, 283, 12992-13000.

Biffinger, J. C., Kim, H. W. and Dimagno, S. G. (2004). The polar hydrophobicity of fluorinated compounds. *Chembiochem*, 5, 622-627.

Birch, H. L., Alderwick, L. J., Appelmelk, B. J., Maaskant, J., Bhatt, A., Singh, A., Nigou, J., Eggeling, L., Geurtsen, J. and Besra, G. S. (2010). A truncated lipoglycan from mycobacteria with altered immunological properties. *Proc Natl Acad Sci U S A*, 107, 2634-2639.

Birch, H. L., Alderwick, L. J., Bhatt, A., Rittmann, D., Krumbach, K., Singh, A., Bai, Y., Lowary, T. L., Eggeling, L. and Besra, G. S. (2008). Biosynthesis of mycobacterial arabinogalactan: identification of a novel α(1→3) arabinofuranosyltransferase. *Mol Microbiol*, 69, 1191-1206.

Bloom, B. R. and Murray, C. J. (1992). Tuberculosis: commentary on a re-emergent killer. *Science*, 257, 1055-1064.

Brennan, P. and Ballou, C. E. (1968). Biosynthesis of mannophosphoinositides by *Mycobacterium phlei*. Enzymatic acylation of the dimannophosphoinositides. *J Biol Chem*, 243, 2975-2984.

Brennan, P. J. and Nikaido, H. (1995). The envelope of mycobacteria. *Annu Rev Biochem*, 64, 29-63.

Brosch, R., Gordon, S. V., Marmiesse, M., Brodin, P., Buchrieser, C., Eiglmeier, K., Garnier, T., Gutierrez, C., Hewinson, G., Kremer, K., Parsons, L. M., Pym, A. S., Samper, S., Van Soolingen, D. and Cole, S. T. (2002). A new evolutionary scenario for the *Mycobacterium tuberculosis* complex. *Proc Natl Acad Sci U S A*, 99, 3684-3689.

Broussy, S., Coppel, Y., Nguyen, M., Bernadou, J. and Meunier, B. (2003). ^{1}H and ^{13}C NMR characterization of hemiamidal isoniazid-NAD(H) adducts as possible inhibitors of InhA reductase of *Mycobacterium tuberculosis*. *Chemistry*, 9, 2034-2038.

Buschiazzo, A., Ugalde, J. E., Guerin, M. E., Shepard, W., Ugalde, R. A. and Alzari, P. M. (2004). Crystal structure of glycogen synthase: homologous enzymes catalyze glycogen synthesis and degradation. *EMBO J*, 23, 3196-3205.

Bussey, L. B. and Switzer, R. L. (1993). The *degA* gene product accelerates degradation of *Bacillus subtilis* phosphoribosylpyrophosphate amidotransferase in *Escherichia coli*. *J Bacteriol*, 175, 6348-6353.

Bussmann, M., Baumgart, M. and Bott, M. (2010). RosR (cg1324), a hydrogen peroxide-sensitive MarR-type transcriptional regulator of *Corynebacterium glutamicum*. *Journal of Biological Chemistry*, 285, 29305-29318.

Caminero, J. A., Sotgiu, G., Zumla, A. and Migliori, G. B. (2010). Best drug treatment for multidrug-resistant and extensively drug-resistant tuberculosis. *Lancet Infect Dis*, 10, 621-629.

Campbell, J., Singh, A. K., Swoboda, J. G., Gilmore, M. S., Wilkinson, B. J. and Walker, S. (2012). An antibiotic that inhibits a late step in wall teichoic acid biosynthesis induces the cell wall stress stimulon in *Staphylococcus aureus*. *Antimicrob Agents Chemother*, 56, 1810-1820.

Cerdeno-Tarraga, A. M., Efstratiou, A., Dover, L. G., Holden, M. T., Pallen, M., Bentley, S. D., Besra, G. S., Churcher, C., James, K. D., De Zoysa, A., Chillingworth, T., Cronin, A., Dowd, L., Feltwell, T., Hamlin, N., Holroyd, S., Jagels, K., Moule, S., Quail, M. A., Rabbinowitsch, E., Rutherford, K. M., Thomson, N. R., Unwin, L., Whitehead, S., Barrell, B. G. and Parkhill, J. (2003). The complete genome sequence and analysis of *Corynebacterium diphtheriae* NCTC13129. *Nucleic Acids Res*, 31, 6516-6523.

Chakraborty, S., Gruber, T., Barry, C. E., 3rd, Boshoff, H. I. and Rhee, K. Y. (2013). *Para*-aminosalicylic acid acts as an alternative substrate of folate metabolism in *Mycobacterium tuberculosis*. *Science*, 339, 88-91.

Chatterjee, D., Bozic, C. M., Mcneil, M. and Brennan, P. J. (1991). Structural features of the arabinan component of the lipoarabinomannan of *Mycobacterium tuberculosis*. *J Biol Chem*, 266, 9652-9660.

Chatterjee, D., Hunter, S. W., Mcneil, M. and Brennan, P. J. (1992). Lipoarabinomannan. Multiglycosylated form of the mycobacterial mannosylphosphatidylinositols. *J Biol Chem*, 267, 6228-6233.

Chatterjee, D., Khoo, K. H., Mcneil, M. R., Dell, A., Morris, H. R. and Brennan, P. J. (1993). Structural definition of the non-reducing termini of mannose-capped LAM from *Mycobacterium tuberculosis* through selective enzymatic degradation and fast atom bombardment-mass spectrometry. *Glycobiology*, 3, 497-506.

Choi, K. H., Kremer, L., Besra, G. S. and Rock, C. O. (2000). Identification and substrate specificity of β-ketoacyl (acyl carrier protein) synthase III (mtFabH) from *Mycobacterium tuberculosis*. *J Biol Chem*, 275, 28201-28207.

Cholo, M. C., Steel, H. C., Fourie, P. B., Germishuizen, W. A. and Anderson, R. (2012). Clofazimine: current status and future prospects. *J Antimicrob Chemother*, 67, 290-298.

Christophe, T., Jackson, M., Jeon, H. K., Fenistein, D., Contreras-Dominguez, M., Kim, J., Genovesio, A., Carralot, J. P., Ewann, F., Kim, E. H., Lee, S. Y., Kang, S., Seo, M. J., Park, E. J., Skovierova, H., Pham, H., Riccardi, G., Nam, J. Y., Marsollier, L., Kempf, M., Joly-Guillou, M. L., Oh, T., Shin, W. K., No, Z., Nehrbass, U., Brosch, R., Cole, S. T. and Brodin, P. (2009). High content screening identifies decaprenyl-phosphoribose 2' epimerase as a target for intracellular antimycobacterial inhibitors. *PLoS Pathog*, 5, e1000645.

Claessen, D., Emmins, R., Hamoen, L. W., Daniel, R. A., Errington, J. and Edwards, D. H. (2008). Control of the cell elongation-division cycle by shuttling of PBP1 protein in *Bacillus subtilis*. *Mol Microbiol*, 68, 1029-1046.

Cole, S. T., Brosch, R., Parkhill, J., Garnier, T., Churcher, C., Harris, D., Gordon, S. V., Eiglmeier, K., Gas, S., Barry, C. E., 3rd, Tekaia, F., Badcock, K., Basham, D., Brown, D., Chillingworth, T., Connor, R., Davies, R., Devlin, K., Feltwell, T., Gentles, S., Hamlin, N., Holroyd, S., Hornsby, T., Jagels, K., Krogh, A., Mclean, J., Moule, S., Murphy, L., Oliver, K., Osborne, J., Quail, M. A., Rajandream, M. A., Rogers, J., Rutter, S., Seeger, K., Skelton, J., Squares, R., Squares, S., Sulston, J. E., Taylor, K., Whitehead, S. and Barrell, B. G. (1998). Deciphering the biology of *Mycobacterium tuberculosis* from the complete genome sequence. *Nature*, 393, 537-544.

Collins, M. D., Goodfellow, M. and Minnikin, D. E. (1982a). Fatty acid composition of some mycolic acid-containing coryneform bacteria. *J Gen Microbiol*, 128, 2503-2509.

Collins, M. D., Goodfellow, M. and Minnikin, D. E. (1982b). A survey of the structures of mycolic acids in *Corynebacterium* and related taxa. *J Gen Microbiol*, 128, 129-149.

Crellin, P. K., Brammananth, R. and Coppel, R. L. (2011). Decaprenylphosphoryl-β-D-ribose 2'-epimerase, the target of benzothiazinones and dinitrobenzamides, is an essential enzyme in *Mycobacterium smegmatis*. *PLoS One*, 6, e16869.

Crellin, P. K., Kovacevic, S., Martin, K. L., Brammananth, R., Morita, Y. S., Billman-Jacobe, H., Mcconville, M. J. and Coppel, R. L. (2008). Mutations in *pimE* restore lipoarabinomannan synthesis and growth in a *Mycobacterium smegmatis lpqW* mutant. *J Bacteriol*, 190, 3690-3699.

Cremer, J., Eggeling, L. and Sahm, H. (1991). Control of the lysine biosynthesis sequence in *Corynebacterium glutamicum* as analyzed by overexpression of the individual corresponding genes. *Applied and Environmental Microbiology*, 57, 1746-1752.

Cren, S., Gurcha, S. S., Blake, A. J., Besra, G. S. and Thomas, N. R. (2004). Synthesis and biological evaluation of new inhibitors of UDP-Gal*f* transferase--a key enzyme in M. tuberculosis cell wall biosynthesis. *Org Biomol Chem*, 2, 2418-2420.

Crick, D. C., Mahapatra, S. and Brennan, P. J. (2001). Biosynthesis of the arabinogalactan-peptidoglycan complex of *Mycobacterium tuberculosis*. *Glycobiology*, 11, 107R-118R.

Crick, D. C., Schulbach, M. C., Zink, E. E., Macchia, M., Barontini, S., Besra, G. S. and Brennan, P. J. (2000). Polyprenyl phosphate biosynthesis in *Mycobacterium tuberculosis* and *Mycobacterium smegmatis*. *J Bacteriol*, 182, 5771-5778.

Crubezy, E., Ludes, B., Poveda, J. D., Clayton, J., Crouau-Roy, B. and Montagnon, D. (1998). Identification of *Mycobacterium* DNA in an Egyptian Pott's disease of 5,400 years old. *C R Acad Sci III*, 321, 941-951.

Cui, T., Zhang, L., Wang, X. and He, Z. G. (2009). Uncovering new signaling proteins and potential drug targets through the interactome analysis of *Mycobacterium tuberculosis*. *BMC Genomics*, 10, 118.

D'elia, M. A., Henderson, J. A., Beveridge, T. J., Heinrichs, D. E. and Brown, E. D. (2009). The N-acetylmannosamine transferase catalyzes the first committed step of teichoic acid assembly in *Bacillus subtilis* and *Staphylococcus aureus*. *J Bacteriol*, 191, 4030-4034.

D'elia, M. A., Millar, K. E., Beveridge, T. J. and Brown, E. D. (2006). Wall teichoic acid polymers are dispensable for cell viability in *Bacillus subtilis*. *J Bacteriol*, 188, 8313-8316.

Daffe, M., Brennan, P. J. and Mcneil, M. (1990). Predominant structural features of the cell wall arabinogalactan of *Mycobacterium tuberculosis* as revealed through characterization of oligoglycosyl alditol fragments by gas chromatography/mass spectrometry and by ^{1}H and ^{13}C NMR analyses. *J Biol Chem*, 265, 6734-6743.

Daniel, T. M. (2006). The history of tuberculosis. *Respir Med*, 100, 1862-1870.

Daniel, V. S. and Daniel, T. M. (1999). Old Testament biblical references to tuberculosis. *Clin Infect Dis*, 29, 1557-1558.

Davies, G. J., Ducros, V. M., Varrot, A. and Zechel, D. L. (2003). Mapping the conformational itinerary of β-glycosidases by X-ray crystallography. *Biochem Soc Trans*, 31, 523-527.

Davis, A. L. (2000). A historical perspective on tuberculosis and its control. In H. E. Reichman LB (Ed.) Tuberculosis: a comprehensive international approach (pp. 3-54) New York: Marcel Dekker.

De Arruda, M. V., Colli, W. and Zingales, B. (1989). Terminal β-D-galactofuranosyl epitopes recognized by antibodies that inhibit *Trypanosoma cruzi* internalization into mammalian cells. *Eur J Biochem*, 182, 413-421.

De Smet, K. A., Kempsell, K. E., Gallagher, A., Duncan, K. and Young, D. B. (1999). Alteration of a single amino acid residue reverses fosfomycin resistance of recombinant MurA from *Mycobacterium tuberculosis*. *Microbiology*, 145 (Pt 11), 3177-3184.

Debarber, A. E., Mdluli, K., Bosman, M., Bekker, L. G. and Barry, C. E., 3rd (2000). Ethionamide activation and sensitivity in multidrug-resistant *Mycobacterium tuberculosis*. *Proc Natl Acad Sci U S A*, 97, 9677-9682.

Delmas, C., Gilleron, M., Brando, T., Vercellone, A., Gheorghui, M., Riviere, M. and Puzo, G. (1997). Comparative structural study of the mannosylated-lipoarabinomannans from *Mycobacterium bovis* BCG vaccine strains: characterization and localization of succinates. *Glycobiology*, 7, 811-817.

Dinadayala, P., Kaur, D., Berg, S., Amin, A. G., Vissa, V. D., Chatterjee, D., Brennan, P. J. and Crick, D. C. (2006). Genetic basis for the synthesis of the immunomodulatory mannose caps of lipoarabinomannan in *Mycobacterium tuberculosis*. *J Biol Chem*, 281, 20027-20035.

Dobson, G., Minnikin, D., Minnikin, S., Parlett, J., Goodfellow, M., Ridell, M. And Magnusson, M (1985). Systematic analysis of complex mycobacterial lipids. In M. G. a. D. E. Minnikin (Ed.) Chemical Methods in Bacterial Systematics (pp. 237-265) London: Academic Press.

Dobson G., M. D. E., Minnikin S. M., Parlett J. H., Goodfellow M., Ridell M., and Magnusson M. (1985). Systematic analysis of complex mycobacterial lipids In M. D. E. Goodfellow M. (Ed.) Chemical Methods in Bacterial Systematics (pp. 237–265) London: Academic Press.

Dover, L. G., Cerdeno-Tarraga, A. M., Pallen, M. J., Parkhill, J. and Besra, G. S. (2004). Comparative cell wall core biosynthesis in the mycolated pathogens, *Mycobacterium tuberculosis* and *Corynebacterium diphtheriae*. *FEMS Microbiol Rev*, 28, 225-250.

Draper, P., Khoo, K. H., Chatterjee, D., Dell, A. and Morris, H. R. (1997). Galactosamine in walls of slow-growing mycobacteria. *Biochem J*, 327 (Pt 2), 519-525.

Dutta, R. K. (1980). Clofazimine and dapsone--a combination therapy in erythema nodosum leprosum syndrome. *Lepr India*, 52, 252-259.

Escuyer, V. E., Lety, M. A., Torrelles, J. B., Khoo, K. H., Tang, J. B., Rithner, C. D., Frehel, C., Mcneil, M. R., Brennan, P. J. and Chatterjee, D. (2001). The role of the *embA* and *embB*

gene products in the biosynthesis of the terminal hexaarabinofuranosyl motif of *Mycobacterium smegmatis* arabinogalactan. *J Biol Chem*, 276, 48854-48862.

Fahey, R. C. (2013). Glutathione analogs in prokaryotes. *Biochimica Et Biophysica Acta-General Subjects*, 1830, 3182-3198.

Feng, J., Che, Y. S., Milse, J., Yin, Y. J., Liu, L., Ruckert, C., Shen, X. H., Qi, S. W., Kalinowski, J. and Liu, S. J. (2006). The gene *Ncgl2918* encodes a novel maleylpyruvate isomerase that needs mycothiol as cofactor and links mycothiol biosynthesis and gentisate assimilation in *Corynebacterium glutamicum*. *Journal of Biological Chemistry*, 281, 10778-10785.

Flint, J., Nurizzo, D., Harding, S. E., Longman, E., Davies, G. J., Gilbert, H. J. and Bolam, D. N. (2004). Ligand-mediated dimerization of a carbohydrate-binding molecule reveals a novel mechanism for protein-carbohydrate recognition. *J Mol Biol*, 337, 417-426.

Fortun, J., Martin-Davila, P., Navas, E., Perez-Elias, M. J., Cobo, J., Tato, M., De La Pedrosa, E. G., Gomez-Mampaso, E. and Moreno, S. (2005). Linezolid for the treatment of multidrug-resistant tuberculosis. *J Antimicrob Chemother*, 56, 180-185.

Frunzke, J., Engels, V., Hasenbein, S., Gatgens, C. and Bott, M. (2008). Co-ordinated regulation of gluconate catabolism and glucose uptake in *Corynebacterium glutamicum* by two functionally equivalent transcriptional regulators, GntR1 and GntR2. *Molecular Microbiology*, 67, 305-322.

Gao, J., Qiao, S. and Whitesides, G. M. (1995). Increasing binding constants of ligands to carbonic anhydrase by using "greasy tails". *J Med Chem*, 38, 2292-2301.

Garcia-Nafria, J., Baumgart, M., Bott, M., Wilkinson, A. J. and Wilson, K. S. (2010). The *Corynebacterium glutamicum* aconitase repressor: scratching around for crystals. *Acta Crystallogr Sect F Struct Biol Cryst Commun*, 66, 1074-1077.

Garcia-Nafria, J., Baumgart, M., Turkenburg, J. P., Wilkinson, A. J., Bott, M. and Wilson, K. S. (2013). Crystal and solution studies reveal that the transcriptional regulator *AcnR* of *Corynebacterium glutamicum* is regulated by Citrate-Mg^{2+} binding to a non-canonical pocket. *Journal of Biological Chemistry*, 288, 15800-15812.

George, K. M., Yuan, Y., Sherman, D. R. and Barry, C. E., 3rd (1995). The biosynthesis of cyclopropanated mycolic acids in *Mycobacterium tuberculosis*. Identification and functional analysis of CMAS-2. *J Biol Chem*, 270, 27292-27298.

Giganti, D., Alegre-Cebollada, J., Urresti, S., Albesa-Jove, D., Rodrigo-Unzueta, A., Comino, N., Kachala, M., Lopez-Fernandez, S., Svergun, D. I., Fernandez, J. M. and Guerin, M. E. (2013). Conformational plasticity of the essential membrane-associated mannosyltransferase PimA from mycobacteria. *J Biol Chem*, 288, 29797-29808.

Ginsberg, A. M. Drugs in development for tuberculosis. *Drugs*, 70, 2201-2214.

Ginsburg, A. S., Sun, R., Calamita, H., Scott, C. P., Bishai, W. R. and Grosset, J. H. (2005). Emergence of fluoroquinolone resistance in *Mycobacterium tuberculosis* during continuously dosed moxifloxacin monotherapy in a mouse model. *Antimicrob Agents Chemother*, 49, 3977-3979.

Giraud, M. F., Leonard, G. A., Field, R. A., Berlind, C. and Naismith, J. H. (2000). RmlC, the third enzyme of dTDP-L-rhamnose pathway, is a new class of epimerase. *Nat Struct Biol*, 7, 398-402.

Gloster, T. M., Meloncelli, P., Stick, R. V., Zechel, D., Vasella, A. and Davies, G. J. (2007). Glycosidase inhibition: an assessment of the binding of 18 putative transition-state mimics. *J Am Chem Soc*, 129, 2345-2354.

Goffin, C. and Ghuysen, J. M. (2002). Biochemistry and comparative genomics of SxxK superfamily acyltransferases offer a clue to the mycobacterial paradox: presence of penicillin-susceptible target proteins versus lack of efficiency of penicillin as therapeutic agent. *Microbiol Mol Biol Rev*, 66, 702-738, table of contents.

Goodfellow, M. and Minnikin, D. E. (1981). Identification of *Mycobacterium chelonei* by thin-layer chromatographic analysis of whole-organism methanolysates. *Tubercle*, 62, 285-287.

Gradmann, C. (2006). Robert Koch and the white death: from tuberculosis to tuberculin. *Microbes Infect*, 8, 294-301.

Grassberger, M. A., Turnowsky, F. and Hildebrandt, J. (1984). Preparation and antibacterial activities of new 1,2,3-diazaborine derivatives and analogues. *J Med Chem*, 27, 947-953.

Guerardel, Y., Maes, E., Elass, E., Leroy, Y., Timmerman, P., Besra, G. S., Locht, C., Strecker, G. and Kremer, L. (2002). Structural study of lipomannan and lipoarabinomannan from *Mycobacterium chelonae*. Presence of unusual components with α1,3-mannopyranose side chains. *J Biol Chem*, 277, 30635-30648.

Guerin, M. E., Kaur, D., Somashekar, B. S., Gibbs, S., Gest, P., Chatterjee, D., Brennan, P. J. and Jackson, M. (2009a). New insights into the early steps of phosphatidylinositol mannoside biosynthesis in mycobacteria: PimB' is an essential enzyme of *Mycobacterium smegmatis*. *J Biol Chem*, 284, 25687-25696.

Guerin, M. E., Kordulakova, J., Alzari, P. M., Brennan, P. J. and Jackson, M. (2010). Molecular basis of phosphatidyl-*myo*-inositol mannoside biosynthesis and regulation in mycobacteria. *J Biol Chem*, 285, 33577-33583.

Guerin, M. E., Kordulakova, J., Schaeffer, F., Svetlikova, Z., Buschiazzo, A., Giganti, D., Gicquel, B., Mikusova, K., Jackson, M. and Alzari, P. M. (2007). Molecular recognition and interfacial catalysis by the essential phosphatidylinositol mannosyltransferase PimA from mycobacteria. *J Biol Chem*, 282, 20705-20714.

Guerin, M. E., Schaeffer, F., Chaffotte, A., Gest, P., Giganti, D., Kordulakova, J., Van Der Woerd, M., Jackson, M. and Alzari, P. M. (2009b). Substrate-induced conformational changes in the essential peripheral membrane-associated mannosyltransferase PimA from mycobacteria: implications for catalysis. *J Biol Chem*, 284, 21613-21625.

Gurcha, S. S., Baulard, A. R., Kremer, L., Locht, C., Moody, D. B., Muhlecker, W., Costello, C. E., Crick, D. C., Brennan, P. J. and Besra, G. S. (2002). Ppm1, a novel polyprenol monophosphomannose synthase from *Mycobacterium tuberculosis*. *Biochem J*, 365, 441-450.

Haagsma, A. C., Abdillahi-Ibrahim, R., Wagner, M. J., Krab, K., Vergauwen, K., Guillemont, J., Andries, K., Lill, H., Koul, A. and Bald, D. (2009). Selectivity of TMC207

towards mycobacterial ATP synthase compared with that towards the eukaryotic homologue. *Antimicrob Agents Chemother*, 53, 1290-1292.

Haites, R. E., Morita, Y. S., Mcconville, M. J. and Billman-Jacobe, H. (2005a). Function of phosphatidylinositol in mycobacteria. *J Biol Chem*, 280, 10981-10987.

Haites, R. E., Morita, Y. S., Mcconville, M. J. and Jacobe, H. B. (2005b). Function of phosphatidylinositol in mycobacteria. *Journal of Biological Chemistry*, 280, 10981-10987.

Hanahan, D. (1983). Studies on transformation of *Escherichia coli* with plasmids. *Journal of Molecular Biology*, 166, 557-580.

Hartman, M. C., Jiang, S., Rush, J. S., Waechter, C. J. and Coward, J. K. (2007). Glycosyltransferase mechanisms: impact of a 5-fluoro substituent in acceptor and donor substrates on catalysis. *Biochemistry*, 46, 11630-11638.

Hayman, J. (1984). *Mycobacterium ulcerans*: an infection from Jurassic time? *Lancet*, 2, 1015-1016.

Helen D. Donoghue, O. Y.-C. L., David E. Minnikin, Gurdyal S. Besra, John H. Taylor and Mark Spigelman (2010). Tuberculosis in Dr Granville's mummy: a molecular re-examination of the earliest known Egyptian mummy to be scientifically examined and given a medical diagnosis. *Proc. R. Soc. B*, 277, 51-56.

Henkin, T. M. (1996). The role of CcpA transcriptional regulator in carbon metabolism in *Bacillus subtilis*. *FEMS Microbiol Lett*, 135, 9-15.

Henrickson, C. V., Smith, P. F. (1966). Growth response of Mycoplasma to carotenoid pigments and carotenoid intermediates. *Microbiology*, 45, 73-82.

Hentschel, E., Will, C., Mustafi, N., Burkovski, A., Rehm, N. and Frunzke, J. (2013). Destabilized eYFP variants for dynamic gene expression studies in *Corynebacterium glutamicum*. *Microbial Biotechnology*, 6, 196-201.

Hernick, M. (2013). Mycothiol: a target for potentiation of rifampin and other antibiotics against *Mycobacterium tuberculosis*. *Expert Review of Anti-Infective Therapy*, 11, 49-67.

Heyer, A., Gaetgens, C., Hentschel, E., Kalinowski, J., Bott, M. and Frunzke, J. (2012). The two-component system ChrSA is crucial for haem tolerance and interferes with HrrSA in haem-dependent gene regulation in *Corynebacterium glutamicum*. *Microbiology-Sgm*, 158, 3020-3031.

Horcajada, C., Guinovart, J. J., Fita, I. and Ferrer, J. C. (2006). Crystal structure of an archaeal glycogen synthase: insights into oligomerization and substrate binding of eukaryotic glycogen synthases. *J Biol Chem*, 281, 2923-2931.

Huang, H., Scherman, M. S., D'haeze, W., Vereecke, D., Holsters, M., Crick, D. C. and Mcneil, M. R. (2005). Identification and active expression of the *Mycobacterium tuberculosis* gene encoding 5-phospho-α-D-ribose-1-diphosphate: decaprenyl-phosphate 5-phosphoribosyltransferase, the first enzyme committed to decaprenylphosphoryl-D-arabinose synthesis. *J Biol Chem*, 280, 24539-24543.

Huitric, E., Verhasselt, P., Koul, A., Andries, K., Hoffner, S. and Andersson, D. I. (2010). Rates and mechanisms of resistance development in *Mycobacterium tuberculosis* to a novel diarylquinoline ATP synthase inhibitor. *Antimicrob Agents Chemother*, 54, 1022-1028.

Hunter, S. W. and Brennan, P. J. (1990). Evidence for the presence of a phosphatidylinositol anchor on the lipoarabinomannan and lipomannan of *Mycobacterium tuberculosis*. *J Biol Chem*, 265, 9272-9279.

Hurdle, J. G., Lee, R. B., Budha, N. R., Carson, E. I., Qi, J., Scherman, M. S., Cho, S. H., Mcneil, M. R., Lenaerts, A. J., Franzblau, S. G., Meibohm, B. and Lee, R. E. (2008). A microbiological assessment of novel nitrofuranylamides as anti-tuberculosis agents. *J Antimicrob Chemother*, 62, 1037-1045.

Iain C. Sutcliffe, A. K. B., Lynn G. Dover (2010). The Rhodococcal Cell Envelope: Composition, Organisation and Biosynthesis. In H. M. Alvarez (Ed.) Biology of Rhodococcus (pp. 29-71): Springer Berlin Heidelberg.

Imkamp, F. M. (1981). Clofazimine (lamprene or B663) in lepra reactions. *Lepr Rev*, 52, 135-140.

Ioannou, A., Cini, E., Timofte, R. S., Flitsch, S. L., Turner, N. J. and Linclau, B. (2011). Heavily fluorinated carbohydrates as enzyme substrates: oxidation of tetrafluorinated galactose by galactose oxidase. *Chem Commun (Camb)*, 47, 11228-11230.

Iwainsky, H. (1988). Mode of action, biotransformation and pharmacokinetics of antituberculosis drugs in animals and man. In K. Bartmann (Ed.) Antituberculosis Drugs (pp. 457–465) Berlin: Springer-Verlag.

Jackson, M. and Brennan, P. J. (2009). Polymethylated polysaccharides from Mycobacterium species revisited. *J Biol Chem*, 284, 1949-1953.

Jackson, M., Crick, D. C. and Brennan, P. J. (2000). Phosphatidylinositol is an essential phospholipid of mycobacteria. *J Biol Chem*, 275, 30092-30099.

Jackson, M., Raynaud, C., Laneelle, M. A., Guilhot, C., Laurent-Winter, C., Ensergueix, D., Gicquel, B. and Daffe, M. (1999). Inactivation of the antigen 85C gene profoundly affects the mycolate content and alters the permeability of the *Mycobacterium tuberculosis* cell envelope. *Mol Microbiol*, 31, 1573-1587.

Jamaluddin, H., Tumbale, P., Withers, S. G., Acharya, K. R. and Brew, K. (2007). Conformational changes induced by binding UDP-2F-galactose to α-1,3 galactosyltransferase-implications for catalysis. *J Mol Biol*, 369, 1270-1281.

Jankute, M., Grover, S., Rana, A. K. and Besra, G. S. (2012). Arabinogalactan and lipoarabinomannan biosynthesis: structure, biogenesis and their potential as drug targets. *Future Microbiol*, 7, 129-147.

Johansen, S. K., Maus, C. E., Plikaytis, B. B. and Douthwaite, S. (2006). Capreomycin binds across the ribosomal subunit interface using *tlyA*-encoded 2'-O-methylations in 16S and 23S rRNAs. *Mol Cell*, 23, 173-182.

Kacem, R., De Sousa-D'auria, C., Tropis, M., Chami, M., Gounon, P., Leblon, G., Houssin, C. and Daffe, M. (2004). Importance of mycoloyltransferases on the physiology of *Corynebacterium glutamicum*. *Microbiology*, 150, 73-84.

Karimova, G., Fayolle, C., Gmira, S., Ullmann, A., Leclerc, C. and Ladant, D. (1998a). Charge-dependent translocation of Bordetella pertussis adenylate cyclase toxin into eukaryotic cells: implication for the in vivo delivery of CD8(+) T cell epitopes into antigen-presenting cells. *Proc Natl Acad Sci U S A*, 95, 12532-12537.

Karimova, G., Pidoux, J., Ullmann, A. and Ladant, D. (1998b). A bacterial two-hybrid system based on a reconstituted signal transduction pathway. *Proc Natl Acad Sci U S A*, 95, 5752-5756.

Karimova, G., Ullmann, A. and Ladant, D. (2000). A bacterial two-hybrid system that exploits a cAMP signaling cascade in *Escherichia coli*. *Methods Enzymol*, 328, 59-73.

Kaur, D., Berg, S., Dinadayala, P., Gicquel, B., Chatterjee, D., Mcneil, M. R., Vissa, V. D., Crick, D. C., Jackson, M. and Brennan, P. J. (2006). Biosynthesis of mycobacterial lipoarabinomannan: role of a branching mannosyltransferase. *Proc Natl Acad Sci U S A*, 103, 13664-13669.

Kaur, D., Brennan, P. J. and Crick, D. C. (2004). Decaprenyl diphosphate synthesis in *Mycobacterium tuberculosis*. *J Bacteriol*, 186, 7564-7570.

Kaur, D., Guerin, M. E., Skovierova, H., Brennan, P. J. and Jackson, M. (2009). Chapter 2: Biogenesis of the cell wall and other glycoconjugates of *Mycobacterium tuberculosis*. *Adv Appl Microbiol*, 69, 23-78.

Kaur, D., Mcneil, M. R., Khoo, K. H., Chatterjee, D., Crick, D. C., Jackson, M. and Brennan, P. J. (2007). New insights into the biosynthesis of mycobacterial lipomannan arising from deletion of a conserved gene. *J Biol Chem*, 282, 27133-27140.

Kaur, D., Obregon-Henao, A., Pham, H., Chatterjee, D., Brennan, P. J. and Jackson, M. (2008). Lipoarabinomannan of Mycobacterium: mannose capping by a multifunctional terminal mannosyltransferase. *Proc Natl Acad Sci U S A*, 105, 17973-17977.

Keilhauer, C., Eggeling, L. and Sahm, H. (1993). Isoleucine synthesis in *Corynebacterium glutamicum* - Molecular analysis of the *ilvb-ilvn-ilvc* Operon. *Journal of Bacteriology*, 175, 5595-5603.

Khoo, K. H., Dell, A., Morris, H. R., Brennan, P. J. and Chatterjee, D. (1995a). Inositol phosphate capping of the nonreducing termini of lipoarabinomannan from rapidly growing strains of *Mycobacterium*. *J Biol Chem*, 270, 12380-12389.

Khoo, K. H., Dell, A., Morris, H. R., Brennan, P. J. and Chatterjee, D. (1995b). Structural definition of acylated phosphatidylinositol mannosides from *Mycobacterium tuberculosis*: definition of a common anchor for lipomannan and lipoarabinomannan. *Glycobiology*, 5, 117-127.

Khoo, K. H., Douglas, E., Azadi, P., Inamine, J. M., Besra, G. S., Mikusova, K., Brennan, P. J. and Chatterjee, D. (1996). Truncated structural variants of lipoarabinomannan in ethambutol drug-resistant strains of *Mycobacterium smegmatis*. Inhibition of arabinan biosynthesis by ethambutol. *J Biol Chem*, 271, 28682-28690.

Kinoshita, S., Udaka, S. and Shimono, M. (1957). Studies of amino acid fermentation. I. Production of L-glutamic acid by various microorganisms. *J Gen Appl Microbiol*, 3, 193-205.

Klaffl, S., Brocker, M., Kalinowski, J., Eikmanns, B. and Bott, M. (2013). Complex regulation of the PEP carboxykinase gene *pck* and characterization of its GntR-type regulator IolR as a repressor of *myo*-inositol utilization genes in *Corynebacterium glutamicum*. *Journal of Bacteriology*, 195, 4283-4296.

Klopper, M., Warren, R. M., Hayes, C., Gey Van Pittius, N. C., Streicher, E. M., Muller, B., Sirgel, F. A., Chabula-Nxiweni, M., Hoosain, E., Coetzee, G., David Van Helden, P., Victor, T. C. and Trollip, A. P. (2013). Emergence and spread of extensively and totally drug-resistant tuberculosis, South Africa. *Emerg Infect Dis*, 19, 449-455.

Koch, R. (1891). A further communication on a remedy for Tuberculosis. *Br Med J*, 1, 125-127.

Kordulakova, J., Gilleron, M., Mikusova, K., Puzo, G., Brennan, P. J., Gicquel, B. and Jackson, M. (2002). Definition of the first mannosylation step in phosphatidylinositol mannoside synthesis. PimA is essential for growth of mycobacteria. *J Biol Chem*, 277, 31335-31344.

Kordulakova, J., Gilleron, M., Puzo, G., Brennan, P. J., Gicquel, B., Mikusova, K. and Jackson, M. (2003). Identification of the required acyltransferase step in the biosynthesis of the phosphatidylinositol mannosides of mycobacterium species. *J Biol Chem*, 278, 36285-36295.

Koul, A., Dendouga, N., Vergauwen, K., Molenberghs, B., Vranckx, L., Willebrords, R., Ristic, Z., Lill, H., Dorange, I., Guillemont, J., Bald, D. and Andries, K. (2007). Diarylquinolines target subunit c of mycobacterial ATP synthase. *Nat Chem Biol*, 3, 323-324.

Kovacevic, S., Anderson, D., Morita, Y. S., Patterson, J., Haites, R., Mcmillan, B. N., Coppel, R., Mcconville, M. J. and Billman-Jacobe, H. (2006). Identification of a novel protein with a role in lipoarabinomannan biosynthesis in mycobacteria. *J Biol Chem*, 281, 9011-9017.

Kowalska, H., Pastuszak, I. and Szymona, M. (1980). A mannoglucokinese of *Mycobacterium tuberculosis* H37Ra. *Acta Microbiol Pol*, 29, 249-257.

Kremer, L., Douglas, J. D., Baulard, A. R., Morehouse, C., Guy, M. R., Alland, D., Dover, L. G., Lakey, J. H., Jacobs, W. R., Jr., Brennan, P. J., Minnikin, D. E. and Besra, G. S. (2000). Thiolactomycin and related analogues as novel anti-mycobacterial agents targeting KasA and KasB condensing enzymes in *Mycobacterium tuberculosis*. *J Biol Chem*, 275, 16857-16864.

Kremer, L., Dover, L. G., Carrere, S., Nampoothiri, K. M., Lesjean, S., Brown, A. K., Brennan, P. J., Minnikin, D. E., Locht, C. and Besra, G. S. (2002a). Mycolic acid biosynthesis and enzymic characterization of the β-ketoacyl-ACP synthase A-condensing enzyme from *Mycobacterium tuberculosis*. *Biochem J*, 364, 423-430.

Kremer, L., Dover, L. G., Morbidoni, H. R., Vilcheze, C., Maughan, W. N., Baulard, A., Tu, S. C., Honore, N., Deretic, V., Sacchettini, J. C., Locht, C., Jacobs, W. R., Jr. and Besra, G. S. (2003). Inhibition of InhA activity, but not KasA activity, induces formation of a KasA-containing complex in mycobacteria. *J Biol Chem*, 278, 20547-20554.

Kremer, L., Dover, L. G., Morehouse, C., Hitchin, P., Everett, M., Morris, H. R., Dell, A., Brennan, P. J., Mcneil, M. R., Flaherty, C., Duncan, K. and Besra, G. S. (2001). Galactan

biosynthesis in *Mycobacterium tuberculosis*. Identification of a bifunctional UDP-galactofuranosyltransferase. *J Biol Chem*, 276, 26430-26440.

Kremer, L., Gurcha, S. S., Bifani, P., Hitchen, P. G., Baulard, A., Morris, H. R., Dell, A., Brennan, P. J. and Besra, G. S. (2002b). Characterization of a putative α-mannosyltransferase involved in phosphatidylinositol trimannoside biosynthesis in *Mycobacterium tuberculosis*. *Biochem J*, 363, 437-447.

Krings, E., Krumbach, K., Bathe, B., Kelle, R., Wendisch, V. F., Sahm, H. and Eggeling, L. (2006). Characterization of myo-inositol utilization by *Corynebacterium glutamicum*: the stimulon, identification of transporters, and influence on L-lysine formation. *Journal of Bacteriology*, 188, 8054-8061.

Lange, B. M., Rujan, T., Martin, W. and Croteau, R. (2000). Isoprenoid biosynthesis: the evolution of two ancient and distinct pathways across genomes. *Proc Natl Acad Sci U S A*, 97, 13172-13177.

Lange, C., Rittmann, D., Wendisch, V. F., Bott, M. and Sahm, H. (2003). Global expression profiling and physiological characterization of *Corynebacterium glutamicum* grown in the presence of L-valine. *Applied and Environmental Microbiology*, 69, 2521-2532.

Larsen, M. H., Vilcheze, C., Kremer, L., Besra, G. S., Parsons, L., Salfinger, M., Heifets, L., Hazbon, M. H., Alland, D., Sacchettini, J. C. and Jacobs, W. R., Jr. (2002). Overexpression of *inhA*, but not *kasA*, confers resistance to isoniazid and ethionamide in *Mycobacterium smegmatis*, *M. bovis* BCG and *M. tuberculosis*. *Mol Microbiol*, 46, 453-466.

Lea-Smith, D. J., Martin, K. L., Pyke, J. S., Tull, D., Mcconville, M. J., Coppel, R. L. and Crellin, P. K. (2008). Analysis of a new mannosyltransferase required for the synthesis of phosphatidylinositol mannosides and lipoarbinomannan reveals two lipomannan pools in *corynebacterineae*. *J Biol Chem*, 283, 6773-6782.

Lee, A., Wu, S. W., Scherman, M. S., Torrelles, J. B., Chatterjee, D., Mcneil, M. R. and Khoo, K. H. (2006). Sequencing of oligoarabinosyl units released from mycobacterial arabinogalactan by endogenous arabinanase: identification of distinctive and novel structural motifs. *Biochemistry*, 45, 15817-15828.

Lee, A. S., Teo, A. S. and Wong, S. Y. (2001). Novel mutations in ndh in isoniazid-resistant *Mycobacterium tuberculosis* isolates. *Antimicrob Agents Chemother*, 45, 2157-2159.

Lee, H. N., Jung, K. E., Ko, I. J., Baik, H. S. and Oh, J. I. (2012a). Protein-protein interactions between histidine kinases and response regulators of *Mycobacterium tuberculosis* H37Rv. *J Microbiol*, 50, 270-277.

Lee, M., Lee, J., Carroll, M. W., Choi, H., Min, S., Song, T., Via, L. E., Goldfeder, L. C., Kang, E., Jin, B., Park, H., Kwak, H., Kim, H., Jeon, H. S., Jeong, I., Joh, J. S., Chen, R. Y., Olivier, K. N., Shaw, P. A., Follmann, D., Song, S. D., Lee, J. K., Lee, D., Kim, C. T., Dartois, V., Park, S. K., Cho, S. N. and Barry, C. E., 3rd (2012b). Linezolid for treatment of chronic extensively drug-resistant tuberculosis. *N Engl J Med*, 367, 1508-1518.

Lee, R., Monsey, D., Weston, A., Duncan, K., Rithner, C. and Mcneil, M. (1996). Enzymatic synthesis of UDP-galactofuranose and an assay for UDP-galactopyranose mutase based on high-performance liquid chromatography. *Anal Biochem*, 242, 1-7.

Lee, R. E., Brennan, P. J. and Besra, G. S. (1997). Mycobacterial arabinan biosynthesis: the use of synthetic arabinoside acceptors in the development of an arabinosyl transfer assay. *Glycobiology*, 7, 1121-1128.

Lee, R. E., Brennan, P. J. and Besra, G. S. (1998). Synthesis of β-D-arabinofuranosyl-1-monophosphoryl polyprenols: examination of their function as mycobacterial arabinosyl transferase donors. *Bioorg Med Chem Lett*, 8, 951-954.

Lee, Y. H. and Helmann, J. D. (2013). Reducing the level of undecaprenyl pyrophosphate synthase has complex effects on susceptibility to cell wall antibiotics. *Antimicrob Agents Chemother*.

Li, W., Xin, Y., Mcneil, M. R. and Ma, Y. (2006). *rmlB* and *rmlC* genes are essential for growth of mycobacteria. *Biochem Biophys Res Commun*, 342, 170-178.

Lin, P. L., Dartois, V., Johnston, P. J., Janssen, C., Via, L., Goodwin, M. B., Klein, E., Barry, C. E., 3rd and Flynn, J. L. (2012). Metronidazole prevents reactivation of latent *Mycobacterium tuberculosis* infection in macaques. *Proc Natl Acad Sci U S A*, 109, 14188-14193.

Liu, J. and Mushegian, A. (2003). Three monophyletic superfamilies account for the majority of the known glycosyltransferases. *Protein Sci*, 12, 1418-1431.

Liu, P., Sharon, A. and Chu, C. K. (2008). Fluorinated Nucleosides: Synthesis and Biological implication. *J Fluor Chem*, 129, 743-766.

Loewenberg, S. (2012). India reports cases of totally drug-resistant tuberculosis. *Lancet*, 379, 205.

Lovering, A. L., Lee, S. S., Kim, Y. W., Withers, S. G. and Strynadka, N. C. (2005). Mechanistic and structural analysis of a family 31 α-glycosidase and its glycosyl-enzyme intermediate. *J Biol Chem*, 280, 2105-2115.

Ludwiczak, P., Brando, T., Monsarrat, B. and Puzo, G. (2001). Structural characterization of *Mycobacterium tuberculosis* lipoarabinomannans by the combination of capillary electrophoresis and matrix-assisted laser desorption/ionization time-of-flight mass spectrometry. *Anal Chem*, 73, 2323-2330.

Ma, Y., Pan, F. and Mcneil, M. (2002). Formation of dTDP-rhamnose is essential for growth of mycobacteria. *J Bacteriol*, 184, 3392-3395.

Ma, Y., Stern, R. J., Scherman, M. S., Vissa, V. D., Yan, W., Jones, V. C., Zhang, F., Franzblau, S. G., Lewis, W. H. and Mcneil, M. R. (2001). Drug targeting *Mycobacterium tuberculosis* cell wall synthesis: genetics of dTDP-rhamnose synthetic enzymes and development of a microtiter plate-based screen for inhibitors of conversion of dTDP-glucose to dTDP-rhamnose. *Antimicrob Agents Chemother*, 45, 1407-1416.

Mahapatra, S., Crick, D. C. and Brennan, P. J. (2000). Comparison of the UDP-N-acetylmuramate:L-alanine ligase enzymes from *Mycobacterium tuberculosis* and Mycobacterium leprae. *J Bacteriol*, 182, 6827-6830.

Mai, D., Jones, J., Rodgers, J. W., Hartman, J. L. T., Kutsch, O. and Steyn, A. J. (2011). A screen to identify small molecule inhibitors of protein-protein interactions in mycobacteria. *Assay Drug Dev Technol*, 9, 299-310.

Makarov, V., Manina, G., Mikusova, K., Mollmann, U., Ryabova, O., Saint-Joanis, B., Dhar, N., Pasca, M. R., Buroni, S., Lucarelli, A. P., Milano, A., De Rossi, E., Belanova, M., Bobovska, A., Dianiskova, P., Kordulakova, J., Sala, C., Fullam, E., Schneider, P., Mckinney, J. D., Brodin, P., Christophe, T., Waddell, S., Butcher, P., Albrethsen, J., Rosenkrands, I., Brosch, R., Nandi, V., Bharath, S., Gaonkar, S., Shandil, R. K., Balasubramanian, V., Balganesh, T., Tyagi, S., Grosset, J., Riccardi, G. and Cole, S. T. (2009). Benzothiazinones kill *Mycobacterium tuberculosis* by blocking arabinan synthesis. *Science*, 324, 801-804.

Makarov, V., Riabova, O. B., Yuschenko, A., Urlyapova, N., Daudova, A., Zipfel, P. F. and Mollmann, U. (2006). Synthesis and antileprosy activity of some dialkyldithiocarbamates. *J Antimicrob Chemother*, 57, 1134-1138.

Manina, G., Bellinzoni, M., Pasca, M. R., Neres, J., Milano, A., Ribeiro, A. L., Buroni, S., Skovierova, H., Dianiskova, P., Mikusova, K., Marak, J., Makarov, V., Giganti, D., Haouz, A., Lucarelli, A. P., Degiacomi, G., Piazza, A., Chiarelli, L. R., De Rossi, E., Salina, E., Cole, S. T., Alzari, P. M. and Riccardi, G. (2010). Biological and structural characterization of the *Mycobacterium smegmatis* nitroreductase NfnB, and its role in benzothiazinone resistance. *Mol Microbiol*, 77, 1172-1185.

Manjunatha, U. H., Boshoff, H., Dowd, C. S., Zhang, L., Albert, T. J., Norton, J. E., Daniels, L., Dick, T., Pang, S. S. and Barry, C. E., 3rd (2006a). Identification of a nitroimidazo-oxazine-specific protein involved in PA-824 resistance in *Mycobacterium tuberculosis*. *Proc Natl Acad Sci U S A*, 103, 431-436.

Manjunatha, U. H., Lahiri, R., Randhawa, B., Dowd, C. S., Krahenbuhl, J. L. and Barry, C. E., 3rd (2006b). Mycobacterium leprae is naturally resistant to PA-824. *Antimicrob Agents Chemother*, 50, 3350-3354.

Mann, F. M., Thomas, J. A. and Peters, R. J. (2011). *Rv0989c* encodes a novel (E)-geranyl diphosphate synthase facilitating decaprenyl diphosphate biosynthesis in *Mycobacterium tuberculosis*. *FEBS Lett*, 585, 549-554.

Marks, P. A. (1956). A newer pathway of carbohydrate metabolism; the pentose phosphate pathway. *Diabetes*, 5, 276-283.

Marrakchi, H., Laneelle, G. and Quemard, A. (2000). InhA, a target of the antituberculous drug isoniazid, is involved in a mycobacterial fatty acid elongation system, FAS-II. *Microbiology*, 146 (Pt 2), 289-296.

Marshall, G. (1949). Individuality in medicine. *Br Med J*, 2, 941-944.

Matsumoto, M., Hashizume, H., Tomishige, T., Kawasaki, M., Tsubouchi, H., Sasaki, H., Shimokawa, Y. and Komatsu, M. (2006). OPC-67683, a nitro-dihydro-imidazooxazole derivative with promising action against tuberculosis in vitro and in mice. *PLoS Med*, 3, e466.

Maus, C. E., Plikaytis, B. B. and Shinnick, T. M. (2005a). Molecular analysis of cross-resistance to capreomycin, kanamycin, amikacin, and viomycin in *Mycobacterium tuberculosis*. *Antimicrob Agents Chemother*, 49, 3192-3197.

Maus, C. E., Plikaytis, B. B. and Shinnick, T. M. (2005b). Mutation of *tlyA* confers capreomycin resistance in *Mycobacterium tuberculosis*. *Antimicrob Agents Chemother*, 49, 571-577.

Mccarthy, T. R., Torrelles, J. B., Macfarlane, A. S., Katawczik, M., Kutzbach, B., Desjardin, L. E., Clegg, S., Goldberg, J. B. and Schlesinger, L. S. (2005). Overexpression of *Mycobacterium tuberculosis manB*, a phosphomannomutase that increases phosphatidylinositol mannoside biosynthesis in *Mycobacterium smegmatis* and mycobacterial association with human macrophages. *Mol Microbiol*, 58, 774-790.

Mcneil, M., Daffe, M. and Brennan, P. J. (1990). Evidence for the nature of the link between the arabinogalactan and peptidoglycan of mycobacterial cell walls. *J Biol Chem*, 265, 18200-18206.

Mcneil, M., Daffe, M. and Brennan, P. J. (1991). Location of the mycolyl ester substituents in the cell walls of mycobacteria. *J Biol Chem*, 266, 13217-13223.

Mcneil, M., Wallner, S. J., Hunter, S. W. and Brennan, P. J. (1987). Demonstration that the galactosyl and arabinosyl residues in the cell-wall arabinogalactan of *Mycobacterium leprae* and *Mycobacterium tuberculosis* are furanoid. *Carbohydr Res*, 166, 299-308.

Mcneil, M. R., Robuck, K. G., Harter, M. and Brennan, P. J. (1994). Enzymatic evidence for the presence of a critical terminal hexa-arabinoside in the cell walls of *Mycobacterium tuberculosis*. *Glycobiology*, 4, 165-173.

Mdluli, K., Sherman, D. R., Hickey, M. J., Kreiswirth, B. N., Morris, S., Stover, C. K. and Barry, C. E., 3rd (1996). Biochemical and genetic data suggest that InhA is not the primary target for activated isoniazid in *Mycobacterium tuberculosis*. *J Infect Dis*, 174, 1085-1090.

Mdluli, K., Slayden, R. A., Zhu, Y., Ramaswamy, S., Pan, X., Mead, D., Crane, D. D., Musser, J. M. and Barry, C. E., 3rd (1998). Inhibition of a *Mycobacterium tuberculosis* β-ketoacyl ACP synthase by isoniazid. *Science*, 280, 1607-1610.

Meniche, X., De Sousa-D'auria, C., Van-Der-Rest, B., Bhamidi, S., Huc, E., Huang, H., De Paepe, D., Tropis, M., Mcneil, M., Daffe, M. and Houssin, C. (2008). Partial redundancy in the synthesis of the D-arabinose incorporated in the cell wall arabinan of *Corynebacterineae*. *Microbiology*, 154, 2315-2326.

Metzger, L. E. T. and Raetz, C. R. (2009). Purification and characterization of the lipid A disaccharide synthase (LpxB) from *Escherichia coli*, a peripheral membrane protein. *Biochemistry*, 48, 11559-11571.

Middlebrook, G. and Dressler, S. H. (1954). Clinical evaluation of isoniazid. *Am Rev Tuberc*, 70, 1102-1103.

Migliori, G. B., Sotgiu, G., Gandhi, N. R., Falzon, D., Deriemer, K., Centis, R., Hollm-Delgado, M. G., Palmero, D., Perez-Guzman, C., Vargas, M. H., D'ambrosio, L., Spanevello, A., Bauer, M., Chan, E. D., Schaaf, H. S., Keshavjee, S., Holtz, T. H. and Menzies, D. (2013). Drug resistance beyond extensively drug-resistant tuberculosis: individual patient data meta-analysis. *Eur Respir J*, 42, 169-179.

Mikusova, K., Huang, H., Yagi, T., Holsters, M., Vereecke, D., D'haeze, W., Scherman, M. S., Brennan, P. J., Mcneil, M. R. and Crick, D. C. (2005). Decaprenylphosphoryl arabinofuranose, the donor of the D-arabinofuranosyl residues of mycobacterial arabinan, is formed via a two-step epimerization of decaprenylphosphoryl ribose. *J Bacteriol*, 187, 8020-8025.

Mikusova, K., Mikus, M., Besra, G. S., Hancock, I. and Brennan, P. J. (1996). Biosynthesis of the linkage region of the mycobacterial cell wall. *J Biol Chem*, 271, 7820-7828.

Mikusova, K., Slayden, R. A., Besra, G. S. and Brennan, P. J. (1995). Biogenesis of the mycobacterial cell wall and the site of action of ethambutol. *Antimicrob Agents Chemother*, 39, 2484-2489.

Mills, J. A., Motichka, K., Jucker, M., Wu, H. P., Uhlik, B. C., Stern, R. J., Scherman, M. S., Vissa, V. D., Pan, F., Kundu, M., Ma, Y. F. and Mcneil, M. (2004). Inactivation of the mycobacterial rhamnosyltransferase, which is needed for the formation of the arabinogalactan-peptidoglycan linker, leads to irreversible loss of viability. *J Biol Chem*, 279, 43540-43546.

Minnikin, D. E. (1982). Lipids: complex lipids, their chemistry, biosynthesis and roles. In C. R. a. J. Stanford (Ed.) The Biology of the Mycobacteria (pp. 95-185) London: Academic Press.

Minnikin, D. E., Goodfellow, M. & Collins, M. D. (1978). *Lipid composition in the classification and identification of coryneform and related taxa.* . London: London Academic Press.

Minnikin, D. E., Kremer, L., Dover, L. G. and Besra, G. S. (2002). The methyl-branched fortifications of *Mycobacterium tuberculosis*. *Chem Biol*, 9, 545-553.

Minnikin, D. E., Minnikin, S. M., Goodfellow, M. and Stanford, J. L. (1982). The mycolic acids of *Mycobacterium chelonei*. *J Gen Microbiol*, 128, 817-822.

Minnikin, D. E. a. G., M. (1980). Lipid composition in the classification and identification of acid-fast bacteria. In R. G. B. M. Goodfellow (Ed.) Microbiological Classification and Identification (pp. 189-256) London: Academic Press.

Mishra, A. K., Alderwick, L. J., Rittmann, D., Tatituri, R. V., Nigou, J., Gilleron, M., Eggeling, L. and Besra, G. S. (2007). Identification of an α(1→6) mannopyranosyltransferase (MptA), involved in *Corynebacterium glutamicum* lipomanann biosynthesis, and identification of its orthologue in *Mycobacterium tuberculosis*. *Mol Microbiol*, 65, 1503-1517.

Mishra, A. K., Alderwick, L. J., Rittmann, D., Wang, C., Bhatt, A., Jacobs, W. R., Jr., Takayama, K., Eggeling, L. and Besra, G. S. (2008). Identification of a novel α(1→6) mannopyranosyltransferase MptB from *Corynebacterium glutamicum* by deletion of a conserved gene, *NCgl1505*, affords a lipomannan- and lipoarabinomannan-deficient mutant. *Mol Microbiol*, 68, 1595-1613.

Mishra, A. K., Batt, S., Krumbach, K., Eggeling, L. and Besra, G. S. (2009). Characterization of the *Corynebacterium glutamicum* Δ*pimB'* Δ*mgtA* double deletion mutant and the role of *Mycobacterium tuberculosis* orthologues *Rv2188c* and *Rv0557* in glycolipid biosynthesis. *J Bacteriol*, 191, 4465-4472.

Mishra, A. K., Driessen, N. N., Appelmelk, B. J. and Besra, G. S. (2011a). Lipoarabinomannan and related glycoconjugates: structure, biogenesis and role in *Mycobacterium tuberculosis* physiology and host-pathogen interaction. *FEMS Microbiol Rev*.

Mishra, A. K., Driessen, N. N., Appelmelk, B. J. and Besra, G. S. (2011b). Lipoarabinomannan and related glycoconjugates: structure, biogenesis and role in *Mycobacterium tuberculosis* physiology and host-pathogen interaction. *FEMS Microbiol Rev*, 35, 1126-1157.

Mishra, A. K., Driessen, N. N., Appelmelk, B. J. and Besra, G. S. (2011c). Lipoarabinomannan and related glycoconjugates: structure, biogenesis and role in *Mycobacterium tuberculosis* physiology and host-pathogen interaction. *FEMS Microbiology Reviews*, 35, 1126-1157.

Moker, N., Brocker, M., Schaffer, S., Kramer, R., Morbach, S. and Bott, M. (2004). Deletion of the genes encoding the MtrA-MtrB two-component system of *Corynebacterium glutamicum* has a strong influence on cell morphology, antibiotics susceptibility and expression of genes involved in osmoprotection. *Mol Microbiol*, 54, 420-438.

Möker, N., Brocker, M., Schaffer, S., Kramer, R., Morbach, S. and Bott, M. (2004). Deletion of the genes encoding the MtrA-MtrB two-component system of *Corynebacterium glutamicum* has a strong influence on cell morphology, antibiotics susceptibility and expression of genes involved in osmoprotection. *Molecular Microbiology*, 54, 420-438.

Morita, Y. S., Fukuda, T., Sena, C. B. C., Yamaryo-Botte, Y., Mcconville, M. J. and Kinoshita, T. (2011). Inositol lipid metabolism in mycobacteria: Biosynthesis and regulatory mechanisms. *Biochimica Et Biophysica Acta-General Subjects*, 1810, 630-641.

Morita, Y. S., Patterson, J. H., Billman-Jacobe, H. and Mcconville, M. J. (2004). Biosynthesis of mycobacterial phosphatidylinositol mannosides. *Biochem J*, 378, 589-597.

Morita, Y. S., Sena, C. B., Waller, R. F., Kurokawa, K., Sernee, M. F., Nakatani, F., Haites, R. E., Billman-Jacobe, H., Mcconville, M. J., Maeda, Y. and Kinoshita, T. (2006). PimE is a polyprenol-phosphate-mannose-dependent mannosyltransferase that transfers the fifth mannose of phosphatidylinositol mannoside in mycobacteria. *J Biol Chem*, 281, 25143-25155.

Morlock, G. P., Metchock, B., Sikes, D., Crawford, J. T. and Cooksey, R. C. (2003). ethA, *inhA*, and *katG* loci of ethionamide-resistant clinical *Mycobacterium tuberculosis* isolates. *Antimicrob Agents Chemother*, 47, 3799-3805.

Movahedzadeh, F., Smith, D. A., Norman, R. A., Dinadayala, P., Murray-Rust, J., Russell, D. G., Kendall, S. L., Rison, S. C., Mcalister, M. S., Bancroft, G. J., Mcdonald, N. Q., Daffe, M., Av-Gay, Y. and Stoker, N. G. (2004a). The *Mycobacterium tuberculosis* ino1 gene is essential for growth and virulence. *Mol Microbiol*, 51, 1003-1014.

Movahedzadeh, F., Smith, D. A., Norman, R. A., Dinadayala, P., Murray-Rust, J., Russell, D. G., Kendall, S. L., Rison, S. C. G., Mcalister, M. S. B., Bancroft, G. J., Mcdonald, N. Q., Daffe, M., Av-Gay, Y. and Stoker, N. G. (2004b). The *Mycobacterium tuberculosis ino1* gene is essential for growth and virulence. *Molecular Microbiology*, 51, 1003-1014.

Movahedzadeh, F., Wheeler, P. R., Dinadayala, P., Av-Gay, Y., Parish, T., Daffe, M. and Stoker, N. G. (2010). Inositol monophosphate phosphatase genes of *Mycobacterium tuberculosis*. *BMC Microbiol*, 10, 50.

Murray, C. J. and Salomon, J. A. (1998). Modeling the impact of global tuberculosis control strategies. *Proc Natl Acad Sci U S A*, 95, 13881-13886.

Musser, J. M. (1992). Clinical relevance of streptococcal pyrogenic exotoxins in streptococcal toxic shock-like syndrome and other severe invasive infections. *Pediatr Ann*, 21, 821-822, 825-828.

Neres, J., Pojer, F., Molteni, E., Chiarelli, L. R., Dhar, N., Boy-Rottger, S., Buroni, S., Fullam, E., Degiacomi, G., Lucarelli, A. P., Read, R. J., Zanoni, G., Edmondson, D. E., De Rossi, E., Pasca, M. R., Mckinney, J. D., Dyson, P. J., Riccardi, G., Mattevi, A., Cole, S. T. and Binda, C. (2012). Structural basis for benzothiazinone-mediated killing of *Mycobacterium tuberculosis*. *Sci Transl Med*, 4, 150ra121.

Nerlich, A. G., Haas, C. J., Zink, A., Szeimies, U. and Hagedorn, H. G. (1997). Molecular evidence for tuberculosis in an ancient Egyptian mummy. *Lancet*, 350, 1404.

Newton, G. L., Arnold, K., Price, M. S., Sherrill, C., Delcardayre, S. B., Aharonowitz, Y., Cohen, G., Davies, J., Fahey, R. C. and Davis, C. (1996). Distribution of thiols in microorganisms: mycothiol is a major thiol in most actinomycetes. *J Bacteriol*, 178, 1990-1995.

Newton, G. L., Buchmeier, N. and Fahey, R. C. (2008). Biosynthesis and functions of mycothiol, the unique protective thiol of Actinobacteria. *Microbiol Mol Biol Rev*, 72, 471-494.

Nguyen, C. C. and Saier, M. H., Jr. (1995). Phylogenetic, structural and functional analyses of the LacI-GalR family of bacterial transcription factors. *FEBS Lett*, 377, 98-102.

Niebisch, A. and Bott, M. (2001). Molecular analysis of the cytochrome bc_1-aa_3 branch of the *Corynebacterium glutamicum* respiratory chain containing an unusual diheme cytochrome c_1. *Archives of Microbiology*, 175, 282-294.

Niebisch, A., Kabus, A., Schultz, C., Weil, B. and Bott, M. (2006). Corynebacterial protein kinase G controls 2-oxoglutarate dehydrogenase activity via the phosphorylation status of the OdhI protein. *Journal of Biological Chemistry*, 281, 12300-12307.

Nigou, J. and Besra, G. S. (2002). Characterization and regulation of inositol monophosphatase activity in *Mycobacterium smegmatis*. *Biochem J*, 361, 385-390.

Nigou, J., Gilleron, M., Brando, T. and Puzo, G. (2004). Structural analysis of mycobacterial lipoglycans. *Appl Biochem Biotechnol*, 118, 253-267.

Nigou, J., Gilleron, M. and Puzo, G. (1999). Lipoarabinomannans: characterization of the multiacylated forms of the phosphatidyl-myo-inositol anchor by NMR spectroscopy. *Biochem J*, 337 (Pt 3), 453-460.

Nigou, J., Gilleron, M. and Puzo, G. (2003). Lipoarabinomannans: from structure to biosynthesis. *Biochimie*, 85, 153-166.

Nikonenko, B. V., Protopopova, M., Samala, R., Einck, L. and Nacy, C. A. (2007). Drug therapy of experimental tuberculosis (TB): improved outcome by combining SQ109, a new diamine antibiotic, with existing TB drugs. *Antimicrob Agents Chemother*, 51, 1563-1565.

Ning, B. and Elbein, A. D. (1999). Purification and properties of mycobacterial GDP-mannose pyrophosphorylase. *Arch Biochem Biophys*, 362, 339-345.

Noll, H. and Bloch, H. (1953). A toxic lipid component of the tubercle bacillus (cord factor). II. Occurrence in chloroform extracts of young and older bacterial cultures. *Am Rev Tuberc*, 67, 828-852.

Noll, H., Bloch, H., Asselineau, J. and Lederer, E. (1956). The chemical structure of the cord factor of *Mycobacterium tuberculosis*. *Biochim Biophys Acta*, 20, 299-309.

Norman, R. A., Mcalister, M. S. B., Murray-Rust, J., Movahedzadeh, F., Stoker, N. G. and Mcdonald, N. Q. (2002). Crystal structure of inositol 1-phosphate synthase from *Mycobacterium tuberculosis*, a key enzyme in phosphatidylinositol synthesis. *Structure*, 10, 393-402.

Nuermberger, E. L., Yoshimatsu, T., Tyagi, S., O'brien, R. J., Vernon, A. N., Chaisson, R. E., Bishai, W. R. and Grosset, J. H. (2004). Moxifloxacin-containing regimen greatly reduces time to culture conversion in murine tuberculosis. *Am J Respir Crit Care Med*, 169, 421-426.

Osborne, R. (2013). First novel anti-tuberculosis drug in 40 years. *Nat Biotechnol*, 31, 89-91.

Pan, F., Jackson, M., Ma, Y. and Mcneil, M. (2001). Cell wall core galactofuran synthesis is essential for growth of mycobacteria. *J Bacteriol*, 183, 3991-3998.

Pantano, S., Alber, F., Lamba, D. and Carloni, P. (2002). NADH interactions with WT- and S94A-acyl carrier protein reductase from *Mycobacterium tuberculosis*: an ab initio study. *Proteins*, 47, 62-68.

Pasca, M. R., Degiacomi, G., Ribeiro, A. L., Zara, F., De Mori, P., Heym, B., Mirrione, M., Brerra, R., Pagani, L., Pucillo, L., Troupioti, P., Makarov, V., Cole, S. T. and Riccardi, G. (2010). Clinical isolates of *Mycobacterium tuberculosis* in four European hospitals are uniformly susceptible to benzothiazinones. *Antimicrob Agents Chemother*, 54, 1616-1618.

Pathak, A. K., Pathak, V., Maddry, J. A., Suling, W. J., Gurcha, S. S., Besra, G. S. and Reynolds, R. C. (2001). Studies on α(1→5) linked octyl arabinofuranosyl disaccharides for mycobacterial arabinosyl transferase activity. *Bioorg Med Chem*, 9, 3145-3151.

Pathak, A. K., Pathak, V., Seitz, L., Gurcha, S. S., Besra, G. S., Riordan, J. M. and Reynolds, R. C. (2007). Disaccharide analogs as probes for glycosyltransferases in *Mycobacterium tuberculosis*. *Bioorg Med Chem*, 15, 5629-5650.

Pathak, A. K., Pathak, V., Suling, W. J., Gurcha, S. S., Morehouse, C. B., Besra, G. S., Maddry, J. A. and Reynolds, R. C. (2002). Studies on n-octyl-5-(α-D-arabinofuranosyl)-β-D-galactofuranosides for mycobacterial glycosyltransferase activity. *Bioorg Med Chem*, 10, 923-928.

Pathak, A. K., Pathak, V., Suling, W. J., Riordan, J. R., Gurcha, S. S., Besra, G. S. and Reynolds, R. C. (2009). Synthesis of deoxygenated α(1→5)-linked arabinofuranose disaccharides as substrates and inhibitors of arabinosyltransferases of *Mycobacterium tuberculosis*. *Bioorg Med Chem*, 17, 872-881.

Patterson, J. H., Waller, R. F., Jeevarajah, D., Billman-Jacobe, H. and Mcconville, M. J. (2003). Mannose metabolism is required for mycobacterial growth. *Biochem J*, 372, 77-86.

Peek, S. F., Cote, P. J., Jacob, J. R., Toshkov, I. A., Hornbuckle, W. E., Baldwin, B. H., Wells, F. V., Chu, C. K., Gerin, J. L., Tennant, B. C. and Korba, B. E. (2001). Antiviral activity of clevudine [L-FMAU, (1-(2-fluoro-5-methyl-β, L-arabinofuranosyl) uracil)] against woodchuck hepatitis virus replication and gene expression in chronically infected woodchucks (Marmota monax). *Hepatology*, 33, 254-266.

Persson, K., Ly, H. D., Dieckelmann, M., Wakarchuk, W. W., Withers, S. G. and Strynadka, N. C. (2001). Crystal structure of the retaining galactosyltransferase LgtC from *Neisseria meningitidis* in complex with donor and acceptor sugar analogs. *Nat Struct Biol*, 8, 166-175.

Pesnot, T., Jorgensen, R., Palcic, M. M. and Wagner, G. K. (2010). Structural and mechanistic basis for a new mode of glycosyltransferase inhibition. *Nat Chem Biol*, 6, 321-323.

Pitarque, S., Larrouy-Maumus, G., Payre, B., Jackson, M., Puzo, G. and Nigou, J. (2008). The immunomodulatory lipoglycans, lipoarabinomannan and lipomannan, are exposed at the mycobacterial cell surface. *Tuberculosis (Edinb)*, 88, 560-565.

Protopopova, M., Hanrahan, C., Nikonenko, B., Samala, R., Chen, P., Gearhart, J., Einck, L. and Nacy, C. A. (2005). Identification of a new antitubercular drug candidate, SQ109, from a combinatorial library of 1,2-ethylenediamines. *J Antimicrob Chemother*, 56, 968-974.

Puech, V., Chami, M., Lemassu, A., Laneelle, M. A., Schiffler, B., Gounon, P., Bayan, N., Benz, R. and Daffe, M. (2001). Structure of the cell envelope of corynebacteria: importance of the non-covalently bound lipids in the formation of the cell wall permeability barrier and fracture plane. *Microbiology*, 147, 1365-1382.

Qasba, P. K., Ramakrishnan, B. and Boeggeman, E. (2005). Substrate-induced conformational changes in glycosyltransferases. *Trends Biochem Sci*, 30, 53-62.

Quinones-Soto, S. and Roth, J. R. (2011). Effect of growth under selection on appearance of chromosomal mutations in *Salmonella enterica*. *Genetics*, 189, 37-53.

Qureshi, N., Takayama, K., Jordi, H. C. and Schnoes, H. K. (1978). Characterization of the purified components of a new homologous series of alpha-mycolic acids from *Mycobacterium tuberculosis* H37Ra. *J Biol Chem*, 253, 5411-5417.

Radmacher, E., Stansen, K. C., Besra, G. S., Alderwick, L. J., Maughan, W. N., Hollweg, G., Sahm, H., Wendisch, V. F. and Eggeling, L. (2005). Ethambutol, a cell wall inhibitor of *Mycobacterium tuberculosis*, elicits L-glutamate efflux of *Corynebacterium glutamicum*. *Microbiology*, 151, 1359-1368.

Rainczuk, A. K., Yamaryo-Botte, Y., Brammananth, R., Stinear, T. P., Seemann, T., Coppel, R. L., Mcconville, M. J. and Crellin, P. K. (2012). The lipoprotein LpqW is essential for the mannosylation of periplasmic glycolipids in Corynebacteria. *J Biol Chem*, 287, 42726-42738.

Raman, K. and Chandra, N. (2008). *Mycobacterium tuberculosis* interactome analysis unravels potential pathways to drug resistance. *BMC Microbiol*, 8, 234.

Ramaswamy, S. V., Amin, A. G., Goksel, S., Stager, C. E., Dou, S. J., El Sahly, H., Moghazeh, S. L., Kreiswirth, B. N. and Musser, J. M. (2000). Molecular genetic analysis of nucleotide polymorphisms associated with ethambutol resistance in human isolates of *Mycobacterium tuberculosis*. *Antimicrob Agents Chemother*, 44, 326-336.

Ramseier, T. M., Bledig, S., Michotey, V., Feghali, R. and Saier, M. H., Jr. (1995). The global regulatory protein FruR modulates the direction of carbon flow in *Escherichia coli*. *Mol Microbiol*, 16, 1157-1169.

Rana, A. K., Singh, A., Gurcha, S. S., Cox, L. R., Bhatt, A. and Besra, G. S. (2012). Ppm1-encoded polyprenyl monophosphomannose synthase activity is essential for lipoglycan synthesis and survival in mycobacteria. *PLoS One*, 7, e48211.

Raymond, J. B., Mahapatra, S., Crick, D. C. and Pavelka, M. S., Jr. (2005). Identification of the *namH* gene, encoding the hydroxylase responsible for the N-glycolylation of the mycobacterial peptidoglycan. *J Biol Chem*, 280, 326-333.

Rengarajan, J., Sassetti, C. M., Naroditskaya, V., Sloutsky, A., Bloom, B. R. and Rubin, E. J. (2004). The folate pathway is a target for resistance to the drug para-aminosalicylic acid (PAS) in mycobacteria. *Mol Microbiol*, 53, 275-282.

Reyes, P. and Heidelberger, C. (1965). Fluorinated Pyrimidines. Xxv. The inhibition of thymidylate synthetase from ehrlich ascites carcinoma cells by pyrimidine Analogs. *Biochim Biophys Acta*, 103, 177-179.

Roos, A. K., Andersson, C. E., Bergfors, T., Jacobsson, M., Karlen, A., Unge, T., Jones, T. A. and Mowbray, S. L. (2004). *Mycobacterium tuberculosis* ribose-5-phosphate isomerase has a known fold, but a novel active site. *J Mol Biol*, 335, 799-809.

Roos, A. K., Burgos, E., Ericsson, D. J., Salmon, L. and Mowbray, S. L. (2005). Competitive inhibitors of *Mycobacterium tuberculosis* ribose-5-phosphate isomerase B reveal new information about the reaction mechanism. *J Biol Chem*, 280, 6416-6422.

Rozwarski, D. A., Grant, G. A., Barton, D. H., Jacobs, W. R., Jr. and Sacchettini, J. C. (1998). Modification of the NADH of the isoniazid target (InhA) from *Mycobacterium tuberculosis*. *Science*, 279, 98-102.

Sacksteder, K. A., Protopopova, M., Barry, C. E., 3rd, Andries, K. and Nacy, C. A. (2012). Discovery and development of SQ109: a new antitubercular drug with a novel mechanism of action. *Future Microbiol*, 7, 823-837.

Saltini, C. (2006). Chemotherapy and diagnosis of tuberculosis. *Respir Med*, 100, 2085-2097.

Sambrook, J. and Russell, D. W. (2001). *Molecular cloning: A laboratory manual*. NY: Cold Spring Harbor Laboratory Press.

Sassetti, C. M., Boyd, D. H. and Rubin, E. J. (2003). Genes required for mycobacterial growth defined by high density mutagenesis. *Mol Microbiol*, 48, 77-84.

Scarsdale, J. N., Kazanina, G., He, X., Reynolds, K. A. and Wright, H. T. (2001). Crystal structure of the *Mycobacterium tuberculosis* beta-ketoacyl-acyl carrier protein synthase III. *J Biol Chem*, 276, 20516-20522.

Schaeffer, M. L., Agnihotri, G., Volker, C., Kallender, H., Brennan, P. J. and Lonsdale, J. T. (2001). Purification and biochemical characterization of the *Mycobacterium tuberculosis* β-ketoacyl-acyl carrier protein synthases KasA and KasB. *J Biol Chem*, 276, 47029-47037.

Schafer, A., Tauch, A., Jager, W., Kalinowski, J., Thierbach, G. and Puhler, A. (1994). Small mobilizable multi-purpose cloning vectors derived from the *Escherichia coli* Plasmids pK18 and pK19: Selection of defined deletions in the chromosome of *Corynebacterium glutamicum*. *Gene*, 145, 69-73.

Scherman, H., Kaur, D., Pham, H., Skovierova, H., Jackson, M. and Brennan, P. J. (2009). Identification of a polyprenylphosphomannosyl synthase involved in the synthesis of mycobacterial mannosides. *J Bacteriol*, 191, 6769-6772.

Scherman, M. S., Kalbe-Bournonville, L., Bush, D., Xin, Y., Deng, L. and Mcneil, M. (1996). Polyprenylphosphate-pentoses in mycobacteria are synthesized from 5-phosphoribose pyrophosphate. *J Biol Chem*, 271, 29652-29658.

Schröder, J., Jochmann, N., Rodionov, D. A. and Tauch, A. (2010). The Zur regulon of *Corynebacterium glutamicum* ATCC 13032. *BMC Genomics*, 11:12 doi 10.1186/1471-2164-11-12.

Schulbach, M. C., Mahapatra, S., Macchia, M., Barontini, S., Papi, C., Minutolo, F., Bertini, S., Brennan, P. J. and Crick, D. C. (2001). Purification, enzymatic characterization, and inhibition of the Z-farnesyl diphosphate synthase from *Mycobacterium tuberculosis*. *J Biol Chem*, 276, 11624-11630.

Scorpio, A. and Zhang, Y. (1996). Mutations in *pncA*, a gene encoding pyrazinamidase/nicotinamidase, cause resistance to the antituberculous drug pyrazinamide in tubercle bacillus. *Nat Med*, 2, 662-667.

Seidel, M., Alderwick, L. J., Birch, H. L., Sahm, H., Eggeling, L. and Besra, G. S. (2007a). Identification of a novel arabinofuranosyltransferase AftB involved in a terminal step of cell wall arabinan biosynthesis in *Corynebacterineae*, such as *Corynebacterium glutamicum* and *Mycobacterium tuberculosis*. *J Biol Chem*, 282, 14729-14740.

Seidel, M., Alderwick, L. J., Sahm, H., Besra, G. S. and Eggeling, L. (2007b). Topology and mutational analysis of the single Emb arabinofuranosyltransferase of *Corynebacterium glutamicum* as a model of Emb proteins of *Mycobacterium tuberculosis*. *Glycobiology*, 17, 210-219.

Severn, W. B., Furneaux, R. H., Falshaw, R. and Atkinson, P. H. (1998). Chemical and spectroscopic characterisation of the phosphatidylinositol manno-oligosaccharides from *Mycobacterium bovis* AN5 and WAg201 and *Mycobacterium smegmatis* MC^2 155. *Carbohydr Res*, 308, 397-408.

Shi, L., Berg, S., Lee, A., Spencer, J. S., Zhang, J., Vissa, V., Mcneil, M. R., Khoo, K. H. and Chatterjee, D. (2006). The carboxy terminus of EmbC from *Mycobacterium smegmatis* mediates chain length extension of the arabinan in lipoarabinomannan. *J Biol Chem*, 281, 19512-19526.

Shi, W., Zhang, X., Jiang, X., Yuan, H., Lee, J. S., Barry, C. E., 3rd, Wang, H., Zhang, W. and Zhang, Y. (2011). Pyrazinamide inhibits trans-translation in *Mycobacterium tuberculosis*. *Science*, 333, 1630-1632.

Singh, R., Manjunatha, U., Boshoff, H. I., Ha, Y. H., Niyomrattanakit, P., Ledwidge, R., Dowd, C. S., Lee, I. Y., Kim, P., Zhang, L., Kang, S., Keller, T. H., Jiricek, J. and Barry, C. E., 3rd (2008). PA-824 kills nonreplicating *Mycobacterium tuberculosis* by intracellular NO release. *Science*, 322, 1392-1395.

Skovierova, H., Larrouy-Maumus, G., Pham, H., Belanova, M., Barilone, N., Dasgupta, A., Mikusova, K., Gicquel, B., Gilleron, M., Brennan, P. J., Puzo, G., Nigou, J. and Jackson, M. (2010). Biosynthetic origin of the galactosamine substituent of Arabinogalactan in *Mycobacterium tuberculosis*. *J Biol Chem*, 285, 41348-41355.

Skovierova, H., Larrouy-Maumus, G., Zhang, J., Kaur, D., Barilone, N., Kordulakova, J., Gilleron, M., Guadagnini, S., Belanova, M., Prevost, M. C., Gicquel, B., Puzo, G., Chatterjee, D., Brennan, P. J., Nigou, J. and Jackson, M. (2009). AftD, a novel essential arabinofuranosyltransferase from mycobacteria. *Glycobiology*, 19, 1235-1247.

Sotgiu, G., Centis, R., D'ambrosio, L., Alffenaar, J. W., Anger, H. A., Caminero, J. A., Castiglia, P., De Lorenzo, S., Ferrara, G., Koh, W. J., Schecter, G. F., Shim, T. S., Singla, R., Skrahina, A., Spanevello, A., Udwadia, Z. F., Villar, M., Zampogna, E., Zellweger, J. P., Zumla, A. and Migliori, G. B. (2012). Efficacy, safety and tolerability of linezolid containing regimens in treating MDR-TB and XDR-TB: systematic review and meta-analysis. *Eur Respir J*, 40, 1430-1442.

Sreevatsan, S., Stockbauer, K. E., Pan, X., Kreiswirth, B. N., Moghazeh, S. L., Jacobs, W. R., Jr., Telenti, A. and Musser, J. M. (1997). Ethambutol resistance in *Mycobacterium tuberculosis*: critical role of *embB* mutations. *Antimicrob Agents Chemother*, 41, 1677-1681.

Stamm, L. M., Morisaki, J. H., Gao, L. Y., Jeng, R. L., Mcdonald, K. L., Roth, R., Takeshita, S., Heuser, J., Welch, M. D. and Brown, E. J. (2003). *Mycobacterium marinum* escapes from phagosomes and is propelled by actin-based motility. *J Exp Med*, 198, 1361-1368.

Steingart, K. R., Jotblad, S., Robsky, K., Deck, D., Hopewell, P. C., Huang, D. and Nahid, P. (2011). Higher-dose rifampin for the treatment of pulmonary tuberculosis: a systematic review. *Int J Tuberc Lung Dis*, 15, 305-316.

Studier, F. W. and Moffatt, B. A. (1986). Use of bacteriophage T7 RNA polymerase to direct selective high-level expression of cloned genes. *Journal of Molecular Biology*, 189, 113-130.

Subramaniam, V., Gurcha, S. S., Besra, G. S. and Lowary, T. L. (2005). Modified mannose disaccharides as substrates and inhibitors of a polyprenol monophosphomannose-dependent α-(1→6)-mannosyltransferase involved in mycobacterial lipoarabinomannan biosynthesis. *Bioorg Med Chem*, 13, 1083-1094.

Swint-Kruse, L. and Matthews, K. S. (2009). Allostery in the LacI/GalR family: variations on a theme. *Current Opinion in Microbiology*, 12, 129-137.

Szczepina, M. G., Zheng, R. B., Completo, G. C., Lowary, T. L. and Pinto, B. M. (2010). STD-NMR studies of two acceptor substrates of GlfT2, a galactofuranosyltransferase from *Mycobacterium tuberculosis*: epitope mapping studies. *Bioorg Med Chem*, 18, 5123-5128.

Tahlan, K., Wilson, R., Kastrinsky, D. B., Arora, K., Nair, V., Fischer, E., Barnes, S. W., Walker, J. R., Alland, D., Barry, C. E., 3rd and Boshoff, H. I. (2012). SQ109 targets MmpL3, a membrane transporter of trehalose monomycolate involved in mycolic acid donation to the cell wall core of *Mycobacterium tuberculosis*. *Antimicrob Agents Chemother*, 56, 1797-1809.

Takayama, K. and Goldman, D. S. (1970). Enzymatic synthesis of mannosyl-1-phosphoryl-decaprenol by a cell-free system of *Mycobacterium tuberculosis*. *J Biol Chem*, 245, 6251-6257.

Takayama, K. and Kilburn, J. O. (1989). Inhibition of synthesis of arabinogalactan by ethambutol in *Mycobacterium smegmatis*. *Antimicrob Agents Chemother*, 33, 1493-1499.

Takayama, K., Schnoes, H. K. and Semmler, E. J. (1973). Characterization of the alkali-stable mannophospholipids of *Mycobacterium smegmatis*. *Biochim Biophys Acta*, 316, 212-221.

Takiff, H. E., Salazar, L., Guerrero, C., Philipp, W., Huang, W. M., Kreiswirth, B., Cole, S. T., Jacobs, W. R., Jr. and Telenti, A. (1994). Cloning and nucleotide sequence of *Mycobacterium tuberculosis gyrA* and *gyrB* genes and detection of quinolone resistance mutations. *Antimicrob Agents Chemother*, 38, 773-780.

Taniguchi, H., Aramaki, H., Nikaido, Y., Mizuguchi, Y., Nakamura, M., Koga, T. and Yoshida, S. (1996). Rifampicin resistance and mutation of the *rpoB* gene in *Mycobacterium tuberculosis*. *FEMS Microbiol Lett*, 144, 103-108.

Tatituri, R. V., Alderwick, L. J., Mishra, A. K., Nigou, J., Gilleron, M., Krumbach, K., Hitchen, P., Giordano, A., Morris, H. R., Dell, A., Eggeling, L. and Besra, G. S. (2007). Structural characterization of a partially arabinosylated lipoarabinomannan variant isolated from a *Corynebacterium glutamicum ubiA* mutant. *Microbiology*, 153, 2621-2629.

Telenti, A., Philipp, W. J., Sreevatsan, S., Bernasconi, C., Stockbauer, K. E., Wieles, B., Musser, J. M. and Jacobs, W. R., Jr. (1997). The *emb* operon, a gene cluster of *Mycobacterium tuberculosis* involved in resistance to ethambutol. *Nat Med*, 3, 567-570.

Thanbichler, M., Iniesta, A. A. and Shapiro, L. (2007). A comprehensive set of plasmids for vanillate- and xylose-inducible gene expression in *Caulobacter crescentus*. *Nucleic Acids Research*, 35:20 doi:10.1093/nar/gkm818.

Thomas, J. P., Baughn, C. O., Wilkinson, R. G. and Shepherd, R. G. (1961). A new synthetic compound with antituberculous activity in mice: ethambutol (dextro-2,2'-(ethylenediimino)-di-l-butanol). *Am Rev Respir Dis*, 83, 891-893.

Torrelles, J. B., Desjardin, L. E., Macneil, J., Kaufman, T. M., Kutzbach, B., Knaup, R., Mccarthy, T. R., Gurcha, S. S., Besra, G. S., Clegg, S. and Schlesinger, L. S. (2009). Inactivation of *Mycobacterium tuberculosis* mannosyltransferase *pimB* reduces the cell wall lipoarabinomannan and lipomannan content and increases the rate of bacterial-induced human macrophage cell death. *Glycobiology*, 19, 743-755.

Trefzer, C., Rengifo-Gonzalez, M., Hinner, M. J., Schneider, P., Makarov, V., Cole, S. T. and Johnsson, K. (2010). Benzothiazinones: prodrugs that covalently modify the decaprenylphosphoryl-β-D-ribose 2'-epimerase DprE1 of *Mycobacterium tuberculosis*. *J Am Chem Soc*, 132, 13663-13665.

Trefzer, C., Skovierova, H., Buroni, S., Bobovska, A., Nenci, S., Molteni, E., Pojer, F., Pasca, M. R., Makarov, V., Cole, S. T., Riccardi, G., Mikusova, K. and Johnsson, K. (2012). Benzothiazinones are suicide inhibitors of mycobacterial decaprenylphosphoryl-β-D-ribofuranose 2'-oxidase DprE1. *J Am Chem Soc*, 134, 912-915.

Turner, B. L., Paphazy, M. J., Haygarth, P. M. and Mckelvie, I. D. (2002). Inositol phosphates in the environment. *Philosophical Transactions of the Royal Society of London Series B-Biological Sciences*, 357, 449-469.

Udwadia, Z. F. (2012). Totally drug-resistant tuberculosis in India: who let the djinn out? *Respirology*, 17, 741-742.

Umeda, M. and Heidelberger, C. (1969). Fluorinated pyrimidines. XXXI. Mechanisms of inhibition of vaccinia virus replication in HeLa cells by pyrimidine nucleosides. *Proc Soc Exp Biol Med*, 130, 24-29.

Van Heijenoort, J. (2001a). Formation of the glycan chains in the synthesis of bacterial peptidoglycan. *Glycobiology*, 11, 25R-36R.

Van Heijenoort, J. (2001b). Recent advances in the formation of the bacterial peptidoglycan monomer unit. *Nat Prod Rep*, 18, 503-519.

Van Ingen, J., Aarnoutse, R. E., Donald, P. R., Diacon, A. H., Dawson, R., Plemper Van Balen, G., Gillespie, S. H. and Boeree, M. J. (2011). Why Do We Use 600 mg of Rifampicin in Tuberculosis Treatment? *Clin Infect Dis*, 52, e194-199.

Vannelli, T. A., Dykman, A. and Ortiz De Montellano, P. R. (2002). The antituberculosis drug ethionamide is activated by a flavoprotein monooxygenase. *J Biol Chem*, 277, 12824-12829.

Varela, C., Rittmann, D., Singh, A., Krumbach, K., Bhatt, K., Eggeling, L., Besra, G. S. and Bhatt, A. (2012). MmpL genes are associated with mycolic acid metabolism in Mycobacteria and Corynebacteria. *Chemistry & Biology*, 19, 498-506.

Veyron-Churlet, R., Bigot, S., Guerrini, O., Verdoux, S., Malaga, W., Daffe, M. and Zerbib, D. (2005). The biosynthesis of mycolic acids in *Mycobacterium tuberculosis* relies on multiple specialized elongation complexes interconnected by specific protein-protein interactions. *J Mol Biol*, 353, 847-858.

Veyron-Churlet, R., Guerrini, O., Mourey, L., Daffe, M. and Zerbib, D. (2004). Protein-protein interactions within the Fatty Acid Synthase-II system of *Mycobacterium tuberculosis* are essential for mycobacterial viability. *Mol Microbiol*, 54, 1161-1172.

Veziris, N., Ibrahim, M., Lounis, N., Chauffour, A., Truffot-Pernot, C., Andries, K. and Jarlier, V. (2009). A once-weekly R207910-containing regimen exceeds activity of the standard daily regimen in murine tuberculosis. *Am J Respir Crit Care Med*, 179, 75-79.

Via, L. E., Cho, S. N., Hwang, S., Bang, H., Park, S. K., Kang, H. S., Jeon, D., Min, S. Y., Oh, T., Kim, Y., Kim, Y. M., Rajan, V., Wong, S. Y., Shamputa, I. C., Carroll, M., Goldfeder, L., Lee, S. A., Holland, S. M., Eum, S., Lee, H. and Barry, C. E., 3rd (2010). Polymorphisms associated with resistance and cross-resistance to aminoglycosides and capreomycin in *Mycobacterium tuberculosis* isolates from South Korean Patients with drug-resistant tuberculosis. *J Clin Microbiol*, 48, 402-411.

Vilcheze, C., Av-Gay, Y., Attarian, R., Liu, Z., Hazbon, M. H., Colangeli, R., Chen, B., Liu, W., Alland, D., Sacchettini, J. C. and Jacobs, W. R., Jr. (2008). Mycothiol biosynthesis is essential for ethionamide susceptibility in *Mycobacterium tuberculosis*. *Mol Microbiol*, 69, 1316-1329.

Vilkas, E. and Lederer, E. (1956). Isolation of a phosphatidyl-inosito-di-D-mannoside from a mycobacterial phosphatide *Bull Soc Chim Biol (Paris)*, 38, 111-121.

Vocadlo, D. J., Davies, G. J., Laine, R. and Withers, S. G. (2001). Catalysis by hen egg-white lysozyme proceeds via a covalent intermediate. *Nature*, 412, 835-838.

Wallis, R. S., Jakubiec, W., Mitton-Fry, M., Ladutko, L., Campbell, S., Paige, D., Silvia, A. and Miller, P. F. (2012). Rapid evaluation in whole blood culture of regimens for XDR-TB containing PNU-100480 (sutezolid), TMC207, PA-824, SQ109, and pyrazinamide. *PLoS One*, 7, e30479.

Wallis, R. S., Jakubiec, W. M., Kumar, V., Silvia, A. M., Paige, D., Dimitrova, D., Li, X., Ladutko, L., Campbell, S., Friedland, G., Mitton-Fry, M. and Miller, P. F. (2010). Pharmacokinetics and whole-blood bactericidal activity against *Mycobacterium tuberculosis* of single doses of PNU-100480 in healthy volunteers. *J Infect Dis*, 202, 745-751.

Wennerhold, J. and Bott, M. (2006). The DtxR regulon of *Corynebacterium glutamicum*. *Journal of Bacteriology*, 188, 2907-2918.

Wennerhold, J., Krug, A. and Bott, M. (2005). The AraC-type regulator RipA represses aconitase and other iron proteins from *Corynebacterium* under iron limitation and is itself repressed by DtxR. *Journal of Biological Chemistry*, 280, 40500-40508.

Wheatley, R., Zheng, R., Richards, M., Lowary, T. and Ng, K. (2012). Tetrameric Structure of the GlfT2 Galactofuranosyltransferase Reveals a Scaffold for the Assembly of Mycobacterial Arabinogalactan. *The Journal of biological chemistry*, 287, 28132-28143.

Wietzerbin, J., Das, B. C., Petit, J. F., Lederer, E., Leyh-Bouille, M. and Ghuysen, J. M. (1974). Occurrence of D-alanyl-(D)-meso-diaminopimelic acid and meso-diaminopimelyl-meso-diaminopimelic acid interpeptide linkages in the peptidoglycan of Mycobacteria. *Biochemistry*, 13, 3471-3476.

Winder, F. G. and Collins, P. B. (1970). Inhibition by isoniazid of synthesis of mycolic acids in *Mycobacterium tuberculosis*. *J Gen Microbiol*, 63, 41-48.

Winder, F. G., Collins, P. B. and Whelan, D. (1971). Effects of ethionamide and isoxyl on mycolic acid synthesis in *Mycobacterium tuberculosis* BCG. *J Gen Microbiol*, 66, 379-380.

Wirth, T., Hildebrand, F., Allix-Beguec, C., Wolbeling, F., Kubica, T., Kremer, K., Van Soolingen, D., Rusch-Gerdes, S., Locht, C., Brisse, S., Meyer, A., Supply, P. and Niemann, S. (2008). Origin, spread and demography of the *Mycobacterium tuberculosis* complex. *PLoS Pathog*, 4, e1000160.

Wolucka, B. A. (2008). Biosynthesis of D-arabinose in mycobacteria - a novel bacterial pathway with implications for antimycobacterial therapy. *FEBS J*, 275, 2691-2711.

Wolucka, B. A. and De Hoffmann, E. (1998). Isolation and characterization of the major form of polyprenyl-phospho-mannose from *Mycobacterium smegmatis*. *Glycobiology*, 8, 955-962.

Wolucka, B. A., Mcneil, M. R., De Hoffmann, E., Chojnacki, T. and Brennan, P. J. (1994). Recognition of the lipid intermediate for arabinogalactan/arabinomannan biosynthesis and its relation to the mode of action of ethambutol on mycobacteria. *J Biol Chem*, 269, 23328-23335.

Yuan, Y., Lee, R. E., Besra, G. S., Belisle, J. T. and Barry, C. E., 3rd (1995). Identification of a gene involved in the biosynthesis of cyclopropanated mycolic acids in *Mycobacterium tuberculosis*. *Proc Natl Acad Sci U S A*, 92, 6630-6634.

Zhang, N., Torrelles, J. B., Mcneil, M. R., Escuyer, V. E., Khoo, K. H., Brennan, P. J. and Chatterjee, D. (2003a). The Emb proteins of mycobacteria direct arabinosylation of lipoarabinomannan and arabinogalactan via an N-terminal recognition region and a C-terminal synthetic region. *Mol Microbiol*, 50, 69-76.

Zhang, Y., Heym, B., Allen, B., Young, D. and Cole, S. (1992). The catalase-peroxidase gene and isoniazid resistance of *Mycobacterium tuberculosis*. *Nature*, 358, 591-593.

Zhang, Y. and Mitchison, D. (2003). The curious characteristics of pyrazinamide: a review. *Int J Tuberc Lung Dis*, 7, 6-21.

Zhang, Y., Wade, M. M., Scorpio, A., Zhang, H. and Sun, Z. (2003b). Mode of action of pyrazinamide: disruption of *Mycobacterium tuberculosis* membrane transport and energetics by pyrazinoic acid. *J Antimicrob Chemother*, 52, 790-795.

Zheng, J., Wei, C., Zhao, L., Liu, L., Leng, W., Li, W. and Jin, Q. (2011). Combining blue native polyacrylamide gel electrophoresis with liquid chromatography tandem mass spectrometry as an effective strategy for analyzing potential membrane protein complexes of *Mycobacterium bovis* bacillus Calmette-Guerin. *BMC Genomics*, 12, 40.

Zumla, A., Nahid, P. and Cole, S. T. (2013). Advances in the development of new tuberculosis drugs and treatment regimens. *Nat Rev Drug Discov*, 12, 388-404.